FREQUENCY RESPONSE MATCHING METHODS FOR THE DESIGN OF DIGITAL CONTROL SYSTEMS

Jianfei Shi, B.E.

Thesis submitted to

Department of Electrical and Electronic Engineering

for the degree of

Master of Engineering Science

The University of Adelaide

July, 1984

awarded 10.10.84

This thesis embodies the results of supervised project work making up two thirds of the work for the degree.

EXAMINER'S REPORT OF M.ENG.SC. THESIS;
J. SHI, "Frequency response matching methods for the design of digital control systems"

ERRATA OR OMISSIONS

p.3-8: the relation for the zero Z_1 in terms of other parameters is omitted. It is

$$Z_1 = \frac{I + \tan(\alpha+90^0)(I^2+R^2-R)}{I-\tan(\alpha+90^0)(1-R)}$$

p.3-10: Fourth line, (correction)

$$b = (C-A)(D+1)-BC$$

p3-12: The term

$$\frac{C^2 + (D-1)^2}{4D}$$

under the square root sign in both expressions should be positive, not negative.

pA-10: Eqn D-16.
The numerator term should be A-B, not A+B.

pA-15 to pA-28 The omission of values for the normalised parameters t_s/T (C/L step time-response) and $\omega_c T$ (O/L frequency-response) render the sets of specifications in each of these domains incomplete.

I recommend that the tables for damping ratio $\xi=0.7$ be recalculated to include these values, and the results be included with an errata sheet in the copies of the thesis.

pA-16: The variables t_s and ω_c should be defined under the appropriate heading.

DEDICATED

TO

MY PARENTS

TABLE OF CONTENTS

ABSTRACT

The frequency response matching technique for the synthesis of digital control systems has been investigated. The basic philosophy of this technique is to design a digital controller so that the frequency response of the designed closed-loop system matches a specified frequency response model. The approaches described in the current literature include Rattan's complex-curve fitting method and Shieh's dominant data matching method.

Two new design methods are proposed in this thesis. The first one is the *iterative complex-curve fitting* (ICCF) design method based on Rattan's algorithm. With its iterative calculations, the new method improves the frequency matching accuracy significantly by eliminating in Rattan's algorithm the frequency dependent weighting factor which severely degrades the matching accuracy at high sampling frequencies. The second one is the *simplex optimization-based* (SIM) design method. With the aid of non-linear constraints on the controller parameters, this method provides a good compromise between the desired system frequency response and the required controller characteristics to avoid problems such as an excessively high controller gain or an oscillatory control signal.

The non-linearity of the Shieh's method in the case of the design of a controller with an integrator is removed by choosing the appropriate controller form and dominant frequency points. As a result, the relevant computational algorithm is considerably simplified.

The determination of a frequency response model from design specifications given in the time, frequency and z- domains is discussed. It is shown that the choice of the model may be critical to the succcess of the frequency matching, in particular when there is discrepancy between the primary frequency range of the system under design and that of the model. To help select an appropriate z-transfer function as a model, an

easy-to-use approach is developed which is based on a comprehensive investigation on the dynamic performances of second-order discrete systems.

A number of design studies is conducted in order to assess the frequency matching design methods. The frequency matching accuracies and time responses of the designed systems form the basis for the comparative evaluation. The results show that ICCF and SIM methods proposed in this thesis are superior to current methods. The effect of the discrepancy between the primary frequency ranges on the matching accuracy and the convergency of optimization algorithms are illustrated as well.

The ***hybrid frequency response*** is defined for the system containing both discrete- and continuous- time components. Unlike the commonly-used ***discrete frequency response*** , which is derived from the system z-transfer function and provides no information about the time response between sampling instants, the hybrid frequency response includes the characteristics of the inter-sampling time response.

DECLARATION

I hereby declare that, (a) the thesis contains no material which has been accepted for the award of any other degree or diploma in any university and that, to the best of my knowledge and belief, the thesis contains no material previously published or written by another person, except where due reference is made in the text of the thesis; and (b) I consent to the thesis being made available for photocopying and loan if applicable.

Jianfei Shi

ACKNOWLEDGEMENTS

It is good fortune to have Dr. M.J. Gibbard as my supervisor. I am deeply indebted for his encouragement throughout the entire postgraduate studies and for his guidance and criticism given in the preparation of this thesis.

I would like to thank Dr. F.J.M. Salzborn, of the Department of Applied Mathematics, for his stimulating lecture in the field of optimization and for his helpful suggestions. I would also like to thank Mr. P. Leppard, of the Department of Statistics, for permission to use his computing program at the early stage of this research project.

I wish to express my gratitude to Dr. B.R. Davis for his help given in many interesting discussions.

The assisstance of the staff of the department is gratefully acknowledged. Special thanks are due to Mr. R.C. Nash for his unsparing support.

As a student from a non-English-speaking country, I am very grateful to Mrs. J. Laurie, of the student counselling service, for her two-year English tutorial work which has helped me to complete this thesis.

Finally, I wish to express my sincere appreciation to the University of Adelaide for the Scholarship for Postgraduate Research which enabled me to pursue my studies towards the degree of Master of Engineering Science in electrical engineering.

LIST OF FIGURES

LIST OF TABLES

LIST OF SYMBOLS AND ABBREVIATIONS

This list summarizes symbols and abbreviations commonly used in this study. The page number indicates the place where the symbol or abbreviation is defined.

Symbol		Page
A	coefficient of a second-order discrete transfer function	3-1
B	coefficient of a second-order discrete transfer function	3-1
C	coefficient of a second-order discrete transfer function	3-1
D	coefficient of a second-order discrete transfer function	3-1
$D(\ )$	transform or frequency response of a digital controller	2-2
E	squared-matching-error function	2-10
or	objective function	2-23
$E(s)$	transfer function of an error signal	2-2
$E(z)$	z-transfer function of an error signal	2-3
$F(s)$	transfer function of a control element in the system feedback loop	2-2
$G(s)$	transfer function of a continuous-time plant	2-2
$G_hG(\ )$	transform or frequency response of a plant with ZOH	2-3
GM	gain margin	3-2
$H(\ )$	transform or frequency response of a closed-loop system	2-3
I	imaginary part of a complex number	2-5
$M(\ )$	transform or frequency response of a closed-loop model	2-3
$M_Q(\ )$	transform or frequency response of a open-loop model	2-3
M_p	maximum overshoot	3-2
M_r	resonance peak value	3-2
$N(\ )$	numerator polynomial	2-9
P	open-loop or closed-loop poles	3-6
$P(\ )$	denominator polynomial	2-9
PM	phase margin	3-2
$Q(\ )$	transform of frequency response of an open-loop system	2-3
R	real part of a complex number	2-5
$R(\ )$	transform of an input signal	2-2
T	sampling period	1-3
T_m	sampling period of a frequency response model	2-14

CHAPTER I

INTRODUCTION

§1.1 Digital control systems

With the great advances in digital computers and microprocessors over the last two decades, significant progress has been made in digital control systems. The applications of these systems have been found in almost all aspects of industry. Compared with their conventional analogue counterparts, digital controllers are usually more reliable in operation, more compact in size, lighter in weight and cheaper in cost. But the most important advantage of digital controllers is their great flexibility in control functions. This unique property enables a digital controller to perform different control functions, in accordance with the latest design changes or adaptive control performances, without modification of the controller hardware.

§1.2 Advantages of frequency response methods

For digital control system synthesis, there are many methods available, among which the frequency response design methods have some distinct advantages in comparison with those in the time and complex z- domains. For instance, the application of the root locus method, a widely used complex z-domain design technique, is limited by the

requirement that the time response of a system under design can be approximated by a pair of dominant poles in its transfer function. On the other hand, in frequency domain analysis, effects of all poles and zeros are taken into account as each of them contributes its share to form the overall system frequency response. The latter provides the facility for handling high-order dynamic systems without having to make the approximation inherent in the former. Furthermore, designs based on time domain synthesis, such as the deadbeat response control technique [1, 14] and the state matching methods [24, 25, 26], are dependent on some specific types of input signals. Their responses to other types of signals may be poor. In contrast with this shortcoming, frequency domain analysis describes the linear system response to any periodic input signals. Moreover, some design methods in the frequency domain allow the designer to characterize the plant of interest by using the results of frequency response measurements directly, rather than by forming a transfer function from these measurements. In practice, the derivation of such a transfer function may be very cumbersome. Finally, it is noteworthy that specifying control performance criteria in the frequency domain is in some cases more reasonable and convenient than in the time or complex z- domains, especially in dealing with high-frequency noises [20].

§1.3 Classification of frequency response methods

Frequency response methods for the digital control system designs can be classified into two categories. The first category covers those graphical design methodologies adopted directly from continuous system synthesis techniques. The best known are the Nyquist plot, Bode plot and Nichols chart methods. In digital control system designs, they are implemented in the W-plane using the bilinear transformation [1, 19]:

$$W = \frac{2}{T} \cdot \frac{z-1}{z+1}, \qquad (1-1)$$

or

$$z = \frac{1 + \frac{WT}{2}}{1 - \frac{WT}{2}}, \qquad (1-2)$$

where T is a sampling period. In many cases, the graphic nature and " cut and try " procedures make it difficult for these methods to be employed in the on-line synthesis of digital controllers, where the simplicity and mathematical formulation of design results are most desirable. The second category comprises the frequency response matching methods which are associated with various complex-curve fitting techniques. An early complex-curve fitting design method was due to Rattan [5], and was followed by the dominant data matching method proposed by Shieh *et al* [4]. In addition to common advantages discussed in section 1.2, their results are formulated in mathematical form and so are amenable to digital computation. It is this feature which offers potential for these methods in more sophisticated designs of digital control systems.

§1.4 Frequency response matching methods

The aim of frequency response matching design methods can be stated as follows:

> *To design the discrete transfer function of a digital controller for a given discrete or continuous plant so that the frequency response of the closed-loop system matches the desired frequency response model as closely as possible.*

To derive a transfer function from a specified complex-curve or a set of known data is not a new idea. Some fundamental work was done in the late 1950's and early 1960's. For instance, Levy [18] proposed the weighted-least-squares complex-curve fitting method in 1959. However, it was not applied to digital control system synthesis until 1975 when Rattan [5] developed a computer-aided design method. Using Levy's complex-curve fitting technique, this method determines the coefficients of the digital

controller by minimizing the weighted-mean-squared error between the frequency response of the closed-loop system under design and that of a continuous model. The only requisites are the z-transfer function of the plant and the transfer function of the continuous model. One of the drawbacks in this method is that a frequency dependent weighting factor is introduced in the error function in the process of linearization. When the sampling period T becomes small, this weighting factor may result in a large deviation in frequency response matching.

A few years later, in 1981, Shieh *et al.* [4] proposed another simple but practical method, called the dominant data matching method. The desired frequency response is specified at several key frequency points, e.g., the gain cross-over frequency, known as the dominant data. The coefficients of the digital controller are then determined so that the frequency response of the system under design will closely match the dominant data. The method becomes complicated when applied to the design of a "type I " system, which has an integrator in its forward path, as shown in Shieh *et al.*'s example [4]. They derived a set of linear and non-linear equations for matching this type of system. However, the Newton-Raphson method used to solve the non-linear equations, as pointed out by Shieh *et al.*, has strict requirements on initial estimates.

§1.5 Summary of the current frequency matching design methods

The frequency response matching methods for the design of digital controllers are recently introduced design approaches. They have been thus far scarcely discussed in relevant textbooks or papers other than those written by the proposers themselves. The advantages of these methods are significant; some examples are given below:

(1) These methods do not require an excessively high sampling frequency for the digital controller.

(2) These methods can be applied to high-order systems without the assumption of

the existence of a pair of dominant poles.

(3) The results of designs are independent of specific types of input signals and therefore can be used for a variety of input signals.

(4) No high-order hold is required.

(5) The solution of these design methods is in mathematical formulation and is amendable to digital computation.

On the other hand, there are also some drawbacks and open questions in the frequency response matching design methods.

(1) There is no guarantee for the open-loop and closed-loop stability of the control system under design.

(2) In the matching process, a closed-loop system is only considered as a whole. Though its realizability is ensured in the design algorithm, the resulting digital controller may be not practical for reasons such as an highly oscillatory controller output in an electromechanical system.

(3) In Rattan's complex-curve fitting method, the matching accuracy may be degraded by a frequency dependent weighting factor.

(4) In Shieh's dominant data matching method, the design of the "type I " system results in a set of non-linear equations whose solution depends on initial values.

(5) The determination of the frequency response models has not been discussed in the literature. In particular, the impact of sampling frequencies on the matching accuracy is ignored.

(6) Designs are carried out via the z-transfer function. For continuous-time plants, the resulting frequency response does not carry the information about the time response between sampling instants.

(7) The relationships between the control specifications of discrete systems given in the time, frequency and complex z-domains have not been well established. Such relationships are essential for selecting discrete frequency response models that satisfy assigned control specifications.

§1.6 Objectives, approaches and achievements

The objectives of this thesis are to evaluate current frequency response matching design methods; to modify these methods to overcome the deficiencies summarized above; and to develop new design methods which improve frequency matching design techniques.

A number of design studies is conducted for the purpose of assessing various frequency matching design methods. The two third-order, continuous-time plants used in the studies possess a sluggish time response and an oscillatory time response, respectively. The plants are compensated according to the same control specifications for a wide range of sampling frequencies. A comparison of the closed-loop designs is based on their accuracy in matching the desired frequency response models and on their unit-step time response performances.

To remove the non-linearity of coefficient equations in Shieh's dominant data matching method in the case of the "type I " system design, this author suggests using a one-order-higher digital controller and choosing appropriate dominant frequency points. As a result, the computational algorithm is significantly simplified, compared with the efforts required by the Newton-Raphson iterative method. More importantly, the designer no longer needs to worry about the initial estimations and the convergency of solutions.

In order to minimize the detrimental effect of the weighting factor in Rattan's complex-curve fitting design method, the author proposes a new method, called the *iterative complex-curve fitting* design method, in which the weighting factor from the current iteration is effectively eliminated by the one from the previous iteration. In comparison with the designs by Rattan's method, as shown in design examples, the matching error can be reduced by the factor of two or three in only $2 \sim 3$ iterations. The corresponding time responses are also improved significantly.

Another important contribution of this thesis is the development of the *simplex optimization-based* frequency matching design method. In this method, the minimization of the frequency matching error is formulated as a non-linear programming problem with a set of non-linear constraints on controller parameters. The solution is then obtained by means of some standard optimization technique such as the simplex method of function minimization. The unique feature of this method is that the controller gain, zeros and poles can be confined to some specified ranges of values. Thus if the plant is open-loop stable and the Nyquist plot of the closed-loop system does not encircle the point of $(-1,\ j0)$ in the $D(z)G_h G(z)$-plane, the closed-loop stability can be guaranteed by locating all controller poles on or inside the unit circle. The dynamic characteristics of the controller also can be improved by confining controller poles and zeros into appropriate regions in the z-plane to avoid, for instance, an oscillatory control signal. The implementation of the upper limit for the controller gain is straightforward.

As a further contribution of this thesis, a systematic and user-oriented approach is presented to determine a discrete frequency response model from control specifications given in one or more of the time, frequency and complex z- domains. The approach is based on an investigation of the dynamic characteristics of the second-order discrete system having a pair of complex poles and a zero. In addition, the sufficient and necessary conditions for an open-loop second-order discrete system to be closed-loop absolutely stable are derived and proved.

Deriving the frequency response of a digital control system from its z-transfer function is the most popular technique. The resulting frequency response is sometimes called the *discrete frequency response* . The disadvantage lies in the fact that, when a plant is a continuous-time system, information about the time response between sampling instants is not provided by the z-transfer function nor by the discrete frequency response. For the frequency response matching design methods, this shortcoming may become severe if the discrete frequency response gives a poor approximation for an actual frequency response in a relevant frequency range when a sampling frequency is low

relative to the closed-loop bandwidth. In this thesis, the *hybrid frequency response* is derived which reveals the actual frequency response of a closed-loop system consisting of both digital and analogue components. Accordingly, the continuous time response of such a system can be accurately predicted from its hybrid frequency response. This unique advantage suggests that the frequency response matching design methods be improved by means of the hybrid frequency response analysis, although lack of time prevented its implementations.

§1.7 The contents

In Chapter II , the problem of the design of a digital controller is defined and is followed by descriptions of the various frequency response matching design methods. In Chapter III the conversion of the control specifications between the time, frequency and complex z- domains for discrete systems is discussed. Based on its results, the approach used for the determination of a desired frequency response model is proposed. Studies for the evaluation of the design methods are described in Chapter IV . After discussing the bases for the design studies, three groups of design examples are presented, each group considering a particular aspect of designs. The time and frequency responses as well as the matching accuracy of the resulting closed-loop systems are shown, along with the comparisons and discussions. Chapter V is devoted to the hybrid frequency response analysis technique. Finally, Chapter VI summarizes the studies and gives general conclusions and recommendations about the frequency matching design methods for the design of digital controllers.

CHAPTER II

FREQUENCY RESPONSE MATCHING DESIGN METHODS

§2.1 Formulation of the design problem

In this study, the control system under design is a linear, time-invariant, single-input/single-output system. The general configuration for the closed-loop system incorporating a digital controller is drawn in Fig. 2-1.

To simplify the synthesis without losing generality, $F(s)$ is assigned to unity. Moreover, the system in Fig. 2-1 is hybrid in nature as it contains components operating with both discrete and continuous signals. The analysis of this system constitutes the investigation in Chapter V and is of interest because its frequency response provides the information about the time response between sampling instants. Chapters II –IV of this thesis, however, will concentrate on the design via the system z-transfer function; a dummy sampler, drawn in dashed lines in Fig. 2-1, is therefore added at the output of system to convert the hybrid system into the discrete-time system as shown in Fig. 2-2.

Define the discrete transfer function for a nth-order digital controller as the ratio of two polynomials:

$$D(z) = \frac{x_0 z^m + x_1 z^{m-1} + \cdots + x_{m-1} z + x_m}{z^n + y_1 z^{n-1} + \cdots + y_{n-1} z + y_n}, \qquad (2-1)$$

where $y_0 = 1$ and $m \leq n$ to ensure the controller is realizable [14].

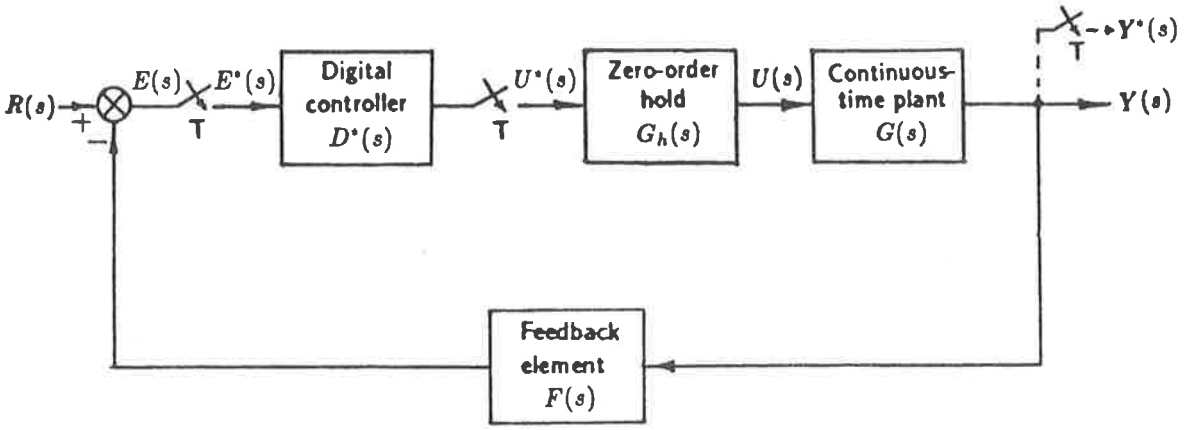

Notation:

$G(s)$ – transfer function of a continuous-time plant

$G_h(s)$– transfer function of a zero-order-hold converting a series of pulses into a continuous-time signal at the input of plant

$D^*(s)$– transfer function of a digital controller, where the notation $X^*(s)$ defines the Laplace transform of $x(kT)$, the sampled form of continuous-time signal $x(t)$

$F(s)$ – transfer function of a control or measurement element in the feedback loop

$R(s)$ – transfer function of an input signal $r(t)$

$Y(s)$ – transfer function of the output signal $y(t)$ of the closed-loop system

$Y^*(s)$ – transfer function of the sampled output signal $y(kT)$

$U^*(s)$ – transfer function of the output signal $U(kT)$ of a digital controller

$E(s)$ – transfer function of an error signal $e(t)$

$E^*(s)$ – discrete transfer function of the sampled error signal $e(kT)$

T – sampling period

Figure 2-1 Configuration of the closed-loop system incorporating a digital controller

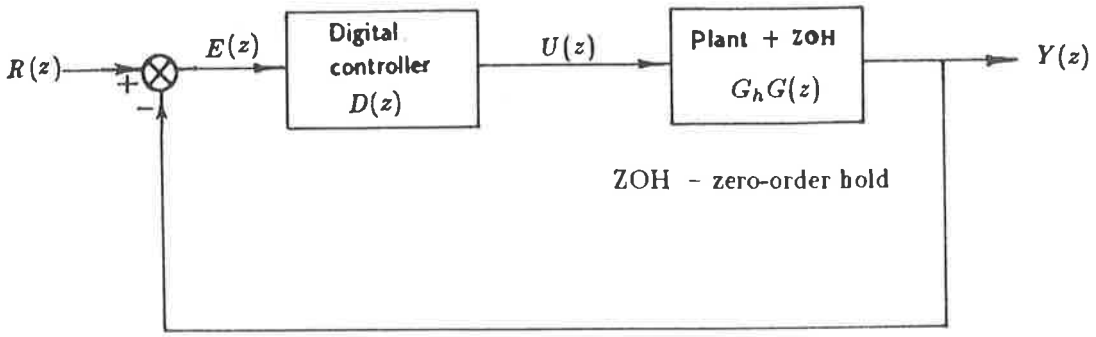

Figure 2-2 Discrete control system with unity feedback

Similarly $G_hG(z)$ is written in the same form:

$$G_hG(z) = \frac{a_0z^q + a_1z^{q-1} + \cdots + a_{q-1}z + a_q}{z^p + b_1z^{p-1} + \cdots + b_{p-1}z + b_p}, \qquad (2-2)$$

where $q \leq p$ and $b_0 = 1$.

For the digital control system defined in Fig. 2-2, the open-loop discrete transfer function is:

$$Q(z) = D(z) \cdot G_hG(z), \qquad (2-3)$$

and the closed-loop discrete transfer function is:

$$H(z) = \frac{Q(z)}{1 + Q(z)} = \frac{D(z)G_hG(z)}{1 + D(z)G_hG(z)}. \qquad (2-4)$$

In addition, $M_Q(j\omega)$ and $M(j\omega)$ are used to denote open-loop and closed-loop frequency response models, respectively. The formulation and determination of these frequency response models will be discussed in detail in Chapter III .

It is well known that the frequency response of a discrete system operating with the sampling frequency $\omega_s = 2\pi/T$ can be obtained by substituting $e^{j\omega T}$ for z in its z-transfer function [1]. Moreover, this frequency response repeats for every $n\omega_s \leq \omega \leq (n+1)\omega_s, n = 0, 1, 2, \ldots$ and the frequency response for $(n+1)\omega_s/2 \leq \omega \leq (n+1)\omega_s$

is just the mirror image of that for $n\omega_s \leq \omega \leq (n+1)\omega/2, n = 0, 1, 2, \ldots$, with respect to the real axis in the complex plane. Hence it is sufficient to consider matching the frequency response over only $0 \leq \omega \leq \omega_p$, where ω_p is called the primary frequency range and is defined as $\omega_p = \omega_s/2$.

Based on the above definitions, the design objective can be explicitly stated as determining the coefficients of the z-transfer function $D(z)$ for the digital controller (see Eq.(2-1)), such that $H(j\omega)$ or $Q(j\omega)$, the closed-loop or open-loop frequency response, whichever is required, will match the specified frequency response model $M(j\omega)$ or $M_Q(j\omega)$ as closely as possible.

§2.2 Dominant Data Matching design method (DDM)

2.2.1 Description of the design method

The Dominant Data Matching method, abbreviated to "DDM" for convenience, was proposed by Shieh *et al.* in 1981 [4] for matching an open-loop frequency response $Q(j\omega)$ to a given set of dominant data. The method was extended before long to multivariable sampled-data control systems for model simplification and digital controller design by the same research group [3]. The dominant data is defined as a set of frequency response values for the open-loop model $M_Q(j\omega_i)$ at some key frequency points $\omega_i, i = 1, 2, \ldots, K$. Usually these points are chosen from the gain cross-over frequency, the phase cross-over frequency and appropriate low frequency points.

The frequency response of the open-loop system can be derived from Eq. (2-3) as:

$$\begin{aligned} Q(j\omega_i) &= D(z)G_hG(z)|_{z=e^{j\omega_i T}} \\ &= D(e^{j\omega_i T})G_hG(e^{j\omega_i T}), \qquad i = 1, 2, \ldots, K. \end{aligned} \tag{2-5}$$

Let R and I represent the real and imaginary part of complex numbers, respectively, then:

$$Q(j\omega_i) = R_Q(\omega_i) + jI_Q(\omega_i); \tag{2-6}$$

$$D(j\omega_i) = R_D(\omega_i) + jI_D(\omega_i); \tag{2-7}$$

$$G_hG(j\omega_i) = R_G(\omega_i) + jI_G(\omega_i). \tag{2-8}$$

For simplicity, rewrite $R_Q(\omega_i)$ as R_{Qi}, $I_Q(\omega_i)$ as $I_{Qi}, \ldots$, etc.. Eqs. (2-6), (2-7) and (2-8), respectively, are then simplified to:

$$Q(j\omega_i) = R_{Qi} + jI_{Qi}; \tag{2-9}$$

$$D(j\omega_i) = R_{Di} + jI_{Di}; \tag{2-10}$$

$$G_hG(j\omega_i) = R_{Gi} + jI_{Gi}. \tag{2-11}$$

Similarly, the open-loop response model is:

$$M_Q(j\omega_i) = R_{M_Qi} + jI_{M_Qi}. \tag{2-12}$$

The design specification now can be expressed as :

$$\begin{aligned} Q(j\omega_i) &= M_Q(j\omega_i) \\ &= R_{M_Qi} + jI_{M_Qi}, \qquad i = 1, 2, \ldots, K. \end{aligned} \tag{2-13}$$

By rearranging Eq. (2-5) and substituting Eqs. (2-10), (2-11) and (2-12) in it, the required controller response is found to be:

$$R_{Di} + jI_{Di} = \frac{R_{M_Qi} + jI_{M_Qi}}{R_{Gi} + jI_{Gi}}, \qquad i = 1, 2, \ldots, K. \tag{2-14}$$

In Eq. (2-14), R_{M_Qi} and I_{M_Qi} are specified, and R_{Gi} and I_{Gi} can be calculated from Eq. (2-8) for the plant with a ZOH.

Substitution of Eq.(2-10) and $z = e^{j\omega T} = \cos\omega T + j\sin\omega T$ into Eq. (2-1) gives:

$$\begin{aligned} D(e^{j\omega_i T}) &= \frac{\sum_{l=0}^{m} x_l \cos(m-l)\omega_i T + j\sum_{l=0}^{m} x_l \sin(m-l)\omega_i T}{\sum_{k=0}^{n} y_k \cos(n-k)\omega_i T + j\sum_{k=0}^{n} y_k \sin(n-k)\omega_i T} \\ &= R_{Di} + jI_{Di}, \qquad i = 1, 2, \ldots, K. \end{aligned} \tag{2-15}$$

where $y_0 = 1$; y_k, $k = 1, 2, \ldots, n$ and x_l, $l = 0, 1, \ldots, m$ are the unknown coefficients to be determined.

Now multiply both sides of Eq. (2-15) by the common denominator and separate out their real and imaginary parts; then by equating the respective real and imaginary parts in the resulting expression the following linear equation matrix can be obtained. Its solution yields the required coefficients of the discrete transfer function for the digital controller.

$$\overline{W}^{\top} = \overline{U}^{-1} \cdot \overline{V} \qquad (2-16)$$

where,

$$\overline{W} = (\; x_0 \; x_1 \; \ldots \; x_m \; y_1 \; \ldots \; y_{n-1} \; y_n \;)$$

and $\overline{W}^{\top}$ is the transpose of $\overline{W}$;

$$\overline{V} = \begin{pmatrix} R_{D1} \cos n\omega_1 T - I_{D1} \sin n\omega_1 T \\ R_{D1} \sin n\omega_1 T + I_{D1} \cos n\omega_1 T \\ \vdots \\ R_{Di} \cos n\omega_i T - I_{Di} \sin n\omega_i T \\ R_{Di} \sin n\omega_i T + I_{Di} \cos n\omega_i T \\ \vdots \\ R_{DK} \cos n\omega_K T - I_{DK} \sin n\omega_K T \\ R_{DK} \sin n\omega_K T + I_{DK} \cos n\omega_K T \end{pmatrix};$$

$$\overline{U} = \begin{pmatrix} a_{11} & a_{12} & \cdots & a_{1(m+1)} & c_{11} & c_{12} & \cdots & c_{1n} \\ b_{11} & b_{12} & \cdots & b_{1(m+1)} & d_{11} & d_{12} & \cdots & d_{1n} \\ \vdots & \vdots & \ddots & \vdots & \vdots & \vdots & \ddots & \vdots \\ a_{i1} & a_{i2} & \cdots & a_{i(m+1)} & c_{i1} & c_{i2} & \cdots & c_{in} \\ b_{i1} & b_{i2} & \cdots & b_{i(m+1)} & d_{i1} & d_{i2} & \cdots & d_{in} \\ \vdots & \vdots & \ddots & \vdots & \vdots & \vdots & \ddots & \vdots \\ a_{K1} & a_{K2} & \cdots & a_{K(m+1)} & c_{K1} & c_{K2} & \cdots & c_{Kn} \\ b_{K1} & b_{K2} & \cdots & b_{K(m+1)} & d_{K1} & d_{K2} & \cdots & d_{Kn} \end{pmatrix},$$

and

$$\left.\begin{aligned} a_{ij} &= \cos(m+1-j)\omega_i T, \\ b_{ij} &= \sin(m+1-j)\omega_i T, \end{aligned}\right\} \quad j = 1, 2, \ldots, m+1$$

$$\left.\begin{aligned} c_{ij} &= -R_{Di} \cos(n-j)\omega_i T + I_{Di} \sin(n-j)\omega_i T, \\ d_{ij} &= -R_{Di} \sin(n-j)\omega_i T - I_{Di} \cos(n-j)\omega_i T. \end{aligned}\right\} \quad j = 1, 2, \ldots, n$$

Suppose the matrix $\overline{C}$ is an enlargement of $\overline{U}$ by $\overline{V}$, i.e., $\overline{C} = (\overline{U} \vdots \overline{V})$. According to the theory of linear algebra, Eq. (2-16) has a unique solution if and only if the number of unknowns, determined by Eq. (2-1), equals the rank of matrix $\overline{C}$, determined by the selected key frequency points. Because in this method, a frequency response is represented in terms of complex numbers, the real and imaginary parts of which are regarded as the dominant data, the number of specified dominant data is always twice the number of selected frequency points. The order of polynomials of $D(z)$, therefore, should be taken in such a way that the sum of $(n+m+1)$ is equal to $2K$.

In practice, however, this requirement may be eased. Assume that K selected frequency points are located reasonably evenly over the frequency range concerned and K is equal to or greater than 4. Then it is conjectured that, for a well-behaved frequency response model, the equation associated with the frequency point which resides between the other points may be discarded from the set of $2K$ linear equations in Eq. (2-16) without significant detriment to the frequency response matching. Unfortunately, this conjecture can not be proved mathematically; but the results of design examples examined in this thesis reveal that the conjecture is well satisfied.

The significance of such an approximation is to reduce the order of a digital controller. The design for $2K$ equations requires a controller the order of which is $n \geq K$, but the design for $(2K-1)$ equations can be implemented by a controller with the order $n \geq (K-1)$.

2.2.2 Deficiencies in and modifications to the DDM method

A problem arises when a "type I " system, which contains an integrator in its forward path, is selected as the model of an open-loop system for a plant without integral characteristics. To fit a "type I " system, Shieh *et al.* proposed to match the dominant data $M_Q(j\omega_i)$ at $\omega = 0$ [4]. However, the infinite value of $I_{M_Q}(j\omega)$ at $\omega = 0$ makes the calculation of Eq. (2-14) impossible. To solve this problem, Shieh *et al.* introduced the

linear transformation $z' = z - 1$ into Eq. (2-3) so that the real part of an open-loop frequency response at $\omega = 0$, $R_e[Q(z')]|_{z'=0}$, can be expressed in terms of coefficients of the new discrete transfer function $Q(z')$. Nevertheless, the resulting equation is non-linear and has to be solved by a method such as Newton-Raphson. Two disadvantages immediately become apparent. Firstly, the convergency of the Newton-Raphson method is highly dependent on initial estimates [4]. Secondly, the estimation of better initial values and the iterative calculations of the Newton-Raphson method increase the overall computational burden significantly.

In this thesis, the author suggests using a higher order controller to overcome these deficiencies in the "type I " system design. The use of a higher order controller enables a designer to select a pair of points one decade apart in a low-frequency band instead of a single point at $\omega = 0$, as Shieh *et al.* proposed. The low-frequency band is considered as $\omega < 0.03\omega_b$, where ω_b is the desired closed-loop bandwidth $(-3db)$. Because the frequency responses at these points are of finite values, Eq. (2-16) can be formulated with no computational difficulty. In matching the "type I " model response, featuring the the magnitude "roll-off" of 20 $db/decade$ and phase lag of 90° in the low frequency band, the algorithm automatically positions an open-loop pole at the point of $(1, j0)$ in the z-plane to form the desired "type I " system. Unlike Shieh's method, no non-linear equation is involved and no initial estimates are required. As a result, the modification proposed by this author not only saves computational effort significantly but also avoids the convergency problem; the only cost is the increment in controller order of one.

Note that in the design of "type I " system, a controller pole is defined at the point of $(1, j0)$ in the z-plane, so that the z-transfer function of a digital controller is

$$D(z) = \frac{x_0 z^m + x_1 z^{m-1} + \cdots + x_{m-1} z + x_m}{(z-1)(z^{n-1} + y_1 z^{n-2} + \cdots + y_{n-2} z + y_{n-1})}, \qquad (2-17)$$

where $m \leq n$. Thus one can solve the other $(m + n)$ unknown coefficients by means of the DDM method. Although this approach may be more efficient and accurate, the

resulting form of linear equations and the associated computer program can not be applied to the design of a system with other type numbers. Hence the design based on Eq. (2-17) is not presented in this study.

§2.3 Complex-Curve Fitting design method (CCF)

The complex-curve fitting technique of Levy [18] has been employed in the synthesis of the z-transfer function of a digital controller so that the frequency response of the closed-loop system will match that of the assigned model. The matching is optimized in the sense of minimum weighted-mean-squared-error. Rattan first presented this elegant method in his doctoral dissertation in 1975 [5]. Since then, he has applied this technique to various digital control system design problems such as discretization of single- and multi-loop continuous-time control systems [6, 7, 3] and model simplification of digital control systems [27]. The essentials of the complex-curve fitting design method, abbreviated to "CCF", are given in this section, and based on Rattan's method.

2.3.1 Rattan's design method

The closed-loop frequency response of the control system defined in Fig. 2-2 is

$$H(j\omega) = \frac{D(z)G_hG(z)}{1 + D(z)G_hG(z)}\Big|_{z=e^{j\omega T}}. \qquad (2-18)$$

Represent $G_hG(j\omega)$ in its real and imaginary parts as:

$$G_hG(j\omega) = R_G(\omega) + jI_G(\omega). \qquad (2-19)$$

Let N and P be a numerator and denominator, respectively, and note that $z = \cos\omega T + j\sin\omega T$. Thus $H(j\omega)$ in Eq. (2-18) can be rewritten as:

$$H(j\omega) = \frac{N_H(j\omega)}{P_H(j\omega)} = \frac{\Phi + j\Theta}{\sigma + j\tau}; \qquad (2-20)$$

where,

$$\Phi = \sum_{i=0}^{m} x_i[R_G(\omega)\cos(i\omega T) + I_G(\omega)\sin(i\omega T)],$$

$$\Theta = \sum_{i=0}^{m} x_i[-R_G(\omega)\sin(i\omega T) + I_G(\omega)\cos(i\omega T)],$$

$$\sigma = 1 + \sum_{i=0}^{m} x_i[R_G(\omega)\cos(i\omega T) + I_G(\omega)\sin(i\omega T)] + \sum_{i=1}^{n} y_i\cos(i\omega T),$$

$$\tau = \sum_{i=0}^{m} x_i[-R_G(\omega)\sin(i\omega T) + I_G(\omega)\cos(i\omega T)] - \sum_{i=1}^{n} y_i\sin(i\omega T).$$

Assume that a desired closed-loop frequency response is

$$M(j\omega) = \frac{N_M(j\omega)}{P_M(j\omega)} = R_M(\omega) + jI_M(\omega). \qquad (2-21)$$

Then the squared-matching-error function to be minimized is defined as:

$$\begin{aligned} E &= \int_0^{\omega_s/2} |M(j\omega) - H(j\omega)|^2 d\omega \\ &= \int_0^{\omega_s/2} \left| M(j\omega) - \frac{N_H(j\omega)}{P_H(j\omega)} \right|^2 d\omega. \end{aligned} \qquad (2-22)$$

To remove the non-linearity which results from differentiating E with respect to controller coefficients, $x_i, i = 0, 1, \ldots, m$ and y_i, $i = 1, 2, \ldots, n$, Eq. (2-22) is modified by including $|P_H(j\omega)|^2$ in the integrand as a weighting factor. The new weighted-squared-error function ε is

$$\begin{aligned} \varepsilon &= \int_0^{\omega_s/2} |P_H(j\omega)|^2 |M(j\omega) - H(j\omega)|^2 d\omega \\ &= \int_0^{\omega_s/2} |P_H(j\omega)M(j\omega) - N_H(j\omega)|^2 d\omega. \end{aligned} \qquad (2-23)$$

The weighting factor $|P_H(j\omega)|^2$ is nonzero for a stable system because for stability all roots of the characteristic equation must lie inside the unit circle in the z-plane.

Substitution of Eqs. (2-20)and (2-21) into Eq. (2-23) gives

$$\varepsilon = \int_0^{\omega_s/2} [(R_M(\omega)\sigma - I_M(\omega)\tau - \Phi)^2 + (R_M(\omega)\tau + I_M(\omega)\sigma - \Theta)^2] d\omega. \qquad (2-24)$$

The minimum of ε can be found by differentiating it with respect to the unknown controller coefficients x_i and y_i, and assigning the derivatives to zero, i.e.,

$$\frac{\partial \varepsilon}{\partial x_i} = 0, \qquad i = 0, 1, \ldots, m; \tag{2-25}$$

$$\frac{\partial \varepsilon}{\partial y_i} = 0, \qquad i = 1, 2, \ldots, n. \tag{2-26}$$

Hence from Eqs. (2-24),(2-25) and (2-26), $(m + n + 1)$ equations can be obtained:

$$\begin{aligned}\frac{\partial \varepsilon}{\partial x_i} &= \int_0^{\omega_s/2} 2(R_M(\omega)\sigma - I_M(\omega)\tau - \Phi)(R_M(\omega)\frac{\partial \sigma}{\partial x_i} - I_M(\omega)\frac{\partial \tau}{\partial x_i} - \frac{\partial \Phi}{\partial x_i})d\omega \\ &\quad + \int_0^{\omega_s/2} 2(R_M(\omega)\tau + I_M(\omega)\sigma - \Theta)(R_M(\omega)\frac{\partial \tau}{\partial x_i} + I_M(\omega)\frac{\partial \sigma}{\partial x_i} - \frac{\partial \Theta}{\partial x_i})d\omega \\ &= 0, \qquad i = 0, 1, \ldots, m;\end{aligned} \tag{2-27}$$

$$\begin{aligned}\frac{\partial \varepsilon}{\partial y_i} &= \int_0^{\omega_s/2} 2(R_M(\omega)\sigma - I_M(\omega)\tau - \Phi)(R_M(\omega)\frac{\partial \sigma}{\partial y_i} - I_M(\omega)\frac{\partial \tau}{\partial y_i})d\omega \\ &\quad + \int_0^{\omega_s/2} 2(R_M(\omega)\tau + I_M(\omega)\sigma - \Theta)(R_M(\omega)\frac{\partial \tau}{\partial y_i} + I_M(\omega)\frac{\partial \sigma}{\partial y_i})d\omega \\ &= 0 \qquad i = 1, 2, \ldots, n.\end{aligned} \tag{2-28}$$

The solution of these equations for the unknowns x_i and y_i is shown in matrix form as following:

$$\overline{\Gamma} = \overline{\Lambda}^{-1} \cdot \overline{\Upsilon}; \tag{2-29}$$

where,

$$\overline{\Gamma} = (\, x_0 \quad x_1 \quad x_2 \quad \ldots \quad x_i \quad \ldots \quad x_m \quad y_1 \quad y_2 \quad \ldots \quad y_i \quad \ldots \quad y_n \,)^{\top};$$

$$\overline{\Upsilon} = (\, L_0 \quad L_1 \quad L_2 \quad \ldots \quad L_i \quad \ldots \quad L_m \quad J_1 \quad J_2 \quad \ldots \quad J_i \quad \ldots \quad J_n \,)^{\top};$$

$$\overline{\Lambda} = \begin{pmatrix}
A_{00} & A_{01} & A_{02} & \cdots & A_{0i} & \cdots & A_{0m} & C_{01} & C_{02} & \cdots & C_{0i} & \cdots & C_{0n} \\
A_{01} & A_{00} & A_{12} & \cdots & A_{1i} & \cdots & A_{1m} & C_{11} & C_{12} & \cdots & C_{1i} & \cdots & C_{1n} \\
A_{02} & A_{12} & A_{00} & \cdots & A_{2i} & \cdots & A_{2m} & C_{21} & C_{22} & \cdots & C_{2i} & \cdots & C_{2n} \\
\vdots & \vdots & \vdots & \ddots & \vdots & \ddots & \vdots & \vdots & \vdots & \ddots & \vdots & \ddots & \vdots \\
A_{0i} & A_{1i} & A_{2i} & \cdots & A_{00} & \cdots & A_{im} & C_{i1} & C_{i2} & \cdots & C_{ii} & \cdots & C_{in} \\
\vdots & \vdots & \vdots & \ddots & \vdots & \ddots & \vdots & \vdots & \vdots & \ddots & \vdots & \ddots & \vdots \\
A_{0m} & A_{1m} & A_{2m} & \cdots & A_{im} & \cdots & A_{00} & C_{m1} & C_{m2} & \cdots & C_{mi} & \cdots & C_{mn} \\
C_{01} & C_{11} & C_{21} & \cdots & C_{i1} & \cdots & C_{m1} & B_{11} & B_{12} & \cdots & B_{1i} & \cdots & B_{1n} \\
C_{02} & C_{12} & C_{22} & \cdots & C_{i2} & \cdots & C_{m2} & B_{12} & B_{11} & \cdots & B_{2i} & \cdots & B_{2n} \\
\vdots & \vdots & \vdots & \ddots & \vdots & \ddots & \vdots & \vdots & \vdots & \ddots & \vdots & \ddots & \vdots \\
C_{0i} & C_{1i} & C_{2i} & \cdots & C_{ii} & \cdots & C_{mi} & B_{1i} & B_{2i} & \cdots & B_{11} & \cdots & B_{in} \\
\vdots & \vdots & \vdots & \ddots & \vdots & \ddots & \vdots & \vdots & \vdots & \ddots & \vdots & \ddots & \vdots \\
C_{0n} & C_{1n} & C_{2n} & \cdots & C_{in} & \cdots & C_{mn} & B_{1n} & B_{2n} & \cdots & B_{in} & \cdots & B_{11}
\end{pmatrix},$$

and

$$A_{ij} = \int_0^{\omega_s/2} [R_M^2(\omega) + I_M^2(\omega) - 2R_M(\omega) + 1](R_G^2(\omega) + I_G^2(\omega)) \cos((i-j)\omega T) d\omega,$$

$$B_{ij} = \int_0^{\omega_s/2} [R_M^2(\omega) + I_M^2(\omega)] \cos((i-j)\omega T) d\omega,$$

$$C_{ij} = \int_0^{\omega_s/2} [(R_M^2(\omega) + I_M^2(\omega) - R_M(\omega))R_G(\omega) - I_M(\omega)I_G(\omega)] \cos((i-j)\omega T) d\omega$$
$$+ \int_0^{\omega_s/2} [(R_M^2(\omega) + I_M^2(\omega) - R_M(\omega))I_G(\omega) + I_M(\omega)R_G(\omega)] \sin((i-j)\omega T) d\omega,$$

$$L_i = -\int_0^{\omega_s/2} [(R_M^2(\omega) + I_M^2(\omega) - R_M(\omega))R_G(\omega) - I_M(\omega)I_G(\omega)] \cos(i\omega T) d\omega$$
$$- \int_0^{\omega_s/2} [(R_M^2(\omega) + I_M^2(\omega) - R_M(\omega))I_G(\omega) + I_M(\omega)R_G(\omega)] \sin(i\omega T) d\omega,$$

$$J_i = -\int_0^{\omega_s/2} [R_M^2(\omega) + I_M^2(\omega)] \cos(i\omega T) d\omega.$$

The choice of the digital controller order mainly rests on the matching accuracy required and the computation time allowed. Data required for the design include m and n, the orders of the polynomials of a controller z-transfer function; $M(j\omega)$, the desired frequency response and $G_hG(z)$, the z-transfer function of the plant with a zero-order hold.

2.3.2 Numerical integration

The great number of integrations involved in solving Eq. (2-29) is one of the main

disadvantages of this method. In this study, these integrations are carried out by means of DCADRE, a numerical integration subroutine from the IMSL programme library [8]. Suppose $F(x)$ is the integral of $f(x)$ over the interval $[a, b]$. Then the DCADRE routine computes $F(x)$ as the sum of estimates for $F(x)$ over suitably chosen subintervals of $[a, b]$. Starting with $[a, b]$ as the first such subinterval, the cautious Romberg extrapolation calculates an acceptable estimate on it. If the result is not satisfactory, the subinterval is divided into two parts of equal length, each of which is then considered as a subinterval for a new estimate. This routine gives fairly accurate results but the computational burden is heavy. For instance, depending much on the behavior of integrands, the calculation of the coefficients for a 3rd-order controller transfer function may require $15 \sim 75$ seconds of CPU time on a VAX-11/780 digital computer.

2.3.3 Detrimental effect of the weighting factor

The effect of the weighting factor $|P_H(j\omega)|^2$ in Eq. (2-23) on the matching accuracy is ignored in Rattan's CCF method as he claimed [5] that the weighting factor was approximately equal to a constant times the absolute value of $P_M(j\omega)$, the denominator term in Eq. (2-21). Nevertheless, this assumption is not valid unless the sampling frequency is low relative to the bandwidth of a closed-loop system. As ω_s increases, the value of weighting factor $|P_H(j\omega)|^2$ in the low-frequency band becomes so small that the consequent deterioration of minimization could bring about considerable deviation in the frequency response matching. This is demonstrated by a numerical example taken from this author's studies.

Assume that the plant under design is

$$G(s) = \frac{100(s + 0.2)}{(s + 2)(s + 0.5 + j6)(s + 0.5 - j6)}; \qquad (2-30)$$

and the closed-loop frequency response model with $T_m = 0.5\ s$ is

$$M(j\omega) = \frac{0.103z + 0.028}{z^2 - 1.424z + 0.555}\Big|_{z=e^{j0.5\omega}}. \qquad (2-31)$$

where T_m denotes the sampling period of a discrete transfer function used as a model. A digital controller is then synthesized by the CCF method at three sampling periods $T = 0.1, 0.3, 0.5\ s$, respectively. The variation of $|P_H(j\omega)|^2$ and the corresponding closed-loop frequency response in each design are shown in Fig. 2-3, from which it is clear that the weighting factor $|P_H(j\omega)|^2$ significantly affects the matching accuracy of designs. In particular, at $T = 0.1\ s$, the value of $|P_H(j\omega)|^2$ reduces to about $-200db$ when $\omega < 0.5\ rad/s$, with the result that the closed-loop frequency response does not match the model at all.

In a later paper [6], Rattan commented further that the effect of $|P_H(j\omega)|^2$ could be easily eliminated, if desired, by dividing the integrand in Eq. (2-23) by $|P_M(j\omega)|^2$ from Eq. (2-21), i.e., by minimizing

$$\varepsilon_m = \int_0^{\omega_s/2} \frac{|P_H(j\omega)|^2}{|P_M(j\omega)|^2} |M(j\omega) - H(j\omega)|^2 d\omega. \qquad (2-32)$$

In the above example, however, it is observed that the ratio $\dfrac{|P_H(j\omega)|^2}{|P_M(j\omega)|^2}$ at $T = 0.1\ s$ is not a constant but varies from -160 to $-100\ db$. Furthermore, because the matching is conducted in terms of the ratio $\dfrac{N_H(j\omega)}{P_H(j\omega)}$ rather than $N_H(j\omega)$ and $P_H(j\omega)$ separately, $P_H(j\omega)$ does not necessarily converge to $P_M(j\omega)$ while minimizing the error $|M(j\omega) - H(j\omega)|$.

To overcome this deficiency in Rattan's CCF method, this author has developed successfully the iterative complex-curve fitting design method in an attempt to eliminate the error-producing effect of the weighting factor $|P_H(j\omega)|^2$. This is presented in the next section.

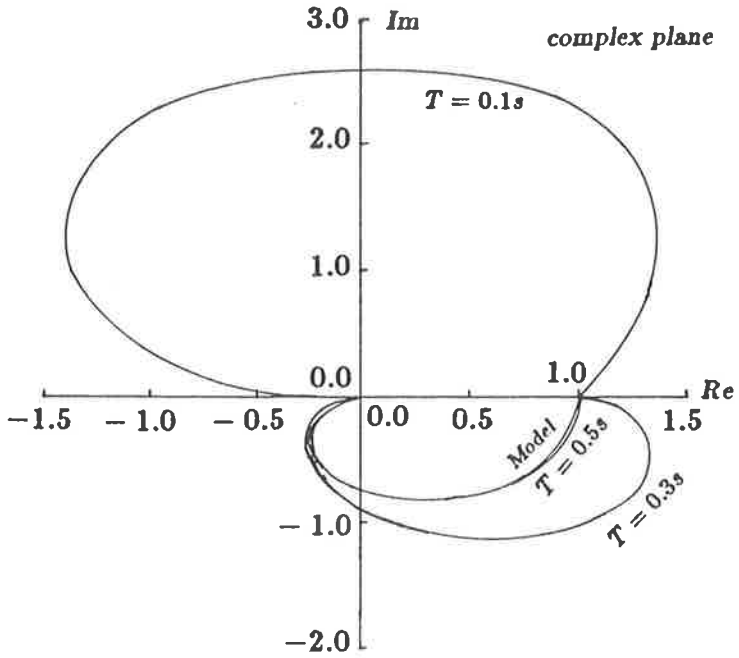

(1) Frequency responses of the closed-loop systems designed by Rattan's CCF method for sampling periods $T = 0.1, 0.3, 0.5$ s

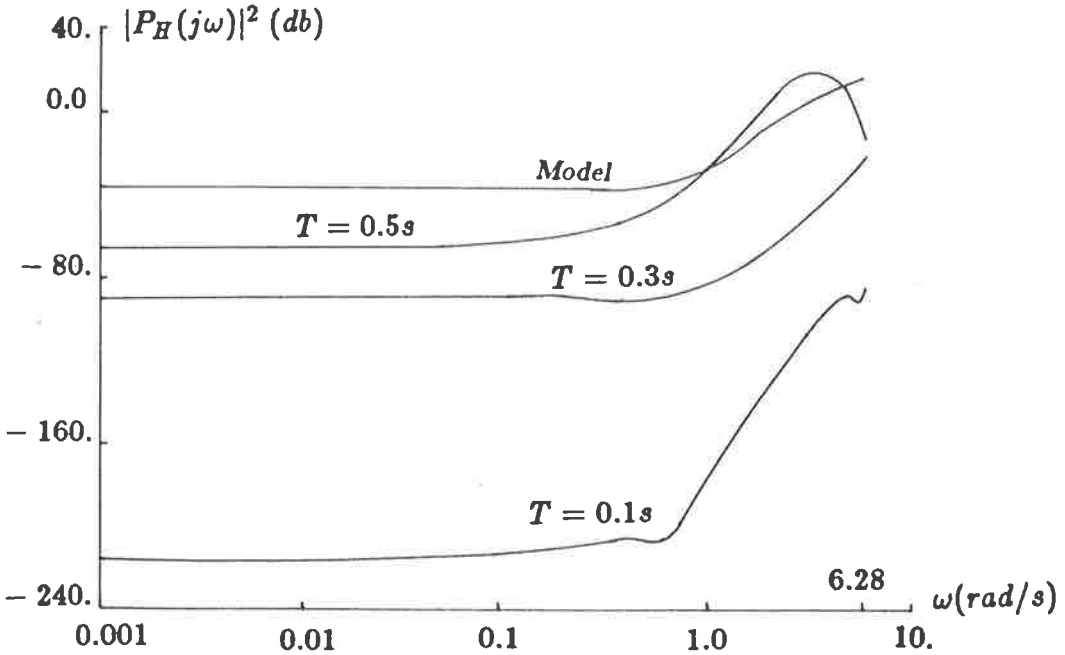

(2) Variation of the weighting factor $|P_H(j\omega)|^2$ as a function of T

Figure 2-3 Effect of the weighting factor $|P_H(j\omega)|^2$ in Rattan's CCF method on the accuracy of frequency matching

§2.4 Iterative Complex-Curve Fitting design method (ICCF)

2.4.1 Description of the ICCF method

On the basis of Rattan's complex-curve fitting design method, this author proposes an iterative algorithm aimed at eliminating the effect of the weighting factor $|P_H(j\omega)|^2$ in the error function Eq. (2-23) in order to reduce the matching error. The new method, called the Iterative Complex-Curve Fitting design method and abbreviated to ICCF, uses the transfer function synthesis technique of Sanathanan and Koerner [13].

Let e and e' denote the squared-error and the weighted-squared-error of matching, respectively:

$$\begin{aligned} e &= |M(j\omega) - H(j\omega)|^2 \\ &= \left| M(j\omega) - \frac{N_H(j\omega)}{P_H(j\omega)} \right|^2 ; \end{aligned} \tag{2-33}$$

$$\begin{aligned} e' &= |P_H(j\omega)|^2 \cdot e \\ &= |P_H(j\omega)M(j\omega) - N_H(j\omega)|^2. \end{aligned} \tag{2-34}$$

Thus the error function E in Eq. (2-22) and the weighted-error function ε in Eq. (2-23) may be rewritten as:

$$\begin{aligned} E &= \int_0^{\omega_s/2} |M(j\omega) - H(j\omega)|^2 d\omega \\ &= \int_0^{\omega_s/2} e \ d\omega; \end{aligned} \tag{2-35}$$

$$\begin{aligned} \varepsilon &= \int_0^{\omega_s/2} |P_H(j\omega)M(j\omega) - N_H(j\omega)|^2 d\omega \\ &= \int_0^{\omega_s/2} e' \ d\omega. \end{aligned} \tag{2-36}$$

If $P_H(j\omega)$ is known, the weighted-error e' can be divided by $|P_H(j\omega)|^2$ so that e' becomes the true error e. But this is impossible because $P_H(j\omega)$ is unknown until the computation is completed. By an iterative process, however, the currently unknown $P_H(j\omega)$ can be approximated from the previous computation result and hence its effect

can be eliminated. In this approach, a new squared-error $e^{*(k)}$ is defined as:

$$e^{*(k)} = \frac{|P_H^{(k)}(j\omega)|^2}{|P_H^{(k-1)}(j\omega)|^2}|M(j\omega) - H^{(k)}(j\omega)|^2; \qquad (2-37)$$

and the corresponding error function $\varepsilon^{*(k)}$ is

$$\begin{aligned}\varepsilon^{*(k)} &= \int_0^{\omega_s/2} e^{*(k)} d\omega \\ &= \int_0^{\omega_s/2} \frac{|P_H^{(k)}(j\omega)|^2}{|P_H^{(k-1)}(j\omega)|^2}|M(j\omega) - H^{(k)}(j\omega)|^2 d\omega;\end{aligned} \qquad (2-38)$$

where the superscript k is the number of the iteration.

Obviously $\varepsilon^{*(k)}$ approaches the true error function E when $P_H^{(k)}(j\omega)$ closes to $P_H^{(k-1)}(j\omega)$, if $P_H(j\omega)$ converges. In other words, the minimum of the matching error function E is reached as the weighting factor $|P_H^{(k)}(j\omega)|^2$ is effectively cancelled by $|P_H^{(k-1)}(j\omega)|^2$.

Based on the new error function $\varepsilon^{*(k)}$ of Eq. (2-38), a set of linear equations (Eq. (2-39)) for the controller coefficients at the kth-iteration, $x_i^{(k)}, i = 0, 1, \ldots, m$ and $y_i^{(k)}, i = 1, 2, \ldots, n$, can be derived by following a similar analysis to that carried out in equations (2-23) to (2-29) of the previous section.

$$\overline{\Gamma} = \overline{\Lambda}^{-1} \cdot \overline{\Upsilon}; \qquad (2-39)$$

where,

$$\overline{\Gamma} = \left(x_0^{(k)} \quad x_1^{(k)} \quad x_2^{(k)} \quad \ldots \quad x_i^{(k)} \quad \ldots \quad x_m^{(k)} \quad y_1^{(k)} \quad y_2^{(k)} \quad \ldots \quad y_i^{(k)} \quad \ldots \quad y_n^{(k)} \right)^{\top};$$

$$\overline{\Upsilon} = (L_0 \quad L_1 \quad L_2 \quad \ldots \quad L_i \quad \ldots \quad L_m \quad J_1 \quad J_2 \quad \ldots \quad J_i \quad \ldots \quad J_n)^{\top};$$

$$\overline{\Lambda} = \begin{pmatrix}
A_{00} & A_{01} & A_{02} & \cdots & A_{0i} & \cdots & A_{0m} & C_{01} & C_{02} & \cdots & C_{0i} & \cdots & C_{0n} \\
A_{01} & A_{00} & A_{12} & \cdots & A_{1i} & \cdots & A_{1m} & C_{11} & C_{12} & \cdots & C_{1i} & \cdots & C_{1n} \\
A_{02} & A_{12} & A_{00} & \cdots & A_{2i} & \cdots & A_{2m} & C_{21} & C_{22} & \cdots & C_{2i} & \cdots & C_{2n} \\
\vdots & \vdots & \vdots & \ddots & \vdots & \ddots & \vdots & \vdots & \vdots & \ddots & \vdots & \ddots & \vdots \\
A_{0i} & A_{1i} & A_{2i} & \cdots & A_{00} & \cdots & A_{im} & C_{i1} & C_{i2} & \cdots & C_{ii} & \cdots & C_{in} \\
\vdots & \vdots & \vdots & \ddots & \vdots & \ddots & \vdots & \vdots & \vdots & \ddots & \vdots & \ddots & \vdots \\
A_{0m} & A_{1m} & A_{2m} & \cdots & A_{im} & \cdots & A_{00} & C_{m1} & C_{m2} & \cdots & C_{mi} & \cdots & C_{mn} \\
C_{01} & C_{11} & C_{21} & \cdots & C_{i1} & \cdots & C_{m1} & B_{11} & B_{12} & \cdots & B_{1i} & \cdots & B_{1n} \\
C_{02} & C_{12} & C_{22} & \cdots & C_{i2} & \cdots & C_{m2} & B_{12} & B_{11} & \cdots & B_{2i} & \cdots & B_{2n} \\
\vdots & \vdots & \vdots & \ddots & \vdots & \ddots & \vdots & \vdots & \vdots & \ddots & \vdots & \ddots & \vdots \\
C_{0i} & C_{1i} & C_{2i} & \cdots & C_{ii} & \cdots & C_{mi} & B_{1i} & B_{2i} & \cdots & B_{11} & \cdots & B_{in} \\
\vdots & \vdots & \vdots & \ddots & \vdots & \ddots & \vdots & \vdots & \vdots & \ddots & \vdots & \ddots & \vdots \\
C_{0n} & C_{1n} & C_{2n} & \cdots & C_{in} & \cdots & C_{mn} & B_{1n} & B_{2n} & \cdots & B_{in} & \cdots & B_{11}
\end{pmatrix},$$

and

$$A_{ij} = \int_0^{\omega_s/2} \frac{1}{|P_H^{(k-1)}(j\omega)|^2}(R_M^2(\omega) + I_M^2(\omega) - 2R_M(\omega) + 1)$$

$$(R_G^2(\omega) + I_G^2(\omega))\cos((i-j)\omega T)d\omega,$$

$$B_{ij} = \int_0^{\omega_s/2} \frac{1}{|P_H^{(k-1)}(j\omega)|^2}[R_M^2(\omega) + I_M^2(\omega)]\cos((i-j)\omega T)d\omega,$$

$$C_{ij} = \int_0^{\omega_s/2} \frac{1}{|P_H^{(k-1)}(j\omega)|^2}[(R_M^2(\omega) + I_M^2(\omega) - R_M(\omega))R_G(\omega) - I_M(\omega)I_G(\omega)]$$

$$\cos((i-j)\omega T)d\omega + \int_0^{\omega_s/2} \frac{1}{|P_H^{(k-1)}(j\omega)|^2}$$

$$[(R_M^2(\omega) + I_M^2(\omega) - R_M(\omega))I_G(\omega) + I_M(\omega)R_G(\omega)]\sin((i-j)\omega T)d\omega,$$

$$L_i = -\int_0^{\omega_s/2} \frac{1}{|P_H^{(k-1)}(j\omega)|^2}[(R_M^2(\omega) + I_M^2(\omega) - R_M(\omega))R_G(\omega) - I_M(\omega)I_G(\omega)]$$

$$\cos(i\omega T)d\omega - \int_0^{\omega_s/2} \frac{1}{|P_H^{(k-1)}(j\omega)|^2}$$

$$[(R_M^2(\omega) + I_M^2(\omega) - R_M(\omega))I_G(\omega) + I_M(\omega)R_G(\omega)]\sin(i\omega T)d\omega,$$

$$J_i = -\int_0^{\omega_s/2} \frac{1}{|P_H^{(k-1)}(j\omega)|^2}[R_M^2(\omega) + I_M^2(\omega)]\cos(i\omega T)d\omega;$$

the superscript k for all A, B, C, L and J is left out for simplicity.

Note that, except for the factor $|P_H^{(k-1)}(j\omega)|^2$ in the denominator of every integrand, Eq. (2-39) is very similar to Eq. (2-29). Let $N_G(j\omega)$ be the numerator of $G_hG(j\omega)$ and $P_G(j\omega)$ the denominator, i.e.,

$$G_hG(j\omega) = \frac{N_G(j\omega)}{P_G(j\omega)}. \tag{2-40}$$

$P_H^{(k-1)}(j\omega)$ can be then expressed as:

$$\begin{aligned} P_H^{(k-1)}(j\omega) =& (x_0^{(k-1)}z^m + x_1^{(k-1)}z^{m-1} + \cdots + x_{m-1}^{(k-1)}z + x_m^{(k-1)}) \cdot N_G(j\omega) \\ &+ (z^n + y_1^{(k-1)}z^{n-1} + \cdots + y_{n-1}^{(k-1)}z + y_n^{(k-1)}) \cdot P_G(j\omega)\Big|_{z=e^{j\omega T}} \end{aligned} \tag{2-41}$$

where, $x_i^{(k-1)}$, $i = 0, 1, \ldots, m$ and $y_i^{(k-1)}$, $i = 1, 2, \ldots, n$ are the known controller coefficients obtained from the $(k-1)$th-iteration.

The initial estimate of $P_H^{(k)}(j\omega)$, namely $P_H^{(0)}(j\omega)$, is assigned to unity. From Eq. (2-38), the error function $\epsilon^{*(k)}$ at $k = 1$ is

$$\begin{aligned} \epsilon^{*(1)} &= \int_0^{\omega_s/2} |P_H^{(1)}(j\omega)|^2 |M(j\omega) - H^{(1)}(j\omega)|^2 d\omega \\ &= \int_0^{\omega_s/2} |P_H^{(1)}(j\omega)M(j\omega) - N_H^{(1)}(j\omega)|^2 d\omega, \end{aligned} \tag{2-42}$$

which is the same as the weighted-squared-error function ϵ in Eq. (2-23). Hence the result of the first iteration is identical to that of Rattan's CCF method.

The number of iterations is determined by the desired matching accuracy and the convergency of $P_H^{(k)}(j\omega)$ to $P_H^{(k-1)}(j\omega)$. In this study, WIAE, a weighted integral absolute error criterion, defined in Eq. (4-5) of section 4.1, is used to assess the matching performance. At kth-iteration, $\text{WIAE}^{(k)}$ is calculated and compared with a specified value for the matching error criterion, say $\epsilon = 0.01$. If $\text{WIAE}^{(k)} \leq \epsilon$, the values of $x_i^{(k)}$, $i = 0, 1, \ldots, m$ and $y_i^{(k)}$, $i = 1, 2, \ldots, n$ are an ideal solution for the coefficients of the controller transfer function; if $\text{WIAE}^{(k)} > \epsilon$, then compare $\text{WIAE}^{(k)}$ with the previous result $\text{WIAE}^{(k-1)}$. When the kth-iteration makes some improvement, i.e., $\text{WIAE}^{(k)} < \text{WIAE}^{(k-1)}$, the values of $x_i^{(k)}$ and $y_i^{(k)}$ are used to evaluate $P_H^{(k)}(j\omega)$ for

the next iteration. Otherwise $P_H(j\omega)$ fails to converge and the values of $x_i^{(k)}$ and $y_i^{(k)}$ should be taken as the most accurate results available. Note that in any case the result of the ICCF method will not be less accurate than that of Rattan's CCF method.

2.4.2 Numerical examples

The iterative complex-curve fitting design method has been tested for a number of design studies in Chapter IV and proved to be one of the most accurate methods. In particular, the examples considered in section 2.3.3 are redesigned by this new method. After just two iterations, the matching errors of the closed-loop systems designed by Rattan's CCF method at $T = 0.1$ and 0.3 s (see Fig. 2-3) are considerably reduced. For $T = 0.5$ s, at which the matching error of CCF's design is insignificant, the result of the ICCF method is close to that of the CCF method. Figure 2-4 shows the frequency responses of the closed-loop systems designed by the ICCF method, together with that of the model $M(j\omega)$.

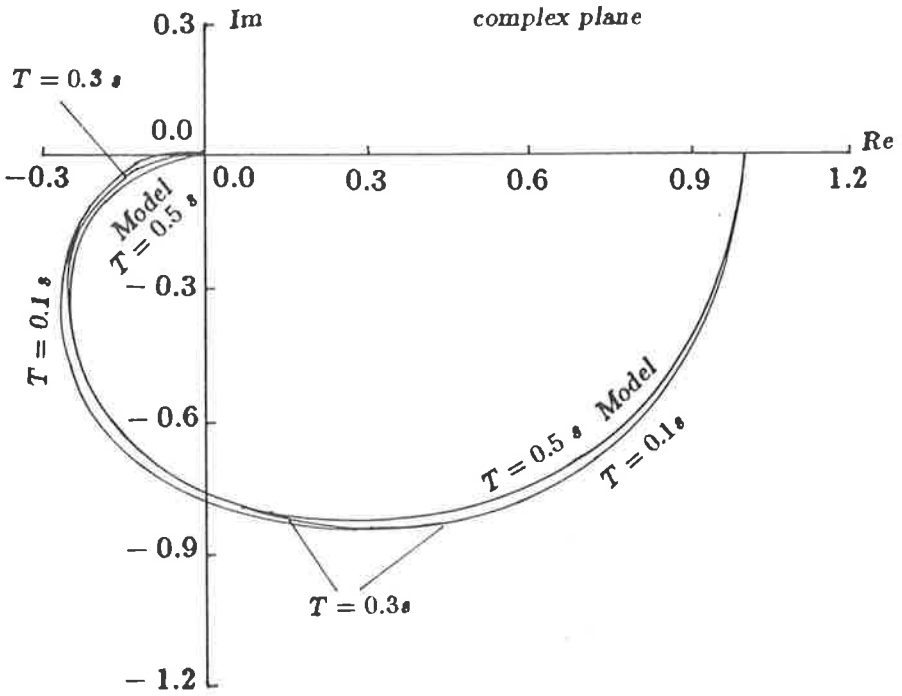

Figure 2-4 Frequency responses of the closed-loop systems designed by the ICCF method

$$\left(\textit{Plant: } G(s) = \frac{100(s+0.2)}{(s+2)(s+0.5+j6)(s+0.5-j6)};\ \textit{Model: } M(j\omega) = \frac{0.103z+0.028}{z^2-1.424z+0.555}\Big|_{z=e^{j0.5\omega}}.\right)$$

§2.5 SIMplex optimization-based design method (SIM)

2.5.1 Control system design via non-linear programming

Non-linear programming is an optimization technique. It has been applied extensively to solve the problem of determining a set of parameters such that the objective function is minimized or maximized, possibly subject to a set of constraints. This objective function and the constraints may be non-linear with respect to the set of parameters.

It is interesting to note that the crux of the frequency matching design methods, such as CCF and ICCF, is the determination of a set of discrete transfer function coefficients, which are optimal in the sense that the matching error function is minimized. These coefficients, namely x_i and y_i in Eq. (2-1), may be subject to constraints that ensure, e.g.,

a) the designed controller is open-loop stable;

b) there is an upper limit on the controller gain;

c) there is no severe oscillation in the controller output signal; etc.

Furthermore, both the error function and constraints are non-linear functions of the controller coefficients. These considerations therefore suggest the possibility of formulating the digital controller design problem as a non-linear programming with constraints.

This approach has been developed in this thesis. The author formulated the non-linear programming problem for the design of z-transfer function of a digital controller, devised the solutions using two optimization algorithms, and assessed these new design methods with the aid of a number of numerical examples. The optimization algorithms used are the simplex method for function minimization and the random searching optimization method.

The new optimization-based methods for the design of digital controllers have

some unique advantages. The significant one compared with the previously discussed methods is that the open-loop stability of a designed controller is guaranteed. Moreover, they offer the facility of including design specifications additional to the frequency response model in the design. These features are implemented by incorporating the appropriate non-linear constraints into the non-linear programming problem.

Of the two optimization algorithms, the simplex method has been proved experimentally to be feasible for and capable of coping with some typical digital controller design tasks (see Chapter IV). It shows superiority over the other methods especially when constraints on a controller output are required. The associated computation time is longer than DDM's, comparable with CCF's and shorter than ICCF's. In contrast with the simplex method, for the same design examples, the random searching optimization method gives inferior accuracy, fails to converge to the minimum in most cases, and imposes a very heavy computational load. Therefore, this method is not recommended for design purposes. It is considered, however, in the next section for sake of completeness because it has been discussed frequently in the literature over the last two years, mainly in the application of time and frequency response matching technique to model simplification problems.

In the remainder of this section, the non-linear programming for the design of a digital controller is formulated first. Then a description of the simplex optimization method will be given, followed by its application to the design of digital controllers.

2.5.2 Formulation of the non-linear programming problem

Suppose that a frequency response $M_Q(j\omega)$ is defined at a set of frequency points ω_i, $i = 1, 2, \ldots, N$, as a desired system open-loop frequency response. The frequency response of an open-loop control system is

$$Q(j\omega) = D(z)G_hG(z)\Big|_{z=e^{j\omega T}}. \qquad (2-43)$$

Instead of the polynomial form of Eq. (2-1), the controller transfer function $D(z)$ is expressed in terms of zeros and poles:

$$D(z) = \frac{x_0(z-z_1)(z-z_2)\cdots(z-z_m)}{(z-p_1)(z-p_2)\cdots(z-p_n)}, \qquad (2-44)$$

where, z_i, $i = 1, 2, \ldots, m$ are zeros and p_i, $i = 1, 2, \ldots, n$ are poles.

Before the objective function is defined, an obstacle in scaling has to be removed for the reason that complex numbers are represented in terms of their magnitudes and phase angles (in degrees). In general, for frequency response of control systems, the range of the magnitude variation is much larger than that of the phase angle variation. Consequently the value of magnitude may be either too heavily weighted or insignificant when included with the value of phase angle in the summation in the error function. The decibel value of the magnitude of a complex number, therefore, is used to replace its normal value. For $Q(j\omega)$, the scaled magnitude is $\vartheta_Q(\omega)$, defined as:

$$\vartheta_Q(\omega) = 20\log_{10}|Q(j\omega)|. \qquad (2-45)$$

Similarly the scaled magnitude of $M_Q(j\omega)$ is

$$\vartheta_{M_Q}(\omega) = 20\log_{10}|M_Q(j\omega)|. \qquad (2-46)$$

Based on the above definitions, the error function, or the objective function, E, can be defined over all N selected frequency points as:

$$E = \sum_{i=1}^{N} \sqrt{[\vartheta_Q(\omega_i) - \vartheta_{M_Q}(\omega_i)]^2 + [\psi_Q(\omega_i) - \psi_{M_Q}(\omega_i)]^2}, \qquad (2-47)$$

where, ψ_Q and ψ_{M_Q} are the phase angle of $Q(j\omega)$ and $M_Q(j\omega)$ in degrees, respectively.

Next, consider appropriate constraints to ensure that the closed-loop system is stable. In this analysis, it is assumed that the plant under design is open-loop stable and the Nyquist plot does not encircle the $(-1, j0)$ point in the $D(z)G_hG(z)$-plane.

Thus, according to the Nyquist stability criterion for digital control systems [1], the closed-loop system is stable if the poles of D(z) satisfy:

$$|p_i| \leq 1, \qquad i = 1, 2, \ldots, n \tag{2-48}$$

In other words, none of p_i, $i = 1, 2, \ldots, n$ is outside the unit circle in the z-plane.

The combination of equations from (2-43) to (2-48) formulates the desired non-linear programming problem for the design of digital controllers as follows:

Minimize

$$\begin{aligned} E &= \sum_{i=1}^{N} \sqrt{[\vartheta_Q(\omega_i) - \vartheta_{M_Q}(\omega_i)]^2 + [\psi_Q(\omega_i) - \psi_{M_Q}(\omega_i)]^2} \\ &= f(x_0; z_1, z_2, \ldots, z_m; p_1, p_2, \ldots, p_n) \end{aligned} \tag{2-49}$$

subject to the non−linear constraints

$$|p_i| \leq 1, \qquad i = 1, 2, \ldots, n.$$

It is rather difficult to solve this non-linear programming problem directly because of the constraints imposed. Fortunately, these constraints may be removed by means of the following transformations in which λ is an auxiliary optimization variable. For poles:

$$\begin{cases} p_{i,i+1} = \mu_p e^{-|\lambda_i|} \cdot e^{\pm j\nu_p \pi e^{-|\lambda_{i+1}|}}, & \text{for a pair of complex conjugate poles;} \\ p_i = \mu_p e^{-|\lambda_i|} - \nu_p, & \text{for a real pole.} \end{cases} \tag{2-50}$$

Similarly, zeros are formed as follows:

$$\begin{cases} z_{i,i+1} = \mu_z e^{-|\lambda_i|} \cdot e^{\pm j\nu_z \pi e^{-|\lambda_{i+1}|}}, & \text{for a pair of complex conjugate zeros;} \\ z_i = \mu_z e^{-|\lambda_i|} - \nu_z, & \text{for a real zero.} \end{cases} \tag{2-51}$$

For a gain x_0, which is always a positive real number,

$$x_0 = \mu_g e^{-|\lambda_0|}. \tag{2-52}$$

In the transformations (2-50), (2-51) and (2-52), the parameters μ_p, μ_z, μ_g and ν_p, ν_z are real numbers which enable a designer to impose the desired constraints on the gain, poles and zeros of $D(z)$. The constraints in Eq. (2-49), for example, can be implemented by setting $\mu_p = \nu_p = 1$ for a pair of complex poles, or $\mu_p = 2$, $\nu_p = 1$ for a pole on the real axis. Thus when λ assumes values from $-\infty$ to $+\infty$, p_i, $i = 1, 2, \ldots, n$, lie on or within the unit circle in the z-plane.

For m zeros, n poles and a gain, there is a total of $(m+n+1)$ auxiliary variables λ_i, $i = 0, 1, \ldots, m+n$. Hence, with the aid of the above transformations, the non-linear programming problem with constraints defined in Eq. (2-49) can be transformed into one free of constraints:

Minimize

$$E = \sum_{i=1}^{N} \sqrt{[\vartheta_Q(\omega_i) - \vartheta_{M_Q}(\omega_i)]^2 + [\psi_Q(\omega_i) - \psi_{M_Q}(\omega_i)]^2} \qquad (2-53)$$

$$= F(\lambda_0, \lambda_1, \ldots, \lambda_{m+n}),$$

where $-\infty \leq \lambda_j \leq +\infty$, $j = 0, 1, \ldots, m+n$.

The optimal values λ_i^*, $i = 0, 1, \ldots, m+n$ indirectly determine the required controller coefficients. The formulation of the objective function $F(\lambda_0, \lambda_1, \ldots, \lambda_{m+n})$ is described in Appendix A.

2.5.3 Simplex method for function minimization

The simplex method, abbreviated to "SIM" for short, is a standard optimization algorithm for solving a variety of non-linear programming problems. Nelder and Mead first proposed this method in 1964 [12] based on the original idea of Spendley *et.al* [15]. Since then it has been widely used. Unlike the gradient optimization techniques, which require the derivatives of an objective function, there is no need for any such mathematical derivations in the SIM method. This is a significant advantage because often the analytic derivative of an objective function is very tedious, if not unavailable.

Since the simplex method has been explained in many standard textbooks on the subject of optimization [28, 29], only a brief description of SIM is presented. For simplicity, a two-dimensional (2-D) non-linear programming problem is used to illustrate the concept; the extension to higher-dimensional problems is straightforward. A flow chart for the simplex method for n-D problem is shown in Fig. 2-5.

In optimization techniques, the *simplex* in n-D space is defined as the figure formed by $n+1$ vertices; the vectors connecting each pair of the vertices are linearly independent. In 2-D space, for instance, the simplex is a triangle.

The most important information for solving a minimization problem is the variation of objective function values in a space. If the directions of such variation can be approximated from comparison of function values at different vertices of a simplex, then the better solution may be obtained along the direction which leads to a reduction in the value of the objective function. This is the essence of the simplex method.

Suppose that the objective functin E in 2-D space is to be minimized, i.e.,

$$\text{Minimize} \qquad E = f(\chi), \qquad \chi \in R^2. \tag{2-54}$$

Take three vertices in R^2, V_0, V_1, V_2, to define the current simplex, which is a triangle as described in Fig. 2-6. Calculate the values of E at these points and compare the results. Call the maximum value, say E_2, E_{max} and the minimum value, say E_0, E_{min}. Denote the corresponding vertices as V_{max} and V_{min}, respectively. Furthermore, $\overline{V}$ is defined as the centroid of the vertices excluding V_{max} and $\overline{V_iV_j}$ as the vector from V_i to V_j.

Three operations, *reflection, expansion* and *contraction*, are introduced to find a new vertex to replace the "worst" vertex V_{max}. Usually, there is good reason to assume that a "better" point lies opposite V_{max}. Such a point, denoted by V_r, can be obtained by the *reflection* defined as:

$$V_r = (1+\alpha)\overline{V} - \alpha V_{max}, \tag{2-55}$$

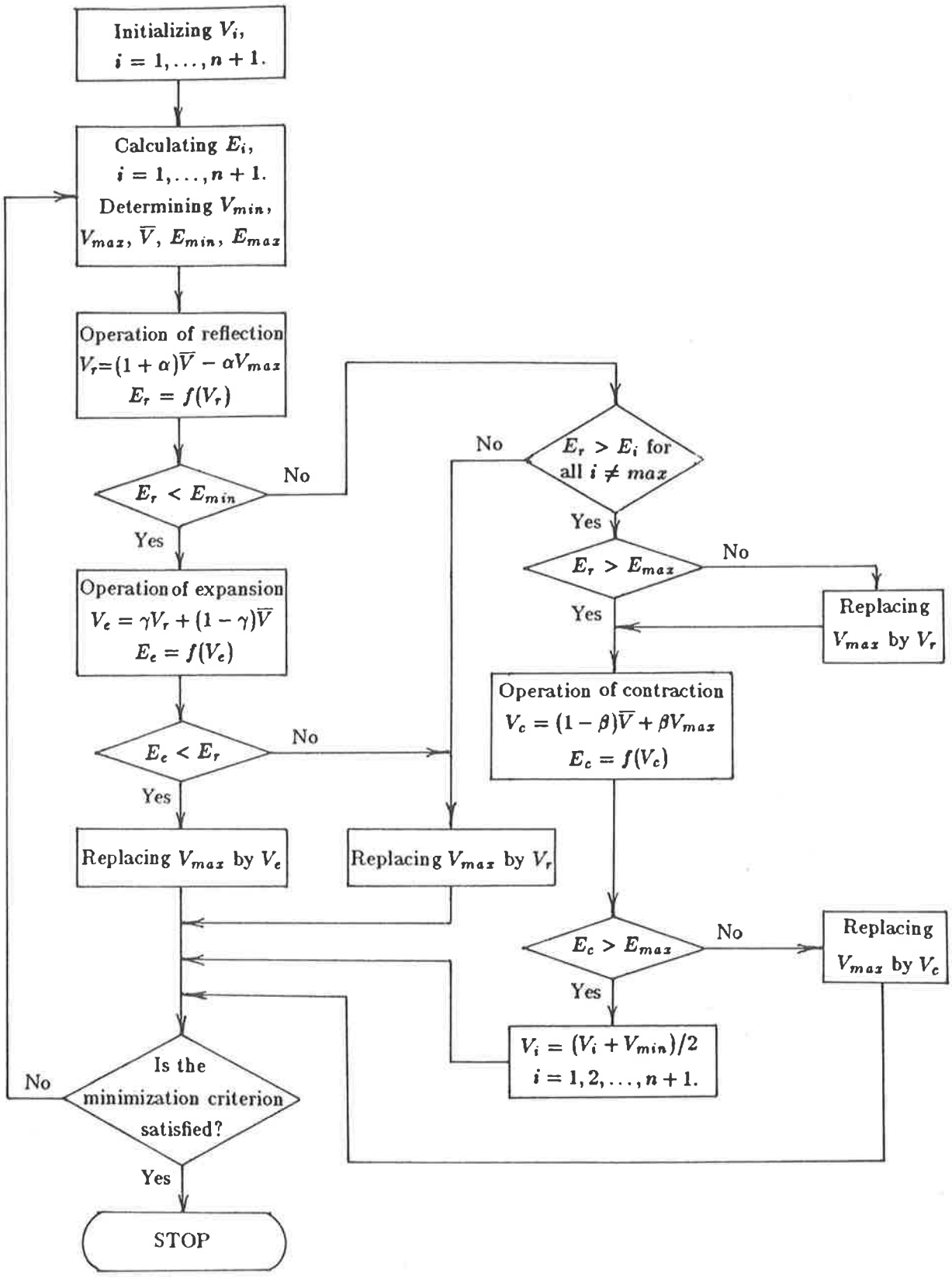

Figure 2-5 Flow chart for the simplex optimization method

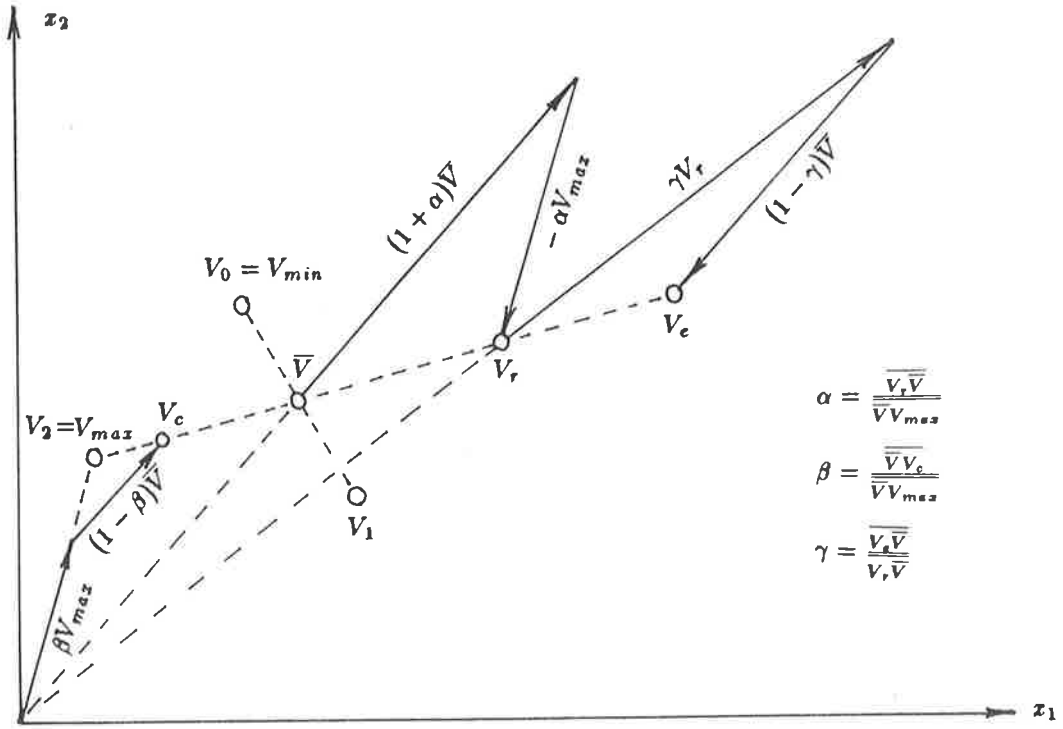

Figure 2-6 Illustration of the simplex method in the 2-dimensional case

where, α is the reflection coefficient, $\alpha > 0$.

Fig. 2-6 shows V_r lying on the extension line of the vector $\overline{V_{max}\overline{V}}$. The distance of $\overline{\overline{V}V_r}$ is dependent on the value of α.

The function value at V_r, namely E_r, will fall into three possible ranges:

(1) $E_{min} \leq E_r \leq E_i$ for any $i \neq \begin{cases} min \\ max \end{cases}$.

Replace V_{max} by V_r so that V_{min}, V_1 and V_r will form a new simplex for subsequent calculations.

(2) $E_r < E_{min}$.

Since V_r gives the "best" point, it may be beneficial to search further in this direction by "expanding" V_r to V_e:

$$V_e = \gamma V_r + (1-\gamma)\overline{V}, \qquad (2-56)$$

where, γ is the *expansion* coefficient, $\gamma > 1$.

V_e is on the extended line of $\overline{\overline{V}V_r}$ as illustrated in Fig 2-6; γ is the ratio of $|\overline{V_e\overline{V}}|$ to $|\overline{\overline{V}V_r}|$. Calculate E_e and form a new simplex of V_{min}, V_1 and V_e if E_e is smaller than E_r. Otherwise the expansion fails and V_{max} is replaced by V_r for the next iteration.

(3) $E_r > E_i$ for all $i \neq max$.

Assign a new V_{max} to be either the original V_{max} or V_r, whichever has the smaller value of E. Then the ***contraction*** coefficient β is used to find the new vertex V_c:

$$V_c = \beta V_{max} + (1-\beta)\overline{V}, \qquad (2-57)$$

with $0 < \beta < 1$.

It is apparent from Fig. 2-6 that V_c is on the straight line between V_{max} and $\overline{V}$. If the contraction is successful, i.e., $E_c < E_{max}$, V_{max} is replaced by V_c in a new simplex. On the other hand, if $E_c \geq E_{max}$, the size of the searching region has to be reduced by replacing all the vertices V_i by $(V_i + V_{min})/2$. The next iteration will start with this new simplex.

The criterion to terminate the process can be one of the followings:

a) a limit on the number of iterations;

b) a limit on the computation time;

c) a desired minimum value,

$$\sum_{i=0}^{n}(E_i - E_{min})^2 < \epsilon, \qquad (2-58)$$

where, ϵ is some specified small number;

d) a lower limit on the size of searching region,

$$|V_i - V_{min}| < S_{min}, \qquad \text{for all } i = 0, 1, \ldots, n, \qquad (2-59)$$

where S_{min} is a specified value.

There is no unique formula for the determination of values of α, β and γ. The author suggests using $\alpha = 1.0$, $\beta = 1.2$ and $\gamma = 0.8$ at the beginning of the experiment. These values may be adjusted later, depending on the optimization process.

Note that at the beginning of optimization, only one vertex V_0 in n-D space needs to be specified by the user. To form a simplex, the other n vertices V_1–V_n are determined from:

$$\begin{cases} r_{ij} = r_{0j}, & \text{if } i \neq j; \\ r_{ij} = r_{0j} + \Delta, & \text{if } i = j; \end{cases} \qquad (2-60)$$
$$i, j = 1, 2, \ldots, n-1, n;$$

where, r_{ij}, $j = 1, 2, \ldots, n$, are the dimensional values of the ith-vertex; Δ is a constant which decides the initial size of simplex and has more significant effect on the convergency and accuracy of optimization than α, β and γ do. From the author's experience, the appropriate value of Δ may vary from 0.7 to 4.5.

Usually as optimization proceeds, the size of a simplex reduces very quickly. Consequently the simplex may become too small before the optimum is found. To avoid this problem, the computer programme in this thesis is designed such that after a number of iterations, say 300, the optimization process will automatically start all over again, with a new simplex in which V_0 is V_{min} in the last iteration and the other n vertices determined by Eq.(2-60). By keeping the simplex under search to a reasonable size, both the convergency and efficiency of the SIM method are remarkably improved.

2.5.4 Application to the design of digital controllers

The simplex method is an optimization algorithm suitable for minimizing a function of n variables without constraints. Note that objective function in Eq. (2-53) formulated for the design of a digital controller is just this type of function. The simplex method, therefore, is applied to solving Eq. (2-53) for the parameters of the digital controller. Since the optimization process is accomplished by a digital computer, the

task of a designer mainly rests on the initialization of design problems, which is to be explained in this section.

Assume that a frequency response model $M_Q(j\omega)$ and the open-loop frequency response $G_hG(j\omega)$ of a plant with a ZOH are given. The formulation of the objective function $E = F(\lambda)$ in Eq. (2-53) is dependent on the pole-zero configuration of $D(z)$, the discrete transfer function of a digital controller. In Eq. (2-44), there is no constraint imposed on the type of poles and zeros of $D(z)$. For instance, for a 3rd-order controller, $D(z)$ may possess 3 real zeros, 1 real pole and a pair of complex conjugate poles; or 1 real zero, a pair of complex zeros and 3 real poles; etc. In this thesis, the configuration of $D(z)$ with 3 real poles and 3 real zeros is adopted for simplicity. Bear it in mind that the poles and zeros of $D(z)$ are the open-loop poles and zeros of the system under design. Thus, in terms of auxiliary variable λ, $D(z)$ may be written as:

$$D(z) = \frac{x_0(z-z_1)(z-z_2)(z-z_3)}{(z-p_1)(z-p_2)(z-p_3)}$$

$$= \frac{(\mu_g e^{-|\lambda_0|})[z-(\mu_z e^{-|\lambda_1|}-\nu_z)][z-(\mu_z e^{-|\lambda_2|}-\nu_z)][z-(\mu_z e^{-|\lambda_3|}-\nu_z)]}{[z-(\mu_p e^{-|\lambda_4|}-\nu_p)][z-(\mu_p e^{-|\lambda_5|}-\nu_p)][z-(\mu_p e^{-|\lambda_6|}-\nu_p)]} \quad (2-61)$$

To start the optimization process, one needs to provide 3 sets of initial values and parameters. They are: (1) initial estimates for the gain, poles and zeros of $D(z)$; (2) the constraints imposed on the gain and pole-zero locations; (3) the selected frequency points ω_i, $i = 1, 2, \ldots, N$.

Choosing the initial gain, poles and zeros of $D(z)$ closer to the optimum is always desirable, as they enable an objective function to converge to the minimum quickly and accurately. The better estimates can be achieved based on the designer's experience and knowledge of plant dynamics. Nevertheless, it is increasingly difficult when the order of a system becomes high. Hence the author suggests an alternative in which the designer may use the DDM method to compensate the plant, and then supply the resulting gain, poles and zeros of $D(z)$ to the optimization process as initial estimates. Because the

computational load of the DDM method is negligible relative to that of optimization-based methods, this combination of the analytic and optimization methods is faster and more accurate. If the DDM method results in some gain or poles or zeros outside the constraints imposed, reassignment is needed to return those parameters to positions within the required regions.

Furthermore, if the optimization algorithm has no strict requirements on initial estimates, one may simply start the optimization process with some arbitrarily-assigned initial estimates. In this thesis, for example, the SIM method is assessed in a number of designs (see sections 4.2 and 4.4) with arbitrarily-assigned 3 poles and 3 zeros, which are all at the same point of $(0.5, j0)$ in the z-plane. All the results of these designs are satisfactory as far as the optimization process is concerned.

Finally it should be pointed out that the computer programme developed in this thesis only requires the values of initial gain, poles and zeros. These values are then converted to the corresponding auxiliary variables λ_i in Eq. (2-53) at the beginning of optimizing iterations.

The parameters for setting the constraints on the gain, poles and zeros of $D(z)$ are μ_g, μ_p, μ_z and ν_p, ν_z. In addition to the system stability, which requires that the poles of $D(z)$ locate within the unit circle, the system dynamic performance may be improved also by further constraining the poles and zeros within some specified areas in the z-plane. Moreover, the upper limit on a controller gain can be readily implemented in a design by selecting an appropriate value of μ_g. More details about the selection of constraints are given in section 4.2.1 with the aid of a numerical example.

Let L_l and L_u be the lower limit and upper limit of real poles and zeros, respectively, the values of μ and ν are then calculated from:

$$\begin{cases} \mu = L_u - L_l \\ \nu = -L_l \end{cases} \qquad (2-62)$$

The number of selected frequency points is related to the smoothness of a complex

curve within the frequency range of interest. Experience has shown that $30 \sim 40$ points are necessary to ensure the accuracy of the frequency response matching. The frequency points are not evenly distributed, rather, they are selected in the weighted manner in which more points are chosen from the frequency range where the gradients change rapidly.

§2.6 Random Searching Optimization-based design method (RSO)

Suppose that, in n-D space, there is a point V_{min} at which the objective function E has its minimum value E_{min}, or a value close to E_{min}. One can search a region $\Omega \in R^n$ assumably large enough to include V_{min} by randomly selecting points within the region and evaluating their function values. The greater the number of random points evaluated, the greater the likelyhood of V_{min} being selected. As the number of evaluations continues to grow, V_{min} will eventually be found. This is the philosophy of the random searching optimization method, abbreviated to "RSO" for short.

In 1973, Luus and Jaakola [11] developed this simple optimization algorithm for solving various non-linear programming problems. In addition to the random searching, they also proposed a systematic reduction of the size of searching region Ω so that the process would proceed more efficiently.

Since 1982, a number of papers [10, 16, 17] has been published by Luus and his colleagues reporting on the applications of this method to the model simplification of discrete and continuous systems. The parameters of a lower-order model are determined in such a way that its time or frequency response will match the corresponding part of the original higher-order system as closely as possible. Successful numerical examples presented in these papers are impressive.

Inspired by the above achievements, this author attempted to extend the RSO

method to the design of digital controllers. In section 2.5.2, non-linear programming is described as a means of designing digital controllers based on the frequency response matching technique, that is,

Minimize

$$E = \sum_{i=1}^{N} \sqrt{[\vartheta_Q(\omega_i) - \vartheta_{M_Q}(\omega_i)]^2 + [\psi_Q(\omega_i) - \psi_{M_Q}(\omega_i)]^2} \qquad (2-53)repeated$$

$$= F(\lambda_0, \lambda_1, \ldots, \lambda_{m+n}).$$

Note that λ_i, $i = 0, 1, \ldots, m+n$ are not subject to any constraints. If the minimum of the objective function E can be found by the random searching, the resulting optimal variables λ_i^* will give the required gain, poles and zeros of a digital controller.

The formulation of non-linear programming and the initialization of a design problem have been discussed in section 2.5. The essential computational steps of the RSO method are given below and illustrated in the flow chart of Fig. 2-7.

(1) Initialize the iteration, the index $j = 0$.

Firstly, set up the initial values $\lambda_i^{*(0)}$ for variables λ_i, $i = 0, 1, \ldots, m+n$ following the same method described in section 2.5.4. Secondly, assign initial sizes to the searching regions, $r_i^{(0)}$, for each variable λ_i. The choice of r is much dependent on experience and knowledge of a dynamic plant. If r is too small, the minimum point may be excluded from the searching region; if too large, the computation time increases significantly. The final action in step 1 is the calculation of the function value $\lambda^{*(0)}$ from Eq. (2-53), i.e.,

$$E^{*(0)} = F(\lambda_0^{*(0)}, \lambda_1^{*(0)}, \ldots, \lambda_{m+n}^{*(0)}).$$

(2) Determine the values of λ at the jth-iteration.

Increase the index j by one, $j = j + 1$.

Take $K \times (m+n+1)$ random numbers $\sigma^{(j)}$ uniformly distributed between -0.5 and $+0.5$. Put them into K sets $\sigma_k^{(j)}$, $k = 1, 2, \ldots, K$, each set containing $m+n+1$

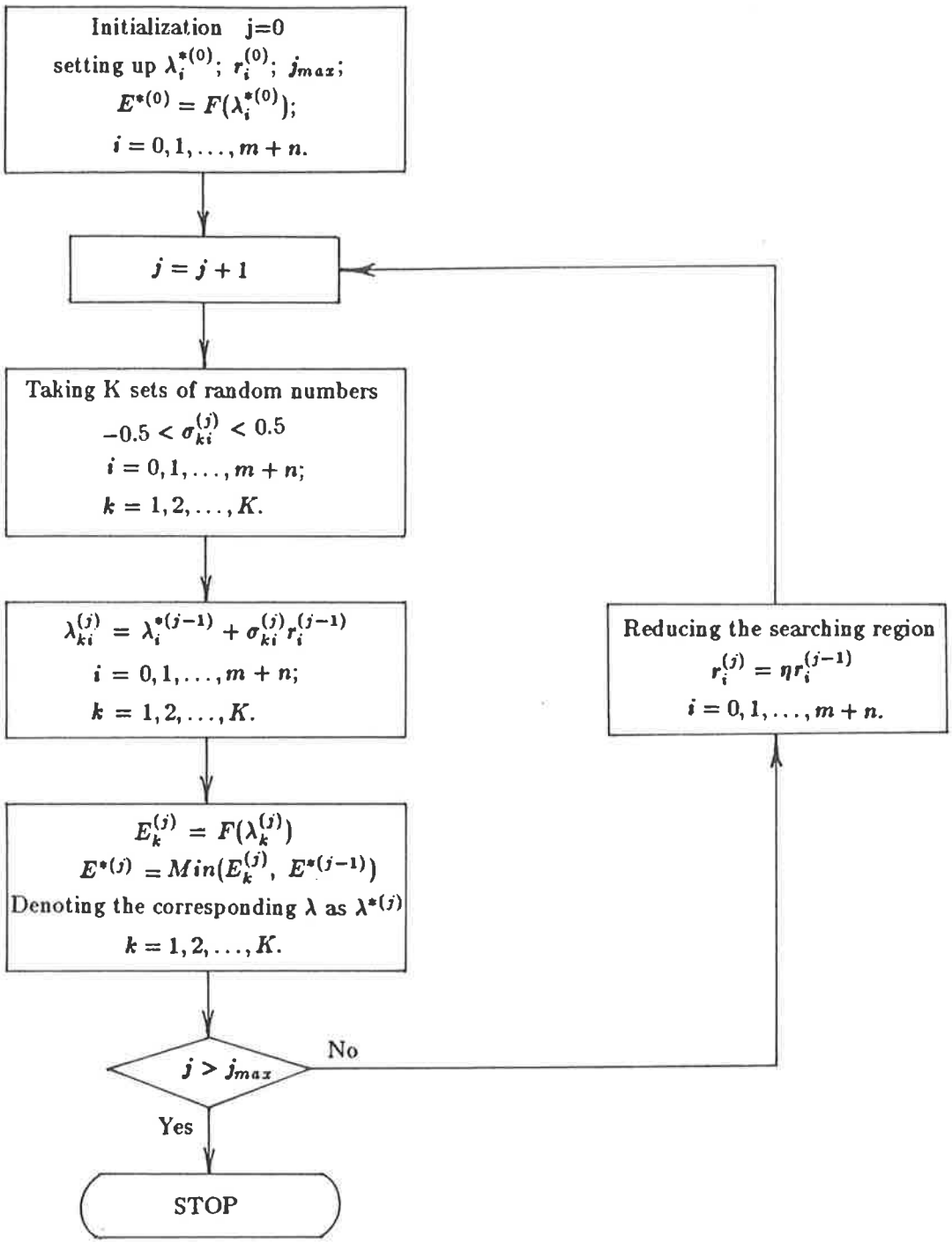

Figure 2-7 Flow chart for the random searching optimization method

numbers $\sigma_{ki}^{(j)}$, $i = 0, 1, \ldots, m+n$. These random numbers are assigned to variables λ_i as determined by

$$\lambda_{ki}^{(j)} = \lambda_i^{*(j-1)} + \sigma_{ki}^{(j)} r_i^{(j-1)}, \qquad (2-63)$$

$$i = 0, 1, \ldots, m+n, \qquad k = 1, 2, \ldots, K.$$

In this thesis, random numbers are generated by the GGUBFS subroutine of the IMSL programme library [9]. The number of sets at each iteration, K, is taken as 100.

(3) Find the minimum function value E^* at the jth-iteration.

Calculate function values $E_k^{(j)}$ from

$$E_k^{(j)} = F(\lambda_{k0}^{(j)}, \lambda_{k1}^{(j)}, \ldots, \lambda_{k(m+n)}^{(j)}), \qquad k = 1, 2, \ldots, K. \qquad (2-64)$$

Determine the minimum value over all sets including $E^{*(j-1)}$ and call it $E^{*(j)}$. Also let the corresponding variables $\lambda_k^{(j)}$ be denoted by $\lambda^{*(j)}$.

(4) Reduce the size of the searching region Ω.

The size of the searching region at $(j+1)$th-iteration is reduced by

$$r_i^{(j+1)} = \eta r_i^{(j)}, \qquad i = 0, 1, \ldots, m+n, \qquad (2-65)$$

where η is a contraction factor and $0 < \eta < 1$.

Usually η is chosen from 0.9 to 0.99. In this thesis, the author uses $\eta = 0.95$.

(5) Start a new iteration.

Go to step (2) and repeat the whole procedure. Continue until the iteration number j exceeds the limit j_{max}. Then halt the process and substitute the optimized variables $\lambda^{*(j_{max})}$ into Eqs. (2-50), (2-51) and (2-52) to obtain the desired poles, zeros and gain of the digital controller. The criterion j_{max} relates to the complexity of the problem, in particular the number of variables. In this thesis, j_{max} is 150 for the problem

in 7-D space. This implies that, over the entire process, 15,000 points are selected and 15,000 function values are calculated. If the number of selected frequency points N in Eq. (2-53) is large, say 30, the computational burden may become extremely heavy.

§2.7 Summary

In this chapter, five methods for the design of digital controllers based on the frequency response matching technique have been presented. Both the theoretical background and operational procedures were discussed. First the dominant data matching method was reviewed as a simple and efficient method. Some modification was suggested in the application of the DDM method to the design of the controller which possesses a pole at the point of $(1, j0)$ in the z-plane. The more elegant method, namely Rattan's complex-curve fitting design method, was then presented. By minimizing the weighted-squred-error function of the matching with the derivative techniques, the design of Rattan's CCF method may reach the optimum. However, it was demonstrated that the detrimental effect of the weighting factor in the error function to be minimized became unacceptable when the sampling frequency ω_s was high relative to the closed-loop bandwidth ω_b. To overcome this deficiency, the iterative complex-curve fitting design method was proposed. The new method eliminates effectively the error-producing weighting factor from the error function by iterative computations. The author also formulated the non-linear programming problem for the design of digital controllers, and devised the solutions using the simplex and the random searching optimization algorithms. These optimization-based design methods feature the facility to incorporate various non-linear constraints in the design in order to ensure the system stability and to improve the system dynamic response. All of these methods will be demonstrated and assessed in Chapter IV .

CHAPTER III

DETERMINATION OF FREQUENCY RESPONSE MODELS

One of fundamental considerations in frequency response matching design techniques is the determination of a frequency response model $M(j\omega)$ from the given performance specifications for a closed-loop control system. This topic, neglected in the previous papers, forms this independent chapter not only because it directly relates to the dynamic performance of a system under design, but also because it has a strong influence upon the effectiveness of the frequency response matching process itself.

In section 3.1, a general description of sources and applications of frequency response models is given; followed by an explanation of using the frequency domain specifications. Section 3.2 deals with the problem of converting specifications between different domains when design goals are assigned in the time or complex z-domain. In order to provide a reliable and easy-to-use solution, a thorough investigation is conducted on a typical second-order discrete system $M(z)$ with:

$$M(z) = \frac{Az + B}{z^2 + Cz + D}. \qquad (3-1)$$

As a result, systematic procedures to determine the parameters A, B, C and D are developed so that the frequency response model $M(j\omega) = M(z)|_{z=e^{j\omega T}}$ can be readily derived for the design specifications given in the time or complex z- domains.

§3.1 Frequency response models

3.1.1 General description of defining a frequency response model

Fig. 3-1 depicts the general relationships between design specifications in different domains, various types of frequency response models and several forms of data presentation.

Though design specifications may be given in many different terms, they are generally classified in three domains: (1) time domain specifications, e.g., the maximum overshoot M_p, defined as the ratio, $\frac{\textit{maximum peak value} - \textit{steady state value}}{\textit{steady state value}}$, expressed in percent; and the time to the first peak, t_p, at which the response of a system to a step change reaches its first peak value; (2) complex z-plane variables, including the system damping ratio ξ, the undamped natural frequency ω_n, etc.; (3) frequency domain specifications such as the phase margin PM and the gain margin GM obtained from an open-loop response, or the resonant frequency ω_r and the resonance peak value M_r obtained from a closed-loop response.

Obviously, for frequency domain synthesis, the specifications in the first two domains have to be converted into the equivalent frequency specifications. Such a conversion will be considered in the next section.

In the third case, the frequency domain specifications may come from two sources. One source is a set of dominant data such as the phase margin, gain margin and closed-loop bandwidth, etc., which define the desired frequency response explicitly at few key frequency points. The second source uses the frequency response of a previously designed system having a desired dynamic performance. This is common in the problem of discretizing an operating continuous-time control system, in which an equivalent digital controller is required to replace an existing analogue controller. A previously designed system, therefore, is often refered to as an existing system in the control literature, though it may not exist physically.

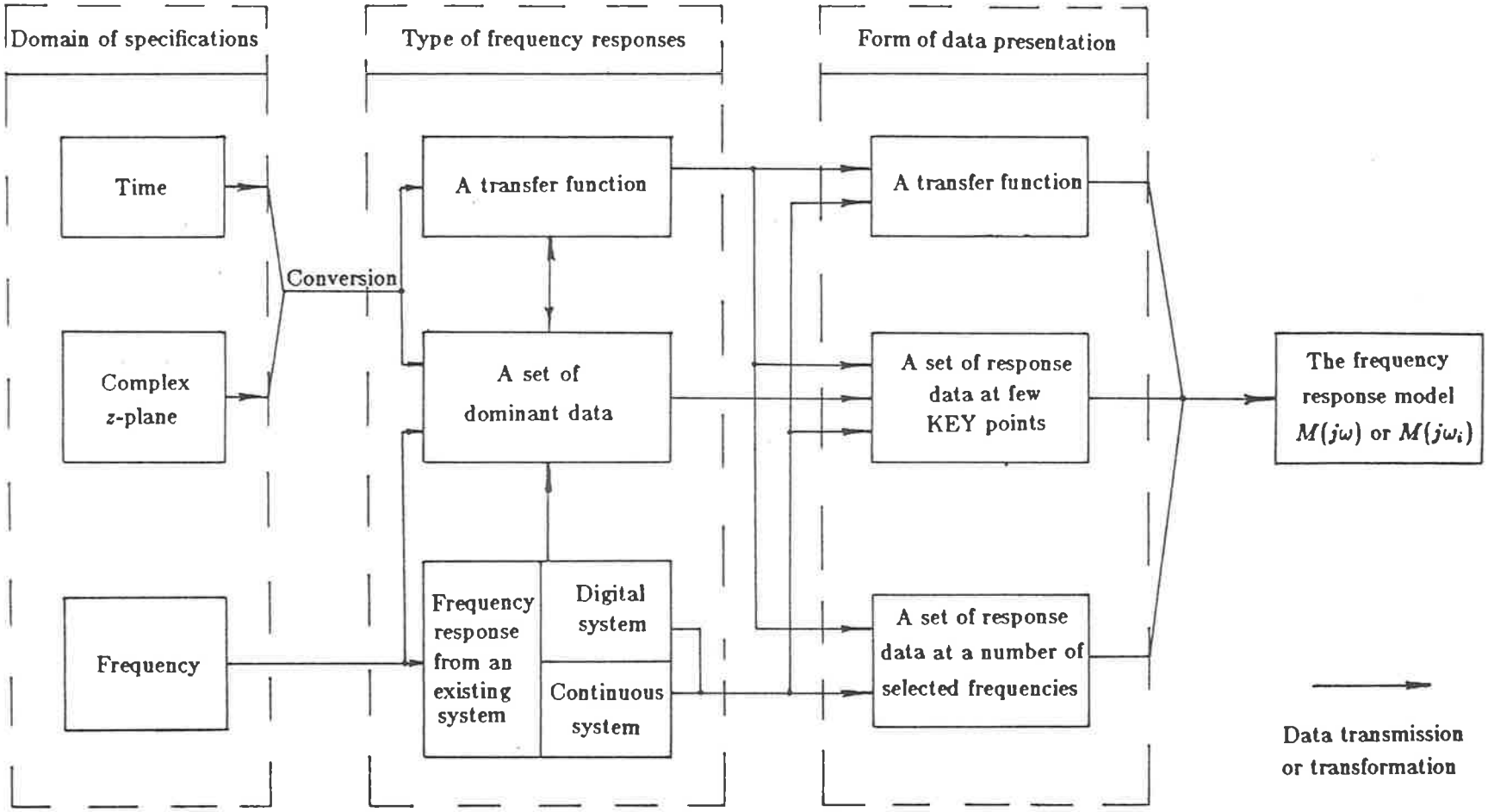

Figure 3-1 Flow chart for determining the frequency response model

Choice of data presentation depends on the design method for which the model is employed. For example, the dominant data matching method requires frequency response data at only few ($4 \sim 5$) key points; while the optimization-based methods (SIM or RSO) need data at a number ($30 \sim 40$) of selected points over an appropriate frequency range to ensure matching accuracy. Furthermore, because of analytical derivatives required in the complex-curve fitting methods for the calculation of the matching error, the frequency response model has to be in transfer function form.

From Fig. 3-1, it can be observed that the frequency responses in transfer function form can be converted to any forms for data presentation. On the other hand, those specified as dominant data type have to be synthesized into a transfer function form before they can be presented in other data forms. This task can be fulfilled by the method proposed in section 3.2.

3.1.2 Limitations on using the frequency response of an existing system as a model

In the problem such as discretizing an existing continuous-time control system, or redesigning an existing digital control system for a new sampling period, it is desirable to retain the original closed-loop frequency response because of its satisfactory dynamic performance. Consequently using this frequency response as the model is logical and convenient. However, some limitations should be borne in mind. The basic consideration is that the effective frequency matching for a digital control system can be conducted only over the primary frequency range ω_p, where $\omega_p = \omega_s/2$ (see section 2.1). Suppose that the sampling period of a digital control system $H_1(z)$ is adjusted from T_1 to T_2 and a new digital controller is required for a new system $H_2(z)$ with the similar frequency response to that of $H_1(z)$. If $H_1(z)$ with T_1 is used as the frequency response model, i.e., $M(j\omega) = H_1(z)|_{z=e^{j\omega T_1}}$, it is impossible for $H_2(j\omega) = H_2(z)|_{z=e^{j\omega T_2}}$ to match $M(j\omega)$ very closely because of the discrepancy in their primary frequency ranges. The distortion in the high frequency band, especially when $T_1 < T_2$, may severely degrade the dynamic performance of $H_2(z)$. In particular, a continuous system can be considered

as a special case in which the sampling period tends to zero and the primary frequency range becomes infinite. Such distortion-producing effects will be carefully examined in the simulation studies of section 4.3.

§3.2 Second-order z-transfer function as a frequency response model

3.2.1 Use of the discrete transfer function as the model

As pointed out by the preceding section, there are mainly two reasons for this part of the discussion. Firstly, the design specifications for digital control systems in the time and complex z-domain need to be converted into the frequency domain. Secondly, in the frequency domain, the specifications assigned in dominant data form have to be converted into a transfer function form, if required by design methods. Such transfer function form is preferably the discrete transfer function to avoid the matching distortion in the high-frequency band as described in section 3.1.2.

For a discrete system having a order higher than two, relations between the specifications in the time, frequency and complex z- domains can be very complicated. In general, however, the dynamic characteristics of most high-order control systems can be well approximated by that of appropriate second-order systems the analysis of which is much simpler than that of the former. Therefore, the second-order discrete transfer function is considered as the most appropriate vehicle to carry the desired performance specifications as a frequency response model.

It is well known that, for continuous second-order systems, the relationships between specifications in the time, frequency and complex s- domains have been expressed accurately in mathematical formulae [20, 21]. In a similar manner, some selected second-order discrete systems in transfer function form are investigated by a number of authors

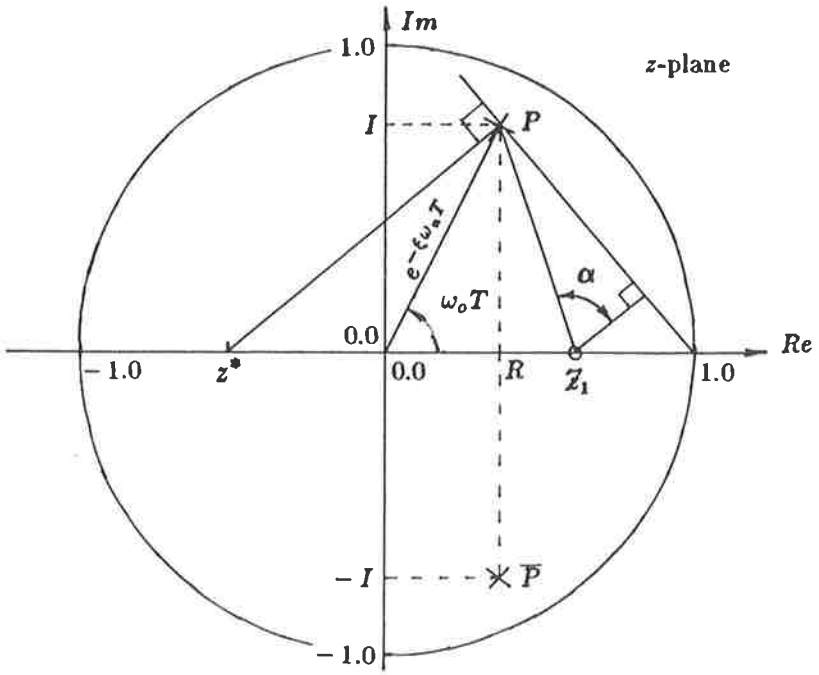

Figure 3-2 Location of the zero Z_1 of $h(z)$ in terms of the parameter α, $h(z) = \frac{A(z-Z_1)}{(z-P)(z-\overline{P})}$

as well. Jury [22] in his pioneering book showed the relationships between a system frequency response and its unit-step time response. But the second-order discrete system that he used was derived from a continuous counterpart so that its zero was closely bounded to the locations of poles. In another elegant representation introduced by Kuo [1], the zero is arbitrarily assigned along the real axis by varying the parameter α as defined graphically in Fig. 3-2, where α is positive if $Z_1 \geq z^*$ or negative otherwise. Using this model, Kuo derived the unit-step time response in terms of complex z-plane variables. Unfortunately he did not use this model consistently in his later frequency domain analysis, and hence did not fill the gap between the specifications in the time domain and those in the frequency domain. For the purpose of seeking a frequency response model, there is also lack of tools to determine the parameters of a discrete transfer function from required design specifications.

These deficiencies are overcome by a thorough investigation carried out on a second-order discrete system having a pair of complex conjugate poles and one zero that can be arbitrarily assigned from $-\infty$ to 1. Specifications and variables from all

three domains are closely linked together. The results of analysis, including coefficients of transfer function, are arranged in mathematical, graphical and tabular forms, which grant a designer the flexibility to choose the better frequency response model in each specific case.

3.2.2 Second-order z-transfer function model

The second-order discrete system with unity feedback, introduced by Kuo [1], is adopted in this analysis. Its open-loop transfer function is $g(z)$ and closed-loop transfer function is $h(z)$,

$$\begin{aligned} h(z) &= \frac{g(z)}{1+g(z)} \\ &= \frac{A(z-Z_1)}{(z-P)(z-\overline{P})} \\ &= \frac{A(z-Z_1)}{(z-e^{-\xi\omega_n T+j\omega_o T})(z-e^{-\xi\omega_n T-j\omega_o T})}; \end{aligned} \tag{3-1}$$

where, A is a closed-loop gain; Z_1 is a real zero; P and $\overline{P}$ are a pair of complex conjugate poles; ξ is the system damping ratio; ω_n is the undamped natural frequency and ω_o is the system oscillatory frequency (see Fig. 3-2).

Note that ω_o is related to ω_n by

$$\omega_o = \omega_n\sqrt{1-\xi^2}. \tag{3-2}$$

Denote the real and imaginary part of P as R and I, respectively, so the poles may be expressed as:

$$P = R + jI, \qquad \text{and} \qquad \overline{P} = R - jI.$$

For short, rewrite $(-AZ_1)$ as B, $(-2\cos\omega_o T e^{-\xi\omega_n T})$ as C, and $(e^{-2\xi\omega_n T})$ as D. Thus Eq. (3-1) becomes:

$$\begin{aligned} h(z) &= \frac{A(z-Z_1)}{(z-e^{-\xi\omega_n T+j\omega_o T})(z-e^{-\xi\omega_n T-j\omega_o T})} \\ &= \frac{Az-AZ_1}{z^2-2\cos\omega_o T e^{-\xi\omega_n T}z+e^{-2\xi\omega_n T}} \\ &= \frac{Az+B}{z^2+Cz+D}. \end{aligned} \tag{3-3}$$

As mentioned before, the zero Z_1 is determined by the parameter α. When α varies from $\alpha^{\circ}_{l.l.}$ to 90°, Z_1 will be set within the range $(-\infty, 1]$, where $\alpha_{l.l.}$ is the lower limit of variation and is derived by this author as:

$$\alpha_{l.l.} = \mathrm{tg}^{-1}\frac{\mathrm{I}}{1-\mathrm{R}} - 90 \qquad (3-4)$$

The derivation of Eq. (3-4) is in Appendix B.

As far as a closed-loop system with certain poles and zeros is concerned, the variation of gain A in Eq. (3-3) does not affect the system transient characteristics but its steady-state response, e.g., the steady-state error e_{ss} which is defined as the difference between the system steady-state output signal and the steady-state input signal. Because e_{ss} is required normally to be as small as possible, the gain of $h(z)$ to a constant signal is assigned to unity. Thus from Eq. (3-1), the system open-loop transfer function is

$$\begin{aligned} g(z) &= \frac{h(z)}{1-h(z)} \\ &= \frac{Az+B}{z^2+(C-A)z+(D-B)}, \end{aligned} \qquad (3-5)$$

with A is determined by:

$$A = \frac{1+C+D}{1-Z_1}.$$

3.2.3 Conversion of specifications between the time and complex z- domains

The investigation embarks with the study of the system time response $y(t)$ to a unit-step input signal. This is based on Kuo's result [1] and the detailed derivations are included in Appendix C. Assume that the maximum value of $y(t)$ occurs at its first response peak. The peak time t_p and the maximum overshoot M_p are expressed in terms of α (in *rad* here), ξ and ω_n, respectively, as follows:

$$t_p = \frac{1}{\omega_n\sqrt{1-\xi^2}}\left[\mathrm{tg}^{-1}\frac{-\xi}{\sqrt{1-\xi^2}} - \alpha + \pi\right]; \qquad (3-6)$$

$$
\begin{aligned}
M_p &= y(t)|_{t=t_p} - 1 \\
&= \sqrt{1-\xi^2}\ |\sec\alpha|\ e^{\frac{-\xi}{\sqrt{1-\xi^2}}[\mathrm{tg}^{-1}\frac{-\xi}{\sqrt{1-\xi^2}}-\alpha+\pi]}.
\end{aligned}
\tag{3-7}
$$

Apparently from Eq. (3-7), the overshoot M_p is only dependent upon α and ξ. Eq. (3-6) shows that t_p is inversely proportional to the system undamped natural frequency ω_n, and that the value of t_p decreases if the zero Z_1 shifts towards the point of $(1,\ j0)$ in the z-plane and increases otherwise.

3.2.4 Frequency response of the open-loop system

The analysis in the frequency domain is covered in this and the next sections. Again, all tedious derivations are left in Appendix D and only the important results are presented here.

From Eq. (3-5), the open-loop frequency response $g(j\omega)$ can be obtained as:

$$
\begin{aligned}
g(j\omega) &= g(z)|_{z=e^{j\omega T}} \\
&= \frac{Az+B}{z^2+(C-A)z+(D-B)}\Big|_{z=e^{j\omega T}} \\
&= \frac{Ae^{j\omega T}+B}{e^{j2\omega T}+(C-A)e^{j\omega T}+(D-B)}.
\end{aligned}
\tag{3-8}
$$

There are two commonly used specifications calculated from open-loop frequency responses, i.e., the phase margin PM and the gain margin GM. In this thesis, the definition of PM is

$$
PM = \psi_g(\omega)|_{\omega=\omega_c} - (-180), \tag{3-9}
$$

where, $\psi_g(\omega)$ is the phase angle of $g(j\omega)$ and ω_c is the gain cross-over frequency at which the magnitude of $g(j\omega)$ equals unity, or 0 db.

In terms of coefficients A, B, C and D, PM and ω_c can be calculated respectively from:

$$
PM = 180 + \mathrm{tg}^{-1}\Big[\frac{\sin\omega_c T(AD-BC-A-2B\cos\omega_c T)}{2B\cos^2\omega_c T+(AD-2AB+BC+A)\cos\omega_c T+u}\Big]; \tag{3-10}
$$

$$\omega_c = \frac{1}{T}\cos^{-1}\left(-\frac{b}{a} \pm \frac{1}{a}\sqrt{b^2 - ad}\,\right); \qquad (3-11)$$

where,

$$a = 4(D - B),$$

$$b = (C - A)(D + 1) + C,$$

$$d = 1 + C^2 + D^2 - 2AC - 2DB - 2(D - B),$$

$$u = BD + AC - A^2 - B^2 - B.$$

It is reasonable to assume that the magnitude of $g(j\omega)$ crosses the level of 0 db only once as ω varies from zero to $\omega_s/2$. This implies that Eq. (3-11) has one and only one solution. Therefore, the sign of the second term inside the parentheses of Eq. (3-11) should be chosen in such a way that $-1 \leq -\frac{b}{a} \pm \frac{1}{a}\sqrt{b^2 - ad} \leq 1$.

The gain margin GM is usually defined in decibels as:

$$GM = -20\log_{10}[\tau_g(\omega)|_{\omega=\omega_g}], \qquad (3-12)$$

where, $\tau_g(\omega)$ is the magnitude of $g(j\omega)$ and ω_g is the frequency at which ψ_g is $-180°$.

In case of an open-loop stable system, The greater the GM is, the larger is the stability margin of the closed-loop system. If the value of GM is negative, the closed-loop system is unstable.

It should be emphasized that, unlike its continuous counterpart, the second-order discrete system is not instability-free even when it is open-loop stable. In fact, the closed-loop stability of a second-order discrete system, as proved by the author in Appendix E, is affected by the open-loop gain, unless the open-loop z-transfer function satisfies all the following conditions:

(1) there are two zeros, and

(2) none of zeros and poles is outside the unit circle in the z-plane, and

(3) there is at least one zero or pole inside the unit circle in the z-plane.

Only in the latter case, the system closed-loop stability is independent of the open-loop gain and is guaranteed.

For the purpose of this thesis, the open-loop systems of interest are confined to those having one zero lying in the range $(-\infty,\ 1\ ]$, one pole inside the unit circle and the other inside or on the unit circle. Thus from the proof in Appendix E and the derivation in Appendix D, the following conclusions can be drawn:

(1) When the open-loop zero and poles are located as specified above, there exists a threshhold for the open-loop gain at and over which the closed-loop system is unstable.

(2) Consequently, for any such system, the gain margin GM has a finite value† which can be determined by (3) or (4) below.

(3) If $|1-D-Z_1C| < 2|Z_1|$, the plot of the phase angle $\psi_g(\omega)$ of $g(j\omega)$ crosses $-180°$ at the frequency ω_g, $0 < \omega_g < \omega_s/2$,

$$\omega_g = \frac{1}{T}\cos^{-1}\Big(\frac{1-D-Z_1C}{2Z_1}\Big), \qquad (3-13)$$

$$\begin{aligned} GM &= -20\log_{10}\tau_g(\omega)|_{\omega=\omega_g} \\ &= -20\log_{10}\Big[\sqrt{\frac{A^2+B^2+2AB\cos\omega_gT}{a\cos^2\omega_gT+2(C-A)(D-B+1)\cos\omega_gT+d+A^2+B^2}}\ \Big], \end{aligned} \qquad (3-14)$$

where, a and d are defined in Eq. (3-11);

(4) If $|1-D-Z_1C| \geq 2|Z_1|$, $\psi_g(\omega)$ will not equal $-180°$ until ω reaches $\omega_s/2$,

$$\begin{aligned} \omega_g &= \frac{\pi}{T} \\ GM &= -20\log_{10}\tau_g(\omega)|_{\omega=\omega_g=\frac{\pi}{T}} \\ &= -20\log_{10}\Big[\frac{A-B}{\sqrt{4(D-B)-2(C-A)(D-B+1)+(C-A)^2+(D-B-1)^2}}\Big]. \end{aligned} \qquad (3-15)$$

† It is well known that the gain margin for an open-loop stable continuous 2nd-order system is infinite.

3.2.5 Frequency response of the closed-loop system

Still another way of evaluating a system frequency characteristics is via its closed-loop response $h(j\omega)$. Specifications, which have been widely used in practice, are the resonance peak value M_r expressed in decibels, the resonant frequency ω_r at which M_r occurs, and the closed-loop bandwidth ω_b at which the magnitude of $h(j\omega)$ equals 0.707, or -3 *db*.

Refering to Appendix D, these quantities are related to system coefficients A, B, C, D and Z_1 as shown in the following equations:

$$M_r = \sqrt{\frac{A^2 + B^2 + 2AB\cos\omega_r T}{4D\cos^2\omega_r T + 2C(1+D)\cos\omega_r T + (D-1)^2 + C^2}}; \qquad (3-16)$$

$$\omega_r = \frac{1}{T}\cos^{-1}\Big[-\frac{A^2+B^2}{2AB} + SIGN(AB)\cdot \sqrt{(\frac{A^2+B^2}{2AB})^2 - \frac{C(1+D)(A^2+B^2)}{4ABD} - \frac{C^2+(D-1)^2}{4D}}\ \Big]$$
$$= \frac{1}{T}\cos^{-1}\Big[\frac{1}{2}[\frac{1+Z_1^2}{Z_1} - SIGN(Z_1)\cdot \sqrt{(\frac{1+Z_1^2}{Z_1})^2 + \frac{C(1+D)(1+Z_1^2)}{Z_1 D} - \frac{C^2+(D-1)^2}{D}}\ ]\Big]; \qquad (3-17)$$

$$\omega_b = \frac{1}{T}\cos^{-1}\Big[\frac{2AB - C - CD}{4D} \pm \frac{1}{4D}\sqrt{(C+CD-2AB)^2 - 4D(1+C^2+D^2-2A^2-2B^2-2D)}\ \Big]. \qquad (3-18)$$

If the magnitude of $h(j\omega)$ does not fall to or below the level of -3 *db*, Eq. (3-18) has no solution. If it crosses the -3 *db* line once, the sign in front of the squared-root in Eq. (3-18) should be taken such that the absolute value of expression in square braces is ≤ 1.

Eq. (3-17) reveals clearly that ω_r is only the function of the zero and pole positions and is independent of the system gain. M_r and ω_r are important specifications as they directly reflect the system transient time response such as M_p and t_p, respectively.

3.2.6 Numerical studies on relationships of various specifications for discrete systems

Equations from (3-6) to (3-18) give for discrete systems a set of mathematical relations between the complex z-domain parameters ξ, ω_n and α, the time response specifications M_p and t_p, and frequency response specifications PM, ω_c, GM, ω_g, ω_r, ω_b and M_r. They are rather complicated even in such a simple second-order case. Instead of using a cumbersome analytical approach, a set of numerical studies for analysis has been carried out; their results are summarized in this section and in Appendix F.

Table A-1 in Appendix F lists a basic set of numerical data which form the relationships between M_p, t_p, ω_b, ω_r, M_r, PM, GM as function of ξ, $\omega_o T$ and α.

To cover typical design specifications for electromechanical control systems, the closed-loop damping ratio ξ is chosen to lie in the range 0.4 to 0.9, α from $-80°$ to $80°$ and $\omega_o T$ from 0.1 to 1.3. In consequence, the closed-loop poles are confined to the shaded area shown in Fig. 3-3. Also given in the table are the parameters of the corresponding discrete systems, including the positions of closed-loop poles and zeros as well as polynomial coefficients A, B, C and D defined in Eq. (3-3). These provide for the designer a z-transfer function for frequency response model after selecting the system performance specifications.

As matter of convenience, normalized variables are used in the table. For example, the peak time t_p is expressed in terms of t_p/T, which approximates the number of samples needed for the system output to reach its first peak value. Moreover, all frequency variables are presented in ωT so that the primary frequency range $0 \sim \omega_s/2$ will be normalized to $0 \sim \pi$.

To help understand the relationships discussed so far, five diagrams are drawn

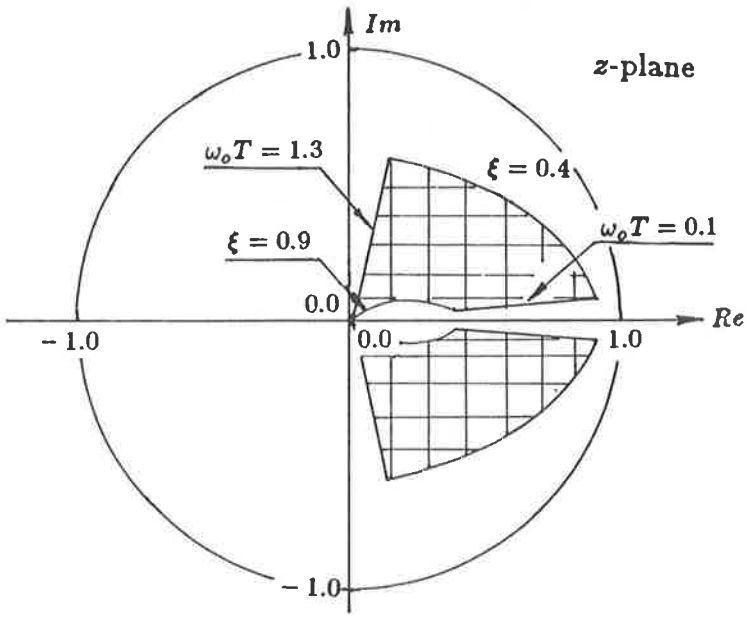

Figure 3-3 Location of the closed-loop poles for the numerical studies. The shaded area is determined by parameter ranges $-80° \leq \alpha \leq 80°$, $0.4 \leq \xi \leq 0.9$, $0.1 \leq \omega_o T \leq 1.3$.

which are based on the data in Table A-1. The first three are devoted to demonstrate the relationships between the specifications in the time and frequency domains. Fig. 3-4 shows the maximum overshoot M_p vs the phase margin PM. M_p against the resonance peak value M_r is plotted in Fig. 3-5 (The curve represents the average value. The deviation is relatively large when M_r<0.6db). The peak time as a ratio t_p/T vs the normalized closed-loop bandwidth $\omega_b T$ is illustrated in Fig. 3-6. A few observations can be drawn from these graphs. Firstly, to design a system at $\omega_o T$=0.7 with $M_p < 30\%$, the phase margin must be greater than 40° and the resonance peak value M_r less than 3 db. Secondly, the hyperbolic relations between $\omega_b T$ and t_p/T differ slightly from the average curve $t_p\omega_b \approx 4.8$ when α and ξ vary over a wide range. The curves in Fig. 3-6 help the designer reach a compromise between speed of response and the required bandwidth ω_b.

Two further diagrams illustrate the time domain specifications as function of the complex z-domain variables ξ, α and ω_o. The relationships shown are the peak time t_p vs ξ, α and ω_o in Fig. 3-7, and the maximum overshoot M_p vs α and ξ in Fig. 3-8.

It is interesting to note that for any fixed value of ξ, the normalized variable $\omega_o t_p$ is a linear function of the parameter α. Furthermore, the effect of the zero Z_1 on the system transient response can be clearly observed by the fact that t_p is reduced at the expense of increasing M_p as α tends to 90°, i.e., the Z_1 shifts closer to the point of (1, j0) in the z-plane.

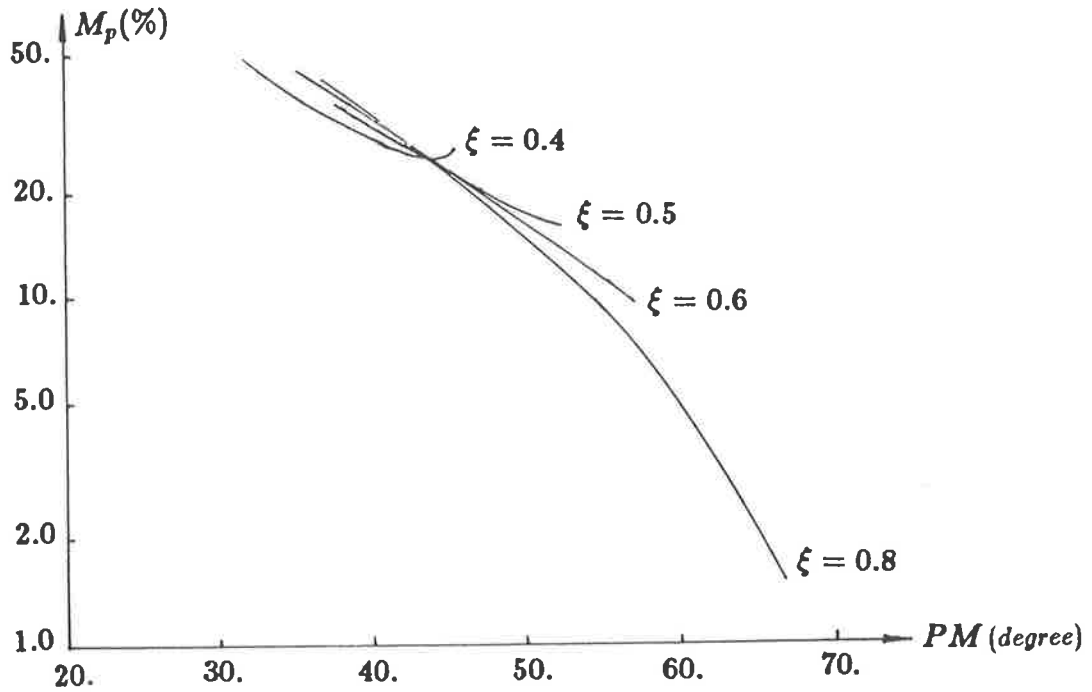

Figure 3-4 Relationship between the maximum overshoot M_p and the phase margin PM at $\omega_o T = 0.7$

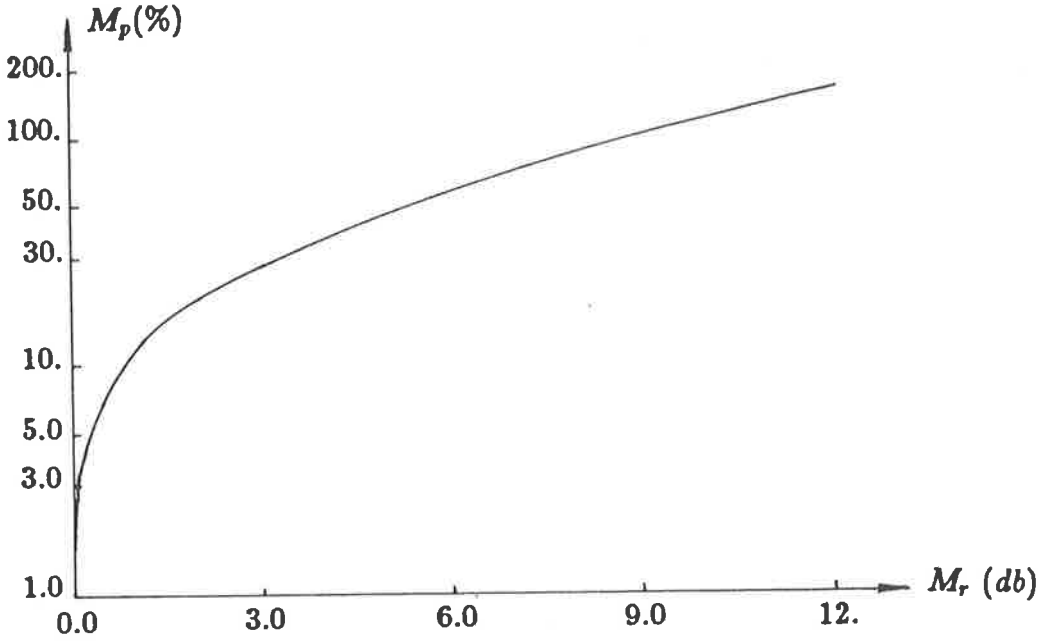

Figure 3-5 Relationship between the maximum overshoot M_p and the resonance peak value M_r

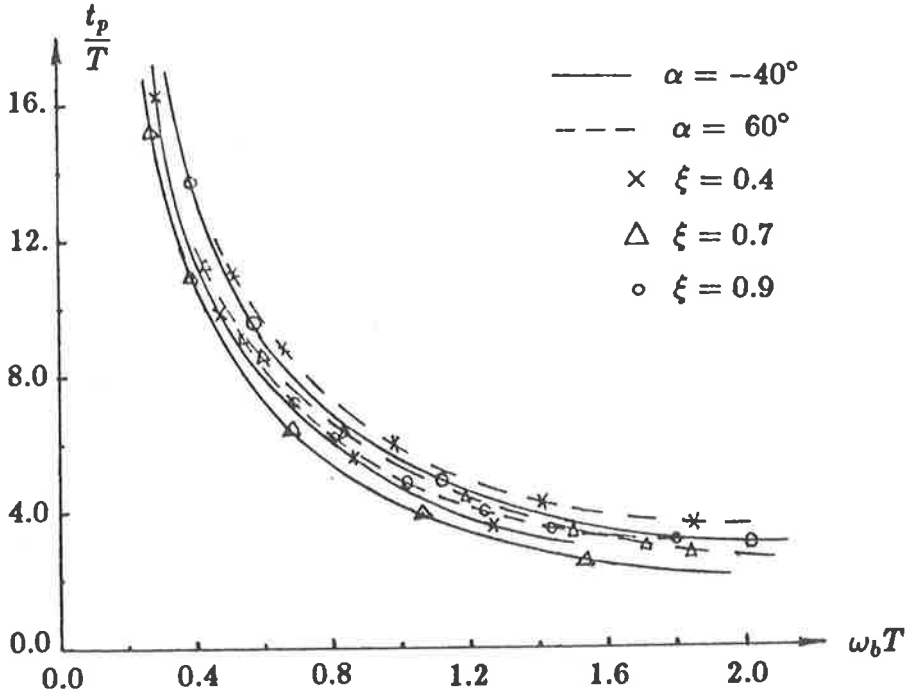

Figure 3-6 Relationship between the peak time ratio $\frac{t_p}{T}$ and the normalized closed-loop bandwidth $\omega_b T$ as a function of α and ξ

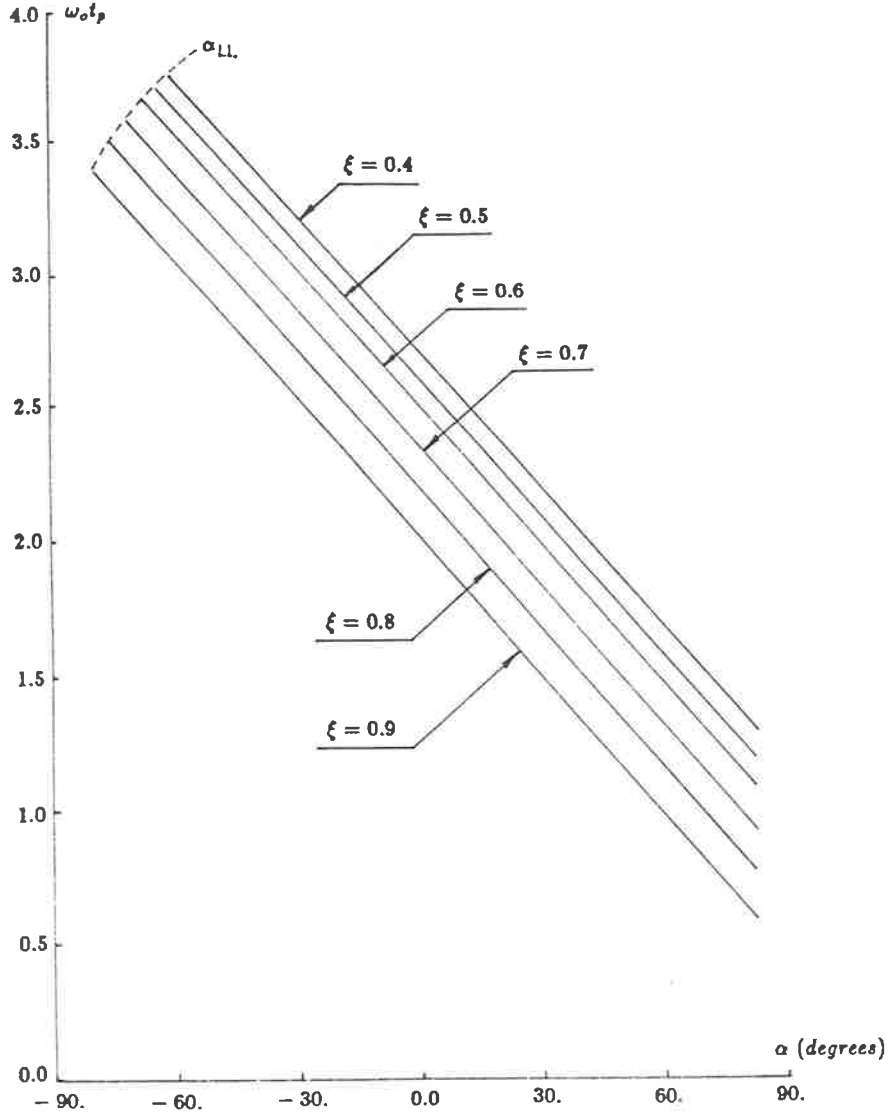

Figure 3-7 Relationship between the normalized peak time $\omega_o t_p$ and α as function of ξ

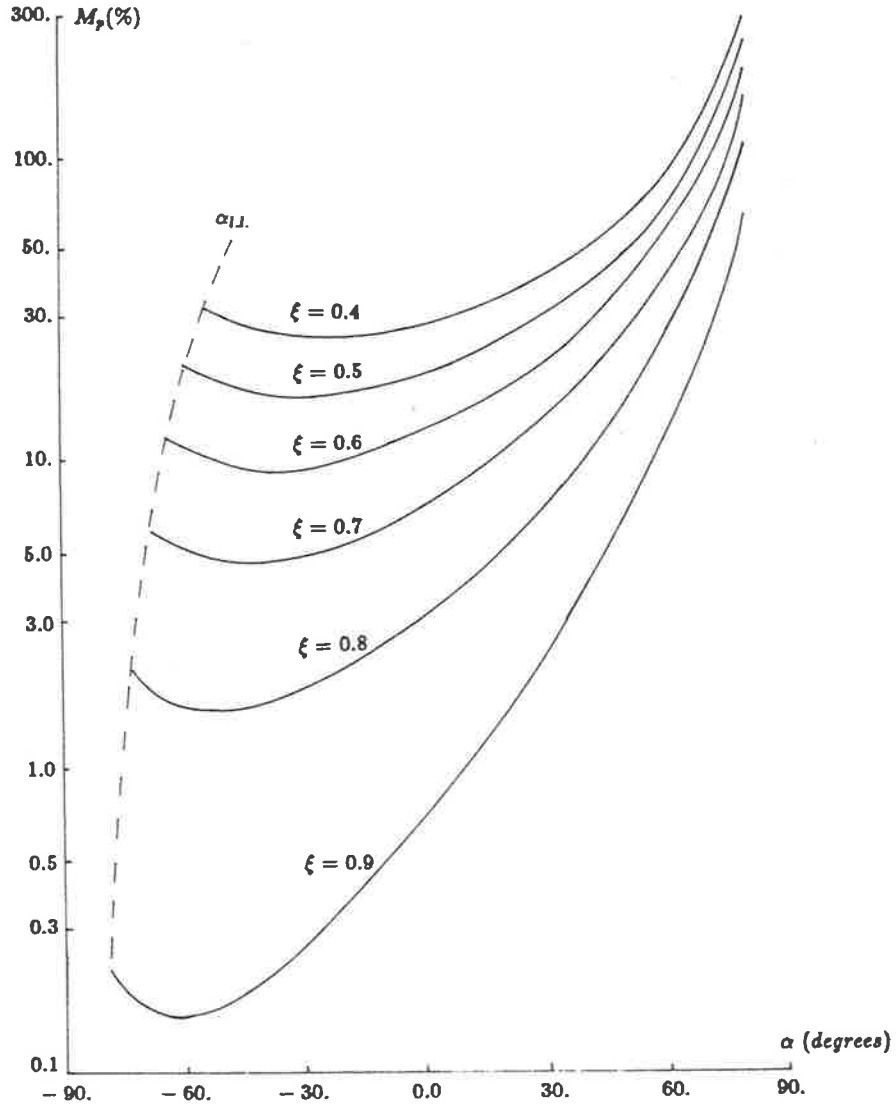

Figure 3-8 Relationship between the maximum overshoot M_p and α as function of ξ

3.2.7 Procedures to define a z-transfer function as a frequency response model

So far the dynamic characteristics of second-order discrete systems have been extensively studied. The results of this investigation are used to establish a frequency response model $M(j\omega)$ from specified control criteria. The form of $M(j\omega)$ based on a discrete second-order transfer function $M(z)$ is

$$\begin{aligned} M(j\omega) &= M(z)|_{z=e^{j\omega T}} \\ &= \left.\frac{Az+B}{z^2+Cz+D}\right|_{z=e^{j\omega T}}. \end{aligned} \qquad (3-19)$$

Hence the specific task is to determine the coefficients A, B, C and D in accordance with desired control specifications. Two cases considered here are:

case 1 – control criteria mainly specified in the complex z-plane;

case 2 – control criteria mainly specified in the time domain.

The recommended procedures are explained with aid of two numerical examples in the remainder of this section.

Case 1

Assume that the desired specifications are: $\omega_n = 0.84\ rad/s$, $\xi = 0.7$, $T = 0.5\ s$ and $t_p \approx 5.0\ s$.

First consider only the specification given in the z-plane. From known ω_n and ξ, the oscillatory frequency ω_o can be calculated by Eq. (3-2):

$$\omega_o = \omega_n\sqrt{1-\xi^2} = 0.6.$$

Then

$$\omega_o T = 0.3.$$

Once $\omega_o T$ and ξ are known, the explicit positions of the closed-loop poles can be readily found from Table A-1, i.e., $P, \overline{P} = 0.712 \pm j0.22$. However, they do not characterize the system performance completely as the zero has a strong influence on the system

transient response. Table A-1 shows, for instance, that as α varies from $-40°$ to $+80°$, the ratio t_p/T decreases from 10.2 to 3.2 and M_p increases from 4.6% up to 159%. Therefore, an additional specification is needed to determine the location of zero. In this example, such a requirement is fulfilled by setting $t_p \approx 5.0\ s$. Notice that $\omega_o t_p$ equals 3.0, then α is found to be $-40°$ from Fig. 3-7 (Fig. 3-8 will be useful if the additional specification is the maximum overshoot M_p). Now look up Table A-1 again, the required $M(z)$ with $\xi = 0.7$, $\omega_o T = 0.3$ and $\alpha = -40°$ is

$$M(z) = \frac{0.103z + 0.028}{z^2 - 1.424z + 0.555};$$

and $M(j\omega)$ is

$$\begin{aligned} M(j\omega) &= M(z)|_{z=e^{j0.5\omega}} \\ &= \frac{0.103e^{j0.5\omega} + 0.028}{e^{j\omega} - 1.424e^{j0.5\omega} + 0.555}. \end{aligned}$$

Case 2

Assume that the desired specifications are: $t_p \approx 5\ s$; $M_p \approx 5\%$; $T = 1.0\ s$ and $\omega_b \approx 0.9\ rad/s$.

Firstly, under the condition $M_p \approx 5\%$, a number of feasible solutions regarding parameters α and ξ may be derived from Fig. 3-8. For further considerations, four sets of α and ξ are taken as listed below:

set I : $\xi = 0.7, \quad \alpha = -60°$;

set II : $\xi = 0.7, \quad \alpha = -30°$;

set III : $\xi = 0.8, \quad \alpha = 19°$;

set IV : $\xi = 0.9, \quad \alpha = 45°$.

Secondly, check up these parameters with the required ω_b by means of Fig. 3-6. It is found that only when ξ is 0.7 and α around $-40°$, ω_b is about 0.9. Hence the parameters set III and IV can be discarded.

Next the values of $\omega_o t_p$ corresponding to parameters of set I and set II are determined from Fig. 3-7 and converted to $\omega_o T$ as values of t_p and T are given. This

leads to two discrete transfer function $M_1(z)$ and $M_2(z)$. $M_1(z)$ is defined by $\xi = 0.7$, $\alpha = -60°$ and $\omega_o T \approx 0.7$, and $M_2(z)$ by $\xi = 0.7$, $\alpha = -30°$ and $\omega_o T \approx 0.6$. Because both of them satisfy all specified criteria, the final decision lies on some minor considerations. Look up Table A-1 to compare the dynamic characteristics and pole-zero locations of $M_1(z)$ and $M_2(z)$. It can be observed that the zero of $M_1(z)$ at $(-8.1,\ j0)$ is too far away from the point of $(1,\ j0)$. On the other hand, the zero of $M_2(z)$ resides near the origin. The direct impact of such a difference is the slower transient step response of $M_1(z)$ comparing with that of $M_2(z)$, as demonstrated in Fig. 3-9. Therefore, finally $M_2(z)$ is chosen as the desired z-transfer function for the frequency response model $M(j\omega)$:

$$M_2(z) = \frac{0.361z + 0.031}{z^2 - 0.917z + 0.308};$$

$$M(j\omega) = M_2(z)|_{z=e^{j\omega}}$$

$$= \frac{0.361e^{j\omega} + 0.031}{e^{j2\omega} - 0.917e^{j\omega} + 0.308}.$$

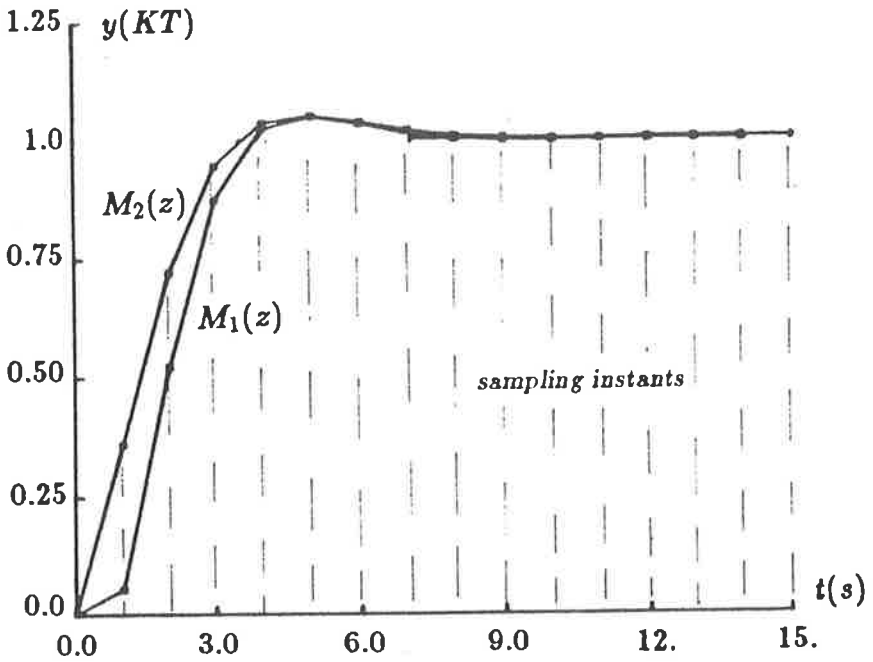

Figure 3-9 Unit-step responses of $M_1(z)$ and $M_2(z)$

CHAPTER IV

DESIGN OF DIGITAL CONTROLLERS BY MEANS OF THE FREQUENCY RESPONSE MATCHING METHODS

§4.1 Introduction

In Chapter II , five frequency response matching design methods have been discussed. They are the dominant data matching method (DDM), the complex-curve fitting method (CCF), the iterative complex-curve fitting method (ICCF), the simplex optimization-based design method (SIM) and the random searching optimization-based design method (RSO). In order to evaluate their effectiveness and practical efficacy, these methods are applied to compensations of various dynamic plants under different conditions. The digital control systems thus designed are then assessed in terms of their performances both in the frequency domain and in the time domain.

In Fig. 4-1 is the block diagram of a closed-loop digital control system to be synthesized in this chapter. It consists of a continuous plant $G(s)$, a zero-order hold $G_h(s)$ and a digital controller with transfer function $D^*(s)$, or z-transfer function $D(z)$, where the notation $X^*(s)$ defines the Laplace transform of $x(kT)$, the sampled or impulse-modulated continuous signal $x(t)$. The system has unity feedback and operates at sampling period T. The problem is to design a controller transfer function $D(z)$ in such a way that the frequency and time responses of the closed-loop system will match those of the desired model as closely as possible.

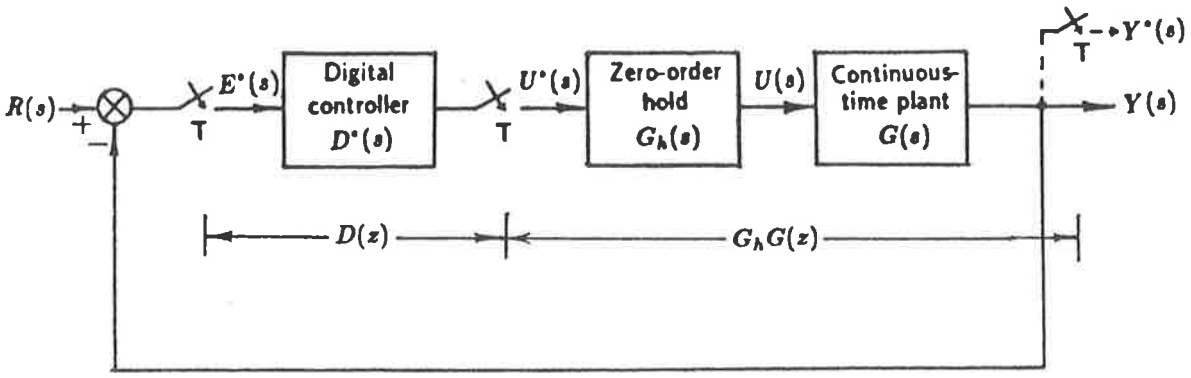

Figure 4-1 Closed-loop digital control system with unity feedback

In addition to the various design studies and discussions in the following sections, some basic information is presented in this section to define the design problem, e.g., the dynamics of the plants, the design specifications, the desired frequency response models, etc.. In particular, section 4.1.1 discusses certain assumptions and the conditions under which the design studies are carried out.

Being sophisticated computer-aided design tools, all frequency response matching design methods have been programmed and run on a VAX-11/780 digital computer. The associated analytical and simulation studies are conducted with the aid of the same computer.

4.1.1 Objectives of the design studies

After having reviewed a number of frequency response matching design methods, an assessment is required to establish the merits and deficiencies of each. In particular, the following set of points may be of interest to a designer:

- To what type of plants can the methods be applied?
- How does the choice of sampling frequency affect the matching accuracy?
- What happens if the control system under design and the model have different primary frequency ranges due to the different sampling frequencies?
- Are there strict requirements on the initial estimates for the optimization-based

design methods?

In order to evaluate the design methods, a comprehensive investigation has been carried out based on over thirty designs. These illustrative designs are organized into three groups as shown in Table 4-1. Each group covers one particular aspect. The purpose of the design studies of Group 1 is to assess the suitability of the design methods for two different types of dynamic plants at various sampling frequencies ranging from 2 to 27 times the desired closed-loop bandwidth ω_b. Note that in this group, specific frequency response models are chosen for each sampling frequency so that the control system being designed always has the same primary frequency range as that of the corresponding model.

In Group 1, all design techniques discussed in Chapter II are evaluated except for the random searching optimization-based design method. Because of its poor convergency properties, the latter is included in a separate set of studies in Group 3.

The design studies of Group 2 consider in Section 4.3 how frequency matching is affected if a control system under design is sampled at period T and the frequency response model of the system is sampled at T_m with $T \neq T_m$, where T_m denotes the sampling period for the model used through out this chapter. A discrete model with a fixed sampling period T_m=0.5 s is employed in five design studies in which sampling periods vary from 0.1 to 2.0 seconds, i.e., some of the periods are shorter than T_m and some longer. In addition, a continuous transfer function is used as a frequency response model for discrete controller designs at sampling frequencies of 4 and 16 times ω_b. This is a common problem which is experienced when an equivalent digital controller is required to replace a continuous unit.

The design method used in the studies of Group 2 is the ICCF method because it is shown in Group 1 to yield results with higher matching accuracy in terms of the matching performance index WIAE, which is the Weighted Integral Absolute-Error criterion defined later in section 4.1.7.

Table 4-1 Objectives of The Design Studies

Group	Objectives	Plant under Design	$T^{\dagger}$	$T_m^{\dagger}$	Methods under Study
1	To demonstrate the applications of four design methods for two types of plant with various sampling frequencies.	I (sluggish time response)	0.5 2.0 4.0	0.5 2.0 4.0	*DDM* *CCF* *ICCF* *SIM*
		II (oscillatory time response)	0.3 0.5	0.3 0.5	
2	To assess the effect of the discrepancy between T and T_m on the frequency response matching and the dynamic characteristic of closed-loop systems.	I	0.1 0.5 2.0	0.5	*ICCF*
		II	0.1 0.5		
		I	0.5 2.0	$0^{\ddagger}$	
3	To evaluate the optimization-based design methods with respect to their convergency, speed of convergency and dependence on initial estimates.	I	0.5	0.5	*SIM* *RSO*

† T–Sampling period of the closed-loop system under design.

T_m–Sampling period of the model to be matched.

‡ A continuous transfer function is used as a model in this subgroup where T_m is assumed zero in the sense that its "sampling frequency" is infinitely fast.

Finally, in the studies of Group 3, two optimization-based design methods, namely SIM and RSO, are assessed with respect to their convergency and speed of convergency. The evaluation is based on the design of a discrete controller for Plant I at T=T_m=0.5 s. The optimization operations for the design start with two sets of different initial values; one is close to the optimum and the other far from the optimum.

4.1.2 Dynamic characteristics of plants

Two third-order continuous dynamic plants have been employed in design studies. The transfer function selected for Plant I is

$$G_1(s) = \frac{(s+1)}{(1.5s+1)(3.5s+1)(5s+1)}. \qquad (4-1)$$

It features an overdamped and sluggish step response which is shown in Fig. 4-2. This response is typical of that of a chemical or thermal process.

Plant II is chosen to be underdamped representing the dynamic performance of an electromechanical system. The following equation gives its transfer function and Fig. 4-3 depicts its oscillatory response for a unit-step input signal.

$$G_2(s) = \frac{100(s+0.2)}{(s+2)(s+0.5+j6)(s+0.5-j6)} \qquad (4-2)$$

Note that its frequency of oscillation is $\omega_{o2} = 6\ rad/s$.

The open-loop frequency responses of Plants I and II are drawn in Figs. 4-4 and 4-5, respectively. Since the two plants will be compensated in accordance with the same control specifications, very distinct digital controllers can be expected in the light of significant differences in the plant characteristics shown in these figures.

4.1.3 Design specifications

The specifications for the dynamic performance of the closed-loop control systems incorporating Plant I and those of the systems incorporating Plant II are identical.

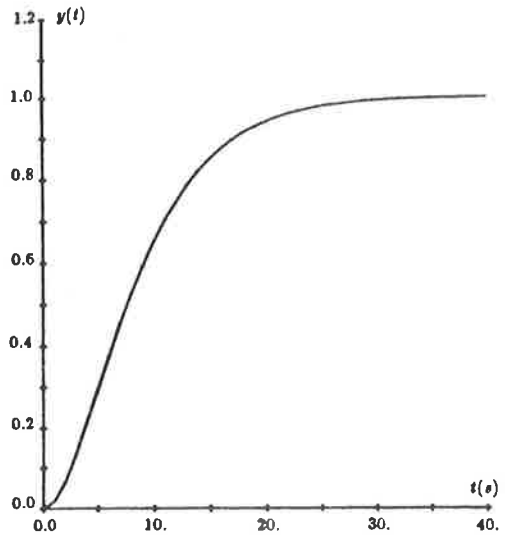

Figure 4-2 Unit-step response of Plant I

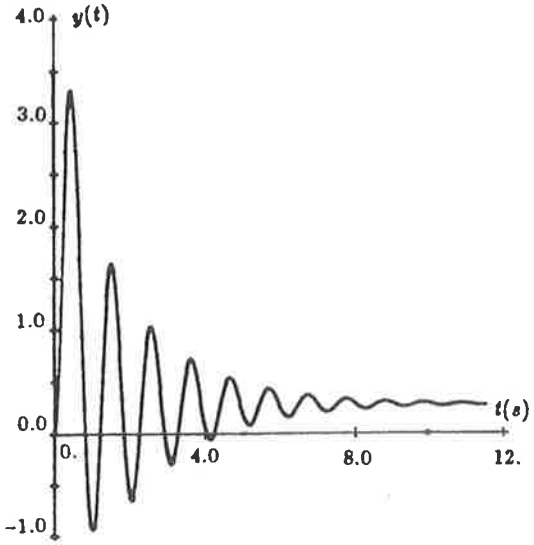

Figure 4-3 Unit-step response of Plant II

They are assigned in terms of closed-loop time responses to a step input signal, as follows:

1. Peak time, $t_p < 6\ s$,
2. Settling time, $t_s < 10\ s$,
3. Maximum overshoot, $M_p < 10\%$,
4. Steady state error, $e_{ss} = 0$;

where the settling time t_s is the time for the response to approach within 5% of its final value.

From the studies of Chapter III (see Fig. 3-6), for $t_p < 6\ s$, the $-3\ db$ bandwidth of the desired closed-loop system, ω_b, is about $0.78\ rad/s$.

4.1.4 Selection of the sampling period

Shannon sampling theorem[19] states that, in order to recover an unknown band-limited signal from its samples, one must sample at a frequency at least equal to twice the highest frequency component in the signal. Accordingly, as far as the design of servo control systems is concerned, the lower bound to the sampling frequency ω_s is twice the required bandwidth ω_b. Also there are many other factors which need to be considered in a practical design. Isermann[14] gives a list of considerations as follows:

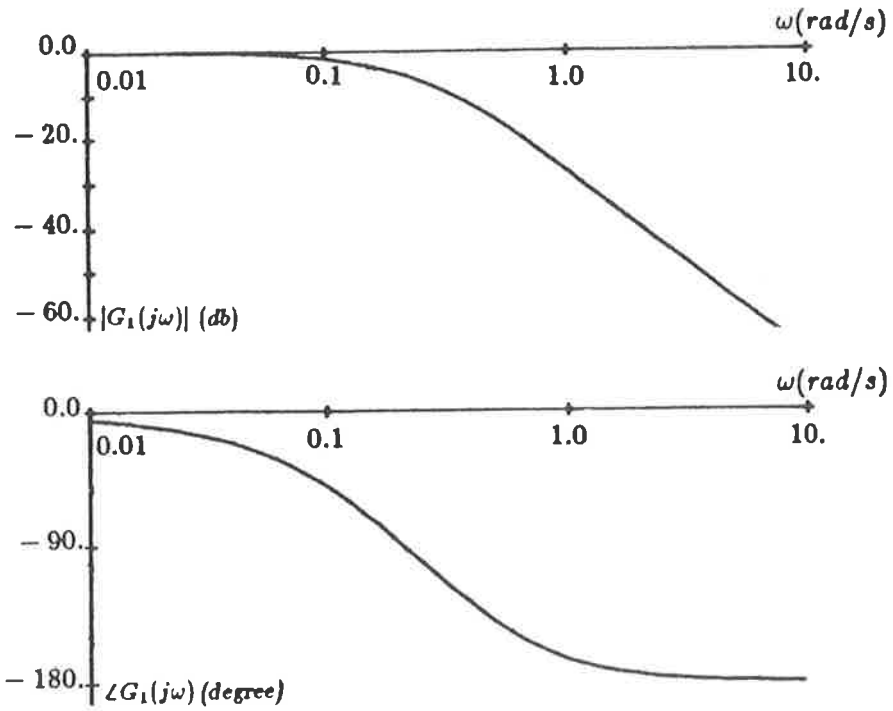

Figure 4-4 Open-loop frequency response of Plant I

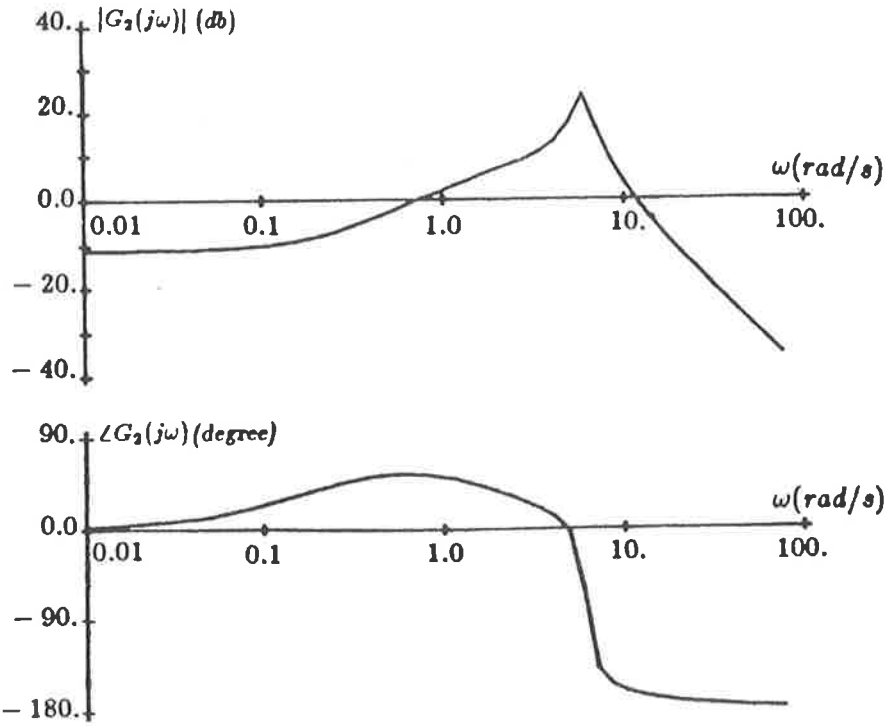

Figure 4-5 Open-loop frequency response of Plant II

- the frequency spectrum of the disturbances;
- the dead time and sum of real time constants of a plant;
- the computational load per control function;
- the control hardware cost;
- the measurement equipment.

Some of these considerations are conflicting. For instance, the control performance deteriorates if the sampling frequency ω_s is too low relative to ω_b, while the computational load and hardware cost increase rapidly if ω_s is too high. Hence a selection of sampling period is basically a compromise among these requirements. Generally speaking, the factor of considerable interest to an engineer is the slowest possible sampling frequency at which the resulting closed-loop system satisfies all performance specifications .

In addition to the considerations pointed out by Isermann, Franklin and Powell [19] show that, for an underdamped plant (like Plant II), its oscillatory response may have a strong influence on the system inter-sample behaviour. This is due to the fact that a digital control system operates effectively in an open-loop mode during the period between sampling instants, hence in this interval the system output may oscillate at the plant damped oscillatory frequency ω_o. From this author's experience, if $\omega_s < 3\omega_o$, the magnitude of the oscillations can be significant and severe ripples on the system output may occur. As an example, in section 4.2 the design of a controller for Plant II at $T = 0.5\ s$, i.e., $\omega_s \approx 2\omega_{o2}$, demonstrates this phenomenon. Furthermore, it should be remembered that the controller synthesis is based on $G_hG(z)$, the z-transfer function of the plant with a ZOH, rather than the continuous plant $G(s)$ itself. In accordance with the Shannon sampling theorem, ω_s should be greater than twice the resonant frequency of plant, which equals ω_o, in order to prevent the plant dynamic characteristics from distortion due to the sample effect. In the case of Plant II , the frequency of oscillation, ω_{o2}, is given in Eq. (4-2) as 6 rad/s; therefore, an appropriate sampling frequency should be, at least, $3\omega_{o2} = 18\ rad/s$, which is far greater than the

closed-loop bandwidth $\omega_b = 0.78\ rad/s$.

Based on the above discussion, a set of sampling periods has been selected for design studies and is given in Table 4-2. The associated range of sampling frequencies is wide; ω_p, the primary frequency range of the closed-loop system, varies about from 1 to 40 times the desired bandwidth ω_b.

Table 4-2 Sampling period T selected for the design studies

T	ω_p $(=\omega_s/2)$	ω_p/ω_b	ω_s/ω_{o2}	Plant under Study
0.1	31.42	40.3	10.47	I , II
0.3	10.47	13.4	3.49	II
0.5	6.28	7.8	2.09	I , II
2.0	1.57	2.0	0.52	I
4.0	0.78	1.0	0.26	I
T is in seconds and ω in rad/s. Note that $\omega_b \approx 0.78$ and $\omega_{o2} = 6$.				

4.1.5 Frequency response models

It has been demonstrated by numerical examples in section 3.2.7 that the desired second-order discrete frequency response model can readily be derived by the method developed in Chapter III . By using this method, four second-order z-transfer functions $M_1 \sim M_4$, each corresponding to a given sampling period, are determined for illustrative designs based on the specifications provided in section 4.1.3. These models are given in Table 4-3 in the order of increasing sampling period, together with the performance parameters of their time responses and the complex z-plane parameters. As explained in

Table 4-3 Frequency response models and their time domain performance parameters for comparison with the control specifications

Model	T_m	z-Transfer Function	t_p	$M_p(\%)$	e_{ss}	t_s	α	$\omega_o T$	ξ
M_1	0.3	$\frac{0.057z+0.007}{z^2-1.611z+0.675}$	4.6	4.6	0.0	3.0	-40	0.2	0.7
M_2	0.5	$\frac{0.103z+0.028}{z^2-1.424z+0.555}$	5.1	4.6	0.0	3.3	-40	0.3	0.7
M_3	2.0	$\frac{0.591z+0.216}{z^2-0.309z+0.116}$	5.6	4.7	0.0	3.6	-40	1.1	0.7
M_4	4.0	$\frac{1.03z-0.113}{z^2-0.094z+0.011}$	4.8	3.7	0.0	3.5	40	1.1	0.9
T and t are in seconds and ω in rad/s.									
Design specifications: $t_p < 6s$; $t_s < 10s$; $M_p < 10\%$; $e_{ss} = 0$.									

Appendix C, the peak time t_p and the maximum overshoot M_p in Table 4-3 are derived from the corresponding continuous time responses of these discrete transfer functions.

4.1.6 Order of the discrete transfer function of a digital controller

The various design methods make differing requirements on the order of the controller transfer function. The complex-curve fitting methods, for instance, allow a designer to start his design with a first-order controller. However, in the dominant data matching method, the controller must, at least, be second-order because a minimum of three points is needed to define a well-behaved complex-curve.

In general, the higher the order of the controller, the more accurate is the matching of frequency responses. But this is achieved at the expense of the complexity of the control function and longer computing time both in design and implementation. As a compromise among these factors, third-order controllers are chosen for all design studies in this chapter.

4.1.7 Simulation and assessment

Following the design of a controller, the performance of a closed-loop system,

which incorporates the digital controller, is simulated on a VAX-11/780 digital computer. Its closed-loop frequency and unit-step responses are calculated for evaluation and comparison. In first part of this section, the formula for the simulation of frequency responses and the methods used for comparison are given. In particular a quantitative figure of merit for the matching accuracy, WIAE, is defined. In the second part, the digital simulation of time responses is described, including the continuous-time output of a closed-loop system and the discrete-time output of a digital controller. Their assessment is based on the performance specifications given in section 4.1.3. Finally the computational burden is pointed out as an important feature in the evaluation.

(a) Simulation and assessment of frequency responses

The discrete frequency response of closed-loop digital control system defined in Fig. 4-1 is

$$H(j\omega) = \frac{D(z)G_hG(z)}{1 + D(z)G_hG(z)}\Big|_{z=e^{j\omega T}} . \qquad (4-3)$$

The frequency matching accuracies of different designs to the assigned model are compared qualitatively through the Bode plots of $H(j\omega)$ and $M(j\omega)$ in the complex plane.

In addition to the direct observation of frequency response plots, a quantitative measurement of the matching error is desirable to indicate the " goodness " of matching performances of various design methods. The commonly-used criterion is the integral absolute error which integrates the error between the frequency response of a closed-loop system and that of a model over a relevant frequency band. The shortcoming of this criterion lies on the fact that the integral over the linear frequency inherently neglects the errors in the low frequency band, the response of which is usually as important as that in the high frequency band. The problem is solved in this thesis by introducing the logarithm frequency in the error integral so that the errors in the low frequency band will be weighted more heavily and the errors in the high frequency band less. This is equivalent to integrating the error between two magnitude curves in the Bode plot except for that, in order to take phase-shift into account, the difference between the two

magnitudes is replaced by the magnitude of the vector difference between two complex functions.

Assume that ω' is a weighted frequency given by:

$$\omega' = \log_{10} \omega. \tag{4-4}$$

Then **WIAE**, the weighted integral absolute error criterion, is defined by this author as:

$$\text{WIAE} = \frac{1}{\omega'_{mat} - \omega'_{l.l.}} \int_{\omega'_{l.l.}}^{\omega'_{mat}} |H(j\omega') - M(j\omega')| d\omega', \tag{4-5}$$

where, $H(j\omega')$ and $M(j\omega')$ are the weighted frequency response of a closed-loop system and a model, and can be calculated from $H(j\omega)$ and $M(j\omega)$, respectively:

$$H(j\omega') = H(j\omega)|_{\omega=10^{\omega'}}, \tag{4-6$_a$}$$

$$M(j\omega') = M(j\omega)|_{\omega=10^{\omega'}}. \tag{4-6$_b$}$$

The upper limit ω'_{mat} is derived from the frequency range ω_{mat} over which the matching of $H(j\omega)$ to $M(j\omega)$ is conducted. The lower limit is zero frequency which can not be converted to a meaningful weighted frequency and therefore a more practical lower frequency limit $\omega_{l.l.}$ is chosen for the integral. In the various design examples of this chapter, there is no significant deviation of the frequency response matching when $\omega < 10^{-4}\ rad/s$. Thus $\omega_{l.l.}$ is assigned to 10^{-4} and the corresponding $\omega'_{l.l.}$ is -4.

The integral absolute error is divided by $\omega'_{mat} - \omega'_{l.l.}$ so that the matching errors of designs with different sampling frequencies can be compared.

Ideally, the design of a digital controller is optimal if the **WIAE** of the closed-loop system is minimum. However, some exceptions should be borne in mind. Firstly, the design studies in this chapter are based on the discrete frequency response that does not carry the information about the inter-sampling performance of the closed-loop system. Secondly, when the design involves very low sampling frequencies, the high accuracy

of matching may not guarantee the closed-loop stability though the model is stable. Furthermore, the practical implementation of the resulting digital controller and all aspects of the closed-loop performance need to be considered. It is therefore necessary to check the continuous time responses as well.

(b) Simulation and assessment of time responses

The time responses at and between sampling instants are simulated by means of the method proposed by Franklin and Powell [19]. According to their derivation, the Laplace transform of the time response of the closed-loop digital control system defined in Fig. 4-1 is

$$Y(s) = R^*(s) \cdot \frac{D^*(s)}{1 + D^*(s)G_hG^*(s)} \cdot G_h(s)G(s) \ . \qquad (4-7)$$

The following are the transforms for a unit-step input signal and a zero-order hold, respectively:

$$R^*(s) = \frac{1}{1 - e^{-Ts}} \ , \qquad (4-8)$$

$$G_h(s) = \frac{1 - e^{-Ts}}{s} \ . \qquad (4-9)$$

Substitution of Eqs. (4-8) and (4-9) into Eq. (4-7) yields

$$Y(s) = \frac{D^*(s)}{1 + D^*(s)G_hG^*(s)} \cdot \frac{G(s)}{s} \ . \qquad (4-10)$$

The first term in Eq. (4-10) corresponds to a train of impulses, i.e.

$$\begin{aligned} \frac{D^*(s)}{1 + D^*(s)G_hG^*(s)} &= k_0 + k_1e^{-Ts} + k_2e^{-2Ts} + \cdots + k_ne^{-nTs} + \cdots \\ &= \sum_{i=0}^{\infty} k_ie^{-iTs} \ . \end{aligned} \qquad (4-11)$$

The values of $k_i, i = 0, 1, 2, \ldots$, can be determined by a long division. Thus, Eq. (4-10) may be rewritten as

$$\begin{aligned} Y(s) &= k_0\frac{G(s)}{s} + k_1e^{-Ts}\frac{G(s)}{s} + \cdots + k_ne^{-nTs}\frac{G(s)}{s} + \cdots \\ &= \sum_{i=0}^{\infty}(k_ie^{-iTs}\frac{G(s)}{s}) \ . \end{aligned} \qquad (4-12)$$

Let $y_g(t)$ be the inverse Laplace transform of $G(s)/s$, i.e.,

$$y_g(t) = L^{-1}\Big[\ \frac{G(s)}{s}\ \Big] \ . \qquad (4-13)$$

Then $y(t)$, the continuous unit-step response of the closed-loop system, can readily be obtained by taking the inverse Laplace transform of $Y(s)$ in Eq. (4-12), as follows:

$$\begin{aligned} y(t) &= L^{-1}[Y(s)] \\ &= \sum_{i=0}^{\infty} L^{-1}\Big[k_i \cdot \frac{G(s)}{s} \cdot e^{-iTs}\Big] \\ &= \sum_{i=0}^{\infty} k_i L^{-1}\Big[\frac{G(s)}{s} \cdot e^{-iTs}\Big] \qquad (4-14) \\ &= \sum_{i=0}^{\infty} k_i y_g(t-iT). \end{aligned}$$

The value of $y(t)$ at any time instant t_a, at or between sampling instants, is

$$y(t_a) = \sum_{i=0}^{n} k_i y_g(t_a - iT) \ , \qquad (4-15)$$

where n is an integer that satisfies

$$n \le \frac{t_a}{T} < (n+1) \ . \qquad (4-16)$$

The unit-step response $y(t)$ is evaluated in accordance with the performance specifications in section 4.1.3. A good design should give a smooth time response between sampling instants.

Consideration also has to be given to $U(kT)$, the output signal of the digital controller, because its performance is an important feature in assessing the practical feasibility of the design.

From Fig. 4-1, the z-transfer function of $U(kT)$ is

$$U(z) = R(z) \cdot \frac{D(z)}{1 + D(z)G_hG(z)} \ . \qquad (4-17)$$

Expanded in power series of z^{-1} , $U(z)$ can be expressed as

$$\begin{aligned} U(z) &= u_0 + u_1 z^{-1} + u_2 z^{-2} + \cdots + u_n z^{-n} + \cdots \\ &= \sum_{k=0}^{\infty} u_k z^{-k} \ . \end{aligned} \qquad (4-18)$$

Taking the inverse z-transform of both sides of Eq. (4-18) yields

$$U(kT) = \sum_{k=0}^{\infty} u_k \delta(t - kT) \ ; \qquad (4-19)$$

where,

$$\delta(t - kT) = \begin{cases} 1, & \text{if } t - kT = 0 \ ; \\ 0, & \text{otherwise.} \end{cases}$$

(c) Computational burden

The last factor to be considered in evaluation of the various methods is the computational burden. In addition to CPU time consumed in each design study, the preliminary work involved should be taken into account as well.

§4.2 Design studies of Group 1 —

Comparison of the various design methods

In this section, the design studies of Group 1 are presented. The studies are based on the design of a digital controller for plants I and II at sampling periods of 0.3, 0.5, 2.0 and 4.0 seconds recommended in Table 4-2. In order to minimize the influence of the difference between T and T_m, in these studies, specific frequency response models from Table 4-3 are assigned for each sampling period so that T_m is the same as T in each design. As a result, a comparison of various design methods is made and given at the end of section.

4.2.1 Designs for Plant I

(a) Choice of the sampling frequency and the models

As described in section 4.1.2, Plant I is an overdamped system. Thus theoretically the choice of sampling frequency is mainly the consideration of ω_b, the desired closed-loop bandwidth.

Design studies start with a sampling period $T = 0.5\ s$ for which ω_s is about 16 times ω_b; model $M_2(j\omega)$ is used as the ideal closed-loop frequency response model. The next design is based on a sampling period $T = 2.0\ s$ and on the model $M_3(j\omega)$. The final study is for the sampling frequency $\omega_s = 1.57\ rad/s$ ($T = 4.0\ s$), which is just twice ω_b, and is based on model $M_4(j\omega)$.

(b) Choice of the dominant data for the DDM method

For the DDM method, the dominant data points are determined from the ideal open-loop frequency response $M_{Qk}(j\omega)$ which in turn, is derived from the closed-loop frequency response model $M_k(j\omega)$,

$$M_{Qk}(j\omega) = \frac{M_k(j\omega)}{1 - M_k(j\omega)}\ , \qquad k = 1, 2, 3, 4. \tag{4-20}$$

Key frequency points $\omega_i, i = 1, 2, 3, 4$, tabulated in Table 4-4, are selected as ω_1 and ω_2 from the low frequency band ($\omega_i < 0.03\omega_b$), ω_3 from the gain cross-over frequency and ω_4 from the high frequency band ($0.9\omega_b < \omega_i < \omega_p$).

(c) Choice of the constraints and initial estimates for the SIM method

There are a few requirements on the initialization of the SIM method. The first step is to set out additional constraints imposed on the gain and pole-zero locations of a controller transfer function $D(z)$, if necessary. In the case of Plant I , the wider closed-loop bandwidth is required for a faster system transient response. This implies that the digital controller under design possesses a frequency response with high gain in the high frequency band near $\omega_s/2$ and so likely yields oscillatory output signal. From

Table 4-4 Dominant data point ω_i (rad/s) used in the design studies based on the DDM method

Plant	T (s)	ω_1	ω_2	ω_3	ω_4
I	0.5	0.002	0.02	0.6	2.6
	2.0	0.002	0.02	0.3	1.3
	4.0	0.0005	0.005	0.275	0.7
II	0.3	0.00033	0.0033	0.666	5.33
	0.5	0.002	0.02	0.6	2.6

the time domain analysis of discrete systems [1], such an oscillation can be avoided if the closed-loop poles are remote to the point $(-1, j0)$ in the z-plane. Therefore, constraints on the poles and zeros of $D(z)$ are needed to position the closed-loop poles away from the $(-1, j0)$ point. Unfortunately, no simple formula is available to choose these constraints. On the basis of the root-locus analysis, the use of "cut and try" procedures may be found helpful and rely on the designer's experience.

The choice of the constraints in this section is explained with one of the design studies, namely the design for Plant I with $T = 2.0\ s$. The poles and zeros of $D(z)G_hG(z)$ are drawn in Fig. 4-6, where the plant zero z_{p1} is very close to $(-1, j0)$. Without additional constraints, the optimization process places a pole slightly to the left of z_{p1} to cancel its influence as shown in Fig. 4-6(a). Consequently on the root locus from this pole to the infinite zero will be a closed-loop pole that is very close to $(-1, j0)$ and causes the oscillation. On the other hand, if two poles of $D(z)$, remote from $(-1, j0)$, are located between z_{p1} and another zero, then the shape of the root locus is changed and a pair of desired complex closed-loop poles can be obtained as shown in Fig. 4-6(b), which is done by the simplex optimization with constraints on the real pole-zero locations, $-0.5 < p_i \leq 1.0$ and $0 < z_i < 1.0$, i=1, 2, 3.

Constraints for designs at other sampling periods are determined following the same philosophy. They are all included in Table 4-5.

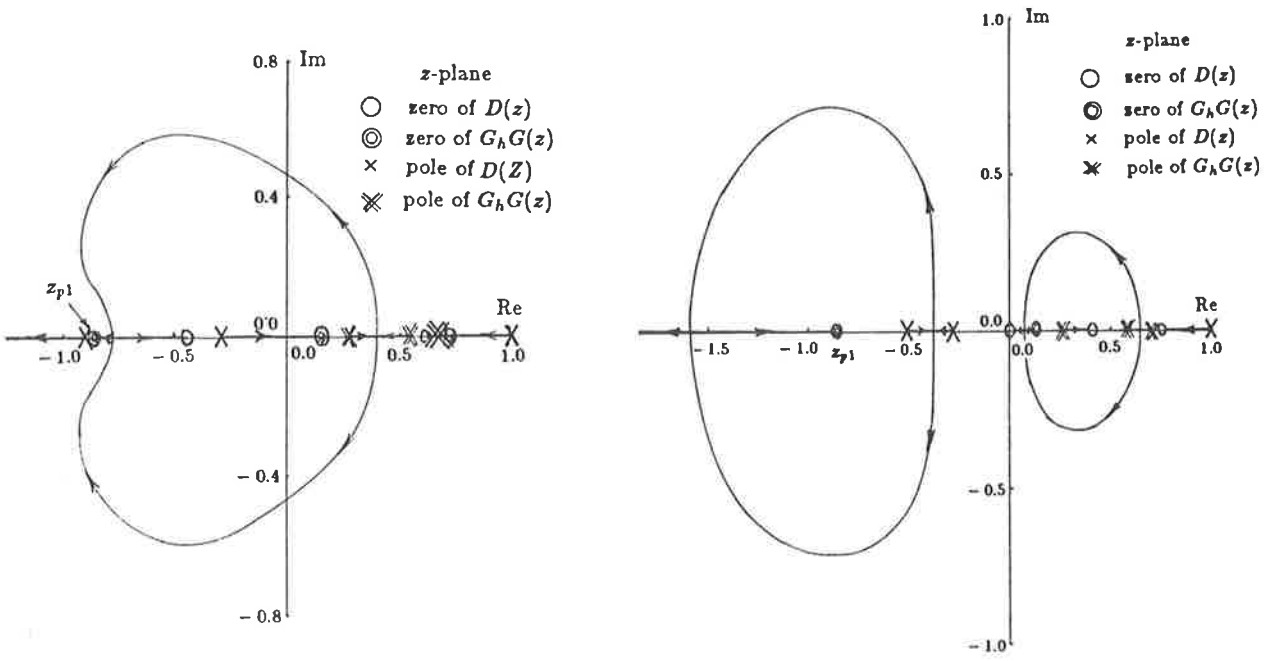

(a) without constraints *(b) with constraints*

Figure 4-6 Root loci of the control systems designed by the SIM method with and without constraints (Plant I , T=2.0 s)

Table 4-5 Constraints on the gain and pole-zero locations of $D(z)$ in the designs for Plant I based on the SIM method

T (s)	Pole p_i	Zero z_i	Gain x_0
0.5	$-0.7 \leq p_i \leq 1.0$	$-0.4 < z_i < 1.0$	$0.0 < x_0$
2.0	$-0.5 \leq p_i \leq 1.0$	$0.0 < z_i < 1.0$	$0.0 < x_0$
4.0	$-0.8 \leq p_i \leq 1.0$	$-0.4 < z_i < 1.0$	$0.0 < x_0 < 4.0$

The second task in the initialization of SIM is to give initial estimates for optimal poles and zeros of $D(z)$. To assess the convergency of the simplex optimization algorithm, all design studies start with a set of arbitrarily-assigned initial values, in which all 3 poles and 3 zeros of $D(z)$ are located at the same point $(0.5, j0)$ in the z-plane. The initial gain x_0 is 10 for $T = 0.5$ s and 2.0 s. For $T = 4.0$ s, $x_0 = 3$ is chosen to satisfy the constraints employed.

(d) Results

Table 4-6 gives the coefficients of the controller transfer functions determined by the various frequency matching design methods (Table 4-6 also includes the design results for Plant II obtained from the following section 4.2.2.). The performance of the resulting closed-loop systems is then assessed by frequency and unit-step response simulation studies. The results of these studies are presented in Fig. 4-7 and 4-8. The values of the performance index **WIAE** for the various designs are compared in Fig. 4-9.

For the DDM, CCF and ICCF methods, the results reveal that the error in the frequency response matching decreases when the sampling frequency ω_s is reduced. In fact, for the designs based on DDM, CCF and ICCF methods with $T = 2.0$ and 4.0 s, all frequency response curves match the model response very closely. Consequently the ICCF gives the same result as the CCF does. As predicted by these excellent frequency response matching performances, the unit-step time responses of the designs based on the DDM, CCF and ICCF methods match those of the discrete models **at sampling instants** as if they were just direct copies. However, ripples on $y(t)$ between those sampling instants become increasingly large as ω_s decreases, until eventually the designs become unacceptable. These ripples are attributed to the oscillation of control signal $U(kT)$ at the input of plant (via a ZOH) as shown in Fig. 4-8.

Because of the constraints imposed on the pole-zero locations of $D(z)$, the designs based on the SIM method for T=2.0 and 4.0 s do not give close matching to the ideal frequency response. But the oscillation of the controller output is effectively minimized. As a result, the magnitude of ripples on $y(t)$ is reduced significantly.

In terms of the time response specification, all designs at $T = 0.5$ s are good. At T=2.0 s, only the design based on SIM meets all requirements of the specification except for peak time t_p being 1.5 s longer than the specified value 6 s. At T=4.0 s, none of the designs completely satisfy the specifications, though the design based on SIM gives a considerably better performance than the others do.

Table 4-6 Coefficients of the controller transfer functions in the design studies of Group 1

Plant	T	Design	$D(z) = \frac{x_0 z^3 + x_1 z^2 + x_2 z + x_3}{z3 + y_1 z^2 + y_2 z + y_3}$						
	(s)	Method	x_0	x_1	x_2	x_3	y_1	y_2	y_3
I	0.5	DDM	18.9879	−40.2125	25.7410	−4.3852	−1.3251	0.1248	0.2003
		CCF	22.2743	−33.5546	6.1884	5.4462	−0.4498	−0.9733	0.4231
		ICCF	22.2743	−33.5546	6.1884	5.4462	−0.4498	−0.9733	0.4231
		SIM	20.2325	−35.0593	14.0921	0.9635	−0.7748	−0.5576	0.3324
	2.0	DDM	9.0752	−6.9073	−2.2502	1.9217	0.2163	−0.9252	−0.2911
		CCF	9.0565	−7.2672	−1.8042	1.8340	0.1651	−0.9113	−0.2538
		ICCF	9.0565	−7.2672	−1.8042	1.8340	0.1651	−0.9113	−0.2538
		SIM	8.8567	−10.2338	2.7490	0.0	−0.2185	−0.6408	−0.1407
	4.0	DDM	4.8825	−4.0124	0.9039	−0.0394	−0.3382	−0.6667	0.0049
		CCF	4.8822	−3.9794	0.8772	−0.0338	−0.3315	−0.6689	0.0004
		ICCF	4.8822	−3.9794	0.8772	−0.0338	−0.3315	−0.6689	0.0004
		SIM	4.0	−2.6288	0.4009	−0.0141	−0.2020	−0.6388	−0.1592
II	0.3	DDM	0.0187	−0.0092	0.0092	−0.0084	−2.6874	2.3896	−0.7022
		CCF	0.0222	0.0140	0.0187	0.0043	−1.1675	−0.6393	0.8068
		ICCF	0.0176	−0.0065	0.0104	−0.0078	−2.5827	2.1848	−0.6021
		SIM	0.0165	0.0013	−0.0003	2.8×10^{-5}	−2.4760	1.9772	−0.5012
	0.5	DDM	0.0319	0.0218	−0.0054	−0.0027	−2.4333	1.9120	−0.4787
		CCF	0.0318	0.0212	−0.0063	−0.0036	−2.4536	1.9479	−0.4943
		ICCF	0.0317	0.0206	−0.0070	−0.0043	−2.4839	2.0088	−0.5249
		SIM	0.0312	0.0263	0.0011	−0.0007	−2.2702	1.5969	−0.3267

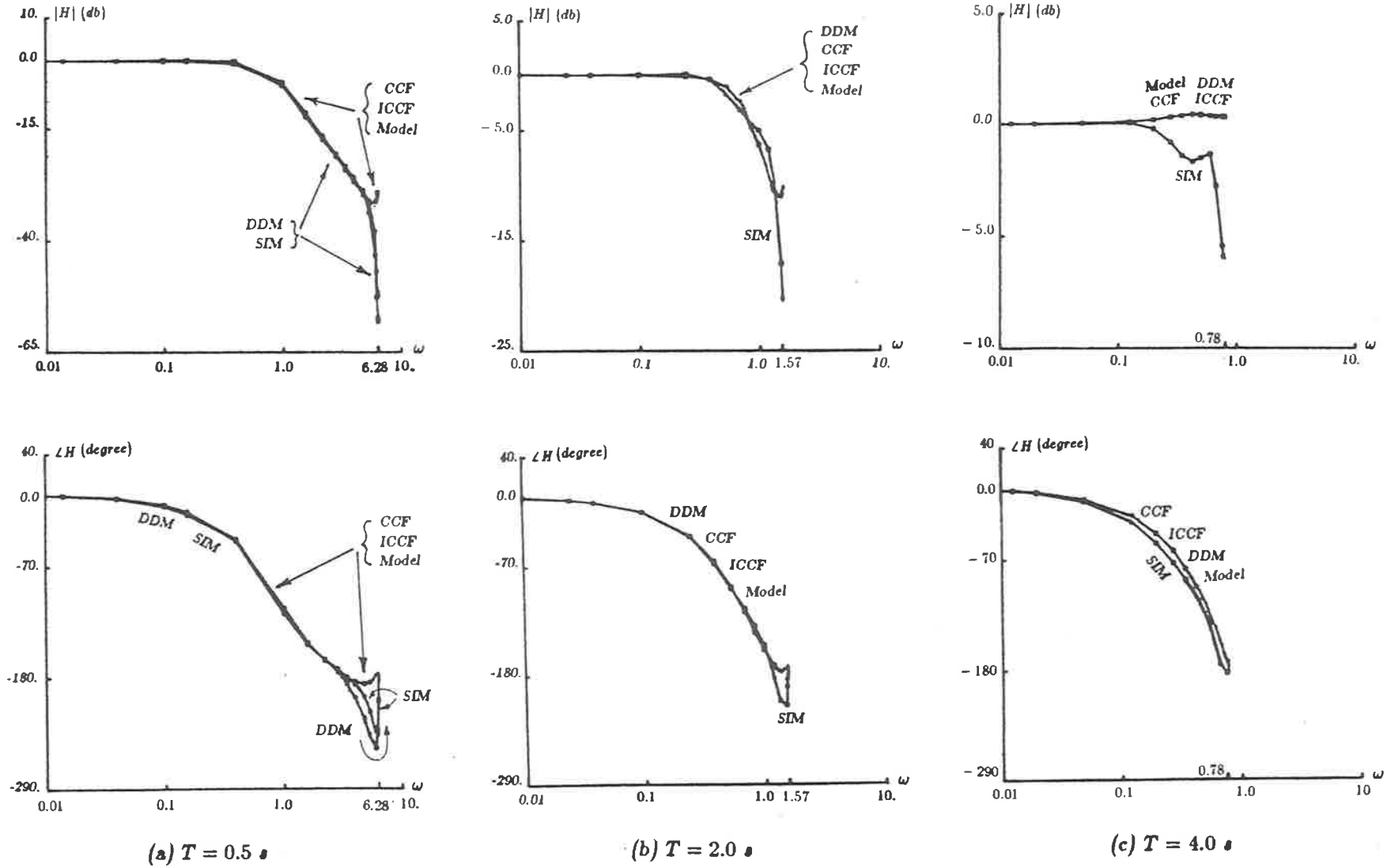

(a) $T = 0.5$ s (b) $T = 2.0$ s (c) $T = 4.0$ s

Figure 4-7 Frequency response of closed-loop systems, $H(j\omega)$, in the design studies of Group 1 for Plant I (ω in rad/s)

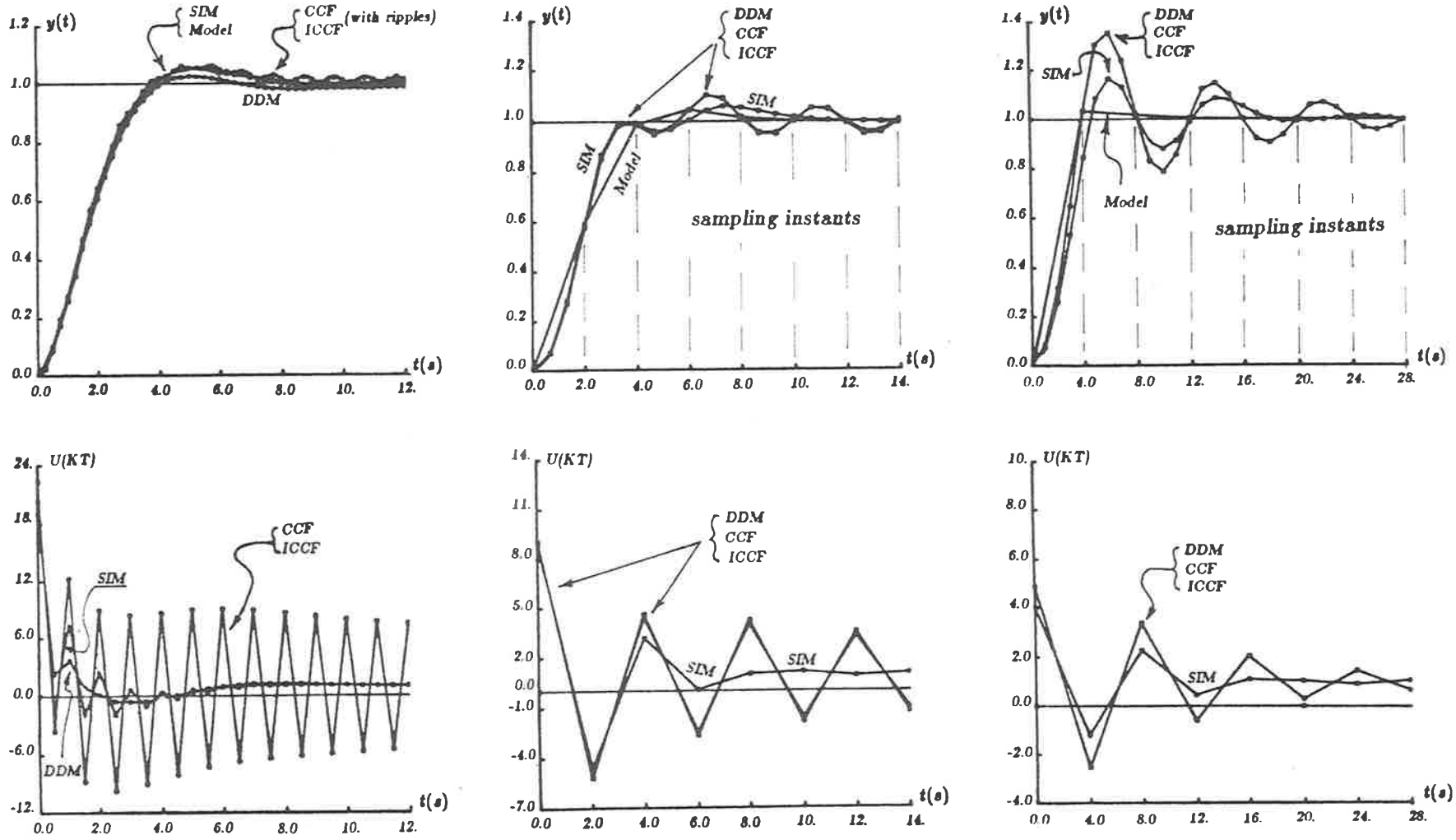

(a) $T = 0.5$ s

(b) $T = 2.0$ s

(c) $T = 4.0$ s

Figure 4-8 Unit-step response $y(t)$ and controller output $U(KT)$ of closed-loop systems in the design studies of Group 1 for Plant I

(Note that $U(KT)$ is a series of pulse signals connecting lines between which are drawn only for purposes of observation.)

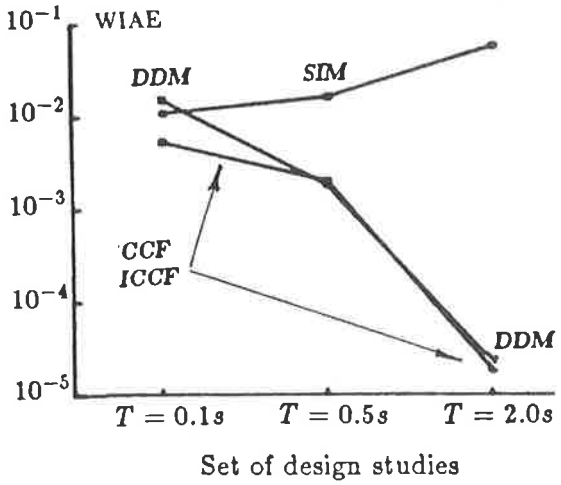

Figure 4-9 Values of WIAE of the closed-loop systems in the design studies of Group 1 for Plant I

4.2.2 Designs for Plant II

(a) Choice of the sampling frequency and the model

Plant II exhibits an underdamped response, the frequency of oscillations being ω_o=6 rad/s; this is a value well above the closed-loop bandwidth $\omega_b = 0.78$ rad/s. Thus ω_o replaces ω_b as the dominant factor determining the sampling period T. According to the conditions outlined in section 4.1.4 and Table 4-2(p.4-9), T=0.3 s (ω_s=21 rad/s) is the longest sampling period from the appropriate choices because the corresponding ω_s is merely 3.5 times ω_o (but 28 times ω_b). However, for the purpose of comparison, controller designs are carried out for $T = 0.5$ s ($\omega_s = 2\omega_o$) as well. The closed-loop frequency response models used in this part studies of Group 1 are therefore restricted to $M_1(j\omega)$ for $T = 0.3$ s, and $M_2(j\omega)$ for $T = 0.5$ s, as defined in Table 4-3(p.4-10).

(b) Choice of the dominant data for the DDM method

The key frequency points are selected from the open-loop response $M_{Qk}(j\omega)$ of Eq. (4-17) to provide the dominant data for DDM design; they are summarized in Table 4-4(p.4-16).

(c) Consideration of the constraints and the initial estimates for the SIM method

Fig. 4-10 shows the magnitudes of $M_{Q1}(j\omega)$, the open-loop frequency response model, and $G_hG(j\omega)$ for $T = 0.3\ s$, as well as that of desired controller frequency response $D(j\omega)$, which is derived from

$$D(j\omega) = \frac{M_{Q1}(j\omega)}{G_hG(j\omega)} \ . \qquad (4-21)$$

From these curves, it is clear that within the frequency band $0.1\omega_s < \omega < \omega_s/2$, the gain of the controller is below $-20\ db$, and so an overdamped control signal can be expected. For the designs based on the SIM method, therefore, no additional constraints are required on the gain and pole-zero locations of $D(z)$. Initial estimates for these poles and zeros are identical with those arbitrarily-assigned to the designs for Plant I , i.e., all at the point $(0.5, j0)$ in the z-plane. The initial value of gain x_o is set to 0.02.

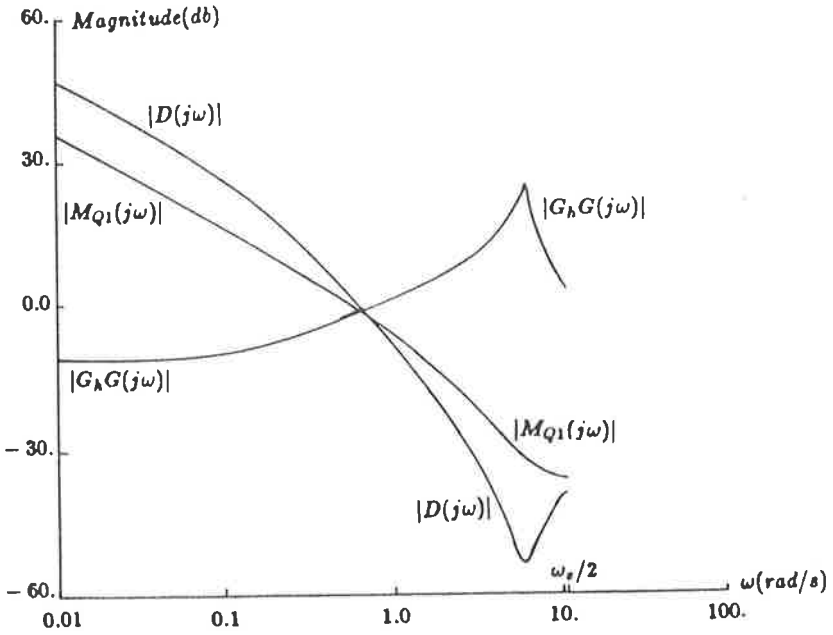

Figure 4-10 Magnitude of frequency responses of Plant II , the model M_{Q1} and the desired digital controller $D(z)$ with T=0.3 s

(d) Results

Once the preparatory work is done, the coefficients of the discrete controller transfer function (see Table 4-6, p.4-20) are readily obtained by running the appropriate computer-aided design programs. The frequency and unit-step time response simulations are presented in Fig. 4-11 and 4-12, respectively. The results based on the ICCF method at T=0.3 s and 0.5 s are from the second iteration. Fig. 4-13 compares the values of WIAE of various designs.

For the DDM, ICCF and SIM methods, it can be seen from Fig. 4-11(a) that, at T=0.3 s, the closed-loop frequency responses of designs agree closely with the model within the frequency band $\omega < 2.0\ rad/s$. From ω=2.0 to $\omega=\omega_p$=6.28, the closed-loop responses diverge from the model in different degrees. However, because their magnitudes in this band are lower than $-20\ db$, the divergences have no significant impact on the corresponding time responses as shown in Fig. 4-12(a). Moreover, as expected, output signals of the resulting controllers are overdamped and follow an almost identical trajectory.

On the other hand, the CCF method yields a closed-loop frequency response with a $2db$ resonant peak at $\omega \approx 0.4\ rad/s$ ($\approx 0.02\omega_s$). Its step response correspondingly presents an excessive overshoot of 18% and a retarded settling time of 12 seconds. The poor performance of CCF at T=0.3 s is due to the error-producing effect of the weighting factor $|P_H(j\omega)|^2$ contained in the objective function E (see section 2.3.3). The weighting factor by which E is multiplied becomes extremely small when $\omega < 0.03\omega_s$. A large matching error is thus introduced in as a resonant peak appears in this frequency band shown in Fig. 4-11(a). By means of the ICCF method, the distortion due to the weighting factor is compensated and the matching error is reduced to nearly the minimum after just one iteration.

At T=0.5 s, each design method works well as all closed-loop frequency responses closely match that of the model in Fig. 4-11(b). Occurrence of ripples on $y(t)$ in Fig. 4-

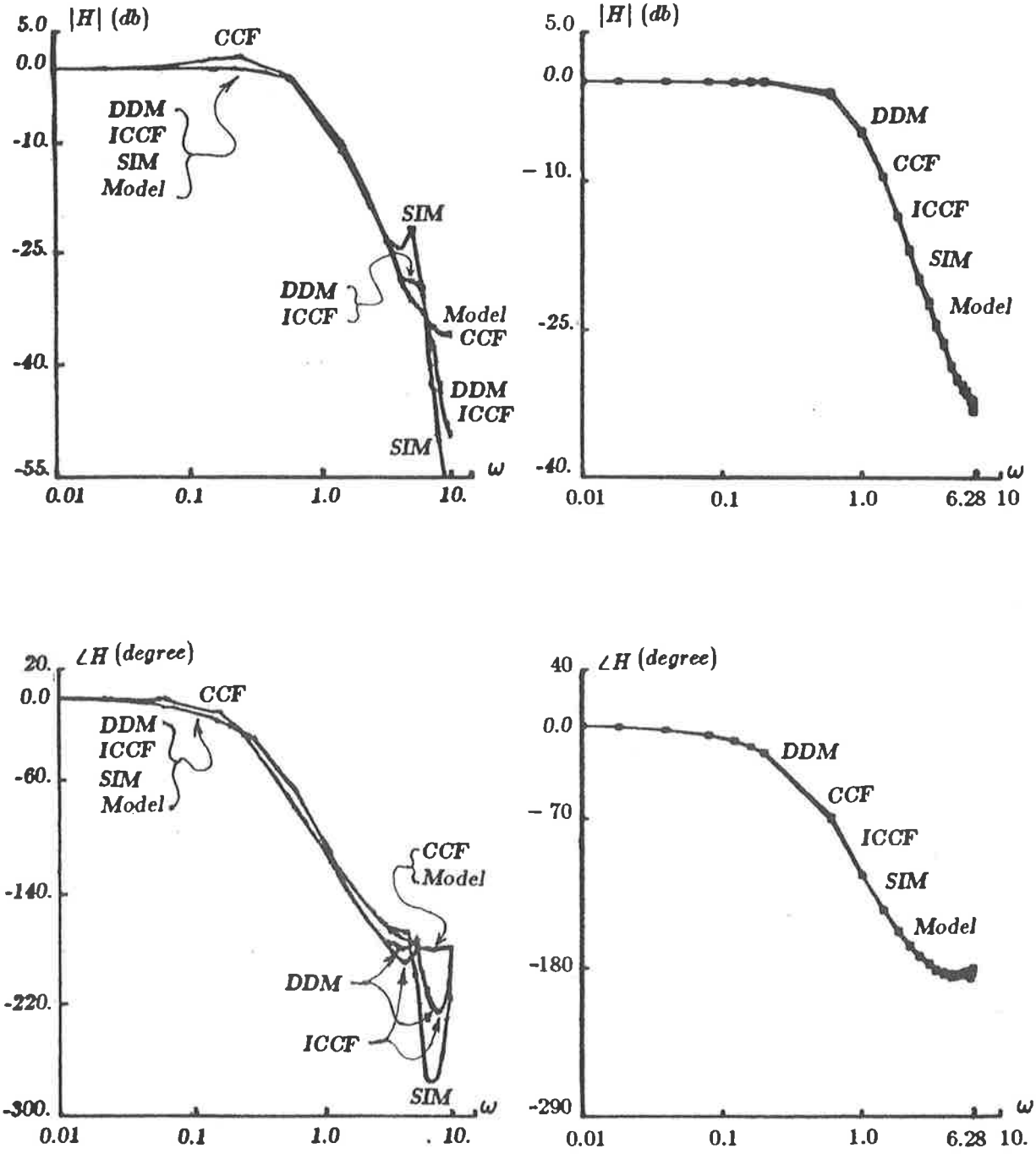

(a) $T = 0.3$ s

(b) $T = 0.5$ s

Figure 4-11 **Frequency response of closed-loop systems, $H(j\omega)$, in the design studies of Group 1 for Plant II** (ω in rad/s)

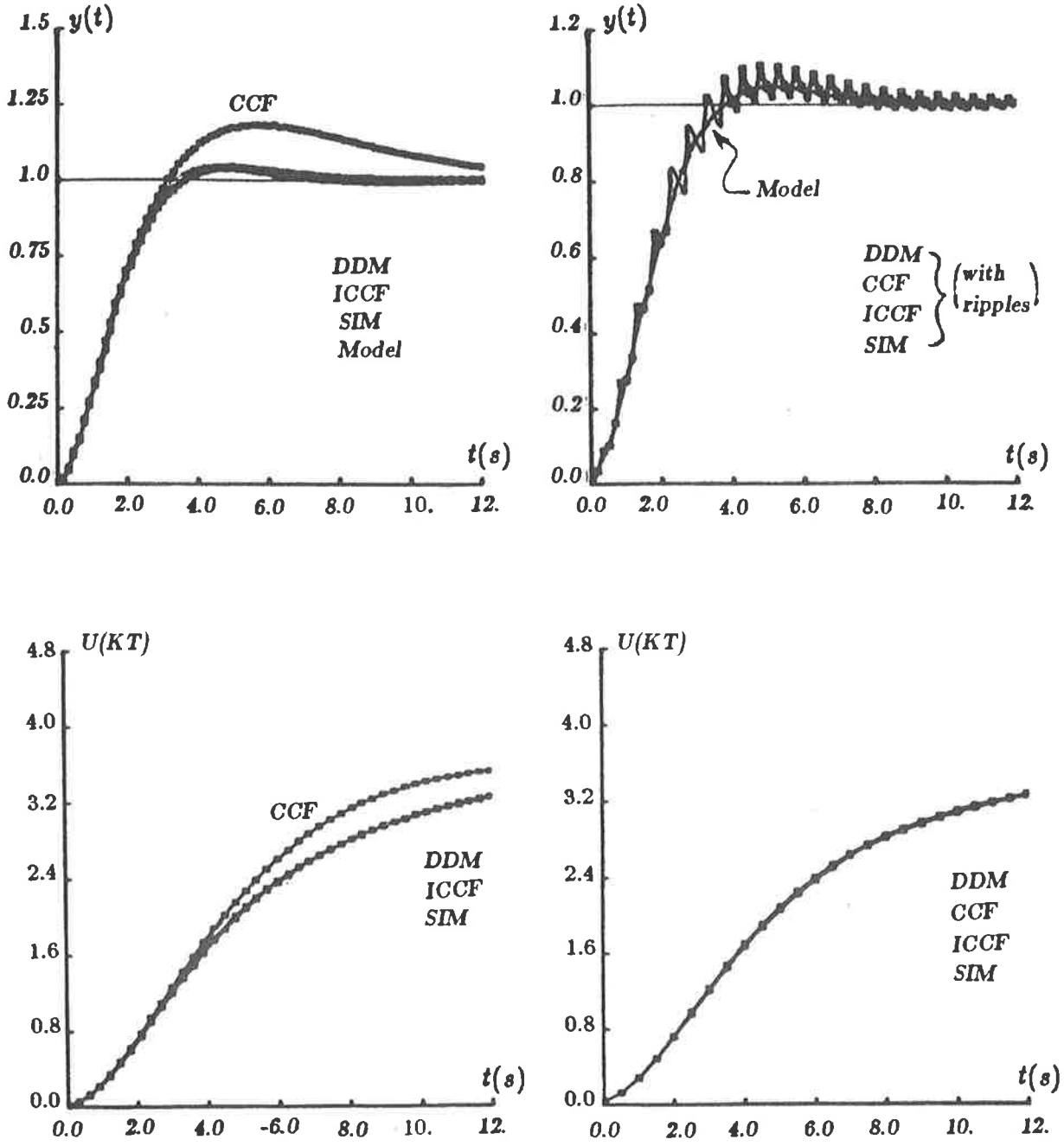

(a) $T = 0.3$ *s*

(b) $T = 0.5$ *s*

Figure 4-12 Unit-step response $y(t)$ *and controller output* $U(KT)$ *of closed-loop systems in the design studies of Group 1 for Plant II . (Note that* $U(KT)$ *is a series of pulse signals connecting lines between which are drawn only for purposes of observation.)*

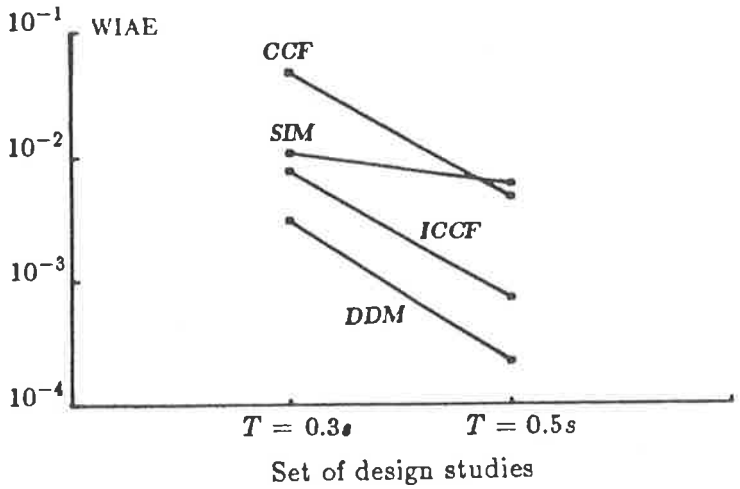

Figure 4-13 Values of WIAE of the closed-loop systems in the design studies of Group 1 for Plant II

12(b) for all designs results from a slow sampling frequency relative to ω_o ($\omega_s \approx 2\omega_o$). This verifies the analysis made in section 4.1.4.

It is important to note that, with T=0.5s, the ripples on $y(t)$ of Plant II in Fig. 4-12(b) look like those on $y(t)$ of Plant I in Fig. 4-8(a) but come for different reasons. The former is due to the oscillatory nature of Plant II and the latter the oscillatory nature of control signals.

4.2.3 Discussions of the simulation results

On the basis of the results from 20 various design studies, this section will discuss some important factors in the application of the frequency response matching design methods. Those of interest include the sampling frequency ω_s, the dynamic characteristic of plant, the feasibility of resulting controllers and the computational burden.

It must be understood that the results are obtained from studies only of the two types of plant specified in section 4.1.2. Thus their validity may be restricted to application to similar types of plant.

(a) Influence of the sampling frequency ω_s

A set of sampling frequencies from 2 to 27 times the closed-loop bandwidth ω_b

has been studied. It is obvious from the comparison of WIAE values in Fig. 4-9 and 4-13 that the matching error of a closed-loop frequency response to a model decreases as ω_s becomes lower, provided no constraints are imposed on controller parameters. This is mainly because the frequency response models tend to be flatter as ω_s decreases. In fact in the time domain, a response resulting from a lower ω_s needs to match fewer specified points than that from a higher ω_s does within a certain time interval. However, such success in frequency matching with a low sampling frequency is achieved at the risk of deterioration of time responses. Ripples on the time response are generally larger for wider sampling intervals as shown in Fig. 4-8 and 4-12, though the responses at sampling instants are accurately matched to the models.

The discrepancy between the frequency and time response matching is a major disadvantage of the technique in which a dummy discrete plant is used instead of the continuous one. An alternative is therefore suggested in Chapter V on the basis of the hybrid frequency response analysis.

(b) Influence of the dynamic characteristic of plants

The comparison of Fig. 4-9 with Fig. 4-13 reveals that the dynamic characteristics of the two types of plants used in the assessment of design methods do not affect the accuracy of frequency response matching significantly. This results from the ability of the mathematical algorithms in these methods to derive various types of controller transfer functions according to given specifications and plants. However, the dynamic characteristic of a plant does have a strong influence on the quality of time response of both closed-loop system and digital controller. Though the closed-loop system may have a satisfactory frequency response obtained from appropriate pole-zero compensations, the distribution of these poles and zeros between the plant and controller can yield unsatisfatory time responses. For instance, when designing a digital controller for an overdamped plant, attention should be paid to the output signal of a controller. On the other hand, in the design for an underdamped plant, the frequency of plant oscillation

ω_o may require a sampling frequency ω_s much higher than that based on the closed-loop bandwidth. Otherwise the ripples on the system output may become unavoidable and intolerable.

(c) constraints on the controller parameters

In the previous frequency matching design methods such as DDM and CCF, the only objective in the design process is to minimize the frequency matching error between the model and closed-loop system. No constraints are imposed on the parameters of resulting controllers. This simplifies the synthesis, but the results may be unsatisfactory for practical applications. A control engineer may have to redesign a resulting control function because of either an excessively high signal amplitude or an oscillatory response at the controller output. Fig. 4-7(a) and Fig. 4-8(a) furnish a convincing example in which the frequency response of a closed-loop system, which incorporates a digital controller designed by the ICCF method, accurately match the model response. However the large magnitude and oscillatory nature of $U(KT)$ are usually found quite unsatisfactory. This example is not exceptional as similar performances can be observed in case of T=2.0 and 4.0 s for the designs by the DDM, CCF and ICCF methods. It can be concluded, therefore, that the design methods only using frequency response matching criteria are unsuitable if they result in controllers with large amplitude oscillatory responses. The controller characteristic should also be considered in the design process.

The contribution of this author is the development of a new design method SIM for overcoming the above deficiencies. SIM enables the designer to confine the gain, poles and zeros of the controller, and indirectly the closed-loop poles and zeros, into some appropriate region in the complex z-plane so that a trade off between the accuracy of frequency matching and the characteristic of a required control signal can be achieved. The designs by SIM shown in Fig. 4-7 and 4-8 successfully demonstrate this unique advantage.

(d) Computational burden

The CPU time (for VAX-11/780) consumed in the design studies is used to estimate the computational burden. For the various design methods, Table 4-7 lists the CPU time taken in a set of design studies for a digital controller for Plant I with T=0.5 second. These values, however, can only serve as rough estimation because the computational burden of the CCF, ICCF and SIM methods depends on the problem under study in various degrees. For example, in the CCF and ICCF method the time required by numerical integrations is highly dependent of the amplitude of integrands.

In general, the DDM method needs the minimal computation as the parameters of the linear equations (see Eq. (2-16)) to be solved can be readily determined. The CCF method with integral operations consumes tens of CPU seconds and is comparable with the SIM method that involves iterative calculations. A heavy burden is imposed by the ICCF method which may take over one hundred CPU seconds.

Except for the SIM method, all frequency matching design methods are thoroughly computerized, and need the minimal preparatory work. When applied to an overdamped plant, the SIM method employs some constraints that may require additional analytical work.

Table 4-7 CPU time consumption of the various design methods in the design studies for Plant I with $T = 0.5$ s of Group 1

Design Method	Number of Iterations	CPU Time(s)
DDM	—	0.3 ~ 0.4
CCF	—	22
ICCF	2	97
ICCF	3	150
SIM	300 ~ 1000	10 ~ 30

4.2.4 Comparison of the design methods

A comparison is made based on the performances of the DDM, CCF, ICCF and SIM methods in the design studies of Group 1. Table 4-8 summarizes the results in a qualitative manner. Since the examples are chosen to represent some typical applications, the author hopes that the table would provide a useful guideline in practice, though the types of plants and the performance specifications from which the results are derived should be borne in mind when refering to a particular case.

4.2.5 Conclusions

In this section, a comparative study has been presented. Four frequency matching design methods were assessed by means of the design of a digital controller for two types of plants with the sampling frequencies chosen from 2 to 27 times ω_b. Some important factors regarding the implementation of the methods were discussed. The result of comparison was given in a tabular form that provides a guideline for the application of these methods.

The frequency response matching design methods can be applied to different types of plants, e.g., an overdamped or underdamped plant. The decrease of sampling frequency may reduce the frequency matching error but increase the ripples between sampling instants. The simplicity and the light computation load of the DDM method distinguish it from the others. The new ICCF method proves its superiority over the CCF method by improving the matching accuracy at high sampling frequencies. Another new method SIM can be employed for designs at low sampling frequencies at which the results of the other methods fail to meet the performance specifications.

Table 4-8 Comparison of the frequency matching design methods

Feature	Frequency Response Matching Design Methods			
	DDM	***CCF***	***ICCF***	***SIM***
Matching Accuracy	high	high but dependent on ω_s	high	high but dependent on constraints
Lower Limit* on the Sampling Frequency (ω_s/ω_b)	≈ 15	≈ 15	≈ 15	≈ 4
Capability to Impose Constraints on Controllers	none	none	none	pole/zero locations & value of gain
Type of Plants†	underdamped	underdamped	underdamped	overdamped
Initialization	simple	simple	simple	additional analysis needed if constraints are required
Computational Burden	light	medium	heavy	medium
Comments		not suitable if $\omega_s > 25\omega_b$		

†These are plants to which the method can be MOST suitably applied.

*** with the design specifications being satisfied.**

§4.3 Design studies of Group 2 — Effect of the discrepancy between the primary frequency range of the model and that of the closed-loop system on the frequency matching

The primary frequency range ω_p of a discrete system, as defined in section 2.1, is the frequency band from 0 to $\omega_s/2$, one half of the sampling frequency. The term *primary* refers to the fact that any part of the frequency response of a discrete system can be constructed from the frequency response for the primary range because the response for $\omega_s/2 \leq \omega \leq \omega_s$ in the complex plane is the mirror image of that for $0 \leq \omega \leq \omega_s/2$ about the real axis, and the response repeats itself every $n\omega_s \leq \omega \leq (n+1)\omega_s, n = 0, 1, 2, \ldots$ [1].

It has been pointed out in section 3.1 that one way to define a frequency response model is to use the frequency response of a previously designed closed-loop system which possesses the desired dynamic performance. Such a system may be equipped with a discrete or continuous controller. The most common example is converting an existing analogue controller into an equivalent digital controller.

The case of the sampling period of an existing discrete system, represented by T_m, being the same as that of the system under design, represented by T, has been discussed in section 4.2. If, however, $T \neq T_m$, then there is a discrepancy between the primary frequency range of the existing system, i.e., the frequency response model, and that of the system under design. In particular, this is always true when an existing controller is analogue because its primary frequency range is infinite in the sense that its "sampling frequency" is infinitely fast.

Fig. 4-14 shows the magnitude of frequency responses of three arbitrarily-selected discrete systems I , II and III , with different sampling periods $T_1 < T_2 < T_3$; the corresponding primary frequency ranges are $\omega_{p1} > \omega_{p2} > \omega_{p3}$, respectively, where $\omega_{pi} = \omega_{si}/2 = \pi/T_i$. Suppose that system II with $T_2 = 0.5\ s$ is the model for the closed-loop system. Digital controllers are to be designed for the systems I and III with $T_1 = 0.1\ s$ and $T_3 = 2.0\ s$ respectively so that their closed-loop frequency responses

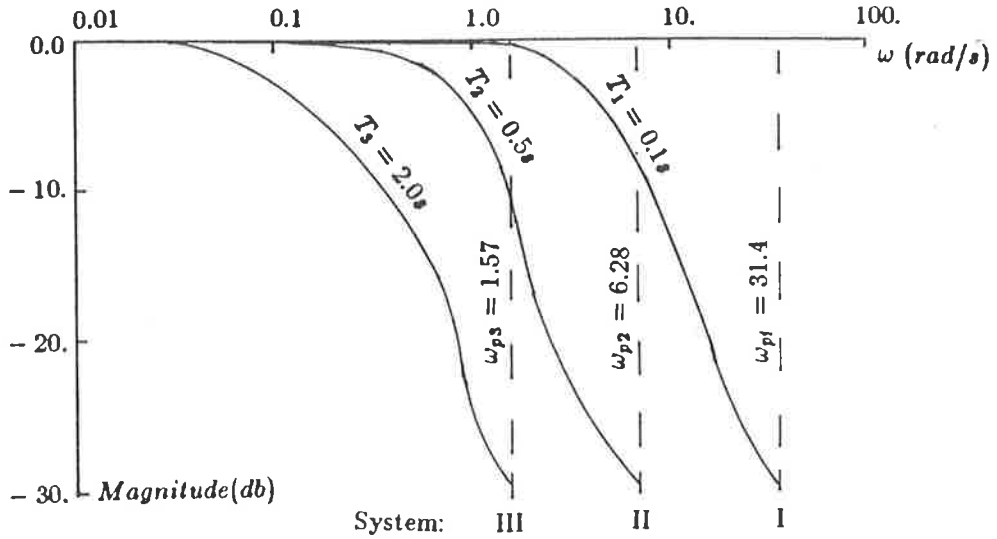

Figure 4-14 Magnitudes of the frequency responses of arbitrarily-selected discrete systems with different primary frequency ranges due to the selection of different sampling periods

will match that of system II . It is evident that system III can only match a part of the frequency response of the model; for system I , the section of primary frequency response from ω_{p2} to ω_{p1} is not defined by the model. In other words, no matter how sophisticated the digital controller is, there must be some degree of distortion in matching. Thus the design studies of Group 2 is devoted to the investigation of the effect of the above-mentioned distortion on the dynamic characteristics of closed-loop systems under design.

In the following section 4.3.1, Plant I is compensated at different sampling periods of $0.1, 0.5$ and 2.0 s to match the frequency response given by the model M_2 with $T_m = 0.5$ s (see Table 4-3, p. 4-10). Section 4.3.2 deals with the compensation of Plant II , the designs of which are also based on M_2 with $T_m = 0.5$ s; the sampling periods tested are $T = 0.1$ and 0.5 s which, as discussed in section 4.1.4, are determined by ω_o, the frequency of oscillation of the open-loop plant. The use of a continuous system frequency response as a model for designing a discrete system is treated in section 4.3.3, followed by discussions and conclusions drawn from the results of these design studies.

Because the purpose of these studies is to assess the effect of differences in the

primary frequency ranges upon the matching accuracy and system performances, only the ICCF method is used in the studies for its relatively high accuracy, and its consistent result without intervention of other factors such as the selection of key points in the DDM method and the initial conditions in the SIM method.

4.3.1 Design studies based on Plant I

Three digital controllers are synthesized for Plant I at three sampling periods so that the frequency responses of the closed-loop systems match the desired frequency response derived from model M_2 with $T_m = 0.5\ s$. These sampling periods are summarized in Table 4-9, where ω_{pm} is defined as $\omega_{pm} = \pi/T_m$. The ratio σ, defined as $\sigma = \dfrac{\omega_p}{\omega_{pm}} = \dfrac{T_m}{T}$, decreases from 5 to 0.25 when the sampling period increases from 0.1 to 2.0 s.

Table 4-9 Sampling period T selected for the design studies of Group 2

T	T_m	ω_p	ω_{pm}	σ
0.1	0.5	31.4	6.28	5.0
0.5	0.5	6.28	6.28	1.0
2.0	0.5	1.57	6.28	0.25
T is in seconds and ω in rad/s.				

The design studies, based on the ICCF method, yield the values for the coefficients of the discrete transfer function of the digital controller given in Table 4-10. In Fig. 4-15(a), the frequency responses of resulting closed-loop systems are shown, together with that of the model. The unit-step time response $y(t)$ and controller output $U(KT)$ are drawn in Fig. 4-15(b). The performance index of frequency matching, WIAE, is shown in Fig. 4-16.

From the simulation results, it is clear that the closest matching is achieved with $T = 0.5\ s$ and $\sigma = 1.0$, that is, when the model and the system under design have

Table 4-10 Coefficients of the controller transfer functions in the design studies of Group 2

Plant	T	Model	$D(z) = \frac{x_0 z^3 + x_1 z^2 + x_2 z + x_3}{z^3 + y_1 z^2 + y_2 z + y_3}$						
	(s)		x_0	x_1	x_2	x_3	y_1	y_2	y_3
I	0.1	M_2*	15.2127	−45.0907	44.5527	−14.6747	−2.8725	2.7454	−0.8729
	0.5		22.2743	−33.5546	6.1884	5.4462	−0.4498	−0.9733	0.4231
	2.0		25.5931	16.6836	−51.4077	19.1605	3.8819	−1.3233	−3.5586
II	0.1		0.0060	−0.0134	0.0117	−0.0037	−2.8379	2.6786	−0.8407
	0.5		0.0317	0.0206	−0.0070	−0.0043	−2.4839	2.0088	−0.5249
I	0.5	M_c†	25.8380	−34.1643	−1.0566	9.7831	−0.2980	−0.9724	0.2704
	2.0		31.8623	21.3322	−66.7114	24.9364	4.3297	−1.1729	−4.1568

*M_2–discrete transfer function with $T_m = 0.5s$.

†M_c–continuous transfer function.

the identical primary frequency range. With $\sigma = 5.0$ ($T = 0.1$ s), the matching error becomes larger but is still acceptable. Note that the undefined section of the frequency response from $\omega_{pm} = 6.28$ to $\omega_p = 31.4$ has the magnitude well below -30 db and thus does not affect the system dynamic performance significantly. On the other hand, when $\sigma = 0.25$ ($T = 2.0$ s), the closed-loop frequency response $H(j\omega)$ matches the ideal frequency response $M_2(j\omega)$ very closely from 0 to $0.85\omega_p \approx 1.3$; only within the range $0.85\omega_{p3} < \omega < \omega_p = 1.57$, $H(j\omega)$ slightly diverges from $M_2(j\omega)$, as is shown in Fig. 4-15(a). Unfortunately, it is this narrow frequency band in which the frequency response proves critical to the system performance; in fact, the design at $T = 2.0$ s results in an unstable system.

4.3.2 Design studies based on Plant II

The same discrete frequency response model, $M_2(j\omega)$ with $T_m = 0.5$ s, is adopted

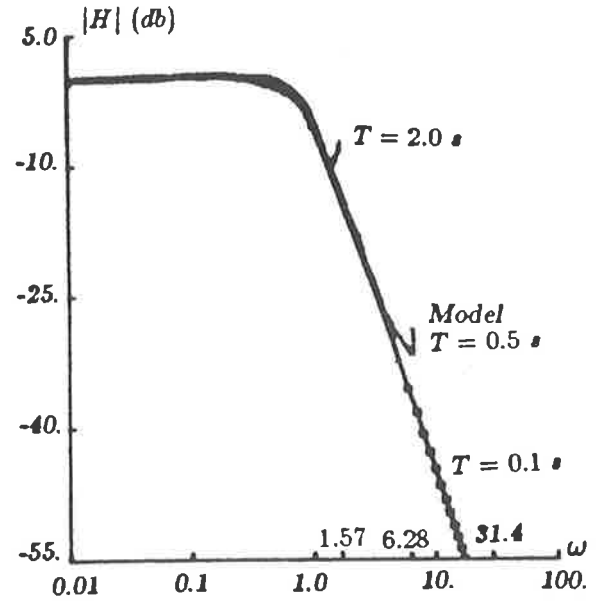

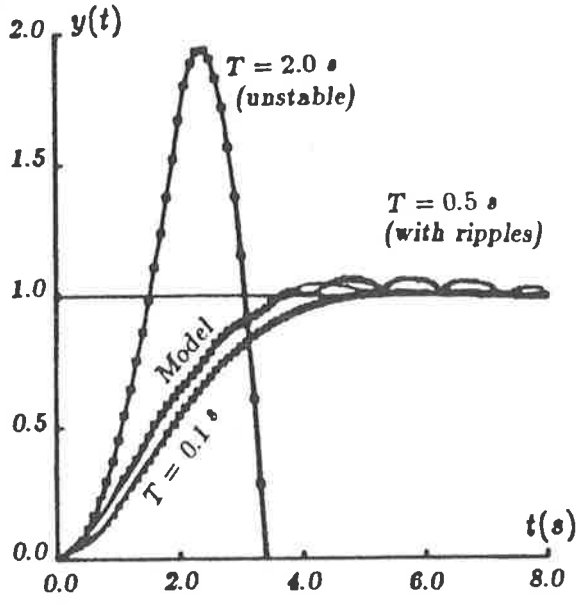

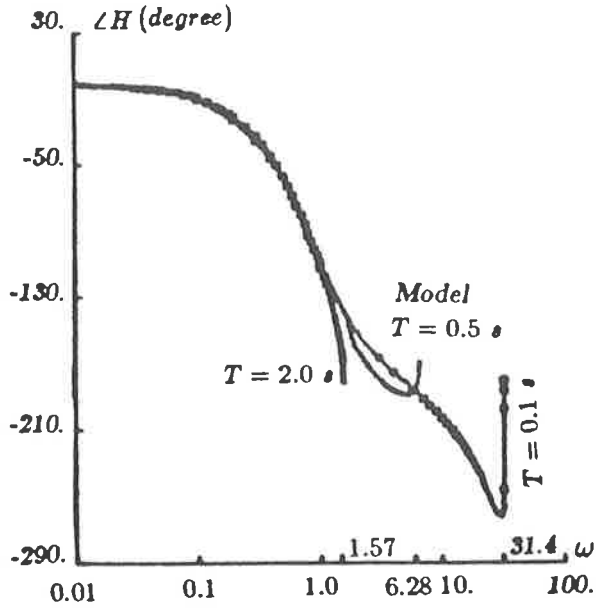

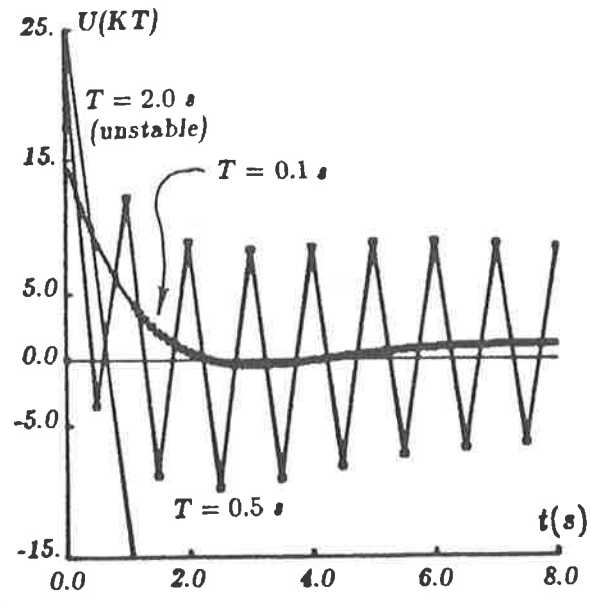

(a) Frequency response $H(j\omega)$ (ω in rad/s)

(b) Unit-step response $y(t)$ and controller output $U(KT)$

Figure 4-15 Frequency and time responses of the closed-loop systems in the design studies of Group 2 for Plant I designed by the ICCF method (Note that $U(KT)$ is a series of pulse signals connecting lines between which are drawn only for purposes of observation.)

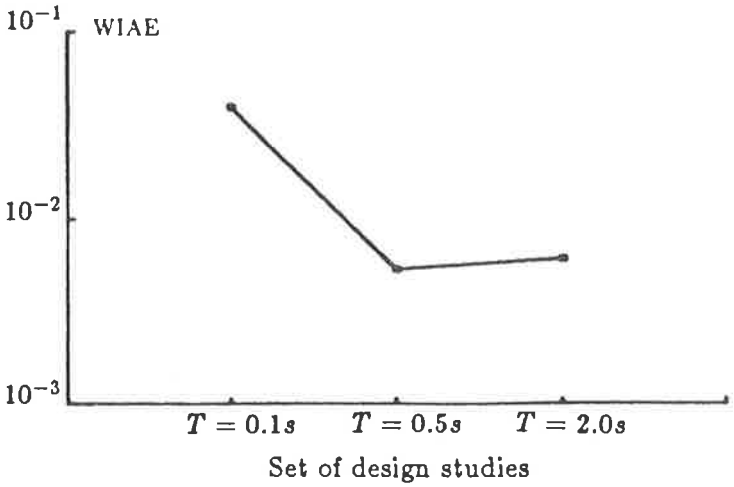

Figure 4-16 Values of WIAE of the closed-loop systems in the design studies of Group 2 for Plant I , designed by the ICCF method

for compensation of Plant II . Two sampling periods used in the studies are $T = 0.1$ and 0.5 s with $\sigma = 0.5$ and 1.0, respectively.

Again by using the ICCF method, two discrete transfer functions are obtained for the digital controller and are shown in Table 4-10. The frequency and time responses of the closed-loop systems in which they are incorporated are drawn in Fig. 4-17. Fig. 4-18 shows the values of matching performance index WIAE of these designs.

As the primary frequency ranges of the systems under design are either larger than or equal to that of the model, the matching performances in both domains are excellent. The only exception is ripples that exist in the time response of the design with $T = 0.5$ s for the reason discussed in section 4.1.4.

4.3.3 Design studies based on matching a continuous frequency response for Plant I

A continuous frequency response in transfer function form $M_c(s)$ is used as a model for designs based on the frequency response matching method. The purpose for this choice is to show how the inevitable difference between the primary frequency range of the closed-loop system under design and that of the continuous model affects the matching performance.

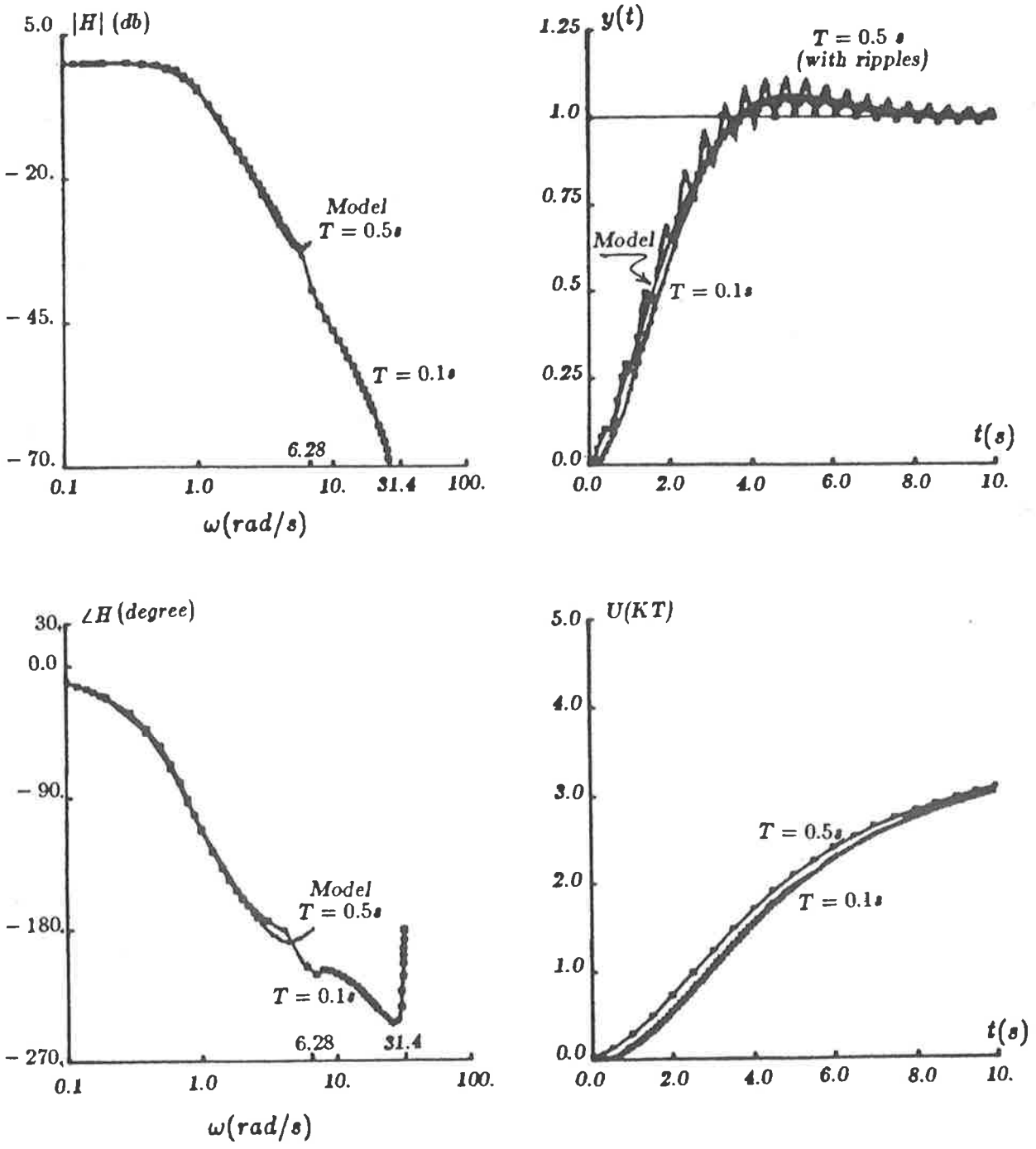

(a) Frequency response $H(j\omega)$

(b) Unit-step response $y(t)$ and controller output $U(KT)$

Figure 4-17 Frequency and time responses of the closed-loop systems in the design studies of Group 2 for Plant II , designed by the ICCF method **(Note that $U(KT)$ is a series of pulse signals connecting lines between which are drawn only for purposes of observation.)**

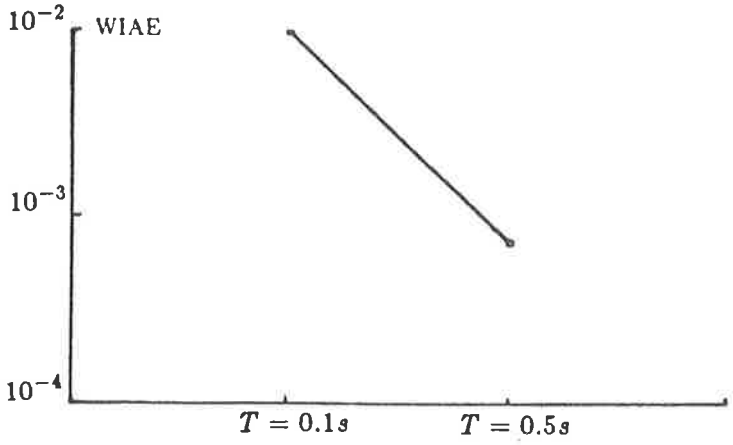

Figure 4-18 Values of WIAE of the closed-loop systems in the design studies of Group 2 for Plant II , designed by the ICCF method

Assume for purposes of comparison that a closed-loop continuous model $M_c(s)$ has the same bandwidth ($\omega_b = 0.78\ rad/s$) as that specified for the discrete model $M_2(j\omega)$, and has a similar unit-step time response to that for the model $M_2(z)$ (with $T_m = 0.5\ s$). Fig. 4-19 shows the similarity of unit-step responses of both discrete and continuous models $M_2(z)$ and $M_c(s)$ at sampling instants. The open-loop transfer function of $M_c(s)$ is

$$M_{Qc}(s) = \frac{150s^3 + 216s^2 + 73.02s + 7.02}{26.25s^6 + 216.625s^5 + 547.65s^4 + 444.075s^3 + 130.1s^2 + 12.3s}. \qquad (4-22)$$

Thus the closed-loop continuous frequency response of the model is

$$M_c(j\omega) = M_c(s)|_{s=j\omega} = \left.\frac{M_{Qc}(s)}{1 + M_{Qc}(s)}\right|_{s=j\omega}. \qquad (4-23)$$

Based on the continuous model $M_c(j\omega)$, design studies for Plant I are carried out for sampling periods of 0.5 and 2.0 s by means of the ICCF method. The coefficients of the discrete transfer functions of the digital controller are calculated and given in Table 4-10, p. 4-37. Simulation results for these designs are presented in Fig. 4-20, together with those of the continuous model. Fig. 4-21 shows the values of WIAE of the resulting closed-loop systems.

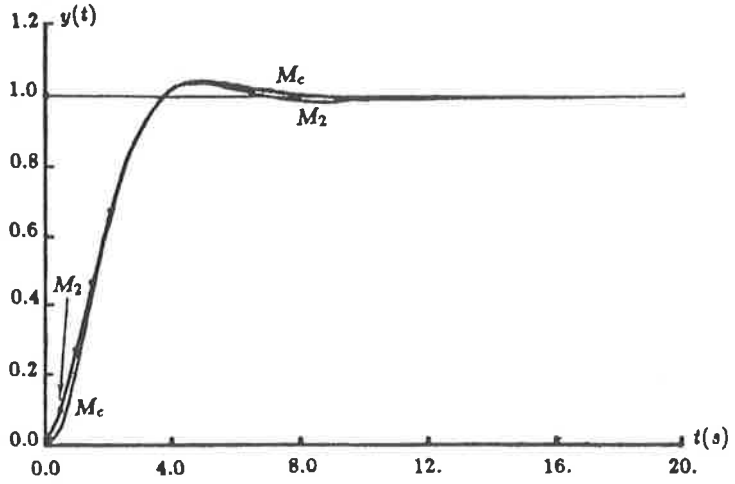

Figure 4-19 Unit-step responses of the continuous model $M_c(s)$ and the discrete model $M_2(z)$ with $T_m = 0.5\ s$

At $T = 0.5s$, the primary frequency range ω_p of the discrete system is 6.28 rad/s, at which the magnitude of $M_c(j\omega)$ is as low as -34 db. Consequently an excellent matching has been achieved by the ICCF method in both the time and frequency domains. When a longer sampling period $T = 2.0s$ is applied, the primary frequency range reduces to $\omega_p = 1.57\ rad/s$, which is about twice the desired frequency bandwidth, $\omega_b = 0.78$. The magnitude of $M_c(j\omega)$ at ω_p is about -10 db. Fig 4-20(a) shows that the frequency response of closed-loop system closely matches that of the model until ω reaches the vicinity of $\omega_p = 1.57$, where a sharp divergence occurs in both the magnitude and phase. Nevertheless, such a close matching to the model over almost the whole primary frequency range does not prevent the system from losing stability.

4.3.4 Discussions of the simulation results

The effect of discrepancy between the primary frequency range of a model and that of a system under design has been demonstrated by the results of eight design studies shown in Table 4-10 and figures from 4-15 to 4-21. By analysing these results, the effect of the discrepancy on similar systems to those evaluated in the above studies can be summarized in Table 4-11 in terms of σ ($\sigma = \frac{\omega_p}{\omega_{pm}} = \frac{T_m}{T}$).

There are two points worthy of emphasis here. First, when $\omega_p < \omega_{pm}$, the

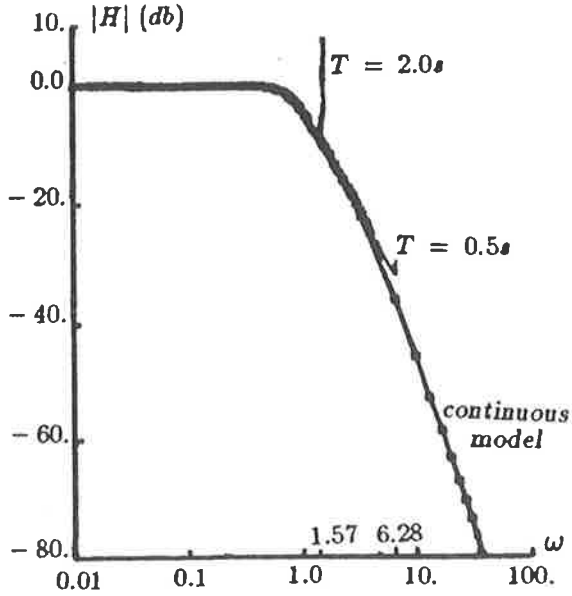

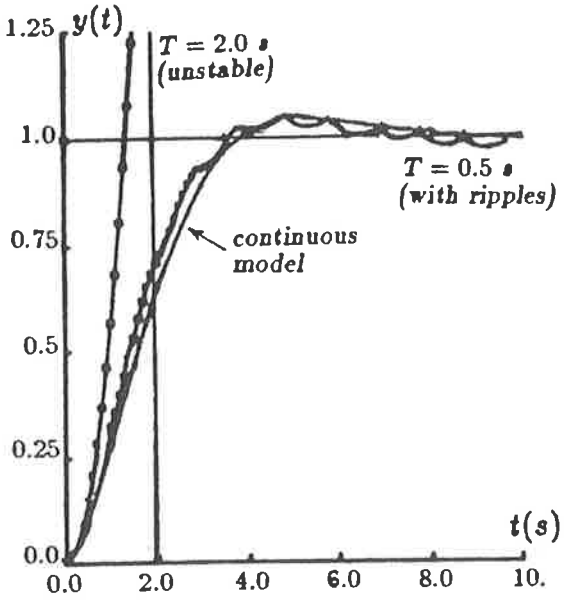

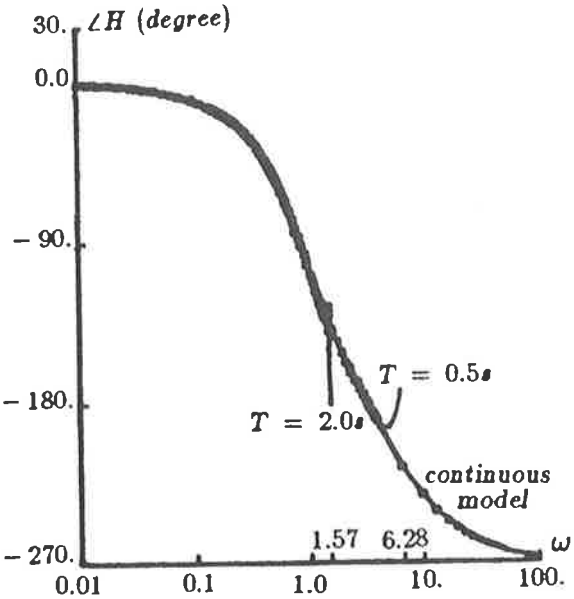

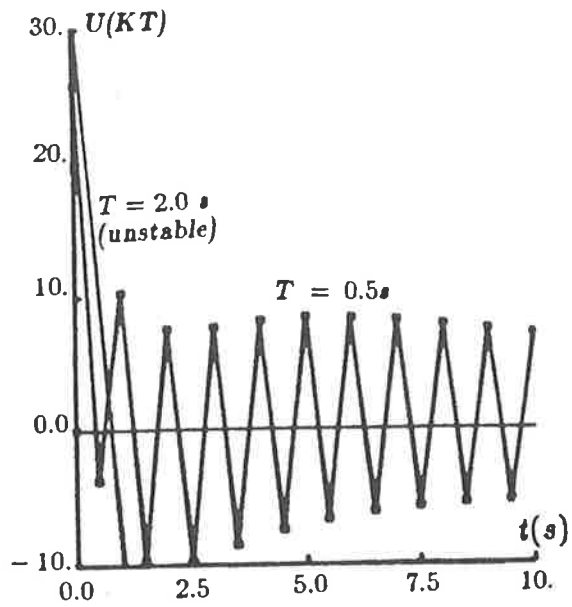

(a) Frequency response $H(j\omega)$ (ω in rad/s)

(b) Unit-step response $y(t)$ and controller output $U(KT)$

Figure 4-20 Frequency and time responses of the closed-loop systems in the design studies of Group 2 for Plant I, designed by the ICCF method, matching the continuous frequency response $M_c(j\omega)$. (Note that $U(KT)$ is a series of pulse signals connecting lines between which are drawn only for purposes of observation.)

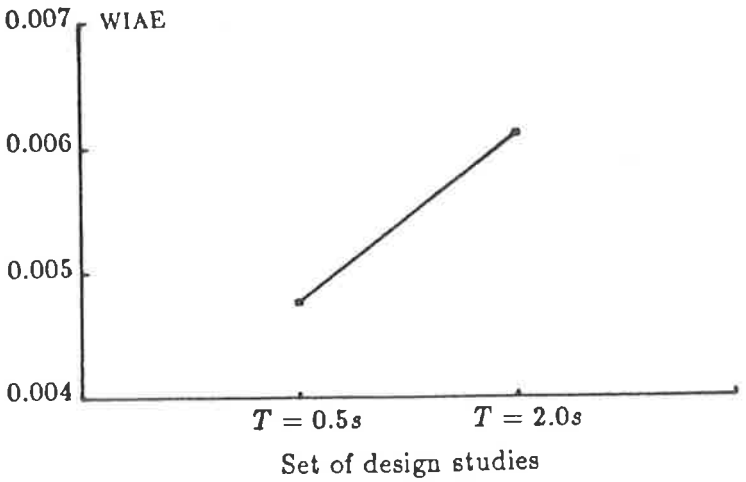

Figure 4-21 Values of WIAE of the closed-loop systems in the design studies of Group 2 for Plant I , designed by the ICCF method, matching the continuous frequency response model $M_c(j\omega)$

distortion in frequency response matching always occurs within a frequency band near to $\omega = \omega_p$. The band is so narrow that WIAE is unable to reflect the impact of the distortion properly, as shown in Figs. 4-16 and 4-21, unless a heavy weighting factor is added to the error in that band. Second, comparison of Figs. 4-15 and 4-20 to Figs. 4-7 and 4-8 with respect to the designs for Plant I at $T = 2.0$ s reveals that, when a low sampling frequency is required, the discrete model with $T_m = T$ is vital for the success of designs as the designs based on the other models with $\omega_{pm} > \omega_p$ failed with instability, no matter whether those models are discrete or continuous.

4.3.5 Conclusions

An investigation on the effect of discrepancy between the primary frequency range of a model and that of a system under design upon the synthesis of a digital controller is presented in this section. The design studies were carried out on Plant I and II . Table 4-11 summarized the results in the order of decreasing σ $(= \frac{\omega_p}{\omega_{pm}})$.

The results of this investigation show that, when $\omega_p < \omega_{pm}$, or $T > T_m$, and $\omega_p < (3 \sim 6)\omega_b$, the discrepancy strongly affects the dynamic characteristic of resulting closed-loop systems. It is suggested, therefore, that a sampling frequency ω_s higher

Table 4-11 Effect of the discrepancy between the primary frequency range of a model and that of a closed-loop system on the design of a digital controller

Value of σ	Value of ω_p		Effects of the discrepancy
$\sigma > 1$	$\omega_p > \omega_{pm}$		The matching error increases but its effect is negligible. Satisfactory results can be expected.
$\sigma = 1$	$\omega_p = \omega_{pm}$		The discrepancy is nil. The minimum of the matching error can be achieved.
$\sigma < 1$	$\omega_p < \omega_{pm}$	$\omega_p > (3 \sim 6)\omega_b$	ω_p is narrower than ω_{pm} but is still much wider than ω_b. Because the failure of the matching occurs at frequencies where the magnitude of response is small, it does not affect the design significantly. (This may occur as T takes some value greater than 0.5 and smaller than 2.0.)
		$\omega_p < (3 \sim 6)\omega_b$	ω_p is narrower than ω_{pm} and is very close to ω_b. The distortion of frequency response near ω_b at which the magnitude is high degrades the dynamic characteristic of the resulting closed-loop system considerably. (At t=2.0s ($\omega_p = 2\omega_b$), the resulting closed-loop system is unstable.)

than $(6 \sim 12)\omega_b$ be used for the design of a digital controller, if the frequency response model is derived from a continuous transfer function or a discrete transfer function with $T_m < T$. On the other hand, if ω_s has to be chosen lower than $(6 \sim 12)\omega_b$, the frequency response model should be specified from an appropriate discrete transfer function with $T_m = T$.

§4.4 Design studies of Group 3 — Evaluation of the optimization-based design methods

In Chapter II , two optimization-based frequency response matching design methods, SIM and RSO, have been discussed. SIM is developed from the simplex optimization algorithm and RSO from the random searching optimization algorithm. Like other optimization methods, the efficacy of these algorithms is highly related to their convergency and speed of convergency, and to their dependence on choices of initial estimates. These aspects of the performances of the SIM and RSO algorithms are therefore the subject of studies described in this section.

4.4.1 Designs with different initial estimates

Design examples are divided into two sets according to the initial estimates for the gain and real pole-zero locations of a controller transfer function $D(z)$. In set A, the optimization operations of SIM and RSO start from a set of arbitrarily-assigned values. They are $0.5, 0.5, 0.5$ for the real poles, $0.5, 0.5, 0.5$ for the zeros and 10 for the gain. Initial values in set B are derived from the controller transfer function obtained using the DDM method so that these values are fairly close to the optimum. In both sets, the designs are carried out for Plant I at $T = 0.5\ s$ to match the model M_2 with $T_m = 0.5\ s$ (see Table 4-3, p. 4-10).

Suppose the optimal parameters of $D(z)$ are those obtained from the more analytical design method ICCF, which gives fairly accurate results in terms of WIAE as shown earlier in section 4.2.

Because the assessment concentrates on the convergency of the optimization algorithms and because the optimal parameters are obtained from the ICCF method without bounds on the pole-zero locations, no constraints are imposed on the designs in this section except for that the controller poles are located on or inside the unit circle of the z-plane for the sake of stability.

Two figures of merits are used for assessing the convergency of the optimization algorithms. One is the frequency matching error E calculated from Eq. (2-47) over 40 frequency points listed in Table 4-12. The other is the consumption of CPU time (for VAX-11/780 digital computer). Moreover, the resulting closed-loop systems are evaluated on the basis of their unit-step time responses with respect to the specifications given in section 4.1.3 (p. 4-5).

Table 4-12 Values of the frequency points (rad/s) used in the calculation of the error E

0.0001	0.002	0.004	0.02	0.04	0.08	0.12	0.16
0.20	0.24	0.28	0.32	0.36	0.40	0.80	1.20
1.60	2.0	2.40	2.60	2.80	3.20	3.60	3.80
4.0	4.20	4.40	4.60	4.80	5.20	5.60	5.72
5.88	6.0	6.08	6.12	6.16	6.20	6.24	6.28

The values of the parameters of the discrete transfer functions for the digital controllers from design studies for Plant I are given in Table 4-13 with their matching errors. Also the table shows the result from the ICCF method. The time and frequemcy response simulations for set A and set B are drawn in Figs. 4-22 and 4-23, respectively.

Fig. 4-22(b) shows the matching error E of the designs based on SIM and RSO in set A as a function of CPU time consumption. It can be observed that SIM brings the matching error E down to the minimum even though the initial estimates are far from optimum. After about 25 s, E is minimized from 2089 to 26. In contrast with SIM, RSO reduces the error E very slowly, and eventually the design of RSO fails to converge to the optimum. This failure results in the sharp differences in the frequency and time responses of the corresponding closed-loop systems, as shown in Fig. 4-22(a) and (c).

In set B, SIM and RSO are used to optimize the controller transfer function,

Table 4-13 Parameters of the z-transfer functions of the digital controllers for the design studies of Group 3 (Plant I , T=0.5s)

Set	Method	E	$D(z) = \frac{x_0(z-z_1)(z-z_2)(z-z_3)}{(z-p_1)(z-p_2)(z-p_3)}$						
			x_0	z_1	z_2	z_3	p_1	p_2	p_3
A	Init.*	2089	10.0	0.5	0.5	0.5	0.5	0.5	0.5
	SIM	26	22.3022	−0.2895	0.8933	0.8963	−0.9751	0.4168	1.0
	RSO	688	27.8182	−1.0	0.9807	0.4769	−1.0	−1.0	1.0
	ICCF	52	22.2743	0.9014	−0.2990	0.9041	−0.9813	0.4311	1.0
B	Init.	524	18.9879	0.2691	0.9240	0.9240	−0.3136	0.6388	1.0
	SIM	24	22.3006	−0.2901	0.8943	0.8951	−0.9751	0.4157	1.0
	RSO	208	21.2804	−0.2020	0.9118	0.8565	−0.9545	0.4042	1.0
	ICCF	52	22.2743	0.9014	−0.2990	0.9014	−0.9813	0.4311	1.0

E — Frequency matching error defined in Eq. (2-47).

*Init. — Initial estimates.

say $D'(z)$, obtained from the DDM method. The parameters of $D'(z)$, which give the matching error $E = 525$, are assigned as the initial values to the optimization operations. As shown in Fig. 4-23(b), after 350 iterations (11 seconds CPU time), E is minimized to 24 by SIM. The optimal parameters of $D(z)$ are almost identical to those obtained from the design of set A. On the other hand, RSO even can not find any solution better than the initial values until 90 seconds CPU time elapses. The performances of the resulting closed-loop systems in the time and frequency domains, as illustrated in Fig. 4-23(a) and (c), are consistent with these optimization results. In order to demonstrate the improvement gained from the optimization operation, the performances of the closed-loop system incorporated with $D'(z)$, based on DDM, are also included in Fig. 4-23.

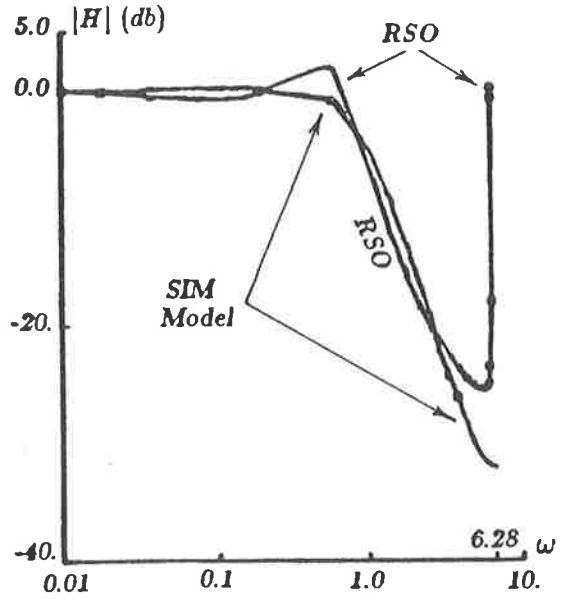

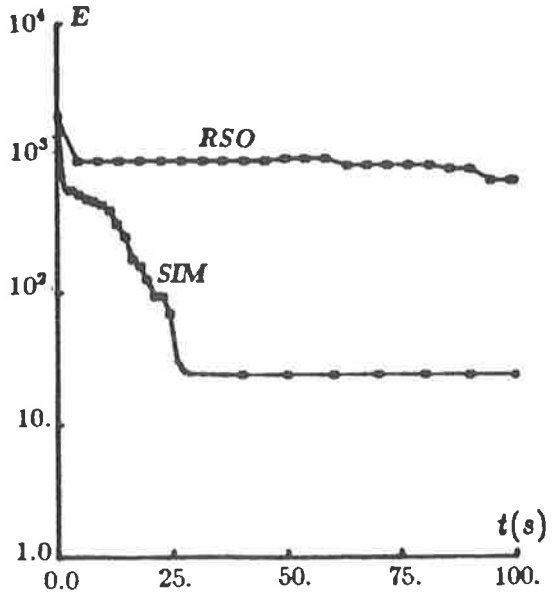

(b) Matching error E vs CPU time

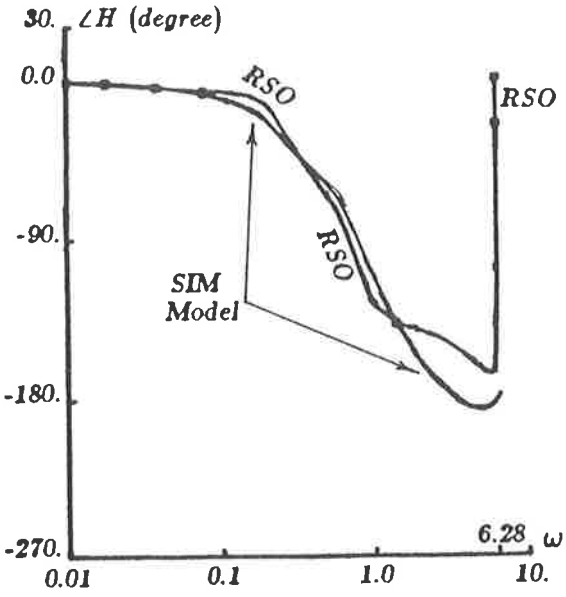

(a) Frequency response $H(j\omega)$
(ω in rad/s)

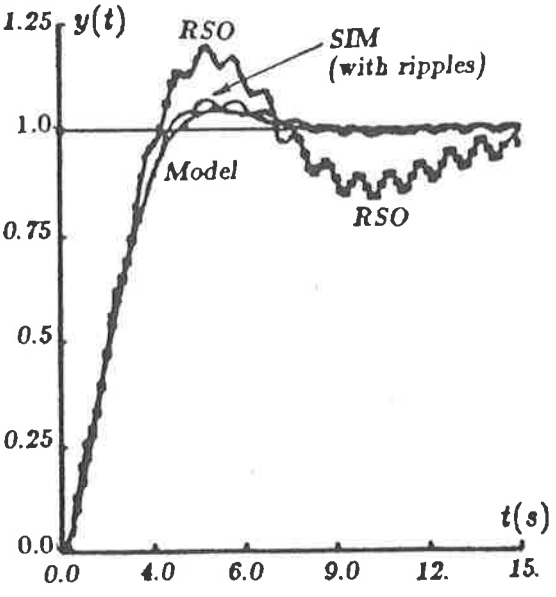

(c) Unit-step response $y(t)$

Figure 4-22 Results of design studies set A in Group 3, based on the SIM and RSO methods with the arbitrarily-assigned initial values(Plant I , T=0.5s)

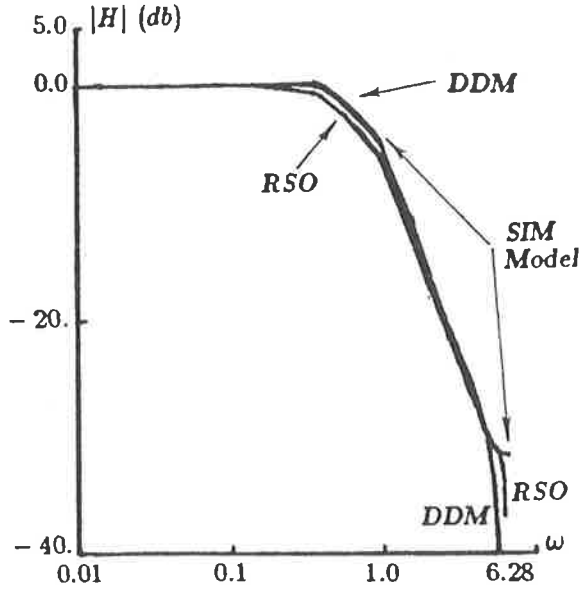

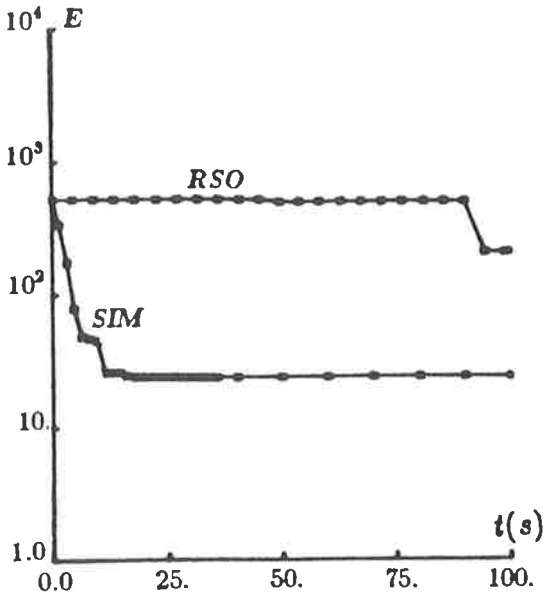

(b) Matching error E vs CPU time

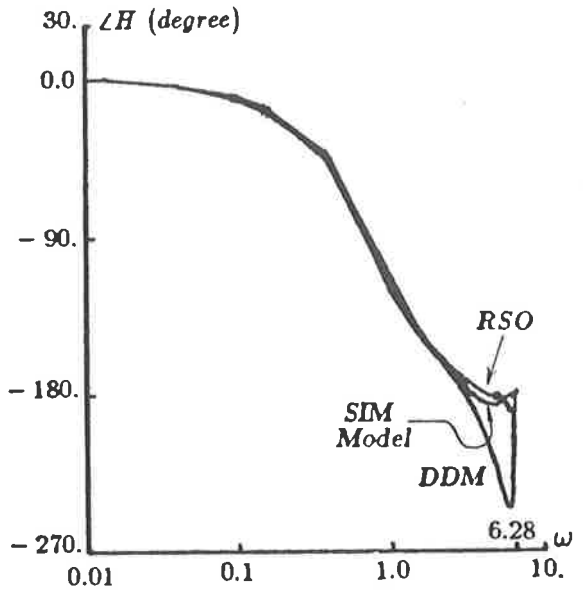

(a) Frequency response $H(j\omega)$
(ω in rad/s)

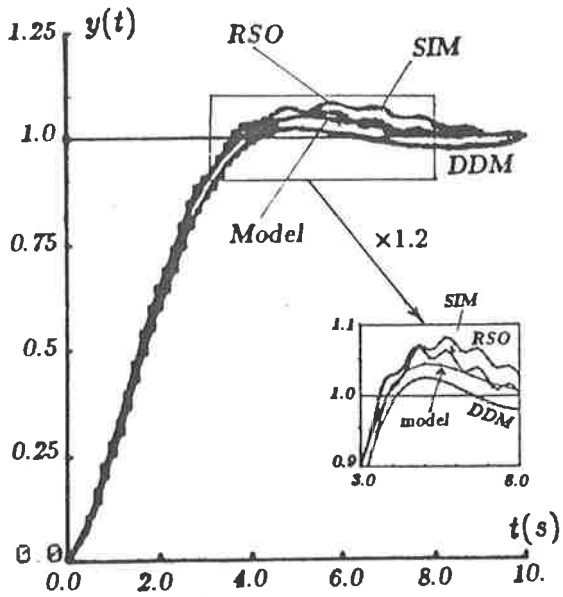

(c) Unit-step response $y(t)$

Figure 4-23 Results of design studies set B in Group 3, based on the SIM and RSO methods with the initial values obtained from the design based on the DDM method(Plant I , T=0.5s)

4.4.2 Conclusions

Two optimization-based design methods, namely SIM and RSO, have been evaluated in this section with respect to their convergency and speed of convergency as well as dependence on initial estimates. It is demonstrated that the SIM method is an effective design method which can bring parameters to the optimal values without strict requirements on initial conditions. This is strongly supported by its successful applications in the design studies of Group 1, in which the controller transfer functions for both Plants I and II are designed by the SIM method with different initial values and sampling periods. The computational burden of SIM much depends on the quality of initial estimates. It is rather heavy but is still comparable with the CCF method and faster than the ICCF method (see Table 4-7, p. 4-31).

It is of interest to note that, in comparison to set A, the combination of DDM and SIM methods, as illustrated in the design studies of set B, has saved CPU time† significantly and also improved the matching accuracy. This suggests that the DDM method be used for the initial design of a controller transfer function, then SIM be employed to optimize the design, if its matching error is not satisfactory. By means of this two-stage design strategy, it is possible that a compromise between speed of computation and high matching accuracy is achieved.

The convergency of the RSO method is so poor that no recommendation can be made on its practical utilization. For this reason RSO is not assessed in section 4.2 together with the other design methods. Because the possibility of the random search striking an optimum becomes extremely small when the number of variables is large, the random searching optimization algorithm seems unable to cope with high-dimensional non-linear programming problems.

† The CPU time required by DDM for matching dominant data at 4 frequency points is only $0.3 \sim 0.5$ s, which is negligible compared to that required by SIM.

CHAPTER V

HYBRID FREQUENCY RESPONSE ANALYSIS

§5.1 Deficiencies of discrete frequency response analysis

In most digital control systems, plants under control are continuous-time systems as described in Fig. 2-1. A digital controller samples a continuous-time signal and generates a sequence of impulse control signals determined by some control algorithm. The control signal is then converted into a continuous-time signal by a ZOH and fed to the input of a continuous-time power amplifier or plant. Because such a system incorporates both the continuous- and discrete- time signals, it is refered to as a ***hybrid*** digital control system. Despite its hybrid nature, the technique commonly used to analyze such a hybrid digital control system is based on its z-transfer function, which is obtained by adding a dummy sampler at the output of the continuous plant as shown by dashed lines in Fig. 2-1. The discretization of the plant makes the task of analysis easier but discards the information about system inter-sampling time response characteristics.

The frequency response derived from the above discretized model of the hybrid system is called the *discrete* frequency response and written as:

$$\begin{aligned} H(j\omega) &= H(z)|_{z=e^{j\omega T}} \\ &= \frac{D(z)G_hG(z)}{1+D(z)G_hG(z)}\Big|_{z=e^{j\omega T}}. \end{aligned} \tag{5-1}$$

The frequency response of this transfer function has been used for analysis and synthesis in the earlier part of this thesis. The design of the hybrid digital control system based

on its discrete frequency response yields the time response only at sampling instants †. As shown in the design studies of Group 1 of Chapter IV , the designs with very low sampling frequencies were not satisfactory. Though the system discrete frequency responses matched the models very closely, significant ripples between sampling instants rendered the designs unacceptable.

§5.2 Hybrid frequency response analysis

In view of the shortcomings of the discrete frequency response, the hybrid frequency response is derived for improving the analysis of hybrid digital control systems.

Fig. 5-1 shows a closed-loop hybrid digital control system that is equivalent to the one defined in Fig. 2-1 and uses the same notation. Then the hybrid frequency response of the closed-loop system is defined as:

$$\begin{aligned} \check{H}(j\omega) &= \frac{Y(j\omega)}{R^*(j\omega)} \\ &= \frac{D^*(j\omega)}{1 + D^*(j\omega)G_hG^*(j\omega)} G_h(j\omega)G(j\omega). \end{aligned} \tag{5-2}$$

Eq. (5-2) is derived from the closed-loop transfer function of the hybrid system with the aid of the block diagram analysis technique [19]. From Fig. 5-1, the transfer functions $Y(s)$, $V(s)$, $U^*(s)$ and $E^*(s)$ can be written as the following:

$$Y(s) = G_h(s)G(s)U^*(s); \tag{5-3}$$

$$V(s) = F(s)Y(s); \tag{5-4}$$

$$U^*(s) = D^*(s)E^*(s); \tag{5-5}$$

$$E^*(s) = R^*(s) - V^*(s). \tag{5-6}$$

† Unlike the others, the SIM design method indirectly restrains the system inter-sampling behaviour by imposing some constraints on controller pole-zero locations.

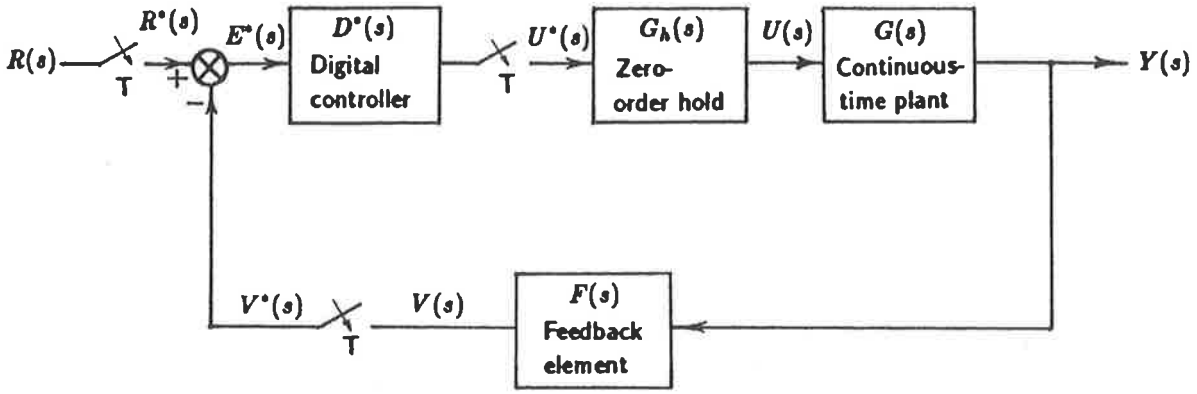

Figure 5-1 Block diagram of a closed-loop hybrid digital control system

According to the relation for the block diagram analysis of sampled-data systems,

$$Y^*(s) = U^*(s)G_hG^*(s); \tag{5-7}$$

$$\begin{aligned} V^*(s) &= FY^*(s) \\ &= FG_hG^*(s)U^*(s). \end{aligned} \tag{5-8}$$

Thus $Y(s)$ in Eq. (5-3) can be rewritten as:

$$\begin{aligned} Y(s) &= G_h(s)G(s)U^*(s) \\ &= G_h(s)G(s)D^*(s)E^*(s) \\ &= G_h(s)G(s)D^*(s)[R^*(s) - V^*(s)] \\ &= G_h(s)G(s)D^*(s)[R^*(s) - FG_hG^*(s)U^*(s)] \\ &= G_h(S)G(s)D^*(s)R^*(s) - FG_hG^*(s)D^*(s)[G_h(s)G(s)U^*(s)] \\ &= G_h(S)G(s)D^*(s)R^*(s) - FG_hG^*(s)D^*(s)Y(s). \end{aligned} \tag{5-9}$$

Y(s) can be then solved from Eq. (5-9):

$$Y(s) = \frac{D^*(s)G_h(s)G(s)}{1 + D^*(s)FG_hG^*(s)}R^*(s). \tag{5-10}$$

Therefore, the closed-loop transfer function of the hybrid system is:

$$\begin{aligned}\breve{H}(s) &= \frac{Y(s)}{R^*(s)} \\ &= \frac{D^*(s)}{1 + D^*(s)FG_hG^*(s)}G_h(s)G(s).\end{aligned} \tag{5-11}$$

Substitution of s by $j\omega$ in Eq. (5-11) yields the hybrid frequency response:

$$\begin{aligned}\breve{H}(j\omega) &= \frac{Y(j\omega)}{R^*(j\omega)} \\ &= \frac{D^*(j\omega)}{1 + D^*(j\omega)FG_hG^*(j\omega)}G_h(j\omega)G(j\omega).\end{aligned} \tag{5-12}$$

The frequency responses of sampled-signals in Eg. (5-12), e.g., $D^*(j\omega)$, $FG_hG^*(j\omega)$, etc., may be obtained by substituting $e^{j\omega T}$ for z in their corresponding z-transfer functions. For instance,

$$D^*(j\omega) = D(z)|_{z=e^{j\omega T}}. \tag{5-13}$$

In the above derivation, there is no approximation or dummy discretization involved and therefore, the hybrid frequency response $\breve{H}(j\omega)$ represents the actual frequency response characteristics of the closed-loop system. In particular, it carries the information about the system inter-sampling behaviour.

After having defined the hybrid frequency response for a hybrid control system, the difference between its discrete and actual frequency responses can be readily determined. Let $D_H^*(j\omega)$ be

$$D_H^*(j\omega) = \frac{D^*(j\omega)}{1 + D^*(j\omega)G_hG^*(j\omega)}. \tag{5-14}$$

Then from Eqs. (5-1) and (5-13), the system discrete frequency response $H(j\omega)$ is

$$H(j\omega) = D_H^*(j\omega)G_hG^*(j\omega). \tag{5-15}$$

The system hybrid frequency response $\breve{H}(j\omega)$ in Eq. (5-12) can be rewritten as

$$\breve{H}(j\omega) = D_H^*(j\omega)G_h(j\omega)G(j\omega). \tag{5-16}$$

The difference between the magnitude of $H(j\omega)$ and that of $\breve{H}(j\omega)$ is thus given by

$$|H(j\omega)| - |\breve{H}(j\omega)| = |D_H^*(j\omega)|[|G_h G^*(j\omega)| - |G_h(j\omega)G(j\omega)|]. \qquad (5-17)$$

Correspondingly the phase shift of $H(j\omega)$ with respect to $\breve{H}(j\omega)$ is

$$\angle H(j\omega) - \angle \breve{H}(j\omega) = \angle G_h G^*(j\omega) - \angle G_h(j\omega)G(j\omega). \qquad (5-18)$$

Equation (5-17) reveals that, if the system discrete frequency response agree with a model very closely, i.e., $H(j\omega) \approx M(j\omega)$, the matching error of the system actual frequency response to the model in magnitude is directly proportional to the discrepancy between the magnitudes of the plant discrete and continuous frequency responses.

§5.3 Numerical example

Three design examples are extracted from the design studies of Group 1 in section 4.2 for comparison between the discrete and hybrid frequency responses. These are designed for Plant I by the ICCF method with $T = 0.5,\ 2.0$ and $4.0\ s$. The frequency response models are $M_2(j\omega)$, $M_3(j\omega)$ and $M_4(j\omega)$ (see Table 4-3, p. 4-10) with $T_m = 0.5,\ 2.0,\ 4.0\ s$, respectively. The coefficients for the digital controllers resulting from the design studies are given in Table 4-6(p. 4-20).

The hybrid and discrete frequency responses of the resulting closed-loop systems with $T = 0.5,\ 2.0,\ 4.0\ s$ are plotted in Fig. 5-2 (a), (b) and (c), respectively, together with the corresponding models. Since the hybrid frequency response from $\omega_s/2$ to ω_s is of interest (and since it cannot be obtained by taking mirror image of that from 0 to $\omega_s/2$ in the complex plane), the frequency responses are plotted from 0.1 to ω_s. Fig. 5-3 shows the time responses of both the models and the closed-loop systems.

From Fig. 5-2 and 5-3, the following observations can be made.

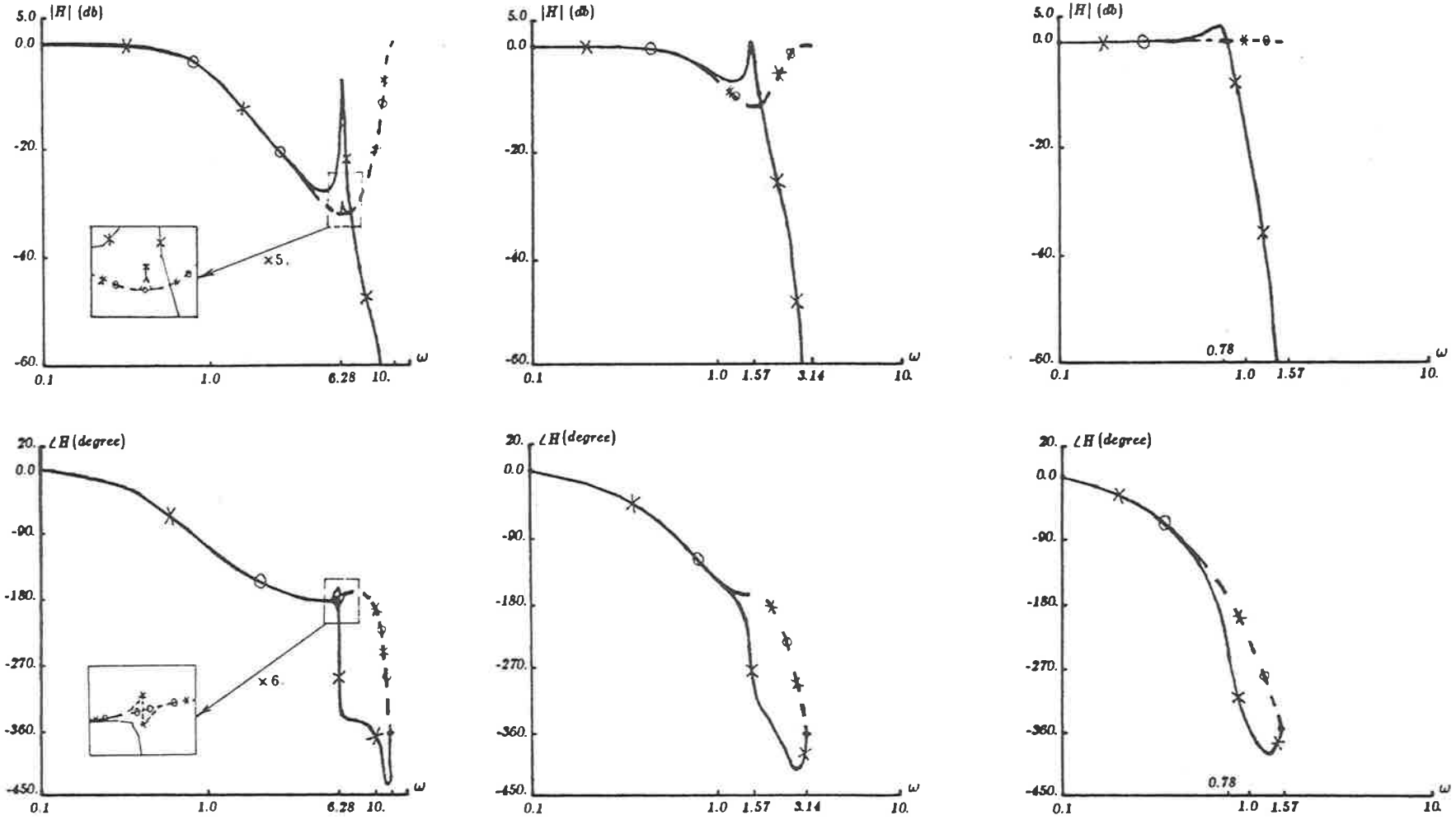

(a) $T = 0.5$ s (b) $T = 2.0$ s (c) $T = 4.0$ s

Figure 5-2 Hybrid and discrete frequency responses of the closed-loop systems for Plant I designed by the ICCF method (ω in rad/s)

(——: hybrid; - - -: discrete; × × ×: closed-loop systems; o o o: Model)

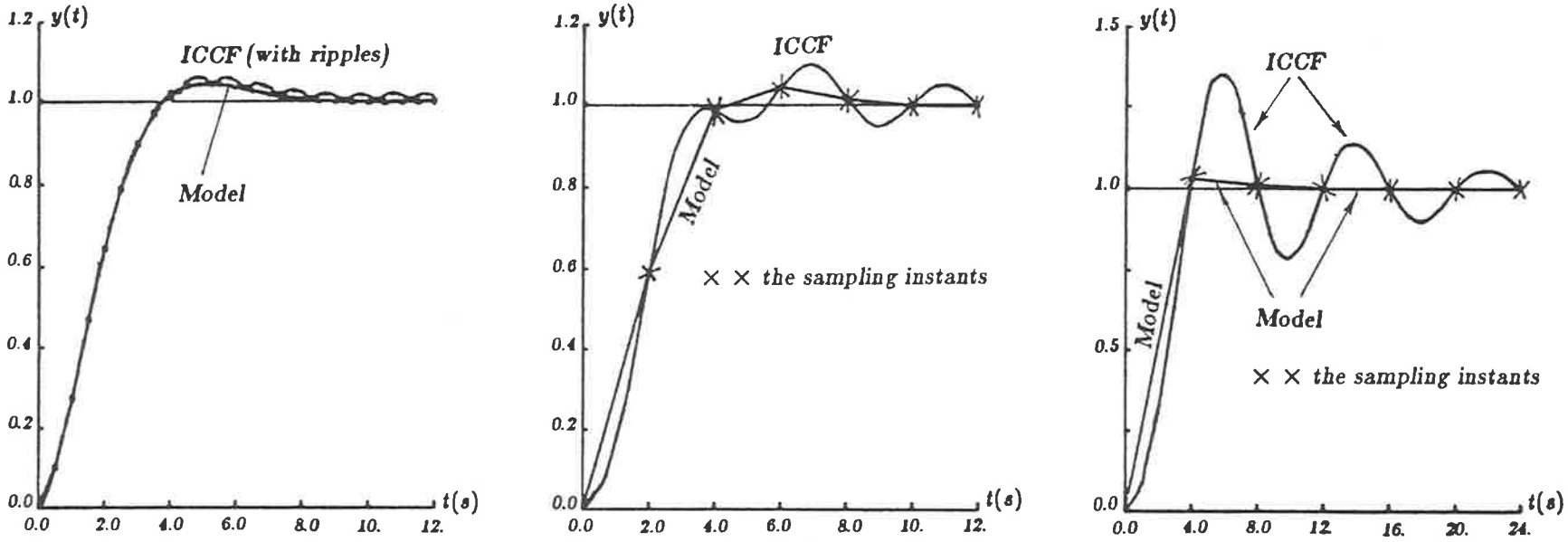

(a) $T = 0.5$ s (b) $T = 2.0$ s (c) $T = 4.0$ s

Figure 5-3 Unit-step time responses of the model and the closed-loop systems for Plant I designed by the ICCF method

(1) The discrete frequency responses of all designs match the corresponding frequency response models very closely.

(2) The continuous time responses of all designs agree closely with the time responses of the discrete models **at sampling instants.**

(3) The magnitudes of hybrid frequency responses in all cases possess a resonant peak at $\omega_p = \omega_s/2$. The gradients of their phase curves vary rapidly in the frequency band near ω_p where the value of phase shift tends to $-360°$.

(4) Ripples on the system continuous time response $y(t)$ emerge after $y(t)$ reaches its first peak. These ripples oscillate at ω_p at which the resonant peak occurs. Their magnitude becomes increasingly large as the sampling frequency decreases and the resonance peak value of the hybrid frequency responses grows.

(5) The relationship between the maximum overshoot M_p of the continuous time responses and the resonance peak value $M_{\breve{H}}$ of the hybrid frequency responses is approximately consistent with the analysis in Chapter III , where Fig. 3-5 shows the relationship between the maximum overshoot and the resonance peak value for second-order systems. For instance at T=2.0 s, $M_{\breve{H}} \approx 0.9$ db, the maximum overshoot is 10%. Furthermore, when T is 4.0 s, $M_{\breve{H}}$ reaches 3 db and the maximum overshoot jumps to 35%. However, in the case of T=0.5 s, the value of $M_{\breve{H}}$ is -3.4 db and the overshoot is 6%. This last set of values is not covered by Fig. 3-5 because the order of the system under study is higher than second and the value of $M_{\breve{H}}$ is lower than 0.6 db(see p.3-14).

It should be pointed out that Plant I (with a ZOH) is an overdamped system with a zero near the point $(-1,\ j0)$ in the z-plane. To match the model, the ICCF method tends to cancel the effect of this zero on the system response by placing a closed-loop pole on the real axis near to -1 point as well. In the frequency domain, this real pole contributes a high resonant peak at ω_p; in the time domain, it yields a controller output containing a slowly decaying "oscillatory" mode whose amplitude changes its sign each sampling instant. The ripples on $y(t)$ therefore oscillate at ω_p.

The resonant peaks on the hybrid frequency responses shown in Fig. 5-2 are mainly due to the deviation of $G_hG^*(j\omega)$, the discrete frequency response of a plant, from $G_h(j\omega)G(j\omega)$, the continuous frequency response of the plant. As an example, in Fig. 5-4 are drawn the magnitudes of $G_hG^*(j\omega)$, $G_h(j\omega)G(j\omega)$ and $D_H^*(j\omega)$ as well as $H(j\omega)$, $\breve{H}(j\omega)$ and $M(j\omega)$ for the case of T=0.5s. With the frequency shifting to $\omega_s/2$, $G_hG^*(j\omega)$ diverges from $G_h(j\omega)G(j\omega)$ and reaches its lowest point at $\omega_s/2$. To compensate $G_hG^*(j\omega)$, the resulting digital controller yields gain peak at $\omega_s/2$ so that $H(j\omega)$ matches the model $M(j\omega)$. However, because the magnitude of $G_h(j\omega)G(j\omega)$ is higher than $G_hG^*(j\omega)$ near $\omega_s/2$, the frequency response of the closed-loop system is over-compensated with an excessively high resonant peak at $\omega_s/2$.

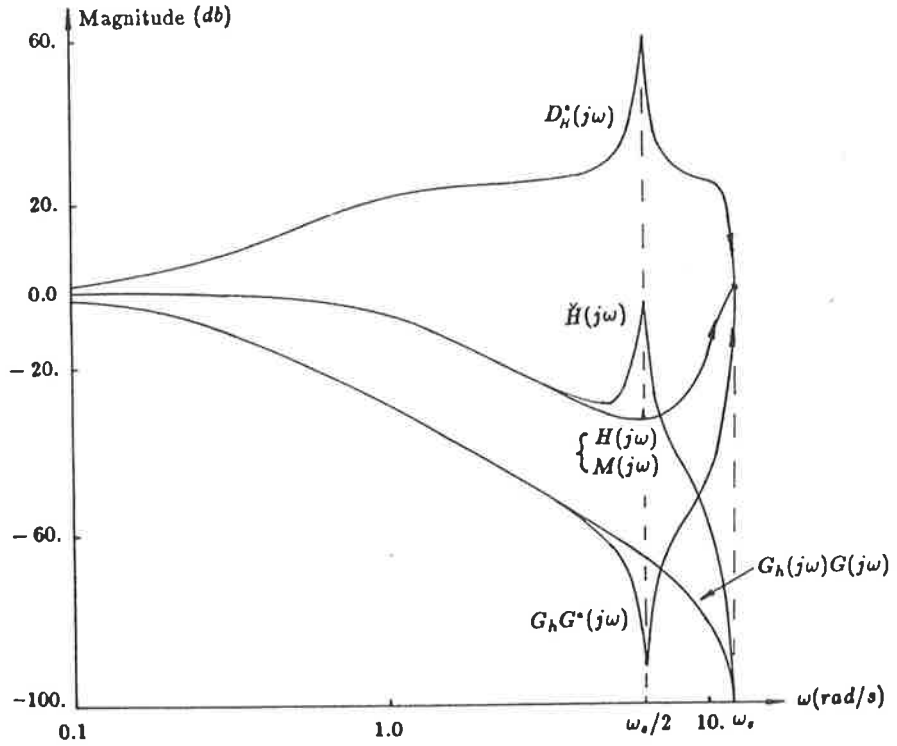

Figure 5-4 Magnitudes of the frequency responses $H(j\omega)$, $\breve{H}(j\omega)$, $M(j\omega)$, $D_H^*(j\omega)$, $G_hG^*(j\omega)$ and $G_h(j\omega)G(j\omega)$ of the hybrid control system for Plant I, designed by ICCF with T=0.5s

§5.4 Conclusions

The hybrid frequency response has been derived in this chapter for closed-loop hybrid control systems consisting of both digital and analogue components. The comparison between the hybrid and discrete frequency responses was demonstrated in the numerical example. Owing to its continuous nature, the hybrid frequency response fully characterizes the true nature of the dynamic performance of the hybrid control system. Consequently the continuous time response can be predicted more accurately by the hybrid frequency response analysis than by the discrete one, which suffers when used for designs with low sampling frequencies due to the lack of information about the system inter-sampling response. Moreover, the investigation shows that, if the discrete frequency response of the resulting closed-loop system matches the model closely, the matching error of the closed-loop actual frequency response to the model is proportional to the difference between the discrete and continuous frequency responses of the plant.

The potential for improvement of frequency response matching design methods based on hybrid frequency response analysis appears promising. For instance, one may match the hybrid frequency response, instead of the discrete response, of a closed-loop control system under design to a specified model so that ripples between sampling instants can be minimized. It is suggested that such a model be a continuous frequency response over a frequency band of interest. The investigation of the hybrid frequency response matching design method is thus a subject worthy of future research work.

CHAPTER VI

SUMMARY AND CONCLUSIONS

The frequency response matching technique for the design of digital controllers has been investigated. The aim of this technique is to design a digital controller so that the frequency response of the resulting closed-loop system matches a specified frequency response model. In addition to the discussion and evaluation of Shieh's dominant data matching design method (DDM) and Rattan's complex-curve fitting design method (CCF), both of which were reported in the literature, the main contributions of this thesis are:

- the development of the iterative complex-curve fitting design method (ICCF) that improves the frequency matching accuracy of the CCF method;
- the development of the simplex optimization-based design method (SIM) which improves the suitability of the frequency response matching design technique for the overdamped plant at low sampling frequencies;
- the assessment of the detrimental effect of the discrepancy between the primary frequency range of a system under design and that of a model upon the matching accuracy and dynamic performance of the resulting system;
- the development of a systematic method for selection of an appropriate discrete frequency response model from performance specifications given in the time, frequency or complex z- domains;

- the definition of the hybrid frequency response which fully characterize a closed-loop system containing both discrete- and continuous- time components.

The initial step in the design by the frequency response matching method is to determine an appropriate frequency response model from a set of performance specifications for the closed-loop control system. This model may be a set of dominant frequency response data, or a discrete or continuous transfer function, depending on the method to be employed. Then the parameters of a digital controller can be determined by means of a number of techniques so that the error, defined in different senses for different methods, between the frequency response of the closed-loop system and that of the model is minimized for frequencies from zero to one-half the sampling frequency.

These methods are analytic in nature and hence are amenable to solutions using general purpose digital computers. For higher order control systems, these methods yield more accurate designs than does the root locus method based on the assumption of the existence of a pair of dominant poles. Moreover, unlike design methods based on the time domain synthesis, the design is independent of the type of input signals and therefore the performance of a resulting closed-loop system is not subject to any restriction on the type of input signal, as in the case, for example, for the design of deadbeat controllers.

Comparative studies are conducted based on the two third-order, continuous-time plants, one being overdamped and the other underdamped. The studies are organized into three groups in order to:

1. evaluate the features of the existing DDM and CCF methods as well as the new ICCF and SIM methods;
2. investigate the effect of discrepancy between the primary frequency range of a closed-loop system and that of a model on the matching accuracy;
3. assess the convergency and speed of convergency of the optimization-based design methods.

The comparative study in Group 1 shows the suitability of the frequency response matching design methods when applied to two different types of plants, i.e., an overdamped plant and an underdamped plant. The decrease in sampling frequency may reduce the error in discrete frequency matching but may increase the ripples between sampling instants. In fact the matching error between the hybrid(actual) frequency response of the closed-loop system and that of the model becomes larger when T grows, as shown in chapter V .

Shieh's DDM method determines the z-transfer function of a controller by matching the system frequency response to a specified model at few dominant frequency points and therefore is the simplest method. The high matching accuracy can be achieved with very light computational burden. But the direct relation between the number of dominant frequency points to be matched and the order of controller may force the designer to choose a very high order controller if more frequency points are required to specify the model. It is shown by this author that the non-linearity of results in Shieh's example[4] for the design of a controller with an integrator can be removed by choosing appropriate dominant frequency points. As a result, the relevant computational algorithm is considerably simplified and the convergency problem is avoided.

Rattan's CCF method minimizes the weighted mean squared error between two frequency responses in transfer function form. At low sampling frequencies, the accuracy of matching is high. On the other hand, at high sampling frequencies, typically $\omega_s \geq 25\omega_b$, the error increases rapidly because the value of the weighting factor becomes extremely small. The numerical integration involved imposes a heavy computational burden on CCF.

The ICCF method proposed in this thesis is based on CCF and is able to eliminate the weighting factor in Rattan's algorithm by using iterative calculations. The matching accuracy at high sampling frequencies can be significantly improved in $2 \sim 3$ iterations. The disadvantage of this method is its heavy computational load.

The DDM, CCF and ICCF methods employ no constraints on the location of

controller poles and zeros in the z-plane. Such constraints might be desirable when controller poles and zeros are required to reside in some specified regions for the sake of system stability and dynamic performance.

The new method SIM enables a designer to confine the controller poles and zeros to desired regions in the z-plane. SIM then searches the optimal poles and zeros within the desired regions by means of the simplex optimization algorithm so that the squared matching error is minimized. When dealing with an overdamped plant with a zero near to $(-1, j0)$ point in the z-plane, SIM yields satisfactory results at low sampling frequencies while the others fail with highly oscillatory control signals and consequent ripples on the system output. The design examples in Group 1 and 3 show that arbitrarily-assigned initial estimates for controller poles and zeros do not affect the convergency of optimization but the speed of convergency. To achieve a compromise between speed of computation and matching accuracy, a two-stage design strategy is suggested in which DDM is employed for the initial design that is then optimized by SIM. Unfortunately there is no simple method to select appropriate constraints and optimization operation parameters in each design case. Therefore a successful selection may be subject to the designer's experience and skill.

RSO is another optimization-based design method formulated by this author. The random searching optimization algorithm employed in RSO is initiated by Luus and is reported to be successful in solving model simplification problems. RSO is evaluated in the design studies of Group 3 and compared with SIM. The performance of RSO is so poor that it could not converge to the optimum after thousands iterations. The failure of RSO is attributed to its dependence on the initial estimates. With a large number of optimization variables, the possibility of the random search striking an optimum becomes extremely small if the initial estimates are not close to the optimum and the size of searching region is large.

Although mathematically the type of plant has little influence on the accuracy of discrete frequency response matching, it does affect the design in terms of time response

characteristics. In particular, in both the overdamped and underdamped plants, ripples between sampling instants are present on the time response of the closed-loop systems. However, the ripples arise for different reasons in each case. For the overdamped plant, the resulting controller frequency characteristic usually possesses high gain in the high frequency band so that its time response is likely to be oscillatory. Such an oscillatory control signal renders the design impractical in many electromechanical control systems. For the underdamped plant, its oscillatory nature may yield ripples because the system is effectively in open-loop mode between sampling instants, typically when $\omega_s < 3\omega_o$, ω_o being the frequency of oscillation of an open-loop plant. Therefore the dynamic characteristics of a plant should be carefully considered when choosing a design method and selecting a sampling frequency.

It must be emphasized that one plant under study possesses a heavily overdamped characteristic and the other a highly underdamped characteristic. Consequently the application of results of these studies may be restricted to similar types of plants only. However, these results provide useful clues to the design of plants the characteristics of which are not as extreme; further studies are required on such plants.

Because of the limited primary frequency range ω_p of discrete systems, the frequency response of a closed-loop system cannot match that of a model very closely if they have different values of ω_p due to different sampling periods. The effect of such discrepancies between the frequency response of the system under design and that of the model has been investigated by design studies for various types of plants. It is demonstrated that, when $\omega_p < \omega_{pm}(T > T_m)$ and $\omega_p < (3 \sim 6)\omega_b$, the discrepancy degrades the performance of the resulting closed-loop systems significantly. The analysis of results suggests that a sampling frequency ω_s higher than $(6 \sim 12)\omega_b$ should be used if the frequency response model is derived from a continuous transfer function or a discrete transfer function with $T_m < T$. On the other hand, if ω_s has to be chosen lower than $(6 \sim 12)\omega_b$, the frequency response model should be specified from an appropriate z-transfer function with $T_m = T$.

To help determine a meaningful frequency response model, which is derived from a second-order z-transfer function and is based on performance specifications framed in one or more of the time, frequency and complex z- domains, a systematic and user-oriented approach is developed and applied to the design studies. The approach is based on a thorough investigation of the dynamic characteristics of second-order discrete systems having a pair of complex poles and a zero. The results are presented in equation, graphical and tabular forms. In addition, the sufficient and necessary conditions for an open-loop second-order discrete system to be closed-loop stable are derived and proved.

As shown in the design studies of Chapter IV , the frequency response matching design method yields a digital controller design for which the discrete frequency response of the closed-loop system perfectly matches the specified discrete frequency response model. However, for the hybrid digital control system containing both discrete and analogue components, it should be borne in mind that there are two fundamental deficiencies in the design based on the discrete frequency response. First, the design derived from discrete frequency response yields the time response only at sampling instants. Second, the discrete frequency response of a plant with a ZOH is an approximation for its continuous counterpart within the primary frequency range $0 \sim \omega_s/2$. The accuracy of the approximation deteriorates when the frequency increases close to $\omega_s/2$. As a result, the closed-loop system may be either over-compensated or under-compensated. One of the usefull contributions in this thesis is therefore the derivation of the actual frequency response of hybrid control systems, refered to as hybrid frequency response. Its application to the analysis of closed-loop dynamic systems is illustrated in an example. It is shown that the system continuous time response can be predicted more accurately by the hybrid frequency response than by the discrete response, especially when the sampling frequency is low. Although lack of time prevented further investigations, the potential for improvement of the frequency response matching design technique based on hybrid frequency response analysis appears promising. Its implementation is worthy of future research work.

In addition to the deficiencies pointed out above, the major disadvantage of the frequency response matching design technique is its uncertainty about the stability of resulting closed-loop systems. Furthermore, the SIM method requires user's experience and skill to determine suitable constraints. If these deficiencies can be overcome, this powerful computer-aided design technique will be widely applicable.

APPENDIX A

Objective function E as function of λ

The objective function E of the non-linear programming problem for the design of a digital controller is defined in Eq. (2-47) as:

$$\begin{aligned} E &= \sum_{i=1}^{N} \sqrt{[\vartheta_Q(\omega_i) - \vartheta_{M_Q}(\omega_i)]^2 + [\psi_Q(\omega_i) - \psi_{M_Q}(\omega_i)]^2} \\ &= f(x_0; z_1, z_2, \ldots, z_m; p_1, p_2, \ldots, p_n), \end{aligned} \qquad (A-1)$$

where,

$$\vartheta_Q(\omega_i) = 20 \log_{10} |Q(j\omega_i)|,$$

$$\vartheta_{M_Q}(\omega_i) = 20 \log_{10} |M_Q(j\omega_i)|,$$

$$\psi_Q(\omega_i) = arg[\ Q(j\omega_i)\ ],$$

$$\psi_{M_Q}(\omega_i) = arg[\ M_Q(j\omega_i)\ ],$$

and $arg[\ \bullet\ ]$ represents the argument or phase angle of $[\ \bullet\ ]$ in degrees.

The system open-loop frequency response is defined in Eq. (2-5) and repeated here:

$$\begin{aligned} Q(j\omega_i) &= D(z)G_hG(z)|_{z=e^{j\omega_i T}} \\ &= D(j\omega_i)G_hG(j\omega_i), \qquad i = 1, 2, \ldots, N. \end{aligned} \qquad (A-2)$$

If Eqs. (2-50), (2-51) and (2-52) are substituted into Eq. (2-44) for $D(z)$, Eq. (A-2) becomes

$$\begin{aligned} Q(j\omega_i) = G_hG(j\omega_i) \cdot \frac{(\mu_g e^{-|\lambda_0|})[e^{j\omega_i T} - (\mu_z e^{-|\lambda_1|} - \nu_z)] \cdots}{[e^{j\omega_i T} - (\mu_p e^{-|\lambda_{m+1}|} - \nu_p)] \cdots} \cdot \\ \cdot \frac{\cdots (e^{j\omega_i T} - e^{-|\lambda_{m-1}|} e^{j\pi e^{-|\lambda_m|}})(e^{j\omega_i T} - e^{-|\lambda_{m-1}|} e^{-j\pi e^{-|\lambda_m|}})}{\cdots (e^{j\omega_i T} - e^{-|\lambda_{m+n-1}|} e^{j\pi e^{-|\lambda_{m+n}|}})(e^{j\omega_i T} - e^{-|\lambda_{m+n-1}|} e^{-j\pi e^{-|\lambda_{m+n}|}})}, \end{aligned} \qquad (A-3)$$

with $i = 1, 2, \ldots, N$.

Note that $G_h G(j\omega_i)$ is known and $M_Q(j\omega_i)$ is specified. The objective function E is therefore a function of λ_i, $i = 0, 1, \ldots, m+n$,

$$E = \sum_{i=1}^{N} \sqrt{[20\log_{10}|Q(j\omega_i)| - 20\log_{10}|M_Q(j\omega_i)|]^2 + [arg[Q(j\omega_i)] - arg[M_Q(j\omega_i)]]^2}$$

$$= F(\lambda_0, \lambda_1, \lambda_2, \ldots, \lambda_{m+n}), \qquad (A-4)$$

where $Q(j\omega_i)$ is defined in Eq. (A-3) and N is the number of selected frequency points.

APPENDIX B

Variation range of the parameter α

The parameter α, defined in Fig. 3-2 and redrawn in Fig. A-1, is introduced by Kuo [1] to describe the position of a real zero Z_1 of $h(z)$ of Eq. (3-1) relative to a pair of complex conjugate poles P and $\overline{P}$. The value of α is positive if Z_1 is to the right of z^*, the vertex of the right triangle $\triangle Pz^*Q$, and is negative otherwise. In an attempt to investigate the dynamic response of $h(z)$, this author derives the bounds on the value of α.

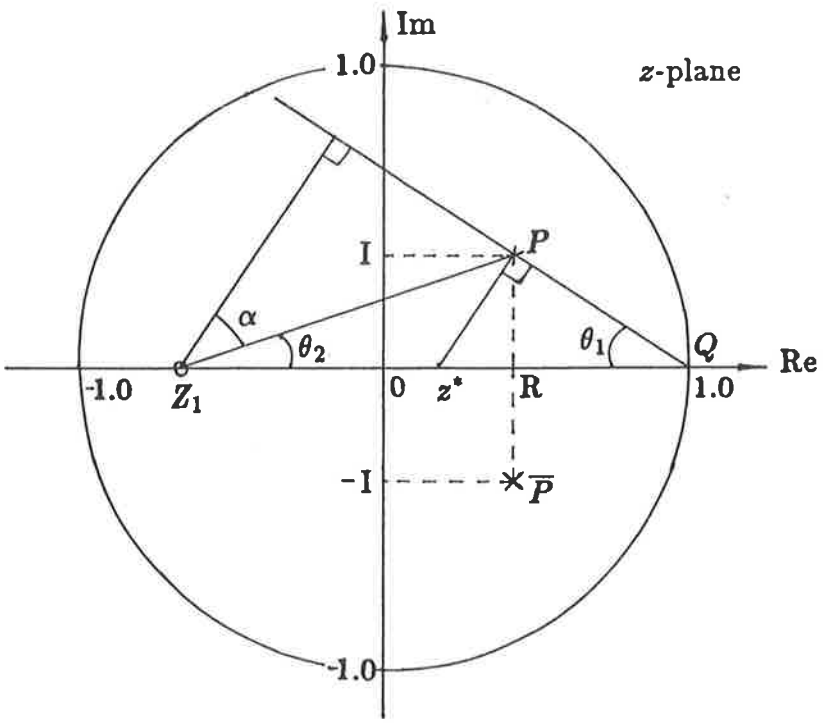

Figure A-1 Position of the zero Z_1 relative to the poles P and $\overline{P}$ in terms of α

It is apparent from the definition that the upper limit on the value of α is $+90°$ as Z_1 approaches the point of $(1,\ j0)$. On the other hand, the lower limit $\alpha_{l.l.}$ is not a constant but a function of the position of the complex poles. Fig. A-1 illustrates the relation between the zero and the poles in terms of α, where R and I represents the real and imaginary part of the complex pole P, respectively.

It is shown in Fig. A-1 that, when Z_1 lies to the left of the point z^* $(\alpha < 0)$,

$$|\alpha| = 90 - \theta_1 - \theta_2.$$

Note that

$$\theta_1 = \mathrm{tg}^{-1}\frac{\mathrm{I}}{1-\mathrm{R}};$$
$$\theta_2 = \mathrm{tg}^{-1}\frac{\mathrm{I}}{\mathrm{R}-\mathrm{Z_1}};$$

and $\theta_2 \to 0$ when $Z_1 \to -\infty$. Thus

$$\begin{aligned}\alpha_{l.l.} &= \lim_{Z_1 \to -\infty} -|\alpha| \\ &= \lim_{Z_1 \to -\infty} (\mathrm{tg}^{-1}\frac{\mathrm{I}}{1-\mathrm{R}} + \mathrm{tg}^{-1}\frac{\mathrm{I}}{\mathrm{R}-\mathrm{Z_1}} - 90) \\ &= \mathrm{tg}^{-1}\frac{\mathrm{I}}{1-\mathrm{R}} - 90.\end{aligned}$$

In summary, for a pair of complex conjugate poles $R \pm jI$, the range of the parameter α is

$$(\mathrm{tg}^{-1}\frac{\mathrm{I}}{1-\mathrm{R}} - 90)° < \alpha < 90°.$$

APPENDIX C

Time response analysis of $h(z)$

The derivation in this section basically follows the work of Kuo [1]. The closed-loop transfer function of the second-order discrete system is defined as:

$$\begin{aligned} h(z) &= \frac{A(z-Z_1)}{(z-P)(z-\overline{P})} \\ &= \frac{A(z-Z_1)}{(z-e^{-\xi\omega_n T+j\omega_o T})(z-e^{-\xi\omega_n T-j\omega_o T})} \\ &= \frac{Az+B}{z^2+Cz+D}. \end{aligned} \qquad (C-1)$$

The time response of $h(z)$ to a unit-step input signal $R(z) = \dfrac{z}{z-1}$ is given by applying the inverse z-transformation on $Y(z)$, the product of $h(z)$ and $R(z)$,

$$\begin{aligned} Y(nT) &= \frac{1}{2\pi j}\oint_\Gamma Y(z)z^{n-1}dz \\ &= \frac{1}{2\pi j}\oint_\Gamma \frac{Az(z-Z_1)}{(z-1)(z-P)(z-\overline{P})}z^{n-1}dz, \end{aligned} \qquad (C-2)$$

where Γ is a closed contour that encloses all singularities of the integrand.

Solving of the contour integration (C-2) by Cauchy's residue theorem yields

$$Y(nT) = 1 + 2\left|\frac{A(P-Z_1)}{(P-1)(P-\overline{P})}\right| \cdot |P|^n \cdot \cos(n\omega_o T + \phi), \qquad (C-3)$$

where

$$\phi = \angle(P-Z_1) - \angle(P-1) - \frac{\pi}{2}.$$

From Fig. 3-1, it can be readily observed that

$$\alpha = \angle(P - Z_1) - \angle(P - 1) + \frac{\pi}{2}. \qquad (C-4)$$

Hence

$$\phi = \alpha - \pi. \qquad (C-5)$$

Further inspection on Fig. 3-1 reveals another important property of α, namely

$$|\sec\alpha| = 2\left|\frac{A(P - Z_1)}{(P-1)(P-\overline{P})}\right|. \qquad (C-6)$$

Substitution of Eqs. (C-5) and (C-6) into Eq. (C-3) leads to:

$$Y(nT) = 1 + |\sec\alpha| \cdot |P|^n \cdot \cos(n\omega_o T + \alpha - \pi). \qquad (C-7)$$

Assume $t = nT$, then

$$|P|^n = |P|^{\frac{t}{T}} = e^{-\xi\omega_n t}, \qquad (C-8)$$

and

$$n\omega_o T = \omega_n\sqrt{1-\xi^2}\cdot t. \qquad (C-9)$$

Thus the discrete unit-step response $Y(nT)$ can be approximated by a continuous function $y(t)$ that passes through all points of $Y(nT)$,

$$y(t) = 1 + |\sec\alpha| \cdot e^{-\xi\omega_n t} \cdot \cos(\omega_n\sqrt{1-\xi^2}\cdot t + \alpha - \pi). \qquad (C-10)$$

The peak values t_p' of $y(t)$ can be found by taking first derivative of $y(t)$ with respect to t and setting $y\prime(t)$ to zero. This results in

$$\mathrm{tg}(\omega_n\sqrt{1-\xi^2}\cdot t_p' + \alpha - n\pi) = \frac{-\xi}{\sqrt{1-\xi^2}}, \qquad (C-11)$$

and

$$t_p' = \frac{1}{\omega_n\sqrt{1-\xi^2}}\left[\mathrm{tg}^{-1}\frac{-\xi}{\sqrt{1-\xi^2}} - \alpha + n\pi\right] \qquad (C-12)$$

with $n = 1, 2, \ldots$. The time t_p for the peak of $y(t)$ corresponds to $n = 1$, i.e.,

$$t_p = \frac{1}{\omega_n \sqrt{1-\xi^2}} \left[\mathrm{tg}^{-1}\left(\frac{-\xi}{\sqrt{1-\xi^2}} \right) - \alpha + \pi \right]. \qquad (C-13)$$

Assume that the maximum value of $y(t)$ occurs at its first peak. Then the maximum overshoot M_p is

$$\begin{aligned} M_p &= y(t)|_{t=t_p} - 1 \\ &= |\sec \alpha| \sqrt{1-\xi^2} \cdot e^{\frac{-\xi}{\sqrt{1-\xi^2}}[\mathrm{tg}^{-1}(\frac{-\xi}{\sqrt{1-\xi^2}}) - \alpha + \pi]}. \end{aligned} \qquad (C-14)$$

Remember that the continuous-time function $y(t)$ represents the discrete function $Y(nT)$ only at the sampling points $t = nT$, $n = 0, 1, 2, \ldots$. Because t_p is not necessarily a multiple of T, the actual maximum overshoot of the discrete system may be not equal to but may be smaller than M_p.

APPENDIX D

Frequency response analysis of $g(z)$ and $h(z)$

The specifications of the open-loop frequency response $g(j\omega)$, such as PM and GM, and those of the closed-loop frequency response $h(j\omega)$, such as ω_r, M_r and ω_b, are derived in this section as functions of the system coefficients A, B, C and D, or functions of ξ, ω_o and α indirectly (see Eqs. (C-1) and (C-4)). The derivations of ω_r and M_r are refered to Jury's work [22].

The frequency response of the open-loop transfer function $g(z)$ of Eq. (3-5) is

$$\begin{aligned} g(j\omega) &= g(z)|_{z=e^{j\omega T}} \\ &= \frac{Ae^{j\omega T}+B}{e^{j2\omega T}+(C-A)e^{j\omega T}+(D-B)}. \end{aligned} \tag{D-1}$$

Substitution of $e^{j\omega T}$ by $\cos\omega T + j\sin\omega T$ gives

$$\begin{aligned} g(j\omega) &= \frac{(A\cos\omega T+B)+jA\sin\omega T}{[\cos 2\omega T+(C-A)\cos\omega T+(D-B)]+j[\sin 2\omega T+(C-A)\sin\omega T]} \\ &= \tau_g(\omega)e^{j\psi_g(\omega)}. \end{aligned} \tag{D-2}$$

The magnitude $\tau_g(\omega)$ is

$$\begin{aligned} \tau_g(\omega) &= |g(j\omega)| \\ &= \sqrt{\frac{A^2+B^2+2AB\cos\omega T}{2(D-B)\cos 2\omega T+2(C-A)(D-B+1)\cos\omega T+(D-B)^2+(C-A)^2+1}}. \end{aligned} \tag{D-3}$$

At the gain cross-over frequency ω_c,

$$\tau_g(\omega_c) = 1,$$

so that

$$A^2 + B^2 + 2AB\cos\omega_c T = 2(D-B)\cos 2\omega_c T + 2(C-A)(D-B+1)\cos\omega_c T + (D-B)^2 + (C-A)^2 + 1; \qquad (D-4)$$

or

$$a\cos^2\omega_c T + 2b\cos\omega_c T + d = 0; \qquad (D-5)$$

where,

$$a = 4(D-B),$$

$$b = C(D-B+1) - A(D+1),$$

$$d = C^2 + D^2 - 2AC - 2DB - 2(D-B) + 1.$$

The solution for $\cos\omega_c T$ from Eq. (D-5) yields the gain cross-over frequency ω_c:

$$\cos\omega_c T = -\frac{b}{a} \pm \frac{1}{a}\sqrt{b^2 - ad}\,; \qquad (D-6)$$

or

$$\omega_c = \frac{1}{T}\cos^{-1}\Big[-\frac{b}{a} \pm \frac{1}{a}\sqrt{b^2 - ad}\,\Big]; \qquad (D-7)$$

where, the sign in front of the term $\frac{1}{a}\sqrt{b^2 - ad}$ should be chosen in such a way that the absolute value of $-\frac{b}{a} \pm \frac{1}{a}\sqrt{b^2 - ad}$ be not greater than unity.

From Eq. (D-2), the phase angle of $g(j\omega)$ can be written as:

$$\psi_g(\omega) = \mathrm{tg}^{-1}\frac{(AD - BC - A - 2B\cos\omega T)\sin\omega T}{2B\cos^2\omega T + (AD - 2AB + BC + A)\cos\omega T + u} \qquad (D-8)$$

with $u = BD + AC - A^2 - B^2 - B$. The commonly-used definition of the phase margin is

$$PM = \psi_g(\omega)|_{\omega=\omega_c} - (-180). \qquad (D-9)$$

Thus, PM can be determined by substituting Eqs. (D-7) and (D-8) into Eq. (D-9),

$$PM = 180 + \mathrm{tg}^{-1}\frac{(AD - BC - A - 2B\cos\omega_c T)\sin\omega_c T}{2B\cos^2\omega_c T + (AD - 2AB + BC + A)\cos\omega_c T + u}, \qquad (D-10)$$

where ω_c is defined in Eqs. (D-7) and (D-5) and u in Eq. (D-8).

Let ω_g be the frequency at which $\psi_g(\omega)$ reaches $-180°$ for the first time, i.e.,

$$\text{tg}[\psi_g(\omega_g)] = \text{tg}(-180) = 0.$$

From Eq. (D-8), the above conditions will be satisfied if:

$$\sin \omega_g T = 0, \tag{D-11}$$

or

$$\cos \omega_g T = \frac{AD - BC - A}{2B}. \tag{D-12}$$

If $|AD - BC - A| < |2B|$, the solution of Eq. (D-12) is given by:

$$\omega_g = \frac{1}{T} \cos^{-1}\left(\frac{AD - BC - A}{2B}\right). \tag{D-13}$$

So the gain margin is

$$\begin{aligned} GM &= -20 \log_{10}[\tau_g(\omega_g)] \\ &= -20 \log_{10} \sqrt{\frac{A^2 + B^2 + 2AB \cos \omega_g T}{4(D-B)\cos^2 \omega_g T + 2(C-A)(D-B+1)\cos \omega_g T + v}} \end{aligned} \tag{D-14}$$

with $v = (C-A)^2 + (D-B-1)^2$. However, if $|AD - BC - A| \geq |2B|$, the phase angle of $g(j\omega)$ will not approach $-180°$ until ωT reaches π as $\sin \pi = 0$. In this case,

$$\omega_g = \frac{\pi}{T}, \tag{D-15}$$

$$GM = -20 \log_{10} \frac{A + B}{\sqrt{4(D-B) - 2(C-A)(D-B+1) + (C-A)^2 + (D-B-1)^2}}. \tag{D-16}$$

The analysis of the closed-loop frequency response $h(j\omega)$ is conducted in a similar manner. From Eq. (3-3),

$$\begin{aligned} h(j\omega) &= h(z)|_{z=e^{j\omega T}} \\ &= \frac{(A \cos \omega T + B) + jA \sin \omega T}{(\cos 2\omega T + C \cos \omega T + D) + j(\sin 2\omega T + C \sin \omega T)} \\ &= \tau_h(\omega) e^{j\psi_h(\omega)}. \end{aligned} \tag{D-17}$$

The magnitude $\tau_h(\omega)$ is

$$\tau_h(\omega) = |h(j\omega)|$$
$$= \sqrt{\frac{\rho + \mu\cos\omega T}{\beta + 2C\gamma\cos\omega T + 2D\cos 2\omega T}}, \qquad (D-18)$$

where,

$$\rho = A^2 + B^2,$$

$$\mu = 2AB,$$

$$\beta = C^2 + D^2 + 1,$$

$$\gamma = D + 1.$$

To determine the resonant frequency ω_r and the resonance peak value M_r, the first derivative of τ_h with respect to ωT is taken as:

$$\frac{d\tau_h(\omega)}{d(\omega T)} = \frac{1}{2}\sqrt{\frac{\beta + 2C\gamma\cos\omega T + 2D\cos 2\omega T}{\rho + \mu\cos\omega T}}\cdot$$
$$\left[\frac{(\rho + \mu\cos\omega T)(2C\gamma\sin\omega T + 4D\sin 2\omega T)}{(\beta + 2C\gamma\cos\omega T + 2D\cos 2\omega T)^2} - \right. \qquad (D-19)$$
$$\left. \frac{\mu\sin\omega T(\beta + 2C\gamma\cos\omega T + 2D\cos 2\omega T)}{(\beta + 2C\gamma\cos\omega T + 2D\cos 2\omega T)^2}\right].$$

At ω_r, the derivative of $\tau_h(\omega)$ is zero and Eq. (D-19) can be simplified to:

$$4D\mu\cos^2\omega_r T + 8\rho D\cos\omega_r T + (2\rho C\gamma - \beta\mu + 2D\mu) = 0. \qquad (D-20)$$

The solution of Eq. (D-20) is

$$\cos\omega_r T = -\frac{\rho}{\mu} + SIGN(\mu)\sqrt{(\frac{\rho}{\mu})^2 - \frac{\rho C\gamma - \frac{1}{2}\beta\mu + D\mu}{2D\mu}}. \qquad (D-21)$$

Here the choice of the sign of the second term on the right side of Eq. (D-21) is based on the fact that the absolute value of $-\frac{\rho}{\mu} + SIGN(\mu)\sqrt{(\frac{\rho}{\mu})^2 - \frac{\rho C\gamma - \frac{1}{2}\beta\mu + D\mu}{2D\mu}}$ is not greater than unity, if ω_r exists. Accordingly,

$$\omega_r = \frac{1}{T}\cos^{-1}\left[-\frac{\rho}{\mu} + SIGN(\mu)\sqrt{(\frac{\rho}{\mu})^2 - \frac{\rho C\gamma - \frac{1}{2}\beta\mu + D\mu}{2D\mu}}\right]. \qquad (D-22)$$

Substitution of A, B, C and D into Eq. (D-18) for ρ, μ, β and γ produces

$$\omega_r = \frac{1}{T}\cos^{-1}\Big[-\frac{A^2+B^2}{2AB} + SIGN(AB)\cdot \sqrt{\Big(\frac{A^2+B^2}{2AB}\Big)^2 - \frac{1}{2} - \frac{C(D+1)(A^2+B^2) - AB(C^2+D^2+1)}{4ABD}}\Big]. \quad (D-23)$$

The magnitude of $h(j\omega)$ at ω_r is called the resonance peak value,

$$M_r = \tau_h(\omega)|_{\omega=\omega_r} = \sqrt{\frac{A^2+B^2+2AB\cos\omega_r T}{4D\cos^2\omega_r T + 2C(1+D)\cos\omega_r T + (D-1)^2 + C^2}}. \quad (D-24)$$

Finally, the closed-loop frequency bandwidth ω_b is defined as the frequency at which the magnitude of $h(j\omega)$ equals 0.707 (-3 db), that is,

$$\tau_h(\omega_b) = \sqrt{\frac{A^2+B^2+2AB\cos\omega_b T}{2D\cos 2\omega_b T + 2C(1+D)\cos\omega_b T + (1+C^2+D^2)}} = 0.707. \quad (D-25)$$

Rearrange Eq. (D-25) as a second-order equation in terms of $\cos\omega_b T$,

$$2D\cos^2\omega_b T + (C+CD-2AB)\cos\omega_b T + \frac{1+C^2+D^2}{2} - (A^2+B^2+D) = 0. \quad (D-26)$$

Its solution provides the required ω_b,

$$\omega_b = \frac{1}{T}\cos^{-1}\Big[\frac{2AB-C-CD}{4D} \pm \frac{1}{4D}\sqrt{(2AB-C-CD)^2 - 4D(1+C^2+D^2-2A^2-2B^2-2D)}\Big]; \quad (D-27)$$

where, the sign of $\sqrt{(2AB-C-CD)^2 - 4D(1+C^2+D^2-2A^2-2B^2-2D)}$ is selected so that the absolute value of the sum in the square brackets is not greater than unity, provided that ω_b exists.

APPENDIX E

Stability of a second-order discrete system

Let $g(z)$ be the open-loop transfer function of a general second-order discrete system and $h(z)$ the transfer function of the corresponding closed-loop system with unity feedback. The forms of these transfer functions are given as follows:

$$g(z) = \frac{k(z^m + a_1 z^{m-1} + a_2)}{z^2 + b_1 z + b_2}; \qquad (E-1)$$

$$h(z) = \frac{g(z)}{1 + g(z)}$$

$$= \frac{k(z^m + a_1 z^{m-1} + a_2)}{z^2 + d_1 z + d_2} \qquad (E-2)$$

with $m = 0, 1, 2$. Then the closed-loop system is absolutely stable with respect to the open-loop gain k, if and only if:

(1) $m = 2$, and

(2) none of open-loop zeros and poles is outside the unit circle in the z-plane, and

(3) there is at least one open-loop zero or pole inside the unit circle in the z-plane.

proof

From the root locus method, it is well known that for the system which has less zeros than poles, or $m < 2$, there must be at least one zero at infinity in the z-plane. Accordingly, as the open-loop gain k increases, at least one closed-loop pole will move to the zero at infinity, i.e., out of the unit circle so that the closed-loop system becomes unstable.

When $m = 2$, the system characteristic equation is

$$\Gamma(z) = z^2 + \frac{a_1 k + b_1}{k+1} z + \frac{a_2 k + b_2}{k+1}. \qquad (E-3)$$

Thus the closed-loop poles are

$$P_{1,2} = -\frac{a_1 k + b_1}{2(k+1)} \pm \frac{1}{2}\sqrt{(\frac{a_1 k + b_1}{k+1})^2 - \frac{4(a_2 k + b_2)}{k+1}}. \qquad (E-4)$$

If P_1 and P_2 are a pair of complex conjugate poles, their magnitude is

$$\begin{aligned} |P_{1,2}| &= \sqrt{(-\frac{a_1 k + b_1}{2(k+1)})^2 + \Big(\frac{1}{2}\sqrt{4\frac{a_2 k + b_2}{k+1} - (\frac{a_1 k + b_1}{k+1})^2}\Big)^2} \\ &= \sqrt{\frac{a_2 k + b_2}{k+1}}. \end{aligned} \qquad (E-5)$$

Suppose that none of the zeros and poles is outside the unit circle, i.e.,

$$|a_2| \leq 1; \qquad |b_2| \leq 1.$$

Also assume that there is at least one zero or pole inside the unit circle, which means that either $|a_2|$ or $|b_2|$, at least, must be less than unity, thus the magnitudes of $P_{1,2}$ are less than unity to any positive k as:

$$|P_{1,2}| = \sqrt{\frac{ka_2 + b_2}{k+1}} < 1 \qquad if\ k > 0.$$

This reveals that the closed-loop poles keep inside the unit circle no matter what the value of the gain k is , and the closed-loop system, therefore, is stable.

If P_1, P_2 are real poles, they must lie between a pair of the zeros or of the open-loop poles, or pairs of the zeros and open-loop poles, hence they are still inside the unit circle and the closed-loop system is stable.

On the other hand, because the closed-loop poles travel from the open-loop poles to zeros as k varies from 0 to $+\infty$, P_1, P_2 may locate on or outside the unit circle if any open-loop zero or pole is outside the unit circle.

Hence the stability criteria is proved.

APPENDIX F

TABLE A-1

Relationships between the design specifications in the time, frequency and complex z- domains for second-order discrete control systems

This is a numerical table that covers the dynamic characteristics of second-order discrete control systems, and serves as a useful tool for discrete system analysis and design. The table is arranged in the order of the complex z-plane variables ξ, α and $\omega_o T$. The ranges covered are $0.4 \sim 0.9$ for ξ, $-80° \sim +80°$ for α and $0.1 \sim 1.3$ for $\omega_o T$. All symbols used in this table are defined originally in Chapter III . For convenience, they are summarized below, together with an explanation of remarks in the table. An example of the use of this table is given in section 3.2.7, p. 3-17.

System Definitions

Open-loop system : $$g(z) = \frac{Az + B}{z^2 + (C - A)z + (D - B)}.$$

Closed-loop system : $$h(z) = \frac{Az + B}{z^2 + Cz + D}.$$

Frequency responses of $g(z)$ and $h(z)$: $$g(j\omega) = g(z)|_{z=e^{j\omega T}}$$ $$h(j\omega) = h(z)|_{z=e^{j\omega T}}$$

Symbols

General

T – Sampling period in seconds.

Complex z-plane variables

ξ – Damping ratio of closed-loop poles.

ω_o – Oscillatory frequency of closed-loop system response in rad/s.

α – Angle in degrees to define the relative location of a zero to a pair of closed-loop poles.

Unit-step time response

t_p – Peak time in seconds.

M_p– Maximum overshoot in percent.

Open-loop frequency response

PM – Phase margin in degrees.

GM – Gain margin in decibels.

Closed-loop frequency response

ω_b – System bandwidth in rad/s.

ω_r – Resonant frequency in rad/s.

M_r– Resonance peak value in decibels.

Remarks and Abbreviations

C/L — Closed-loop.

O/L — Open-loop.

Out of Range — Shown when α is out of the effective range ($\alpha_{l.l.}$, 90°), where $\alpha_{l.l.}$ is defined in Eq. (3-4).

Mono Increasing — Shown when the magnitude of the closed-loop frequency response increases monotonically.

Mono Decreasing — Shown when the magnitude of the closed-loop frequency response decreases monotonically.

O/L Unstable — Shown when an open-loop system is unstable.

C/L SYSTEM IN COMPLEX Z-PLAIN				C/L STEP RES.		C/L FREQUENCY RES.			O/L FREQUENCY RES.		SYSTEM COEFFICIENTS			
α	$\omega_o T$	POLES	ZERO	tp/T	Mp(%)	WbT	WrT	Mr(db)	PM	GM(db)	A	B	C	D
						ξ =0.4								
-80	0.1	0.953+j0.096	Out of Range											
-80	0.2	0.898+j0.182	Out of Range											
-80	0.3	0.838+j0.259	Out of Range											
-80	0.6	0.635+j0.435	Out of Range											
-80	0.7	0.563+j0.475	Out of Range											
-80	0.9	0.420+j0.529	Out of Range											
-80	1.1	0.281+j0.551	Out of Range											
-80	1.3	0.152+j0.546	Out of Range											
-60	0.1	0.953+j0.096	Out of Range											
-60	0.2	0.898+j0.182	Out of Range											
-60	0.3	0.838+j0.259	Out of Range											
-60	0.6	0.635+j0.435	Out of Range											
-60	0.7	0.563+j0.475	Out of Range											
-60	0.9	0.420+j0.529	Out of Range											
-60	1.1	0.281+j0.551	Out of Range											
-60	1.3	0.152+j0.546	Out of Range											
-40	0.1	0.953+j0.096	Out of Range											
-40	0.2	0.898+j0.182	Out of Range											
-40	0.3	0.838+j0.259	Out of Range											
-40	0.6	0.635+j0.435	-1903.597	5.71	26.80	0.929	0.548	2.912	44.98	7.11	0.000	0.322	-1.270	0.592
-40	0.7	0.563+j0.475	-9.873	4.90	26.80	1.074	0.636	2.849	45.63	6.89	0.038	0.378	-1.127	0.543
-40	0.9	0.420+j0.529	-3.515	3.81	26.80	1.351	0.810	2.697	46.97	6.58	0.137	0.480	-0.839	0.456
-40	1.1	0.281+j0.551	-2.201	3.12	26.80	1.605	0.976	2.513	48.32	6.41	0.257	0.565	-0.561	0.383
-40	1.3	0.152+j0.546	-1.611	2.64	26.80	1.830	1.133	2.306	49.61	6.36	0.390	0.628	-0.303	0.322
-30	0.1	0.953+j0.096	Out of Range											
-30	0.2	0.898+j0.182	Out of Range											
-30	0.3	0.838+j0.259	-6.643	10.85	25.58	0.451	0.270	2.713	43.33	11.68	0.012	0.081	-1.676	0.770
-30	0.6	0.635+j0.435	-1.826	5.42	25.58	0.890	0.537	2.618	44.55	9.43	0.114	0.208	-1.270	0.592
-30	0.7	0.563+j0.475	-1.559	4.65	25.58	1.031	0.624	2.574	45.05	8.96	0.162	0.253	-1.127	0.543
-30	0.9	0.420+j0.529	-1.242	3.62	25.58	1.304	0.796	2.470	46.16	8.28	0.275	0.342	-0.839	0.456
-30	1.1	0.281+j0.551	-1.049	2.96	25.58	1.561	0.963	2.347	47.32	7.85	0.401	0.421	-0.561	0.383
-30	1.3	0.152+j0.546	-0.911	2.50	25.58	1.801	1.124	2.216	48.47	7.60	0.533	0.485	-0.303	0.322
-20	0.1	0.953+j0.096	0.103	30.79	25.44	0.150	0.090	2.714	43.11	48.74	0.013	-0.001	-1.905	0.916
-20	0.2	0.898+j0.182	-0.223	15.40	25.44	0.300	0.180	2.697	43.03	26.52	0.036	0.008	-1.796	0.840
-20	0.3	0.838+j0.259	-0.383	10.26	25.44	0.449	0.270	2.685	43.06	19.91	0.068	0.026	-1.676	0.770
-20	0.6	0.635+j0.435	-0.558	5.13	25.44	0.890	0.537	2.617	43.68	13.13	0.207	0.115	-1.270	0.592
-20	0.7	0.563+j0.475	-0.577	4.40	25.44	1.033	0.625	2.585	44.02	12.06	0.264	0.152	-1.127	0.543
-20	0.9	0.420+j0.529	-0.590	3.42	25.44	1.313	0.799	2.512	44.86	10.58	0.388	0.229	-0.839	0.456
-20	1.1	0.281+j0.551	-0.584	2.80	25.44	1.582	0.970	2.428	45.83	9.65	0.519	0.303	-0.561	0.383
-20	1.3	0.152+j0.546	-0.568	2.37	25.44	1.842	1.137	2.343	46.86	9.07	0.649	0.369	-0.303	0.322

C/L SYSTEM IN COMPLEX Z-PLAIN				C/L STEP RES.		C/L FREQUENCY RES.			O/L FREQUENCY RES.		SYSTEM COEFFICIENTS			
α	$\omega_o T$	POLES	ZERO	tp/T	Mo(%)	WbT	WrT	Mr(db)	PM	GM(db)	A	B	C	D
						ξ =0.4								
0	0.1	0.953+j0.096	0.760	27.30	27.84	0.160	0.092	3.182	42.82	33.39	0.047	-0.036	-1.905	0.916
0	0.2	0.898+j0.182	0.573	13.65	27.84	0.319	0.185	3.149	42.21	27.49	0.102	-0.058	-1.796	0.840
0	0.3	0.838+j0.259	0.423	9.10	27.84	0.479	0.277	3.142	41.74	24.06	0.162	-0.068	-1.676	0.770
0	0.6	0.635+j0.435	0.118	4.55	27.84	0.955	0.554	3.103	41.07	18.09	0.365	-0.043	-1.270	0.592
0	0.7	0.563+j0.475	0.047	3.90	27.84	1.113	0.646	3.085	41.06	16.70	0.437	-0.021	-1.127	0.543
0	0.9	0.420+j0.529	-0.062	3.03	27.84	1.427	0.829	3.045	41.28	14.35	0.580	0.036	-0.839	0.456
0	1.1	0.281+j0.551	-0.142	2.48	27.84	1.742	1.011	3.004	41.80	12.36	0.719	0.102	-0.561	0.383
0	1.3	0.152+j0.546	-0.200	2.10	27.84	2.066	1.194	2.968	42.55	10.62	0.848	0.170	-0.303	0.322
20	0.1	0.953+j0.096	0.862	23.81	34.50	0.182	0.097	4.147	41.76	28.28	0.082	-0.071	-1.905	0.916
20	0.2	0.898+j0.182	0.741	11.91	34.50	0.365	0.193	4.132	40.52	22.56	0.168	-0.125	-1.796	0.840
20	0.3	0.838+j0.259	0.635	7.94	34.50	0.548	0.290	4.128	39.49	19.30	0.256	-0.163	-1.676	0.770
20	0.6	0.635+j0.435	0.384	3.97	34.50	1.103	0.580	4.100	37.46	13.90	0.523	-0.201	-1.270	0.592
20	0.7	0.563+j0.475	0.318	3.40	34.50	1.293	0.677	4.087	37.06	12.72	0.609	-0.193	-1.127	0.543
20	0.9	0.420+j0.529	0.202	2.65	34.50	1.683	0.871	4.061	36.63	10.81	0.773	-0.156	-0.839	0.456
20	1.1	0.281+j0.551	0.107	2.16	34.50	2.111	1.066	4.037	36.62	9.27	0.920	-0.099	-0.561	0.383
20	1.3	0.152+j0.546	0.028	1.83	34.50	2.682	1.264	4.021	36.98	7.99	1.047	-0.029	-0.303	0.322
40	0.1	0.953+j0.096	0.911	20.32	49.29	0.227	0.101	5.838	O/L Unstable		0.128	-0.116	-1.905	0.916
40	0.2	0.898+j0.182	0.829	10.16	49.29	0.455	0.202	5.812	O/L Unstable		0.255	-0.211	-1.796	0.840
40	0.3	0.838+j0.259	0.754	6.77	49.29	0.686	0.304	5.806	O/L Unstable		0.379	-0.286	-1.676	0.770
40	0.6	0.635+j0.435	0.559	3.39	49.29	1.416	0.608	5.777	32.50	10.93	0.729	-0.407	-1.270	0.592
40	0.7	0.563+j0.475	0.502	2.90	49.29	1.685	0.710	5.765	31.75	9.91	0.835	-0.419	-1.127	0.543
40	0.9	0.420+j0.529	0.398	2.26	49.29	2.344	0.916	5.738	30.70	8.31	1.024	-0.408	-0.839	0.456
40	1.1	0.281+j0.551	0.305	1.85	49.29	9.990	1.124	5.712	30.17	7.08	1.182	-0.361	-0.561	0.383
40	1.3	0.152+j0.546	0.221	1.56	49.29	9.990	1.336	5.694	30.10	6.10	1.307	-0.289	-0.303	0.322
60	0.1	0.953+j0.096	0.947	16.83	87.94	0.335	0.105	8.910	O/L Unstable		0.213	-0.202	-1.905	0.916
60	0.2	0.898+j0.182	0.896	8.41	87.94	0.677	0.211	8.906	O/L Unstable		0.417	-0.374	-1.796	0.840
60	0.3	0.838+j0.259	0.847	5.61	87.94	1.035	0.317	8.899	O/L Unstable		0.611	-0.518	-1.676	0.770
60	0.6	0.635+j0.435	0.712	2.80	87.94	2.528	0.635	8.854	O/L Unstable		1.117	-0.796	-1.270	0.592
60	0.7	0.563+j0.475	0.670	2.40	87.94	9.990	0.742	8.834	O/L Unstable		1.259	-0.843	-1.127	0.543
60	0.9	0.420+j0.529	0.588	1.87	87.94	9.990	0.959	8.787	O/L Unstable		1.496	-0.880	-0.839	0.456
60	1.1	0.281+j0.551	0.509	1.53	87.94	9.990	1.179	8.736	O/L Unstable		1.674	-0.853	-0.561	0.383
60	1.3	0.152+j0.546	0.433	1.29	87.94	9.990	1.405	8.687	O/L Unstable		1.795	-0.776	-0.303	0.322
80	0.1	0.953+j0.096	0.981	13.34	294.89	0.902	0.108	17.040	O/L Unstable		0.589	-0.578	-1.905	0.916
80	0.2	0.898+j0.182	0.962	6.67	294.89	2.102	0.217	17.023	O/L Unstable		1.134	-1.091	-1.796	0.840
80	0.3	0.838+j0.259	0.943	4.45	294.89	9.990	0.326	17.008	O/L Unstable		1.632	-1.539	-1.676	0.770
80	0.6	0.635+j0.435	0.886	2.22	294.89	9.990	0.655	16.923	O/L Unstable		2.829	-2.507	-1.270	0.592
80	0.7	0.563+j0.475	0.867	1.91	294.89	9.990	0.766	16.884	O/L Unstable		3.128	-2.712	-1.127	0.543
80	0.9	0.420+j0.529	0.828	1.48	294.89	9.990	0.990	16.787	O/L Unstable		3.580	-2.963	-0.839	0.456
80	1.1	0.281+j0.551	0.786	1.21	294.89	9.990	1.220	16.670	O/L Unstable		3.847	-3.025	-0.561	0.383
80	1.3	0.152+j0.546	0.742	1.03	294.89	9.990	1.458	16.537	O/L Unstable		3.947	-2.929	-0.303	0.322

C/L SYSTEM IN COMPLEX Z-PLAIN				C/L STEP RES.		C/L FREQUENCY RES.			O/L FREQUENCY RES.		SYSTEM COEFFICIENTS			
α	$\omega_o T$	POLES	ZERO	tp/T	Mp(%)	WbT	WcT	Mr(db)	PM	GM(db)	A	B	C	D
						ξ =0.5								
-80	0.1	0.939+j0.094	Out of Range											
-80	0.2	0.873+j0.177	Out of Range											
-80	0.3	0.803+j0.249	Out of Range											
-80	0.6	0.584+j0.399	Out of Range											
-80	0.7	0.511+j0.430	Out of Range											
-80	0.9	0.370+j0.466	Out of Range											
-80	1.1	0.240+j0.472	Out of Range											
-80	1.3	0.126+j0.455	Out of Range											
-60	0.1	0.939+j0.094	Out of Range											
-60	0.2	0.873+j0.177	Out of Range											
-60	0.3	0.803+j0.249	Out of Range											
-60	0.6	0.584+j0.399	Out of Range											
-60	0.7	0.511+j0.430	Out of Range											
-60	0.9	0.370+j0.466	Out of Range											
-60	1.1	0.240+j0.472	Out of Range											
-60	1.3	0.126+j0.455	-10.309	2.82	20.87	2.238	1.156	1.789	54.23	5.48	0.086	0.885	-0.253	0.223
-40	0.1	0.939+j0.094	Out of Range											
-40	0.2	0.873+j0.177	Out of Range											
-40	0.3	0.803+j0.249	Out of Range											
-40	0.6	0.584+j0.399	-3.097	5.53	16.66	0.878	0.488	1.233	51.99	9.50	0.081	0.252	-1.167	0.500
-40	0.7	0.511+j0.430	-2.301	4.74	16.66	1.015	0.565	1.189	52.37	9.17	0.129	0.296	-1.021	0.446
-40	0.9	0.370+j0.466	-1.566	3.68	16.66	1.275	0.712	1.089	53.18	8.70	0.239	0.375	-0.739	0.354
-40	1.1	0.240+j0.472	-1.202	3.01	16.66	1.514	0.849	0.978	53.98	8.46	0.363	0.437	-0.481	0.281
-40	1.3	0.126+j0.455	-0.972	2.55	16.66	1.732	0.973	0.868	54.73	8.38	0.492	0.478	-0.253	0.223
-30	0.1	0.939+j0.094	-0.962	31.42	16.30	0.147	0.082	1.240	51.60	25.43	0.006	0.006	-1.878	0.891
-30	0.2	0.873+j0.177	-0.926	15.71	16.30	0.293	0.163	1.239	51.50	20.04	0.025	0.023	-1.746	0.794
-30	0.3	0.803+j0.249	-0.891	10.47	16.30	0.439	0.244	1.228	51.49	17.13	0.053	0.047	-1.607	0.707
-30	0.6	0.584+j0.399	-0.791	5.24	16.30	0.866	0.483	1.167	51.88	12.87	0.186	0.147	-1.167	0.500
-30	0.7	0.511+j0.430	-0.760	4.49	16.30	1.004	0.560	1.140	52.11	12.09	0.241	0.183	-1.021	0.446
-30	0.9	0.370+j0.466	-0.700	3.49	16.30	1.271	0.711	1.078	52.67	11.02	0.361	0.253	-0.739	0.354
-30	1.1	0.240+j0.472	-0.643	2.86	16.30	1.527	0.856	1.013	53.27	10.36	0.487	0.313	-0.481	0.281
-30	1.3	0.126+j0.455	-0.588	2.42	16.30	1.773	0.995	0.951	53.86	10.00	0.611	0.359	-0.253	0.223
-20	0.1	0.939+j0.094	0.526	29.67	16.62	0.149	0.083	1.324	52.05	39.48	0.027	-0.014	-1.878	0.891
-20	0.2	0.873+j0.177	0.240	14.84	16.62	0.298	0.165	1.317	51.68	33.40	0.062	-0.015	-1.746	0.794
-20	0.3	0.803+j0.249	0.054	9.89	16.62	0.446	0.247	1.309	51.42	29.72	0.106	-0.006	-1.607	0.707
-20	0.6	0.584+j0.399	-0.228	4.95	16.62	0.885	0.492	1.268	51.22	19.17	0.271	0.062	-1.167	0.500
-20	0.7	0.511+j0.430	-0.275	4.24	16.62	1.029	0.572	1.250	51.31	16.97	0.333	0.092	-1.021	0.446
-20	0.9	0.370+j0.466	-0.333	3.30	16.62	1.312	0.730	1.211	51.62	14.33	0.461	0.154	-0.739	0.354
-20	1.1	0.240+j0.472	-0.361	2.70	16.62	1.589	0.885	1.171	52.06	12.84	0.588	0.212	-0.481	0.281
-20	1.3	0.126+j0.455	-0.370	2.28	16.62	1.867	1.039	1.138	52.54	11.96	0.708	0.262	-0.253	0.223

C/L SYSTEM IN COMPLEX Z-PLAIN				C/L STEP RES.		C/L FREQUENCY RES.			O/L FREQUENCY RES.		SYSTEM COEFFICIENTS			
α	$\omega_o T$	POLES	ZERO	tp/T	Mp(%)	WbT	WrT	Mr(db)	PM	GM(db)	A	B	C	D
						ξ =0.5								
0	0.1	0.939+j0.094	0.793	26.18	19.10	0.163	0.088	1.809	51.92	31.02	0.061	-0.048	-1.878	0.891
0	0.2	0.873+j0.177	0.626	13.09	19.10	0.327	0.176	1.797	50.94	25.19	0.127	-0.079	-1.746	0.794
0	0.3	0.803+j0.249	0.489	8.73	19.10	0.490	0.264	1.793	50.14	21.81	0.197	-0.096	-1.607	0.707
0	0.6	0.584+j0.399	0.201	4.36	19.10	0.981	0.528	1.773	48.68	16.04	0.416	-0.084	-1.167	0.500
0	0.7	0.511+j0.430	0.133	3.74	19.10	1.145	0.616	1.765	48.45	14.73	0.489	-0.065	-1.021	0.446
0	0.9	0.370+j0.466	0.025	2.91	19.10	1.478	0.792	1.749	48.27	12.54	0.630	-0.016	-0.739	0.354
0	1.1	0.240+j0.472	-0.053	2.38	19.10	1.824	0.969	1.737	48.40	10.75	0.760	0.040	-0.481	0.281
0	1.3	0.126+j0.455	-0.111	2.01	19.10	2.204	1.148	1.738	48.76	9.24	0.874	0.097	-0.253	0.223
20	0.1	0.939+j0.094	0.868	22.69	24.87	0.190	0.095	2.677	50.55	26.93	0.095	-0.083	-1.878	0.891
20	0.2	0.873+j0.177	0.752	11.34	24.87	0.380	0.190	2.682	48.87	21.26	0.191	-0.144	-1.746	0.794
20	0.3	0.803+j0.249	0.650	7.56	24.87	0.571	0.286	2.680	47.48	18.06	0.287	-0.187	-1.607	0.707
20	0.6	0.584+j0.399	0.408	3.78	24.87	1.158	0.572	2.669	44.67	12.82	0.562	-0.229	-1.167	0.500
20	0.7	0.511+j0.430	0.343	3.24	24.87	1.362	0.669	2.664	44.10	11.70	0.646	-0.221	-1.021	0.446
20	0.9	0.370+j0.466	0.232	2.52	24.87	1.796	0.862	2.658	43.39	9.89	0.800	-0.186	-0.739	0.354
20	1.1	0.240+j0.472	0.141	2.06	24.87	2.317	1.060	2.660	43.20	8.49	0.932	-0.131	-0.481	0.281
20	1.3	0.126+j0.455	0.066	1.75	24.87	9.990	1.263	2.676	43.43	7.35	1.039	-0.069	-0.253	0.223
40	0.1	0.939+j0.094	0.910	19.20	37.32	0.238	0.102	4.188	O/L Unstable		0.140	-0.127	-1.878	0.891
40	0.2	0.873+j0.177	0.828	9.60	37.32	0.478	0.205	4.187	O/L Unstable		0.275	-0.228	-1.746	0.794
40	0.3	0.803+j0.249	0.752	6.40	37.32	0.722	0.308	4.184	O/L Unstable		0.405	-0.305	-1.607	0.707
40	0.6	0.584+j0.399	0.557	3.20	37.32	1.508	0.618	4.170	38.82	10.32	0.751	-0.419	-1.167	0.500
40	0.7	0.511+j0.430	0.501	2.74	37.32	1.811	0.722	4.165	37.92	9.35	0.850	-0.426	-1.021	0.446
40	0.9	0.370+j0.466	0.398	2.13	37.32	2.691	0.934	4.157	36.70	7.84	1.021	-0.407	-0.739	0.354
40	1.1	0.240+j0.472	0.308	1.75	37.32	9.990	1.151	4.156	36.14	6.71	1.156	-0.356	-0.481	0.281
40	1.3	0.126+j0.455	0.227	1.48	37.32	9.990	1.377	4.169	36.17	5.84	1.255	-0.285	-0.253	0.223
60	0.1	0.939+j0.094	0.944	15.71	69.94	0.350	0.109	7.031	O/L Unstable		0.224	-0.211	-1.878	0.891
60	0.2	0.873+j0.177	0.891	7.85	69.94	0.708	0.219	7.031	O/L Unstable		0.433	-0.386	-1.746	0.794
60	0.3	0.803+j0.249	0.840	5.24	69.94	1.086	0.328	7.025	O/L Unstable		0.627	-0.527	-1.607	0.707
60	0.6	0.584+j0.399	0.700	2.62	69.94	3.034	0.661	6.993	O/L Unstable		1.108	-0.775	-1.167	0.500
60	0.7	0.511+j0.430	0.656	2.24	69.94	9.990	0.773	6.978	O/L Unstable		1.234	-0.810	-1.021	0.446
60	0.9	0.370+j0.466	0.573	1.75	69.94	9.990	1.002	6.948	O/L Unstable		1.437	-0.823	-0.739	0.354
60	1.1	0.240+j0.472	0.493	1.43	69.94	9.990	1.239	6.919	O/L Unstable		1.578	-0.778	-0.481	0.281
60	1.3	0.126+j0.455	0.416	1.21	69.94	9.990	1.487	6.899	26.11	4.23	1.662	-0.691	-0.253	0.223
80	0.1	0.939+j0.094	0.979	12.22	246.33	0.922	0.115	14.803	O/L Unstable		0.595	-0.583	-1.878	0.891
80	0.2	0.873+j0.177	0.958	6.11	246.33	2.178	0.229	14.801	O/L Unstable		1.131	-1.083	-1.746	0.794
80	0.3	0.803+j0.249	0.937	4.07	246.33	9.990	0.344	14.785	O/L Unstable		1.606	-1.506	-1.607	0.707
80	0.6	0.584+j0.399	0.876	2.04	246.33	9.990	0.694	14.701	O/L Unstable		2.681	-2.348	-1.167	0.500
80	0.7	0.511+j0.430	0.855	1.75	246.33	9.990	0.813	14.662	O/L Unstable		2.928	-2.504	-1.021	0.446
80	0.9	0.370+j0.466	0.812	1.36	246.33	9.990	1.056	14.567	O/L Unstable		3.272	-2.658	-0.739	0.354
80	1.1	0.240+j0.472	0.767	1.11	246.33	9.990	1.309	14.455	O/L Unstable		3.438	-2.638	-0.481	0.281
80	1.3	0.126+j0.455	0.719	0.94	246.33	9.990	1.579	14.330	O/L Unstable		3.454	-2.483	-0.253	0.223

C/L SYSTEM IN COMPLEX Z-PLAIN				C/L STEP RES.		C/L FREQUENCY RES.			O/L FREQUENCY RES.		SYSTEM COEFFICIENTS			
α	$\omega_o T$	POLES	ZERO	tp/T	Mp(%)	WbT	WrT	Mr(db)	PM	GM(db)	A	B	C	D
						ξ =0.6								
-80	0.1	0.923+j0.093	Out of Range											
-80	0.2	0.844+j0.171	Out of Range											
-80	0.3	0.763+j0.236	Out of Range											
-80	0.6	0.526+j0.360	Out of Range											
-80	0.7	0.452+j0.381	Out of Range											
-80	0.9	0.316+j0.399	Out of Range											
-80	1.1	0.199+j0.391	Out of Range											
-80	1.3	0.101+j0.363	Out of Range											
-60	0.1	0.923+j0.093	Out of Range											
-60	0.2	0.844+j0.171	Out of Range											
-60	0.3	0.763+j0.236	Out of Range											
-60	0.6	0.526+j0.360	Out of Range											
-60	0.7	0.452+j0.381	Out of Range											
-60	0.9	0.316+j0.399	Out of Range											
-60	1.1	0.199+j0.391	-5.369	3.22	11.20	1.658	0.774	0.452	57.47	6.87	0.125	0.670	-0.398	0.192
-60	1.3	0.101+j0.363	-2.489	2.73	11.20	1.779	0.788	0.250	58.38	7.15	0.270	0.671	-0.202	0.142
-40	0.1	0.923+j0.093	Out of Range											
-40	0.2	0.844+j0.171	-3.143	15.98	9.50	0.287	0.132	0.354	58.09	17.34	0.013	0.041	-1.687	0.741
-40	0.3	0.763+j0.236	-1.860	10.65	9.50	0.429	0.197	0.344	57.96	15.53	0.039	0.073	-1.526	0.638
-40	0.6	0.526+j0.360	-1.063	5.33	9.50	0.841	0.381	0.300	57.97	12.57	0.172	0.182	-1.053	0.407
-40	0.7	0.452+j0.381	-0.954	4.57	9.50	0.973	0.437	0.281	58.05	12.02	0.228	0.217	-0.905	0.350
-40	0.9	0.316+j0.399	-0.795	3.55	9.50	1.225	0.541	0.242	58.28	11.29	0.349	0.277	-0.633	0.259
-40	1.1	0.199+j0.391	-0.678	2.91	9.50	1.465	0.634	0.204	58.52	10.92	0.474	0.321	-0.398	0.192
-40	1.3	0.101+j0.363	-0.583	2.46	9.50	1.696	0.719	0.175	58.72	10.82	0.594	0.346	-0.202	0.142
-30	0.1	0.923+j0.093	0.381	30.22	9.58	0.145	0.067	0.375	59.54	41.26	0.023	-0.009	-1.846	0.861
-30	0.2	0.844+j0.171	0.069	15.11	9.58	0.289	0.134	0.374	59.04	35.05	0.058	-0.004	-1.687	0.741
-30	0.3	0.763+j0.236	-0.109	10.07	9.58	0.433	0.200	0.368	58.66	30.60	0.101	0.011	-1.526	0.638
-30	0.6	0.526+j0.360	-0.332	5.04	9.58	0.857	0.393	0.342	58.04	17.76	0.266	0.088	-1.053	0.407
-30	0.7	0.452+j0.381	-0.359	4.32	9.58	0.995	0.455	0.331	57.96	16.30	0.328	0.118	-0.905	0.350
-30	0.9	0.316+j0.399	-0.382	3.36	9.58	1.266	0.575	0.308	57.91	14.46	0.453	0.173	-0.633	0.259
-30	1.1	0.199+j0.391	-0.380	2.75	9.58	1.534	0.691	0.288	57.93	13.43	0.576	0.219	-0.398	0.192
-30	1.3	0.101+j0.363	-0.364	2.32	9.58	1.806	0.809	0.276	57.95	12.19	0.689	0.251	-0.202	0.142
-20	0.1	0.923+j0.093	0.664	28.47	10.06	0.150	0.071	0.480	60.19	34.42	0.043	-0.029	-1.846	0.861
-20	0.2	0.844+j0.171	0.430	14.24	10.06	0.300	0.142	0.475	59.40	28.45	0.094	-0.040	-1.687	0.741
-20	0.3	0.763+j0.236	0.260	9.49	10.06	0.450	0.212	0.471	58.76	24.91	0.151	-0.039	-1.526	0.638
-20	0.6	0.526+j0.360	-0.033	4.75	10.06	0.896	0.422	0.455	57.54	18.51	0.343	0.011	-1.053	0.407
-20	0.7	0.452+j0.381	-0.089	4.07	10.06	1.044	0.490	0.448	57.31	16.96	0.409	0.036	-0.905	0.350
-20	0.9	0.316+j0.399	-0.163	3.16	10.06	1.340	0.627	0.436	57.02	14.32	0.538	0.088	-0.633	0.259
-20	1.1	0.199+j0.391	-0.205	2.59	10.06	1.640	0.764	0.428	56.89	12.12	0.659	0.135	-0.398	0.192
-20	1.3	0.101+j0.363	-0.226	2.19	10.06	1.961	0.906	0.431	56.82	10.28	0.767	0.174	-0.202	0.142

C/L SYSTEM IN COMPLEX Z-PLAIN				C/L STEP RES.		C/L FREQUENCY RES.			O/L FREQUENCY RES.		SYSTEM COEFFICIENTS			
α	$\omega_o T$	POLES	ZERO	tp/T	Mp(%)	WbT	WcT	Mr(db)	PM	GM(db)	A	B	C	D
						ξ =0.6								
0	0.1	0.923+j0.093	0.812	24.98	12.29	0.169	0.082	0.877	60.19	28.82	0.077	-0.062	-1.846	0.861
0	0.2	0.844+j0.171	0.657	12.49	12.29	0.338	0.163	0.874	58.75	23.06	0.156	-0.103	-1.687	0.741
0	0.3	0.763+j0.236	0.528	8.33	12.29	0.508	0.245	0.873	57.56	19.76	0.237	-0.125	-1.526	0.638
0	0.6	0.526+j0.360	0.253	4.16	12.29	1.023	0.491	0.869	55.15	14.23	0.474	-0.120	-1.053	0.407
0	0.7	0.452+j0.381	0.187	3.57	12.29	1.199	0.574	0.868	54.66	13.00	0.548	-0.103	-0.905	0.350
0	0.9	0.316+j0.399	0.084	2.78	12.29	1.565	0.741	0.871	54.00	11.02	0.684	-0.057	-0.633	0.259
0	1.1	0.199+j0.391	0.008	2.27	12.29	1.968	0.913	0.883	53.70	9.45	0.801	-0.007	-0.398	0.192
0	1.3	0.101+j0.363	-0.046	1.92	12.29	2.489	1.095	0.910	53.64	8.19	0.899	0.041	-0.202	0.142
20	0.1	0.923+j0.093	0.869	21.49	16.99	0.199	0.093	1.598	58.57	25.54	0.111	-0.096	-1.846	0.861
20	0.2	0.844+j0.171	0.754	10.75	16.99	0.400	0.186	1.598	56.41	19.94	0.219	-0.165	-1.687	0.741
20	0.3	0.763+j0.236	0.654	7.16	16.99	0.602	0.280	1.598	54.62	16.80	0.323	-0.211	-1.526	0.638
20	0.6	0.526+j0.360	0.415	3.58	16.99	1.232	0.563	1.601	51.01	11.76	0.605	-0.251	-1.053	0.407
20	0.7	0.452+j0.381	0.351	3.07	16.99	1.458	0.658	1.604	50.26	10.71	0.686	-0.241	-0.905	0.350
20	0.9	0.316+j0.399	0.244	2.39	16.99	1.964	0.854	1.616	49.29	9.05	0.829	-0.202	-0.633	0.259
20	1.1	0.199+j0.391	0.158	1.95	16.99	2.750	1.057	1.640	48.90	7.80	0.943	-0.149	-0.398	0.192
20	1.3	0.101+j0.363	0.088	1.65	16.99	9.990	1.273	1.684	49.00	6.84	1.031	-0.091	-0.202	0.142
40	0.1	0.923+j0.093	0.906	18.00	27.07	0.252	0.104	2.875	O/L Unstable		0.155	-0.140	-1.846	0.861
40	0.2	0.844+j0.171	0.821	9.00	27.07	0.506	0.209	2.880	51.89	17.24	0.300	-0.246	-1.687	0.741
40	0.3	0.763+j0.236	0.743	6.00	27.07	0.765	0.314	2.880	49.46	14.27	0.435	-0.323	-1.526	0.638
40	0.6	0.526+j0.360	0.544	3.00	27.07	1.628	0.632	2.881	44.62	9.70	0.776	-0.422	-1.053	0.407
40	0.7	0.452+j0.381	0.487	2.57	27.07	1.985	0.741	2.883	43.63	8.78	0.867	-0.422	-0.905	0.350
40	0.9	0.316+j0.399	0.385	2.00	27.07	9.990	0.963	2.894	42.34	7.39	1.018	-0.392	-0.633	0.259
40	1.1	0.199+j0.391	0.296	1.64	27.07	9.990	1.196	2.919	41.87	6.39	1.129	-0.334	-0.398	0.192
40	1.3	0.101+j0.363	0.219	1.38	27.07	9.990	1.447	2.964	42.10	5.65	1.204	-0.264	-0.202	0.142
60	0.1	0.923+j0.093	0.939	14.51	53.89	0.367	0.115	5.428	O/L Unstable		0.237	-0.223	-1.846	0.861
60	0.2	0.844+j0.171	0.881	7.25	53.89	0.745	0.230	5.426	O/L Unstable		0.453	-0.399	-1.687	0.741
60	0.3	0.763+j0.236	0.827	4.84	53.89	1.148	0.346	5.422	O/L Unstable		0.646	-0.534	-1.526	0.638
60	0.6	0.526+j0.360	0.677	2.42	53.89	9.990	0.699	5.403	O/L Unstable		1.097	-0.743	-1.053	0.407
60	0.7	0.452+j0.381	0.631	2.07	53.89	9.990	0.819	5.395	O/L Unstable		1.208	-0.763	-0.905	0.350
60	0.9	0.316+j0.399	0.544	1.61	53.89	9.990	1.068	5.383	O/L Unstable		1.374	-0.748	-0.633	0.259
60	1.1	0.199+j0.391	0.462	1.32	53.89	9.990	1.332	5.379	31.24	4.79	1.478	-0.683	-0.398	0.192
60	1.3	0.101+j0.363	0.385	1.12	53.89	9.990	1.622	5.393	31.45	4.27	1.529	-0.588	-0.202	0.142
80	0.1	0.923+j0.093	0.976	11.02	201.62	0.947	0.123	12.790	O/L Unstable		0.602	-0.588	-1.846	0.861
80	0.2	0.844+j0.171	0.952	5.51	201.62	2.277	0.247	12.781	O/L Unstable		1.126	-1.073	-1.687	0.741
80	0.3	0.763+j0.236	0.929	3.67	201.62	9.990	0.371	12.765	O/L Unstable		1.575	-1.464	-1.526	0.638
80	0.6	0.526+j0.360	0.859	1.84	201.62	9.990	0.753	12.681	O/L Unstable		2.516	-2.162	-1.053	0.407
80	0.7	0.452+j0.381	0.836	1.57	201.62	9.990	0.884	12.641	O/L Unstable		2.709	-2.264	-0.905	0.350
80	0.9	0.316+j0.399	0.787	1.22	201.62	9.990	1.157	12.549	O/L Unstable		2.945	-2.319	-0.633	0.259
80	1.1	0.199+j0.391	0.737	1.00	201.62	9.990	1.451	12.442	O/L Unstable		3.016	-2.222	-0.398	0.192
80	1.3	0.101+j0.363	0.682	0.85	201.62	9.990	1.782	12.328	O/L Unstable		2.960	-2.020	-0.202	0.142

C/L SYSTEM IN COMPLEX Z-PLAIN				C/L STEP RES.		C/L FREQUENCY RES.			O/L FREQUENCY RES.		SYSTEM COEFFICIENTS			
α	$\omega_o T$	POLES	ZERO	tp/T	Mp(%)	WbT	WrT	Mr(db)	PM	GM(db)	A	B	C	D
						ξ =0.7								
-80	0.1	0.902+j0.091	Out of Range											
-80	0.2	0.806+j0.163	Out of Range											
-80	0.3	0.712+j0.220	Out of Range											
-80	0.6	0.458+j0.314	Out of Range											
-80	0.7	0.385+j0.324	Out of Range											
-80	0.9	0.257+j0.324	Out of Range											
-80	1.1	0.154+j0.303	Out of Range											
-80	1.3	0.075+j0.269	Out of Range											
-60	0.1	0.902+j0.091	Out of Range											
-60	0.2	0.806+j0.163	Out of Range											
-60	0.3	0.712+j0.220	Out of Range											
-60	0.6	0.458+j0.314	Out of Range											
-60	0.7	0.385+j0.324	-8.110	4.88	5.03	1.027	0.226	0.012	60.41	8.74	0.053	0.430	-0.770	0.254
-60	0.9	0.257+j0.324	-2.625	3.79	5.03	1.238	Mono Decreasing		60.94	8.76	0.181	0.476	-0.515	0.171
-60	1.1	0.154+j0.303	-1.518	3.10	5.03	1.410	Mono Decreasing		61.43	9.00	0.321	0.487	-0.309	0.116
-60	1.3	0.075+j0.269	-1.025	2.63	5.03	1.563	Mono Decreasing		61.81	9.43	0.458	0.470	-0.150	0.078
-40	0.1	0.902+j0.091	0.190	30.64	4.62	0.142	0.022	0.000	65.38	42.91	0.022	-0.004	-1.804	0.822
-40	0.2	0.806+j0.163	-0.123	15.32	4.62	0.284	0.042	0.003	64.68	33.40	0.057	0.007	-1.611	0.676
-40	0.3	0.712+j0.220	-0.273	10.21	4.62	0.424	0.059	0.002	64.12	24.48	0.103	0.028	-1.424	0.555
-40	0.6	0.458+j0.314	-0.406	5.11	4.62	0.837	0.067	0.000	62.97	17.04	0.279	0.113	-0.917	0.308
-40	0.7	0.385+j0.324	-0.410	4.38	4.62	0.971	0.029	0.000	62.71	16.00	0.343	0.141	-0.770	0.254
-40	0.9	0.257+j0.324	-0.395	3.40	4.62	1.234	Mono Decreasing		62.28	14.73	0.471	0.186	-0.515	0.171
-40	1.1	0.154+j0.303	-0.365	2.79	4.62	1.498	Mono Decreasing		61.90	13.61	0.591	0.216	-0.309	0.116
-40	1.3	0.075+j0.269	-0.328	2.36	4.62	1.777	Mono Decreasing		61.52	11.16	0.699	0.229	-0.150	0.078
-30	0.1	0.902+j0.091	0.611	28.90	4.85	0.147	0.035	0.017	66.76	34.04	0.046	-0.028	-1.804	0.822
-30	0.2	0.806+j0.163	0.356	14.45	4.85	0.295	0.069	0.016	65.74	28.03	0.100	-0.036	-1.611	0.676
-30	0.3	0.712+j0.220	0.183	9.63	4.85	0.441	0.102	0.015	64.88	24.43	0.161	-0.029	-1.424	0.555
-30	0.6	0.458+j0.314	-0.086	4.82	4.85	0.879	0.194	0.012	63.04	17.79	0.361	0.031	-0.917	0.308
-30	0.7	0.385+j0.324	-0.130	4.13	4.85	1.025	0.222	0.011	62.59	16.18	0.428	0.056	-0.770	0.254
-30	0.9	0.257+j0.324	-0.182	3.21	4.85	1.319	0.279	0.010	61.87	13.46	0.556	0.101	-0.515	0.171
-30	1.1	0.154+j0.303	-0.203	2.63	4.85	1.626	0.345	0.011	61.28	11.29	0.671	0.136	-0.309	0.116
-30	1.3	0.075+j0.269	-0.207	2.22	4.85	1.970	0.438	0.014	60.75	9.57	0.770	0.159	-0.150	0.078
-20	0.1	0.902+j0.091	0.726	27.15	5.31	0.156	0.048	0.055	67.52	30.46	0.065	-0.047	-1.804	0.822
-20	0.2	0.806+j0.163	0.522	13.58	5.31	0.311	0.095	0.058	66.17	24.61	0.135	-0.071	-1.611	0.676
-20	0.3	0.712+j0.220	0.368	9.05	5.31	0.467	0.142	0.058	65.03	21.20	0.208	-0.076	-1.424	0.555
-20	0.6	0.458+j0.314	0.084	4.53	5.31	0.939	0.284	0.056	62.57	15.27	0.427	-0.036	-0.917	0.308
-20	0.7	0.385+j0.324	0.027	3.88	5.31	1.098	0.332	0.056	61.99	13.92	0.497	-0.014	-0.770	0.254
-20	0.9	0.257+j0.324	-0.051	3.02	5.31	1.428	0.431	0.058	61.05	11.70	0.625	0.032	-0.515	0.171
-20	1.1	0.154+j0.303	-0.098	2.47	5.31	1.787	0.543	0.064	60.34	9.96	0.735	0.072	-0.309	0.116
-20	1.3	0.075+j0.269	-0.123	2.09	5.31	2.225	0.677	0.077	59.77	8.60	0.827	0.101	-0.150	0.078

C/L SYSTEM IN COMPLEX Z-PLAIN				C/L STEP RES.		C/L FREQUENCY RES.			O/L FREQUENCY RES.		SYSTEM COEFFICIENTS			
α	$\omega_o T$	POLES	ZERO	tp/T	Mp(%)	WbT	WrT	Mr(db)	PM	GM(db)	A	B	C	D
						ξ =0.7								
0	0.1	0.902+j0.091	0.818	23.66	7.02	0.179	0.070	0.280	67.56	26.60	0.098	-0.080	-1.804	0.822
0	0.2	0.806+j0.163	0.668	11.83	7.02	0.359	0.140	0.280	65.55	20.93	0.194	-0.130	-1.611	0.676
0	0.3	0.712+j0.220	0.544	7.89	7.02	0.540	0.211	0.281	63.88	17.73	0.288	-0.157	-1.424	0.555
0	0.6	0.458+j0.314	0.277	3.94	7.02	1.100	0.426	0.288	60.37	12.50	0.542	-0.150	-0.917	0.308
0	0.7	0.385+j0.324	0.214	3.38	7.02	1.298	0.500	0.293	59.58	11.39	0.615	-0.132	-0.770	0.254
0	0.9	0.257+j0.324	0.116	2.63	7.02	1.729	0.655	0.307	58.43	9.64	0.743	-0.086	-0.515	0.171
0	1.1	0.154+j0.303	0.046	2.15	7.02	2.276	0.825	0.331	57.69	8.34	0.846	-0.039	-0.309	0.116
0	1.3	0.075+j0.269	-0.004	1.82	7.02	9.990	1.018	0.371	57.25	7.35	0.925	0.003	-0.150	0.078
20	0.1	0.902+j0.091	0.864	20.17	10.52	0.213	0.089	0.776	65.81	24.01	0.131	-0.113	-1.804	0.822
20	0.2	0.806+j0.163	0.746	10.09	10.52	0.428	0.179	0.781	63.09	18.50	0.254	-0.189	-1.611	0.676
20	0.3	0.712+j0.220	0.643	6.72	10.52	0.646	0.268	0.783	60.87	15.45	0.368	-0.237	-1.424	0.555
20	0.6	0.458+j0.314	0.403	3.36	10.52	1.346	0.544	0.799	56.42	10.68	0.656	-0.264	-0.917	0.308
20	0.7	0.385+j0.324	0.341	2.88	10.52	1.610	0.640	0.808	55.50	9.71	0.733	-0.250	-0.770	0.254
20	0.9	0.257+j0.324	0.237	2.24	10.52	2.275	0.839	0.835	54.29	8.24	0.861	-0.204	-0.515	0.171
20	1.1	0.154+j0.303	0.156	1.83	10.52	9.990	1.056	0.878	53.73	7.19	0.956	-0.149	-0.309	0.116
20	1.3	0.075+j0.269	0.093	1.55	10.52	9.990	1.301	0.943	53.67	6.44	1.023	-0.095	-0.150	0.078
40	0.1	0.902+j0.091	0.898	16.68	18.17	0.269	0.107	1.782	61.74	21.58	0.174	-0.156	-1.804	0.822
40	0.2	0.806+j0.163	0.806	8.34	18.17	0.543	0.214	1.783	58.21	16.25	0.331	-0.267	-1.611	0.676
40	0.3	0.712+j0.220	0.722	5.56	18.17	0.824	0.321	1.786	55.40	13.37	0.473	-0.341	-1.424	0.555
40	0.6	0.458+j0.314	0.513	2.78	18.17	1.807	0.653	1.804	50.02	9.03	0.805	-0.413	-0.917	0.308
40	0.7	0.385+j0.324	0.455	2.38	18.17	2.276	0.768	1.815	48.99	8.19	0.887	-0.404	-0.770	0.254
40	0.9	0.257+j0.324	0.353	1.85	18.17	9.990	1.009	1.847	47.78	6.96	1.015	-0.358	-0.515	0.171
40	1.1	0.154+j0.303	0.266	1.52	18.17	9.990	1.272	1.898	47.52	6.12	1.100	-0.293	-0.309	0.116
40	1.3	0.075+j0.269	0.193	1.28	18.17	9.990	1.575	1.978	48.01	5.55	1.151	-0.223	-0.150	0.078
60	0.1	0.902+j0.091	0.930	13.19	39.20	0.390	0.123	3.959	O/L Unstable		0.255	-0.237	-1.804	0.822
60	0.2	0.806+j0.163	0.865	6.59	39.20	0.794	0.247	3.960	O/L Unstable		0.477	-0.413	-1.611	0.676
60	0.3	0.712+j0.220	0.804	4.40	39.20	1.231	0.372	3.959	O/L Unstable		0.670	-0.538	-1.424	0.555
60	0.6	0.458+j0.314	0.639	2.20	39.20	9.990	0.756	3.958	O/L Unstable		1.085	-0.693	-0.917	0.308
60	0.7	0.385+j0.324	0.589	1.88	39.20	9.990	0.891	3.960	38.20	6.37	1.177	-0.693	-0.770	0.254
60	0.9	0.257+j0.324	0.496	1.47	39.20	9.990	1.175	3.972	37.00	5.41	1.304	-0.648	-0.515	0.171
60	1.1	0.154+j0.303	0.411	1.20	39.20	9.990	1.491	4.002	36.95	4.79	1.371	-0.564	-0.309	0.116
60	1.3	0.075+j0.269	0.333	1.01	39.20	9.990	1.869	4.059	37.91	4.41	1.392	-0.463	-0.150	0.078
80	0.1	0.902+j0.091	0.971	9.70	158.94	0.979	0.137	10.800	O/L Unstable		0.611	-0.593	-1.804	0.822
80	0.2	0.806+j0.163	0.942	4.85	158.94	2.426	0.275	10.790	O/L Unstable		1.121	-1.056	-1.611	0.676
80	0.3	0.712+j0.220	0.914	3.23	158.94	9.990	0.414	10.774	O/L Unstable		1.537	-1.406	-1.424	0.555
80	0.6	0.458+j0.314	0.831	1.62	158.94	9.990	0.846	10.688	O/L Unstable		2.320	-1.928	-0.917	0.308
80	0.7	0.385+j0.324	0.803	1.39	158.94	9.990	0.999	10.649	O/L Unstable		2.455	-1.971	-0.770	0.254
80	0.9	0.257+j0.324	0.746	1.08	158.94	9.990	1.326	10.560	O/L Unstable		2.581	-1.925	-0.515	0.171
80	1.1	0.154+j0.303	0.685	0.88	158.94	9.990	1.703	10.464	O/L Unstable		2.565	-1.758	-0.309	0.116
80	1.3	0.075+j0.269	0.621	0.75	158.94	9.990	2.192	10.371	O/L Unstable		2.453	-1.525	-0.150	0.078

C/L SYSTEM IN COMPLEX Z-PLAIN				C/L STEP RES.		C/L FREQUENCY RES.			O/L FREQUENCY RES.		SYSTEM COEFFICIENTS			
α	$\omega_o T$	POLES	ZERO	tp/T	Mp(%)	WbT	WrT	Mr(db)	PM	GM(db)	A	B	C	D
						$\xi = 0.8$								
-80	0.1	0.871+j0.087	Out of Range											
-80	0.2	0.751+j0.152	Out of Range											
-80	0.3	0.640+j0.198	Out of Range											
-80	0.6	0.371+j0.254	Out of Range											
-80	0.7	0.301+j0.253	Out of Range											
-80	0.9	0.187+j0.236	Out of Range											
-80	1.1	0.105+j0.206	Out of Range											
-80	1.3	0.047+j0.170	Out of Range											
-60	0.1	0.871+j0.087	Out of Range											
-60	0.2	0.751+j0.152	Out of Range											
-60	0.3	0.640+j0.198	-9.209	10.87	1.55	0.440	Mono Decreasing		65.45	13.30	0.017	0.152	-1.281	0.449
-60	0.6	0.371+j0.254	-1.426	5.44	1.55	0.838	Mono Decreasing		64.90	11.93	0.190	0.270	-0.742	0.202
-60	0.7	0.301+j0.253	-1.124	4.66	1.55	0.958	Mono Decreasing		64.79	11.80	0.260	0.293	-0.602	0.155
-60	0.9	0.187+j0.236	-0.772	3.62	1.55	1.185	Mono Decreasing		64.60	11.85	0.404	0.312	-0.374	0.091
-60	1.1	0.105+j0.206	-0.565	2.96	1.55	1.407	Mono Decreasing		64.34	12.27	0.539	0.305	-0.209	0.053
-60	1.3	0.047+j0.170	-0.424	2.51	1.55	1.649	Mono Decreasing		63.95	11.98	0.658	0.279	-0.095	0.031
-40	0.1	0.871+j0.087	0.565	29.12	1.61	0.152	Mono Decreasing		71.99	32.28	0.056	-0.032	-1.742	0.766
-40	0.2	0.751+j0.152	0.299	14.56	1.61	0.303	Mono Decreasing		70.59	26.25	0.122	-0.036	-1.501	0.587
-40	0.3	0.640+j0.198	0.128	9.71	1.61	0.454	Mono Decreasing		69.40	22.61	0.193	-0.025	-1.281	0.449
-40	0.6	0.371+j0.254	-0.106	4.85	1.61	0.907	Mono Decreasing		66.71	15.88	0.416	0.044	-0.742	0.202
-40	0.7	0.301+j0.253	-0.137	4.16	1.61	1.061	Mono Decreasing		66.01	14.29	0.487	0.066	-0.602	0.155
-40	0.9	0.187+j0.236	-0.165	3.24	1.61	1.379	Mono Decreasing		64.80	11.72	0.615	0.101	-0.374	0.091
-40	1.1	0.105+j0.206	-0.168	2.65	1.61	1.734	Mono Decreasing		63.75	9.82	0.723	0.121	-0.209	0.053
-40	1.3	0.047+j0.170	-0.157	2.24	1.61	2.195	Mono Decreasing		62.80	8.46	0.810	0.127	-0.095	0.031
-30	0.1	0.871+j0.087	0.691	27.38	1.80	0.161	Mono Decreasing		73.28	28.73	0.079	-0.054	-1.742	0.766
-30	0.2	0.751+j0.152	0.472	13.69	1.80	0.322	Mono Decreasing		71.49	22.92	0.161	-0.076	-1.501	0.587
-30	0.3	0.640+j0.198	0.313	9.13	1.80	0.483	Mono Decreasing		69.97	19.54	0.245	-0.077	-1.281	0.449
-30	0.6	0.371+j0.254	0.047	4.56	1.80	0.977	Mono Decreasing		66.55	13.71	0.483	-0.022	-0.742	0.202
-30	0.7	0.301+j0.253	0.000	3.91	1.80	1.149	Mono Decreasing		65.68	12.42	0.553	0.000	-0.602	0.155
-30	0.9	0.187+j0.236	-0.059	3.04	1.80	1.517	Mono Decreasing		64.23	10.37	0.677	0.040	-0.374	0.091
-30	1.1	0.105+j0.206	-0.087	2.49	1.80	1.957	Mono Decreasing		63.04	8.88	0.777	0.067	-0.209	0.053
-30	1.3	0.047+j0.170	-0.096	2.11	1.80	2.679	Mono Decreasing		62.05	7.81	0.854	0.082	-0.095	0.031
-20	0.1	0.871+j0.087	0.750	25.63	2.09	0.172	Mono Decreasing		73.95	26.68	0.097	-0.073	-1.742	0.766
-20	0.2	0.751+j0.152	0.560	12.82	2.09	0.344	Mono Decreasing		71.81	20.99	0.194	-0.109	-1.501	0.587
-20	0.3	0.640+j0.198	0.414	8.54	2.09	0.518	Mono Decreasing		70.00	17.75	0.288	-0.119	-1.281	0.449
-20	0.6	0.371+j0.254	0.143	4.27	2.09	1.059	Mono Decreasing		66.01	12.40	0.537	-0.077	-0.742	0.202
-20	0.7	0.301+j0.253	0.089	3.66	2.09	1.252	Mono Decreasing		65.03	11.26	0.607	-0.054	-0.602	0.155
-20	0.9	0.187+j0.236	0.015	2.85	2.09	1.680	Mono Decreasing		63.44	9.50	0.727	-0.011	-0.374	0.091
-20	1.1	0.105+j0.206	-0.029	2.33	2.09	2.247	Mono Decreasing		62.22	8.25	0.821	0.023	-0.209	0.053
-20	1.3	0.047+j0.170	-0.052	1.97	2.09	9.990	Mono Decreasing		61.27	7.36	0.891	0.046	-0.095	0.031

C/L SYSTEM IN COMPLEX Z-PLAIN				C/L STEP RES.		C/L FREQUENCY RES.			O/L FREQUENCY RES.		SYSTEM COEFFICIENTS			
α	$\omega_o T$	POLES	ZERO	tp/T	Mp(%)	WbT	WrT	Mr(db)	PM	GM(db)	A	B	C	D
						ξ =0.8								
0	0.1	0.871+j0.087	0.812	22.14	3.13	0.199	0.033	0.006	73.93	24.07	0.129	-0.105	-1.742	0.766
0	0.2	0.751+j0.152	0.658	11.07	3.13	0.400	0.067	0.007	71.14	18.56	0.249	-0.164	-1.501	0.587
0	0.3	0.640+j0.198	0.531	7.38	3.13	0.604	0.104	0.008	68.83	15.50	0.360	-0.191	-1.281	0.449
0	0.6	0.371+j0.254	0.269	3.69	3.13	1.262	0.235	0.012	64.03	10.72	0.629	-0.169	-0.742	0.202
0	0.7	0.301+j0.253	0.209	3.16	3.13	1.512	0.290	0.015	62.95	9.76	0.699	-0.146	-0.602	0.155
0	0.9	0.187+j0.236	0.119	2.46	3.13	2.135	0.426	0.025	61.32	8.34	0.813	-0.097	-0.374	0.091
0	1.1	0.105+j0.206	0.057	2.01	3.13	9.990	0.607	0.042	60.23	7.36	0.895	-0.051	-0.209	0.053
0	1.3	0.047+j0.170	0.017	1.70	3.13	9.990	0.850	0.072	59.53	6.70	0.953	-0.016	-0.095	0.031
20	0.1	0.871+j0.087	0.849	18.65	5.31	0.237	0.077	0.203	72.22	22.13	0.161	-0.137	-1.742	0.766
20	0.2	0.751+j0.152	0.720	9.33	5.31	0.477	0.155	0.208	68.79	16.77	0.305	-0.219	-1.501	0.587
20	0.3	0.640+j0.198	0.610	6.22	5.31	0.723	0.235	0.212	66.04	13.86	0.432	-0.263	-1.281	0.449
20	0.6	0.371+j0.254	0.362	3.11	5.31	1.562	0.489	0.234	60.70	9.48	0.721	-0.261	-0.742	0.202
20	0.7	0.301+j0.253	0.301	2.66	5.31	1.920	0.583	0.247	59.63	8.64	0.791	-0.238	-0.602	0.155
20	0.9	0.187+j0.236	0.203	2.07	5.31	9.990	0.792	0.281	58.22	7.44	0.899	-0.182	-0.374	0.091
20	1.1	0.105+j0.206	0.130	1.70	5.31	9.990	1.044	0.334	57.52	6.65	0.970	-0.126	-0.209	0.053
20	1.3	0.047+j0.170	0.077	1.43	5.31	9.990	1.365	0.411	57.28	6.15	1.015	-0.078	-0.095	0.031
40	0.1	0.871+j0.087	0.880	15.16	10.37	0.297	0.108	0.841	68.22	20.18	0.203	-0.178	-1.742	0.766
40	0.2	0.751+j0.152	0.774	7.58	10.37	0.601	0.217	0.847	64.05	14.99	0.377	-0.292	-1.501	0.587
40	0.3	0.640+j0.198	0.679	5.05	10.37	0.918	0.327	0.853	60.83	12.24	0.526	-0.357	-1.281	0.449
40	0.6	0.371+j0.254	0.453	2.53	10.37	2.158	0.677	0.890	55.08	8.26	0.842	-0.382	-0.742	0.202
40	0.7	0.301+j0.253	0.393	2.17	10.37	9.990	0.804	0.911	54.11	7.54	0.912	-0.359	-0.602	0.155
40	0.9	0.187+j0.236	0.291	1.68	10.37	9.990	1.083	0.966	53.14	6.54	1.011	-0.294	-0.374	0.091
40	1.1	0.105+j0.206	0.210	1.38	10.37	9.990	1.417	1.048	53.13	5.92	1.068	-0.224	-0.209	0.053
40	1.3	0.047+j0.170	0.145	1.17	10.37	9.990	1.860	1.165	53.71	5.56	1.096	-0.159	-0.095	0.031
60	0.1	0.871+j0.087	0.913	11.67	25.31	0.423	0.136	2.531	O/L Unstable		0.281	-0.256	-1.742	0.766
60	0.2	0.751+j0.152	0.834	5.84	25.31	0.866	0.273	2.533	O/L Unstable		0.513	-0.428	-1.501	0.587
60	0.3	0.640+j0.198	0.760	3.89	25.31	1.359	0.412	2.538	50.79	10.12	0.703	-0.534	-1.281	0.449
60	0.6	0.371+j0.254	0.569	1.95	25.31	9.990	0.853	2.566	44.73	6.68	1.069	-0.608	-0.742	0.202
60	0.7	0.301+j0.253	0.514	1.67	25.31	9.990	1.013	2.583	43.89	6.10	1.138	-0.585	-0.602	0.155
60	0.9	0.187+j0.236	0.414	1.30	25.31	9.990	1.371	2.633	43.46	5.34	1.221	-0.505	-0.374	0.091
60	1.1	0.105+j0.206	0.326	1.06	25.31	9.990	1.820	2.714	44.37	4.92	1.251	-0.408	-0.209	0.053
60	1.3	0.047+j0.170	0.249	0.90	25.31	9.990	2.560	2.837	46.24	4.72	1.248	-0.311	-0.095	0.031
80	0.1	0.871+j0.087	0.961	8.18	116.09	1.027	0.161	8.632	O/L Unstable		0.625	-0.600	-1.742	0.766
80	0.2	0.751+j0.152	0.923	4.09	116.09	2.735	0.323	8.622	O/L Unstable		1.112	-1.027	-1.501	0.587
80	0.3	0.640+j0.198	0.886	2.73	116.09	9.990	0.488	8.606	O/L Unstable		1.483	-1.314	-1.281	0.449
80	0.6	0.371+j0.254	0.777	1.36	116.09	9.990	1.018	8.522	O/L Unstable		2.068	-1.608	-0.742	0.202
80	0.7	0.301+j0.253	0.741	1.17	116.09	9.990	1.215	8.487	O/L Unstable		2.136	-1.583	-0.602	0.155
80	0.9	0.187+j0.236	0.667	0.91	116.09	9.990	1.671	8.412	O/L Unstable		2.151	-1.435	-0.374	0.091
80	1.1	0.105+j0.206	0.591	0.74	116.09	9.990	2.332	8.346	O/L Unstable		2.061	-1.217	-0.209	0.053
80	1.3	0.047+j0.170	0.512	0.63	116.09	9.990	Mono Increasing		O/L Unstable		1.918	-0.982	-0.095	0.031

C/L SYSTEM IN COMPLEX Z-PLAIN				C/L STEP RES.		C/L FREQUENCY RES.			O/L FREQUENCY RES.		SYSTEM COEFFICIENTS			
α	$\omega_o T$	POLES	ZERO	tp/T	Mp(%)	WbT	WrT	Mr(db)	PM	GM(db)	A	B	C	D
						ξ=0.9								
-80	0.1	0.809+j0.081	Out of Range											
-80	0.2	0.649+j0.131	Out of Range											
-80	0.3	0.514+j0.159	Out of Range											
-80	0.6	0.239+j0.164	Out of Range											
-80	0.7	0.180+j0.152	Out of Range											
-80	0.9	0.097+j0.122	-2.949	3.80	0.22	1.424	Mono Decreasing		63.25	8.21	0.210	0.620	-0.194	0.024
-80	1.1	0.047+j0.092	-1.124	3.11	0.22	1.430	Mono Decreasing		64.31	9.65	0.432	0.485	-0.094	0.011
-80	1.3	0.018+j0.066	-0.591	2.63	0.22	1.578	Mono Decreasing		64.66	11.52	0.609	0.360	-0.037	0.005
-60	0.1	0.809+j0.081	0.141	30.69	0.15	0.173	Mono Decreasing		73.77	35.35	0.050	-0.007	-1.619	0.662
-60	0.2	0.649+j0.131	-0.138	15.35	0.15	0.344	Mono Decreasing		72.23	28.50	0.124	0.017	-1.297	0.438
-60	0.3	0.514+j0.159	-0.243	10.23	0.15	0.514	Mono Decreasing		70.94	23.48	0.210	0.051	-1.028	0.290
-60	0.6	0.239+j0.164	-0.268	5.12	0.15	1.020	Mono Decreasing		68.02	14.76	0.478	0.128	-0.478	0.084
-60	0.7	0.180+j0.152	-0.248	4.38	0.15	1.193	Mono Decreasing		67.22	12.84	0.557	0.138	-0.361	0.056
-60	0.9	0.097+j0.122	-0.201	3.41	0.15	1.578	Mono Decreasing		65.74	10.12	0.691	0.139	-0.194	0.024
-60	1.1	0.047+j0.092	-0.155	2.79	0.15	2.099	Mono Decreasing		64.37	8.45	0.794	0.123	-0.094	0.011
-60	1.3	0.018+j0.066	-0.116	2.36	0.15	9.990	Mono Decreasing		63.14	7.45	0.868	0.100	-0.037	0.005
-40	0.1	0.809+j0.081	0.649	27.20	0.21	0.195	Mono Decreasing		77.94	24.73	0.122	-0.080	-1.619	0.662
-40	0.2	0.649+j0.131	0.416	13.60	0.21	0.391	Mono Decreasing		75.17	19.09	0.241	-0.100	-1.297	0.438
-40	0.3	0.514+j0.159	0.258	9.07	0.21	0.591	Mono Decreasing		72.85	15.89	0.352	-0.091	-1.028	0.290
-40	0.6	0.239+j0.164	0.029	4.53	0.21	1.236	Mono Decreasing		67.80	10.72	0.624	-0.018	-0.478	0.084
-40	0.7	0.180+j0.152	-0.004	3.89	0.21	1.486	Mono Decreasing		66.56	9.70	0.692	0.003	-0.361	0.056
-40	0.9	0.097+j0.122	-0.037	3.02	0.21	2.140	Mono Decreasing		64.54	8.23	0.801	0.030	-0.194	0.024
-40	1.1	0.047+j0.092	-0.047	2.47	0.21	9.990	Mono Decreasing		63.02	7.32	0.876	0.041	-0.094	0.011
-40	1.3	0.018+j0.066	-0.045	2.09	0.21	9.990	Mono Decreasing		61.90	6.76	0.927	0.042	-0.037	0.005
-30	0.1	0.809+j0.081	0.701	25.45	0.26	0.208	Mono Decreasing		78.71	23.18	0.144	-0.101	-1.619	0.662
-30	0.2	0.649+j0.131	0.489	12.73	0.26	0.419	Mono Decreasing		75.51	17.69	0.276	-0.135	-1.297	0.438
-30	0.3	0.514+j0.159	0.337	8.48	0.26	0.634	Mono Decreasing		72.87	14.65	0.394	-0.133	-1.028	0.290
-30	0.6	0.239+j0.164	0.091	4.24	0.26	1.355	Mono Decreasing		67.29	9.96	0.666	-0.061	-0.478	0.084
-30	0.7	0.180+j0.152	0.051	3.64	0.26	1.650	Mono Decreasing		65.97	9.07	0.732	-0.037	-0.361	0.056
-30	0.9	0.097+j0.122	0.003	2.83	0.26	2.569	Mono Decreasing		63.92	7.82	0.833	-0.002	-0.194	0.024
-30	1.1	0.047+j0.092	-0.019	2.31	0.26	9.990	Mono Decreasing		62.46	7.04	0.900	0.017	-0.094	0.011
-30	1.3	0.018+j0.066	-0.026	1.96	0.26	9.990	Mono Decreasing		61.45	6.58	0.944	0.024	-0.037	0.005
-20	0.1	0.809+j0.081	0.733	23.71	0.35	0.222	Mono Decreasing		79.03	22.11	0.161	-0.118	-1.619	0.662
-20	0.2	0.649+j0.131	0.536	11.85	0.35	0.447	Mono Decreasing		75.48	16.73	0.304	-0.163	-1.297	0.438
-20	0.3	0.514+j0.159	0.389	7.90	0.35	0.680	Mono Decreasing		72.60	13.80	0.428	-0.167	-1.028	0.290
-20	0.6	0.239+j0.164	0.136	3.95	0.35	1.482	Mono Decreasing		66.66	9.43	0.701	-0.096	-0.478	0.084
-20	0.7	0.180+j0.152	0.091	3.39	0.35	1.832	Mono Decreasing		65.33	8.62	0.764	-0.069	-0.361	0.056
-20	0.9	0.097+j0.122	0.033	2.63	0.35	9.990	Mono Decreasing		63.31	7.51	0.859	-0.028	-0.194	0.024
-20	1.1	0.047+j0.092	0.003	2.16	0.35	9.990	Mono Decreasing		61.95	6.84	0.920	-0.003	-0.094	0.011
-20	1.3	0.018+j0.066	-0.011	1.82	0.35	9.990	Mono Decreasing		61.05	6.44	0.958	0.010	-0.037	0.005

Table 1

C/L SYSTEM IN COMPLEX Z-PLANE				C/L STEP RES.			C/L FREQUENCY RES. (ξ=0.7)			O/L FREQUENCY RES.			SYSTEM COEFFICIENTS			
α	$\omega_o T$	POLES	ZERO	t_p/T	M_p(%)	t_s/T	$\omega_b T$	$\omega_r T$	M_r(db)	PM	GM(db)	$\omega_c T$	A	B	C	D
-60	0.1	0.902+j0.091	Out of Range													
-60	0.2	0.806+j0.163	Out of Range													
-60	0.3	0.712+j0.220	Out of Range													
-60	0.6	0.458+j0.314	Out of Range													
-60	0.7	0.385+j0.324	-8.110	4.88	5.03	5.4	1.027	0.226	0.012	60.41	8.74	0.41	0.053	0.430	-0.770	0.254
-60	0.9	0.257+j0.324	-2.625	3.79	5.03	4.2	1.238	+		60.94	8.76	0.51	0.181	0.476	-0.515	0.171
-60	1.1	0.154+j0.303	-1.518	3.10	5.03	3.4	1.410	+		61.43	9.00	0.59	0.321	0.487	-0.309	0.116
-60	1.3	0.075+j0.269	-1.025	2.63	5.03	2.9	1.563	+		61.81	9.43	0.67	0.458	0.470	-0.150	0.078
-40	0.1	0.902+j0.091	0.190	30.64	4.62	33.3	0.142	0.022	0.000	65.38	42.91	0.09	0.022	-0.004	-1.804	0.822
-40	0.2	0.806+j0.163	-0.123	15.32	4.62	16.6	0.284	0.042	0.003	64.68	33.40	0.18	0.057	0.007	-1.611	0.676
-40	0.3	0.712+j0.220	-0.273	10.21	4.62	11.1	0.424	0.059	0.002	64.12	24.48	0.26	0.103	0.028	-1.424	0.555
-40	0.6	0.458+j0.314	-0.406	5.11	4.62	5.5	0.837	0.067	0.000	62.97	17.04	0.47	0.279	0.113	-0.917	0.308
-40	0.7	0.385+j0.324	-0.410	4.38	4.62	4.8	0.971	0.029	0.000	62.71	16.00	0.53	0.343	0.141	-0.770	0.254
-40	0.9	0.257+j0.324	-0.395	3.40	4.62	3.7	1.234	+		62.28	14.73	0.63	0.471	0.186	-0.515	0.171
-40	1.1	0.154+j0.303	-0.365	2.79	4.62	3.0	1.498	+		61.90	13.61	0.73	0.591	0.216	-0.309	0.116
-40	1.3	0.075+j0.269	-0.328	2.36	4.62	2.6	1.777	+		61.52	11.16	0.81	0.699	0.229	-0.150	0.078
-30	0.1	0.902+j0.091	0.611	28.90	4.85	32.0	0.147	0.035	0.017	66.76	34.04	0.10	0.046	-0.028	-1.804	0.822
-30	0.2	0.806+j0.163	0.356	14.45	4.85	16.0	0.295	0.069	0.016	65.74	28.03	0.20	0.100	-0.036	-1.611	0.676
-30	0.3	0.712+j0.220	0.183	9.63	4.85	10.7	0.441	0.102	0.015	64.88	24.43	0.28	0.161	-0.029	-1.424	0.555
-30	0.6	0.458+j0.314	-0.086	4.82	4.85	5.3	0.879	0.194	0.012	63.04	17.79	0.51	0.361	0.031	-0.917	0.308
-30	0.7	0.385+j0.324	-0.130	4.13	4.85	4.6	1.025	0.222	0.011	62.59	16.18	0.57	0.428	0.056	-0.770	0.254
-30	0.9	0.257+j0.324	-0.182	3.21	4.85	3.6	1.319	0.279	0.010	61.87	13.46	0.69	0.556	0.101	-0.515	0.171
-30	1.1	0.154+j0.303	-0.203	2.63	4.85	2.9	1.626	0.345	0.011	61.28	11.29	0.78	0.671	0.136	-0.309	0.116
-30	1.3	0.075+j0.269	-0.207	2.22	4.85	2.5	1.970	0.438	0.014	60.75	9.57	0.86	0.770	0.159	-0.150	0.078
-20	0.1	0.902+j0.091	0.726	27.15	5.31	31.2	0.156	0.048	0.055	67.52	30.46	0.11	0.065	-0.047	-1.804	0.822
-20	0.2	0.806+j0.163	0.522	13.58	5.31	15.6	0.311	0.095	0.058	66.17	24.61	0.22	0.135	-0.071	-1.611	0.676
-20	0.3	0.712+j0.220	0.368	9.05	5.31	10.4	0.467	0.142	0.058	65.03	21.20	0.31	0.208	-0.076	-1.424	0.555
-20	0.6	0.458+j0.314	0.084	4.53	5.31	5.2	0.939	0.284	0.056	62.57	15.27	0.55	0.427	-0.036	-0.917	0.308
-20	0.7	0.385+j0.324	0.027	3.88	5.31	4.5	1.098	0.332	0.056	61.99	13.92	0.62	0.497	-0.014	-0.770	0.254
-20	0.9	0.257+j0.324	-0.051	3.02	5.31	3.5	1.428	0.431	0.058	61.05	11.70	0.74	0.625	0.032	-0.515	0.171
-20	1.1	0.154+j0.303	-0.098	2.47	5.31	2.8	1.787	0.543	0.064	60.34	9.96	0.83	0.735	0.072	-0.309	0.116
-20	1.3	0.075+j0.269	-0.123	2.09	5.31	2.4	2.225	0.677	0.077	59.77	8.60	0.91	0.827	0.101	-0.150	0.078
0	0.1	0.902+j0.091	0.818	23.66	7.02	30.6	0.179	0.070	0.280	67.56	26.60	0.13	0.098	-0.080	-1.804	0.822
0	0.2	0.806+j0.163	0.668	11.83	7.02	15.3	0.359	0.140	0.280	65.55	20.93	0.25	0.194	-0.130	-1.611	0.676
0	0.3	0.712+j0.220	0.544	7.89	7.02	10.2	0.540	0.211	0.281	63.88	17.73	0.36	0.288	-0.157	-1.424	0.555
0	0.6	0.458+j0.314	0.277	3.94	7.02	5.1	1.100	0.426	0.288	60.37	12.50	0.64	0.542	-0.150	-0.917	0.308
0	0.7	0.385+j0.324	0.214	3.38	7.02	4.4	1.298	0.500	0.293	59.58	11.39	0.71	0.615	-0.132	-0.770	0.254
0	0.9	0.257+j0.324	0.116	2.63	7.02	3.4	1.729	0.655	0.307	58.43	9.64	0.83	0.743	-0.086	-0.515	0.171
0	1.1	0.154+j0.303	0.046	2.15	7.02	2.8	2.276	0.825	0.331	57.69	8.34	0.93	0.846	-0.039	-0.309	0.116
0	1.3	0.075+j0.269	-0.004	1.82	7.02	2.4	•	1.018	0.371	57.25	7.35	1.01	0.925	0.003	-0.150	0.078
20	0.1	0.902+j0.091	0.864	20.17	10.52	31.2	0.213	0.089	0.776	65.81	24.01	0.16	0.131	-0.113	-1.804	0.822
20	0.2	0.806+j0.163	0.746	10.09	10.52	15.6	0.428	0.179	0.781	63.09	18.50	0.30	0.254	-0.189	-1.611	0.676
20	0.3	0.712+j0.220	0.643	6.72	10.52	10.4	0.646	0.268	0.783	60.87	15.45	0.43	0.368	-0.237	-1.424	0.555
20	0.6	0.458+j0.314	0.403	3.36	10.52	5.2	1.346	0.544	0.799	56.42	10.68	0.73	0.656	-0.264	-0.917	0.308
20	0.7	0.385+j0.324	0.341	2.88	10.52	4.5	1.610	0.640	0.808	55.50	9.71	0.81	0.733	-0.250	-0.770	0.254
20	0.9	0.257+j0.324	0.237	2.24	10.52	3.5	2.275	0.839	0.835	54.29	8.24	0.94	0.861	-0.204	-0.515	0.171
20	1.1	0.154+j0.303	0.156	1.83	10.52	2.8	•	1.056	0.878	53.73	7.19	1.04	0.956	-0.149	-0.309	0.116
20	1.3	0.075+j0.269	0.093	1.55	10.52	2.4	•	1.301	0.943	53.67	6.44	1.11	1.023	-0.095	-0.150	0.078
40	0.1	0.902+j0.091	0.898	16.68	18.17	33.3	0.269	0.107	1.782	61.74	21.58	0.19	0.174	-0.156	-1.804	0.822
40	0.2	0.806+j0.163	0.806	8.34	18.17	16.6	0.543	0.214	1.783	58.21	16.25	0.36	0.331	-0.267	-1.611	0.676
40	0.3	0.712+j0.220	0.722	5.56	18.17	11.1	0.824	0.321	1.786	55.40	13.37	0.50	0.473	-0.341	-1.424	0.555
40	0.6	0.458+j0.314	0.513	2.78	18.17	5.5	1.807	0.653	1.804	50.02	9.03	0.84	0.805	-0.413	-0.917	0.308
40	0.7	0.385+j0.324	0.455	2.38	18.17	4.8	2.276	0.768	1.815	48.99	8.19	0.93	0.887	-0.404	-0.770	0.254
40	0.9	0.257+j0.324	0.353	1.85	18.17	3.7	•	1.009	1.847	47.78	6.96	1.07	1.015	-0.358	-0.515	0.171
40	1.1	0.154+j0.303	0.266	1.52	18.17	3.0	•	1.272	1.898	47.52	6.12	1.18	1.100	-0.293	-0.309	0.116
40	1.3	0.075+j0.269	0.193	1.28	18.17	2.6	•	1.575	1.978	48.01	5.55	1.24	1.151	-0.223	-0.150	0.078
60	0.1	0.902+j0.091	0.930	13.19	39.20	37.6	0.390	0.123	3.959	O/L Unstable			0.255	-0.237	-1.804	0.822
60	0.2	0.806+j0.163	0.865	6.59	39.20	18.8	0.794	0.247	3.960	O/L Unstable			0.477	-0.413	-1.611	0.676
60	0.3	0.712+j0.220	0.804	4.40	39.20	12.5	1.231	0.372	3.959	O/L Unstable			0.670	-0.538	-1.424	0.555
60	0.6	0.458+j0.314	0.639	2.20	39.20	6.3	•	0.756	3.958	O/L Unstable			1.085	-0.693	-0.917	0.308
60	0.7	0.385+j0.324	0.589	1.88	39.20	5.4	•	0.891	3.960	38.20	6.37	1.10	1.177	-0.693	-0.770	0.254
60	0.9	0.257+j0.324	0.496	1.47	39.20	4.2	•	1.175	3.972	37.00	5.41	1.25	1.304	-0.648	-0.515	0.171
60	1.1	0.154+j0.303	0.411	1.20	39.20	3.4	•	1.491	4.002	36.95	4.79	1.36	1.371	-0.564	-0.309	0.116
60	1.3	0.075+j0.269	0.333	1.01	39.20	2.9	•	1.869	4.059	37.91	4.41	1.43	1.392	-0.463	-0.150	0.078
80	0.1	0.902+j0.091	0.971	9.70	158.94	48.4	0.979	0.137	10.800	O/L Unstable			0.611	-0.593	-1.804	0.822
80	0.2	0.806+j0.163	0.942	4.85	158.94	24.2	2.426	0.275	10.790	O/L Unstable			1.121	-1.056	-1.611	0.676
80	0.3	0.712+j0.220	0.914	3.23	158.94	16.1	•	0.414	10.774	O/L Unstable			1.537	-1.406	-1.424	0.555
80	0.6	0.458+j0.314	0.831	1.62	158.94	8.1	•	0.846	10.688	O/L Unstable			2.320	-1.928	-0.917	0.308
80	0.7	0.385+j0.324	0.803	1.39	158.94	6.9	•	0.999	10.649	O/L Unstable			2.455	-1.971	-0.770	0.254
80	0.9	0.257+j0.324	0.746	1.08	158.94	5.4	•	1.326	10.560	O/L Unstable			2.581	-1.925	-0.515	0.171
80	1.1	0.154+j0.303	0.685	0.86	158.94	4.4	•	1.703	10.464	O/L Unstable			2.565	-1.758	-0.309	0.116
80	1.3	0.075+j0.269	0.621	0.75	158.94	3.7	•	2.192	10.371	O/L Unstable			2.453	-1.525	-0.150	0.078

+ no resonance • no solution

C/L SYSTEM IN COMPLEX Z-PLAIN				C/L STEP RES.		C/L FREQUENCY RES.			O/L FREQUENCY RES.		SYSTEM COEFFICIENTS			
α	$\omega_o T$	POLES	ZERO	tp/T	Mp(%)	WbT	WrT	Mr(db)	PM	GM(db)	A	B	C	D
						ξ =0.9								
0	0.1	0.809+j0.081	0.775	20.22	0.67	0.253	Mono Decreasing		78.75	20.59	0.191	-0.148	-1.619	0.662
0	0.2	0.649+j0.131	0.599	10.11	0.67	0.511	Mono Decreasing		74.65	15.37	0.351	-0.211	-1.297	0.438
0	0.3	0.514+j0.159	0.462	6.74	0.67	0.782	Mono Decreasing		71.40	12.60	0.486	-0.224	-1.028	0.290
0	0.6	0.239+j0.164	0.204	3.37	0.67	1.789	Mono Decreasing		65.14	8.64	0.761	-0.155	-0.478	0.084
0	0.7	0.180+j0.152	0.152	2.89	0.67	2.341	Mono Decreasing		63.85	7.96	0.820	-0.125	-0.361	0.056
0	0.9	0.097+j0.122	0.080	2.25	0.67	9.990	Mono Decreasing		62.04	7.04	0.903	-0.073	-0.194	0.024
0	1.1	0.047+j0.092	0.038	1.84	0.67	9.990	Mono Decreasing		60.94	6.51	0.953	-0.036	-0.094	0.011
0	1.3	0.018+j0.066	0.014	1.56	0.67	9.990	Mono Decreasing		60.30	6.22	0.982	-0.014	-0.037	0.005
20	0.1	0.809+j0.081	0.805	16.73	1.47	0.293	Mono Decreasing		77.36	19.33	0.220	-0.177	-1.619	0.662
20	0.2	0.649+j0.131	0.647	8.36	1.47	0.595	Mono Decreasing		72.76	14.25	0.399	-0.259	-1.297	0.438
20	0.3	0.514+j0.159	0.519	5.58	1.47	0.916	Mono Decreasing		69.25	11.61	0.544	-0.282	-1.028	0.290
20	0.6	0.239+j0.164	0.262	2.79	1.47	2.300	Mono Decreasing		63.03	7.99	0.820	-0.215	-0.478	0.084
20	0.7	0.180+j0.152	0.206	2.39	1.47	9.990	Mono Decreasing		61.90	7.39	0.875	-0.180	-0.361	0.056
20	0.9	0.097+j0.122	0.124	1.86	1.47	9.990	Mono Decreasing		60.47	6.63	0.948	-0.117	-0.194	0.024
20	1.1	0.047+j0.092	0.071	1.52	1.47	9.990	0.902	0.032	59.77	6.22	0.987	-0.070	-0.094	0.011
20	1.3	0.018+j0.066	0.037	1.29	1.47	9.990	1.586	0.090	59.48	6.01	1.006	-0.038	-0.037	0.005
40	0.1	0.809+j0.081	0.834	13.24	3.70	0.357	0.092	0.115	74.20	17.97	0.259	-0.216	-1.619	0.662
40	0.2	0.649+j0.131	0.695	6.62	3.70	0.728	0.187	0.119	69.05	13.05	0.462	-0.321	-1.297	0.438
40	0.3	0.514+j0.159	0.578	4.41	3.70	1.135	0.288	0.127	65.32	10.56	0.619	-0.358	-1.028	0.290
40	0.6	0.239+j0.164	0.326	2.21	3.70	9.990	0.656	0.175	59.52	7.28	0.898	-0.292	-0.478	0.084
40	0.7	0.180+j0.152	0.266	1.89	3.70	9.990	0.814	0.201	58.72	6.77	0.947	-0.252	-0.361	0.056
40	0.9	0.097+j0.122	0.174	1.47	3.70	9.990	1.222	0.274	58.03	6.16	1.006	-0.175	-0.194	0.024
40	1.1	0.047+j0.092	0.110	1.20	3.70	9.990	1.864	0.382	58.02	5.87	1.030	-0.113	-0.094	0.011
40	1.3	0.018+j0.066	0.066	1.02	3.70	9.990	Mono Increasing		58.28	5.76	1.037	-0.069	-0.037	0.005
60	0.1	0.809+j0.081	0.870	9.75	11.65	0.490	0.156	1.035	66.77	15.98	0.331	-0.288	-1.619	0.662
60	0.2	0.649+j0.131	0.757	4.87	11.65	1.017	0.315	1.043	60.85	11.34	0.579	-0.438	-1.297	0.438
60	0.3	0.514+j0.159	0.657	3.25	11.65	1.650	0.480	1.058	56.88	9.06	0.761	-0.500	-1.028	0.290
60	0.6	0.239+j0.164	0.420	1.62	11.65	9.990	1.051	1.146	51.99	6.25	1.044	-0.439	-0.478	0.084
60	0.7	0.180+j0.152	0.358	1.39	11.65	9.990	1.290	1.193	51.82	5.86	1.083	-0.388	-0.361	0.056
60	0.9	0.097+j0.122	0.255	1.08	11.65	9.990	1.942	1.318	52.64	5.44	1.115	-0.284	-0.194	0.024
60	1.1	0.047+j0.092	0.176	0.89	11.65	9.990	Mono Increasing		54.15	5.32	1.112	-0.195	-0.094	0.011
60	1.3	0.018+j0.066	0.116	0.75	11.65	9.990	Mono Increasing		55.69	5.35	1.096	-0.128	-0.037	0.005
80	0.1	0.809+j0.081	0.934	6.26	68.99	1.123	0.213	5.842	O/L Unstable		0.651	-0.608	-1.619	0.662
80	0.2	0.649+j0.131	0.872	3.13	68.99	9.990	0.431	5.834	O/L Unstable		1.097	-0.956	-1.297	0.438
80	0.3	0.514+j0.159	0.812	2.09	68.99	9.990	0.658	5.822	O/L Unstable		1.388	-1.127	-1.028	0.290
80	0.6	0.239+j0.164	0.641	1.04	68.99	9.990	1.467	5.776	O/L Unstable		1.689	-1.083	-0.478	0.084
80	0.7	0.180+j0.152	0.586	0.89	68.99	9.990	1.838	5.766	O/L Unstable		1.681	-0.986	-0.361	0.056
80	0.9	0.097+j0.122	0.480	0.70	68.99	9.990	Mono Increasing		32.83	3.61	1.596	-0.765	-0.194	0.024
80	1.1	0.047+j0.092	0.378	0.57	68.99	9.990	Mono Increasing		37.20	3.77	1.475	-0.558	-0.094	0.011
80	1.3	0.018+j0.066	0.285	0.48	68.99	9.990	Mono Increasing		42.66	4.07	1.355	-0.387	-0.037	0.005

BIBLIOGRAPHY

1. Kuo, B. C.: *Digital Control Systems*, Holt, Rinehart and Winston Inc., 1980.

2. Rattan, K. S.: "Digital Redesign of Existing Multiloop Continuous Control Systems", *Proc. of 1981 Joint Automatic Control Conference*, Va., USA, Vol. 1.

3. Shieh, L. S.: "Model Simplification and Digital Design of Multivariable Sampled-Data Control Systems via a Dominant-Data Matching Method", *Proc. of IFAC Symposium on Theory and Application of Digital Control*, New Delhi, January 1982.

4. Shieh, L. S., Chang, Y. F., and Yates, R. E.: "A Dominant-Data Matching Method for Digital Control Systems Modeling and Design", *IEEE Trans. on Industrial Electronics and Control Instrumentation*, Vol. IECI-28, No. 4, November 1981, pp. 390-396.

5. Rattan, K. S.: *Computer-Aided Design of Sampled-Data Control Systems via Complex-Curve Fitting*, Ph.D Dissertation, The University of Kentucky, 1975.

6. Rattan, K. S., and Yeh, H. H.: "Discretizing Continuous-Data Control Systems", *Computer-Aided Design*, Vol. 10, No. 5, September 1978, pp. 299-306.

7. Rattan, K. S.: "Conversion of Existing Continuous Control Systems into Digital Control Systems", *Proc. of American Control Conference*, 1982, pp. 46-51.

8. "DCADRE", IMSL Library Manual, IMSL Inc., November 1979.

9. "GGUBFS", IMSL Library Manual, IMSL Inc.

10. Luus, R.: "Optimization in Model Reduction", *Int. J. Control*, Vol. 32, No. 5, pp. 741-747.

11. Luus, R., and Jaakola, T. H. I.: "Optimization by Direct Search and Systematic Reduction of the Size of Search Region", *AIChE Journal*, Vol. 19, No. 4, July 1973, pp. 760-766.

12. Nelder, J. A., and Mead, R.: "A Simplex Method for Function Minimization", *The Computer Journal*, Vol. 7, 1964, pp. 308-313.

13. Sanathanan, C. K., and Koerner, J.: "Transfer Function Synthesis as a Ratio of Two Complex Polynomials", *IEEE Trans. on Automatic Control*, January 1963, pp.56-58.

14. Isermann, R.: *Digital Control Systems*, Springer–Verlag, 1981.

15. Spendley, W., Hext, G. R., and Himsworth, F. R.: "Sequential Application of Simplex Designs Optimization and Evolutionary Operation", *Technometrics*, Vol. 4, 1962, p.441.

16. Yang, S. M., and Luus, R.: "Optimization in Linear System Reduction", *Electronics Letters*, Vol. 19, No. 16, August 4, 1983.

17. Yang, S. M., and Luus, R.: "A Note on Model Reduction of Digital Control Systems", *Int. J. Control*, Vol. 37, 1983, pp. 437-439.

18. Levy, E. C.: "Complex-Curve Fitting", *IRE Trans. on Automatic Control*, AC-4, 1959, pp. 37-43.

19. Franklin, G. F., and Powell, J. D.: *Digital Control of Dynamic Systems*, Addison–Wesley Publishing Company, 1980.

20. Ogata, K.: *Modern Control Engineering*, Prentice-Hall, 1970.

21. Shieh, L. S., Wei, Y-J. P., Chow, H-Z., and Yates, R. E.: "Determination of Equivalent Dominant Poles and Zeros Using Industrial Specifications", *IEEE Trans. on Industrial Electronics and Control Instrumentation*, Vol. IECI-26, No. 3, August 1979, pp. 125-133.

22. Jury, E. I.: *Sampled-Data Control Systems*, John Wiley & Sons, Inc., 1958.

23. Katz, P.: *Digital Control Using Microprocessors*, Prentice-Hall International, Inc., 1981.

24. Kuo, B. C., Singh, G., and Yackel, R. A.: "Digital Approximation of Continuous-Data Control Systems by Point-by-Point State Comparison", *Computer and Electrical Engineering*, Vol. 1, 1973, pp. 155-170.

25. Yackel, R. A., Kuo, B. C., and Singh, G.: "Digital Redesign of Continuous Systems by Matching of States at Multiple Sampling Periods", *Automatica*, Vol. 10, 1974, pp. 105-111.

26. Singh, G., Kuo, B. C., and Yackel, R. A.: "Digital Approximation by Point-by-Point State Matching with Higher-Order Holds", *Int. J. Control*, Vol. 20, 1974, pp. 81-90.

27. Pujara, L. R., and Rattan, K. S.: "A Frequency Matching Method for Model Reduction of Digital Control Systems", *Int. J. Control*, Vol. 35, 1982, pp. 139-148.

28. Dixon, L. C. W.: *Non-linear Optimization*, English Universities Press, London, 1972.

29. Fan, M. Y., and Zhang, Y.: *Optimization Technique Fundamentals*, Tsing-Hua University Press, Beijing, 1981, (in Chinese).